UNIVERSITÄT LEIPZIG

REPORT

Institute für Physik
The Physics Institutes

2003

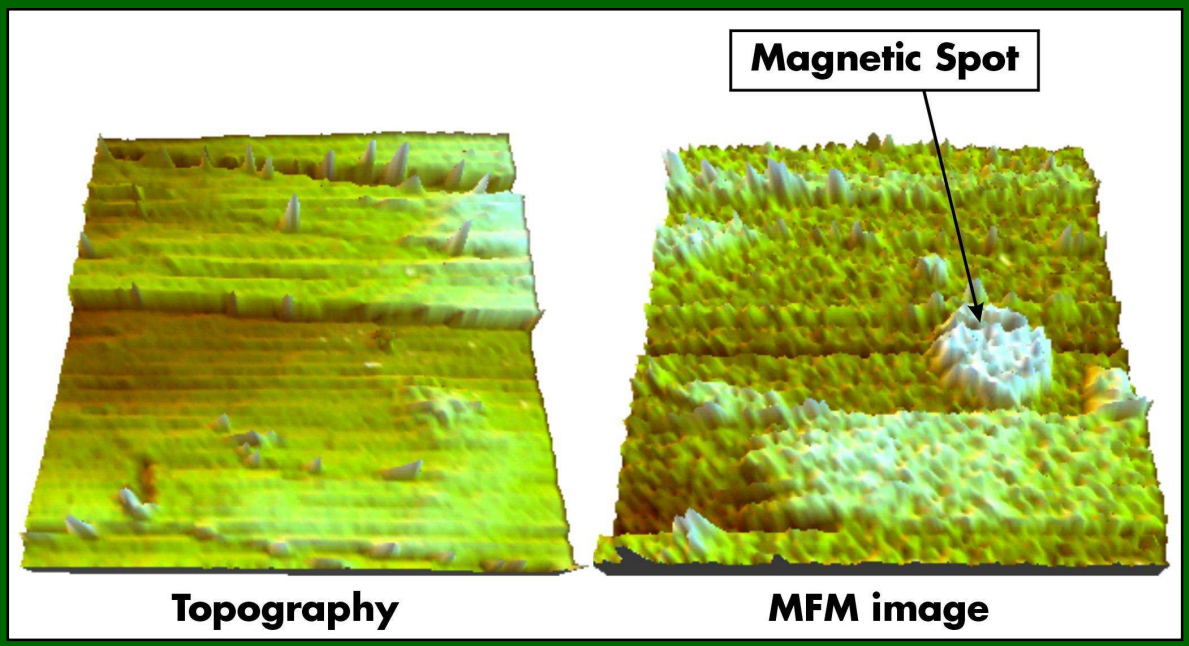

The Physics Institutes of Universität Leipzig, Report 2003
M. Grundmann, ed.
ISBN 3-934178-33-2

Printed in Germany by
MERKUR Druck und Kopierzentrum GmbH, Leipzig

on-line available at
http://www.uni-leipzig.de/~exph2/report_2003.pdf

Front cover

Topography (*left*) and magnetic-force gradient (*right*) images of a highly oriented graphite surface (7.6×7.6 μm^2) irradiated with a ~1 μm diameter proton microbeam (dose ~ 0.1 $nC/\mu m^2$) with the LIPSION accelerator. The magnetic spot is clearly recognized in the magnetic image, whereas no change in the topography is observed.
Irradiation: D. Spemann, Measurement: K.-H. Han

Back cover

top: Arrangement of isotropic droplets in a homogeneous smectic film at steps of film thickness, observed by reflection microscopy under monochromatic illumination, image size: (260 μm × 190 μm).
bottom: Array of ZnO nanowhiskers grown on sapphire using pulsed laser deposition.

Institut für Experimentelle Physik I
Institut für Experimentelle Physik II
Institut für Theoretische Physik
Fakultät für
Physik und Geowissenschaften
Universität Leipzig

Institute for Experimental Physics I
Institute for Experimental Physics II
Institute for Theoretical Physics
Faculty of Physics and Geosciences
Universität Leipzig

Report 2003

Addresses

Institute for Experimental Physics I
Linnéstraße 5
D-04103 Leipzig, Germany
Phone: +49 341 9732 551
Fax: +49 341 9732 599
WWW: http://www.uni-leipzig.de/~gasse/nysid_a/inst/exp_1.htm

Institute for Experimental Physics II
Linnéstraße 5
D-04103 Leipzig, Germany
Phone: +49 341 9732 650
Fax: +49 341 9732 668
WWW: http://www.uni-leipzig.de/~exph2/

Institute for Theoretical Physics
Vor dem Hospitaltore 1
D-04103 Leipzig, Germany
Phone: +49 341 9732 420
Fax: +49 341 9732 548
WWW: http://www.physik.uni-leipzig.de/
Mailing address: Augustusplatz 10/11, 04109 Leipzig, Germany

Contents

Preface

In this report the Institutes of Physics of the Universität Leipzig present their scientific activities and major achievements in the year 2003.

In July the DFG 'Forschergruppe' (Research Group) 522 (speaker: Prof. Dr. Marius Grundmann, www.uni-leipzig.de/∼for522) *Architecture of nano- and micro-dimensional building blocks* took up work. Physicists, chemists, mineralogists and mathematicians jointly research on three-dimensionally designed nanostructures, such as whiskers/wires, scrolls and spirals. Four projects are at our faculty, two at the Faculty of Chemistry and Mineralogy of the University of Leipzig, one project is at the Leibniz-Institute for Surface Modification (IOM), Leipzig and one at the Max-Planck-Institute for Mathematics in the Natural Sciences (MPI-MiS), Leipzig.

The group 'Physics of Interfaces' (head: Prof. Dr. J. Kärger) coordinates the EC-sponsored project TROCAT in which nine groups from five countries are jointly exploring the interrelation between molecular diffusion and conversion in heterogeneous catalysis. These activities will be continued within a Network of Excellence of the 6th frame program of the EC (INSIDE-PORES). With special focus on diffusion in zeolites Prof. Kärger and his team initiated an international (British, French, German) research group ("Internationale Forschergruppe") jointly sponsored by EPSR, CNRS and DFG. The activities of this collaboration will be of particular benefit for the International Research Training Group ('Europäisches Graduiertenkolleg') dedicated to 'Diffusion in Porous Media', which starts to operate in summer term 2004 comprising groups from our institute, from the institutes of Theoretical Physics and of Chemical Technology (Faculty of Chemistry and Mineralogy) together with colleagues of the universities of Amsterdam, Delft and Eindhoven. Prof. Kärger and his group highly appreciates the presence of Prof. Douglas Morris Ruthven who received in 2002 the Humboldt Research Award.

The research team of Prof. Kremer is defining at the moment new activities after the leave of three staff members (Prof. Grande, who retired, Prof. Stannarius, Prof. Papadakis). In the nearer future it is planned to strengthen the activities in the field of biophysics and biotechnology. In the course of this a large research project within the 'Sächsischen Biotechnologieinitiative' was prolonged. Furthermore, against tough competition, the team of Prof. Kremer successfully applied for an extended grant within a newly established DFG-Schwerpunktprogramm 'Nano- and Microfluidics: From the molecular motion to macroscopic flow'.

The BMBF 'Nachwuchsgruppe' (Young Research Team) *Nano-Spintronics*, lead by Dr. Heidemarie Schmidt (www.uni-leipzig.de/∼nse), started its work in July 2003 and has in the meantime already succeeded with the realization of room temperature ferromagnetic ZnO doped with transition metals.

The research performed at the Institute for Theoretical Physics covers a wide range fields. We would like to mention the following papers of which we think that they deserve particular attention:

The 'Habilitationsschrift' of our colleague Olaf Richter who deceased in 2004:
Physically reasonable solutions to the Ernst equation and their twistor theory.

C. Landim, J. Quastel, M. Salmhofer, H-T. Yau, *Superdiffusivity of Asymmetric Exclusion Process, in Dimensions One and Two*, Communications in Mathematical Physics 244 (2004) 455-481

S. Derkachov, D. Karakhanyan and R. Kirschner, *Universal R operator with Jordanian deformation of conformal symmetry*, Nucl. Phys. B 681 (2004) 295, [arXiv:nlin.si/0310019]

M. Brede, U. Behn, *Patterns in randomly evolving networks: Idiotypic networks*, Phys. Rev. E **67**, 031920-1/18 (2003).

M. Bachmann, W. Janke, *Multicanonical Chain Growth Algorithm*, Phys. Rev. Lett. **91** (2003) 208105-1–4

Prof. Dr. Ralf Stannarius received a call from the University of Magdeburg, where he took over a chair (C4-position) for non-linear physics. Prof. Dr. Christine Papadakis received a call from the Technical University of Munich for a C3-professorship at the chair of Experimental Physics IV (Prof. Dr. Winfried Petry). We wish both all the best in their new positions.

Our colleague for many years Dr. Bernd Rheinländer has been appointed as extraordinary professor at our faculty. His initiative and achievements in the field of ellipsometry are the basis of many exciting results. Dr. Andreas Pöppl has been appointed extraordinary professor for his achievements and excellence in the field of electron paramagnetic resonance.

We are grateful to many funding agencies which are acknowledged in the individual contributions. We appreciate their support which is essential for our work. We like to thank the University for generously supporting us in the framework of the 'HbfG-Verfahren' with a new helium liquifier, to be installed in the fall of 2004, and equipment for advanced characterization of optoelectronic devices.

Leipzig, April 2004

F. Kremer
M. Grundmann
K. Sibold
Directors

2

Structure and Staff of the Institutes

2.1 Institute for Experimental Physics I

2.1.1 Office of the Director

Prof. Dr. Friedrich Kremer (director)
Prof. Dr. Jörg Kärger (vice director)

2.1.2 Physics of Anisotropic Fluids, Physik anisotroper Fluide

Prof. Dr. Friedrich Kremer

Secretary

Karin Girke

Technical staff

Ines Grünwald
Dipl.-Ing. Jörg Reinmuth
Dipl.-Phys. Wiktor Skokow

Academic staff

Priv.-Doz. Dr. Ralf Stannarius
Dr. Christine Papadakis

PhD candidates

Dipl.-Phys. Tune B. Bonné
Dipl.-Chem. Peter Busch

Dipl.-Phys. Lutz Hartmann
Dipl.-Phys. Thomas John
M. Sc. Julius Tsuwi Kazungu
Dipl.-Phys. Kati Kegler
Dipl.-Biochem. Mathias Salomo
Dipl.-Phys. Heidrun Schüring
Dipl.-Phys. Anatoli Serghei
Dipl.-Biochem. Marc Struhalla
M. Sc. Michael Tammer

2.1.3 Physics of Interfaces, Grenzflächenphysik

Prof. Dr. Jörg Kärger

Secretary

Dipl.-Chem. Katrin Kunze

Technical staff

Dipl.-Ing. Bernd Knorr
Dipl.-Phys. Cordula Bärbel Krause
Lutz Moschkowitz
Ing. Dagmar Prager

Academic staff

Prof. Dr. Peter Bräuer
Priv.-Doz. Dr. Horst Ernst
Prof. Dr. Dieter Freude
Dr. Karen Friedemann
Dr. Petrik Galvosas
Dr. Wilfried Heink
Prof. (i.R.) Dr. Dr. h.c. Harry Pfeifer
Dr. Andreas Schüring
Dr. Frank Stallmach
Priv.-Doz. Dr. Brigitte Staudte
Priv.-Doz. Dr. Sergey Vasenkov

PhD candidates

Dipl.-Phys. Christian Chmelik
Dipl.-Chem. Stefan Gröger
Dipl.-Phys. Johanna Kanellopoulos
Dipl.-Phys. Pavel Kortunov
Dipl.-Chem. Enrico Lehmann

Dipl.-Phys. Thomas Loeser
Dipl.-Phys. Andreas Brzank
Dipl.-Phys. Denis Schneider

2.1.4 Polymer Physics, Polymerphysik

Prof. Dr. Dieter Geschke

Technical staff

Christine Adolph
Dipl.-Ing. Hans-Jürgen Rauchfuß
Dipl.-Phys. Uwe Weber

Academic staff

PD Dr. Martin Helmstedt
Dr. Jianjun Li

2.1.5 Soft Matter Physics, Physik der weichen Materie

Prof. Dr. Josef A. Käs

Secretary

Claudia Hanisch

Technical staff

Dipl. Phys. Bernd Kohlstrunk
PTA Undine Dietrich
CTA Elke Westphal

Academic staff

Prof. Dr. Herbert Schmiedel
Prof. Dr. Mathias Lösche (on leave of absence)
Dr. Jochen Guck
Dr. Carsten Selle

PhD candidates

Brian Gentry
David Smith
Allen Ehrlicher
Timo Betz
Daniel Koch
Bjoern Stuhrmann
Michael Goegler
Vanessa Bell
Falk Wottawah
Stefan Schinkinger
Bryan Lincoln
Kristian Franze
Jens Gerdelmann
Claudia Brunner
Florian Huber
Susanne Ebert
Frank Sauer
Karla Müller
Thomas Siegemund

Students

Maren Romeyke
Mireille Martin
Natalie Bordag
Marlis Wilke

2.2 Institute for Experimental Physics II

2.2.1 Office of the Director

Prof. Dr. Marius Grundmann (director)
Prof. Dr. Tilman Butz (vice director)

2.2.2 Nuclear Solid State Physics, Nukleare Festkörperphysik

Prof. Dr. Tilman Butz

Technical staff

Dipl.-Ing. Bernd Krause
PTA Raimund Wipper

Academic staff

Dr. Dietmar Lehmann
Dr. Tilo Reinert
Dr. Jiři Škopek
Priv.-Doz. Dr. Wolfgang Tröger
Dr. Jürgen Vogt

PhD candidates

Dipl.-Phys. Frank Heinrich
Dipl.-Phys. Christoph Meinecke
Dipl.-Phys. Frank Menzel
Dipl.-Phys. Daniel Spemann

Students

Anja Fiedler
Sven Friedemann
Pedro Hugo Ferreira Natal da Luz

2.2.3 Physics of Dielectric Solids, Physik dielektrischer Festkörper

Prof. Dr. Dieter Michel

Secretary

Mrs. Ursula Seibt

Academic staff

apl. Prof. Dr. Rolf Böttcher (Hochschuldozent)
apl. Prof. Dr. Andreas Pöppl
Prof. Dr. Georg Völkel
Dr. habil. Horst Braeter
Dr. André Pampel
Dr. Venkatesan Umamaheswari
Dr. Marlen Gutjahr
Dr. Samir Mulla Osman

Technicians

Dr. Winfried Böhlmann
Dipl.-Ing. Joachim Hoentsch
Dipl.-Phys. Gert Klotzsche

Physical-technical assistent

Mrs. Ursula Heinich

Ph. D. candidates

Emre Erdem
Özlen F. Erdem
Abdoulaye Taye
Nagarajan Vijayasarathi

Students

Andreas Bunge
Eike Bierwirth

External members

Dima Yaskov
Pavel Sedykh
Maria Popova
(PhD Students from St. Petersburg State University)

2.2.4 Semiconductor Physics, Halbleiterphysik

Prof. Dr. Marius Grundmann

Secretary

Mrs. Gabriele Adami-Kirschey

Technical staff

Dipl.-Phys. Gabriele Benndorf
Ing. Gisela Biehne
Dipl. Ing. Holger Hochmuth
Dipl.-Phys. Jörg Lenzner
PTA Gabriele Ramm
PTA Roswitha Riedel

Academic staff

Dr. Michael Lorenz
Priv.-Doz. Dr. Rainer Pickenhain
apl. Prof. Dr. Bernd Rheinländer
Dr. Heidemarie Schmidt

PhD candidates

Dipl.-Phys. Jens Bauer
Dipl.-Phys. Daniel Fritsch
Dipl.-Phys. Karsten Goede
M.Sc. Erick Guzmán Ramirez
Susanne Hardt
Dipl.-Phys. Susanne Heitsch
Dipl.-Phys. Tino Hofmann
Dipl.-Phys. Thomas Nobis
Dipl.-Ing. Stefan Jaensch
Dipl.-Phys. Andreas Rahm
Dipl.-Phys. Rüdiger Schmidt-Grund
Dipl.-Phys. Alexander Weber
Dipl.-Phys. Holger von Wenckstern

Students

Chengnui Bekeny
Anke Carstens
Wolfram Czakai
Wadinga Fomba
Marcus Gonschorek
Claudia Krahmer
Marcus Schillgalies

Swen Weinhold
Gregor Zimmermann

2.2.5 Solid-state Optics and Acoustics, Festkörperoptik und -akustik

Prof. Dr. Wolfgang Grill

Secretary

Mrs. Gabriele Adami-Kirschey

Technical staff

Phys.-Lab. Adelheid Geyer
PTA Hans-Joachim vom Hofe
Dipl.-Phys. Friedrich Jilek
Dipl.-Ing. (FH) Ulrike Teschner

Academic staff

Dr. Stefan Knauth
Dr. Zbigniew Kojro
Dr. Volker Riede
Privatdozent Dr. rer. nat. habil. Mathias Schubert
Privatdozent Dr. rer. nat. habil. Reinhold Wannemacher

PhD candidates

Nurdin Ashkenov, M. Sc.
Dipl.-Phys. Jens Jahny
Carsten Bundesmann (Staatsexamen Physik)
Dipl.-Phys. Oliver Lenkeit
Dipl. Phys. Claas Middendorf
Wilfred Ngwa, M. Sc.
Evgeny Twerdowski, M. Sc.

Students

Albert Kamanyi
Shou Wei Dong

2.2.6 Superconductivity and Magnetism, Supraleitung und Magnetismus

Prof. Dr. Pablo Esquinazi

Technical staff

Mr. Klaus Grünwald
Dipl.-Krist. Annette Setzer
Mrs. Monika Steinhardt

Academic staff

Dr. Alberto Bollero Real
Dr. Kyoo-hyun Han
Dr. Roland Höhne
Dr. Hans-Christoph Semmelhack
Dr. Michael Ziese

PhD candidates

Dipl.-Phys. Heiko Kempa
Dipl.-Phys. Roberto Ocaña

Students

Andreas Glaser
Ulrike Köhler
Uwe Schaufuß
Kristian Schindler
Konstantin Ulrich

2.3 Institute for Theoretical Physics

2.3.1 Office of the Director

Prof. Dr. Klaus Sibold (director)

Secretaries

Gabriele Menge
Gloria Salzer
Lea Voigt

Library

Elfriede Thiele

2.3.2 Quantum Field Theory, Quantenfeldtheorie

Prof. Dr. Gerd Rudolph

Academic staff

Priv.-Doz. Dr. Michael Bordag
Prof. Dr. Bodo Geyer
Dr. Olaf Richter[1]
Prof. Dr. Gerd Rudolph
Dr. Matthias Schmidt
Dr. Dmitri V. Vassilevich

Retired

Prof. em. Armin Uhlmann
Prof. em. Wolfgang Weller

Permanent Guests

Doz. Dr. Peter Alberti
Dr. Bernd Crell
Dr. Christian Fleischhack

PhD candidates

M.Sc. Szymon Charzynski
M.Sc. Igor Drosdow
Dipl.-Phys. Jörg Eilers

[1]Dr. Olaf Richter died on November 16, 2003.

Dipl.-Phys. Stefan Neumeier
M.Sc. Alexei Strelchenko

Students

Elisabeth Fischer
Tobias Fischer
Nicole Große
Alexander Hertsch
Oliver Witzel

2.3.3 Theory of Elementary Particles, Theorie der Elementarteilchen

Prof. Dr. Klaus Sibold

Academic staff

PD Dr. Roland Kirschner
PD Dr. Arwed Schiller
Dr. Yi Liao
Dr. Paul Heslop

PhD Students

Christoph Dehne
Alexander Ivanov
Yong Zhang

Students

Robert Feldmann
Tobias Reichenbach

2.3.4 Theory of Condensed Matter, Festkörpertheorie

Prof. Dr. Dieter Ihle (spokesperson)
Prof. Dr. Ulrich Behn
Prof. Dr. Adolf Kühnel (i.R.)

Academic staff

Privatdozent Dr. Winfried Kolley

PhD candidates

Dipl.-Phys. Markus Brede
Dipl.-Phys. Iren Junger
Dipl.-Phys. Thomas John
Dipl.-Phys. Micaela Krieger-Hauwede

Students

Otto Edgar Martin

2.3.5 Computational Quantum Field Theory, Computerorientierte Quantenfeldtheorie

Prof. Dr. Wolfhard Janke

Academic Staff

Dr. Michael Bachmann
Dr. Elmar Bittner
Dr. Peter Crompton
Dr. habil. Adriaan Schakel
Dr. Martin Weigel

PhD Students

Dipl.-Phys. Andreas Nußbaumer
Dipl.-Phys. Thomas Vogel
M.Sc. Sandro Wenzel

Students

Goetz Kähler
Axel Krinner
Eric Lorenz
Rodrigo Megaides
Reinhard Schiemann
Stefan Schnabel

2.3.6 Molecular Dynamics/Computer Simulations, Molekulardynamik/Computersimulationen

Academic staff

Dr. rer. nat. habil. Horst Vörtler (Sprecher)
PD Dr. rer. nat. habil. Siegfried Fritzsche
Prof. Dr. rer. nat. habil. Reinhold Haberlandt
Dr. rer. nat. Andreas Schüring (seit 8/2003)
Dr. rer. nat. Viatcheslav Kormilets (seit 4/2003)

PhD students

BC Arthorn Loisruangsin

2.3.7 Statistical Physics, Statistische Physik

Prof. Dr. Manfred Salmhofer

Academic staff

Dr. Oliver Lauscher

PhD students

Walter Pedra

Students

Christoph Husemann

3

Institute for Experimental Physics I

3.1 Physics of Anisotropic Fluids

3.1.1 Introduction

The year 2003 was a year of changes. In April Ralf Stannarius left the group to take over a chair for experimental physics at the University of Magdeburg. In September Christine Papadakis started with her professorship at the TU Munich. The members of the old team in Leipzig wish both all the best in their new positions. The research in the classical topics (molecular dynamics as studied by broadband dielectric spectroscopy and time-resolved Fourier Transform-Spectroscopy) developed well. Additionally new activities have emerged. The optical tweezer experiments are in good progress and routinely it is possible now to measure the viscoelastic properties of single chains of DNA. This open new perspectives for instance to study DNA protein interaction in great detail on a single molecule level. Concerning the funding of our research in 2004 we are in a comfortable position: Two major grants were approved one to continue the single molecule experiments with optical tweezers and one within the DFG-Schwerpunkt 1104: Nano- and microfluidics: From the molecular motion to the continuous flow. Two further applications are in preparation. This provides excellent support and strong encouragement for our research.

Friedrich Kremer

3.1.2 New developments in the preparation of nanometric thin films

F. Kremer, A. Serghei

This project aims to develop new methods to prepare nanometric thin layers, which would enable one to investigate the influence of confinement on the molecular dynamics of thin polymeric films. Additionally, the preparation should provide an easy way to adjust the interactions at the interfaces, which will allow us to emphasize their role in the dynamics under confinement. One approach to be followed is to use silica nano-colloids as spacers between two flat conductive electrodes (silicon wafers). This procedure starts with the preparation of an empty condenser with a well-defined separation between the electrodes in a nanometric range. After annealing, the measurement of the capacity (of the empty condenser) provides an additional way to control the thickness. The polymer is filled by capillarity, the filling factor being easily estimated from the capacity measurement of the filled condenser. Our first results using this method are presented in Fig. 1, for polyisoprene bulk (using 50 μm glass fibers) and thin films (450 nm and 50 nm colloids as spacers). As expected, two relaxation processes are observed: the segmental and the normal mode, corresponding to the segmental and the chain end-to-end fluctuations. In agreement with our previous study [1] both relaxation processes are not shifted with decreasing the film thickness down to a thickness of 50 nm. Another approach we want to develop is to use nanostructures as spacers between two silicon wafers. This procedure reduces itself essentially to selective etching of a SiO layer (deposited by evaporation on a silicon wafer), which enables the formation of a nanometric pattern (array of steps) with a well-defined height.

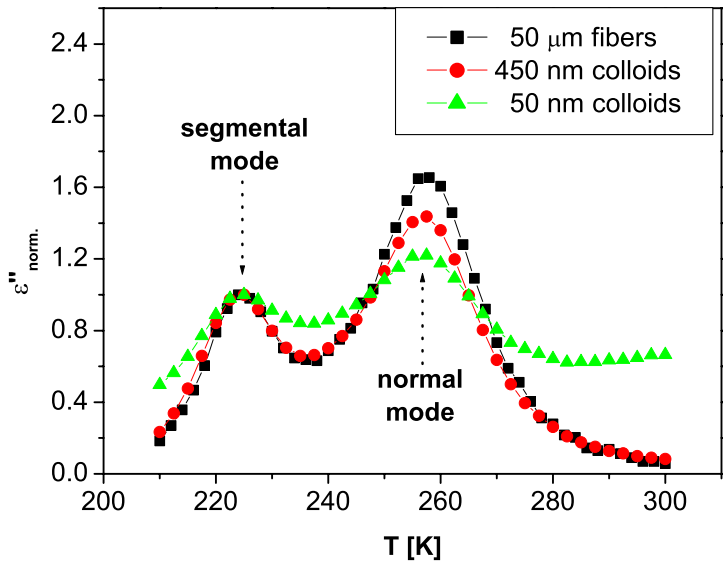

Fig. 1: The temperature dependence of the normalized dielectric loss at 770 Hz for polyisoprene (Mw=5000) bulk and thin films, as indicated.

[1] A. Serghei, F. Kremer, Phys. Rev. Lett. 91, 165702 (2003).

* *The underlined author is the principal investigator of the project.*

3.1.3 Fluctuation of terminal subchains in thin films of polyisoprene

F. Kremer, A. Serghei

A novel relaxation process (confinement-induced mode) was detected in thin cis-1,4-polyisoprene films (Fig. 1a) investigated by Broadband Dielectric Spectroscopy. Additionally to the segmental and the normal mode, originating from the segmental and chain end-to-end fluctuations, the confinement-inducted mode shows up when the film thickness becomes comparable with the chain extension, arising from the fluctuations of the terminal subchains formed by the immobilization of the chain segments at the interface (Fig. 1b). This molecular model explains most of the features observed in the experiment, being also in a full-qualitative agreement with the results revealed by the simulations of the chains as ideal random walks: a) the confinement-induced mode becomes faster with decreasing film thickness (experiment) because the terminal subchains become in average shorter (simulation); b) its relaxation strength increases with increasing confinement on the expense of that of the normal mode (exp.) because the relative number of the immobilized chains increases with decreasing film thickness, while the relative number of the free (non-immobilized) chains decreases (sim.); c) the confinement-induced mode shows no molecular weight dependence (exp.) because with increasing the length of the chain increases also its probability to come in contact with the immobilizing interface (sim.); d) the relaxation rate of normal mode is not affected by the confinement down to thicknesses comparable with the chain extension (exp.) because even for such small films a certain fraction of free (non-immobilized) chains still exists (sim.), which exhibits a bulk-like dynamics; e) the segmental mode is not affected by the confinement because it takes place on a length scale much smaller than the film thickness.

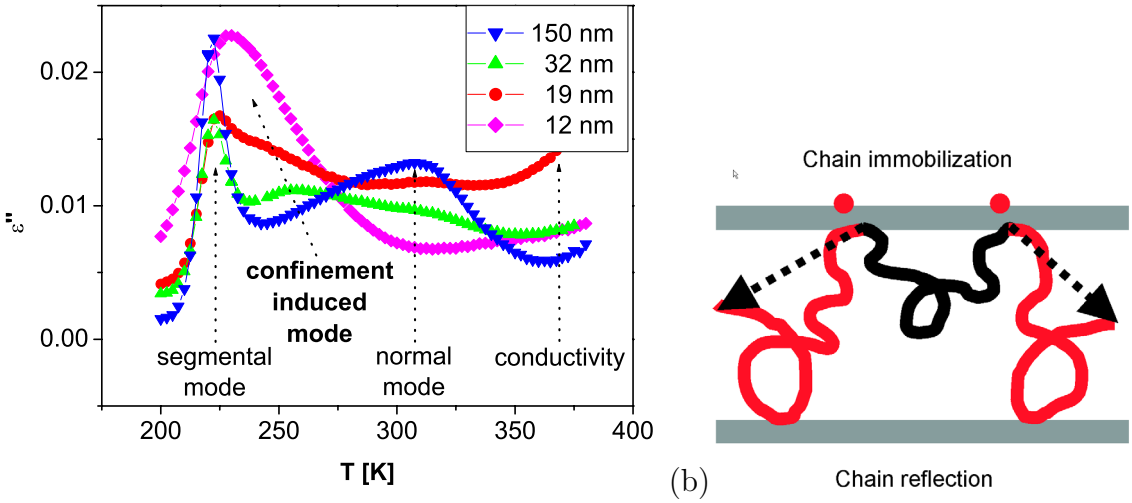

(a) (b)

Fig. 1: (a) Dielectric loss versus temperature for different thicknesses. (b) Terminal subchains formed by immobilization of chain segments at an interface.

[1] A. Serghei, F. Kremer, Phys. Rev. Lett. 91, 165702 (2003).
[2] A. Serghei, F. Kremer, W. Kob, EJP E 12, 143 (2003)

Collaborators: W. Kob (Université Montpellier, France)

3.1.4 Glass transition and molecular dynamics in grafted and spin-coated PDMS layers

F. Kremer, L. Hartmann

Thin polymer films are an ideal system to study the influence of finite size effects on the polymer dynamics [1-3]. We focus on measurements of dipole fluctuations by Broadband Dielectric Spectroscopy to reveal deviations from the bulk behaviour when reducing the film thickness. In case of poly(dimethyl siloxane) (PDMS) we have studied the influence of different preparation techniques (thin grafted and spin cast films [3]) on the molecular dynamics of this particular polymer besides that of mere variation of the film thickness [2]. In thin films of grafted PDMS of thickness d above and below the radius of gyration R_g we find bulk-like behavior for $d = 41\,\mathrm{nm} > R_g$ whereas for $d < R_g$ the dynamic glass transition (α-relaxation) is by up to two orders of magnitude faster than in the bulk (Fig. 1). The latter finding is explained by an altered chain conformation compared to the bulk which presumably leads to an increased free volume as a consequence of the grafting procedure. The α-relaxation in spin cast films compares well with that of the bulk with respect to the thermal activation down to a film thickness d of 14 nm. However, in these films an additional relaxation shows up which is faster than any relaxation in the bulk. To explain this, we assume that in spin cast films only a part of the chains (close to the upper film surface) experiences an altered chain conformation leading to this faster relaxation. This interpretation is supported by the values obtained for the dielectric strength $\Delta\epsilon$. In all films the ac-relaxation related to fluctuations in the amorphous fraction of PDMS above crystallization has been observed showing no particular dependence of the

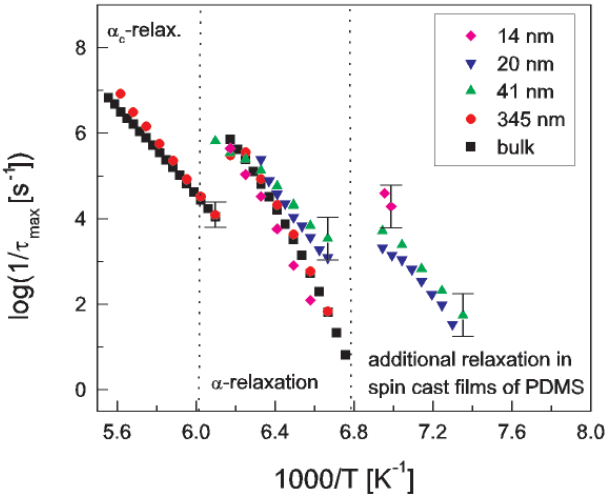

Fig. 1: Activation plot for PDMS of a molecular weight of 1.4×10^5 g/mol in the bulk (black symbols) and as spin cast films (full colored symbols).

[1] L. Hartmann, K. Fukao, F. Kremer, Chapter in book: "Broadband Dielectric Spectroscopy", p. 433, (Springer Verlag, Berlin, (2002), F. Kremer, A. Schönhals (Eds.)
[2] L. Hartmann, F. Kremer, P. Pouret, L. Léger, J. Chem. Phys. 118, 6052 (2003).
[3] F. Kremer, L. Hartmann, A. Serghei, P. Pouret, L. Léger, Eur. Phys. J. E. 12, 139 (2003).

Collaborators: Prof. Dr. L. Léger (Collège de France, Paris, France)

3.1.5 Molecular dynamics in alternating maleimide copolymers as studied by Broadband Dielectric Spectroscopy

F.Kremer, J.Tsuwi

Structural segments consisting of alkyl and perfluoroalkyl groups covalently linked by a C-C bond are well known for their microphase separation resulting in highly ordered bulk structures. The use of such materials for surface modification is numerous because of the resulting low surface free energy. We are employing Broadband Dielectric Spectroscopy to study the molecular dynamics in a set of poly (alkene-*alt*-*N*-(perfluoro-)alkylmaleimide) copolymers with two types of side chains: alkyl or perfluoroalkyl. Generally, four relaxation regions are observed for copolymers with alkyl side chains (Fig. 1a), while three processes are observed for the perfluorinated copolymer systems (Fig. 1b).

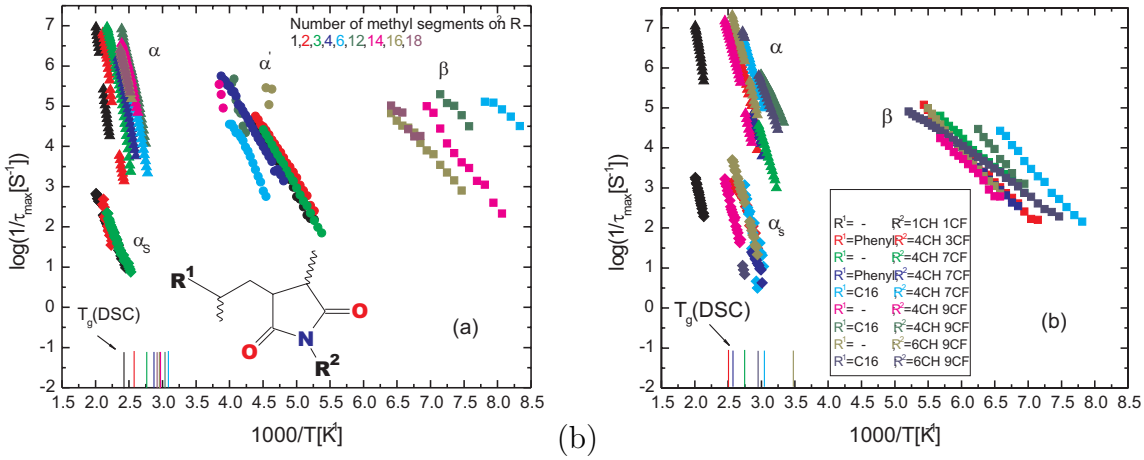

(a) (b)

Fig. 1: (a) Activation plot showing four relaxation processes (β, α', α, α_s) for unfluorinated copolymer systems and inset: maleimide unit with two side chains R^1 and R^2. (b) Activation plot with three processes for perfluorinated copolymers.

The low temperature β-process is assigned to libration motion of CH_3 at the end of alkyl side chain, described by Arrhenius-type temperature dependence. The α'-process is assigned to an out-of-plane motion of the succinimide ring while the a-process is assigned to an in-plane fluctuation of one maleimide ring. The slowest as-process is assigned to fluctuations of 2-3 maleimide rings that constitute the helical superstructure of the copolymers. In contrast, the perfluorinated polymer systems show three relaxation regions only. The faster process at low temperatures is assigned to the librational motion of the CF_3 end group while the other two processes are the α- and α_s- processes assigned as earlier.

[1] Song, K.,Twieg., J.R., Rabolt, J.F., Macromolecules 23,3712 (1990).
[2] Bailey, J., Walker, S.M., Polymer 13, 561 (1972).
[3] Block H., Lord, P.W., Walker, S.M., Polymer 16, 739 (1975).
[4] Cubbon R.C.P, Journal of Polymer Science: Part C 16, 387-392 (1967). [5] Baltá-Calleja, F.J., Ramos J.G., Barrales-Rienda, J.M., Kolloid-Z. und Z. Polymere 250, 474-481 (1972).
[6] Tsuwi, J., Appelhans, D., Kremer, F., to be submitted to Macromolecules

Collaborators: D. Appelhans (IPF Dresden, Germany)

3.1.6 Dielectric relaxation of inverse miniemulsions

F.Kremer, J.Tsuwi

Miniemulsions are specifically formulated heterophase systems where stable nanodroplets of one phase are dispersed in a second continuous phase. These nanodroplets are envisaged to act as nanoreactors of polymer reactions resulting in polymer dispersions when appropriate reaction initiators are introduced. We focus on dielectric measurements of miniemulsions in the microwave frequencies to study nanodroplet stability.

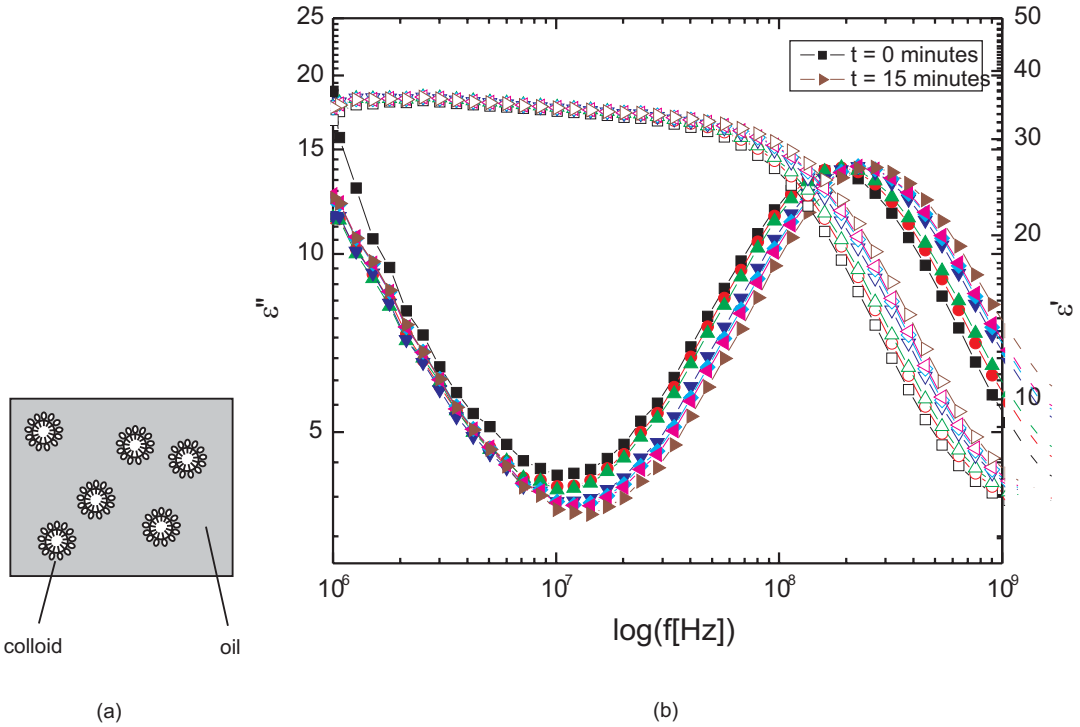

Fig. 1: (a) Miniemulsion composed of nanodroplets (colloids) dispersed in a continuous medium of oil. (b) Real part (ϵ', closed symbols) and imaginary part (ϵ", open symbols) of dielectric function versus frequency for time-dependence measurement of miniemulsion with 0.5% surfactant concentration.

The dielectric spectra of miniemulsions are analyzed by considering the relaxation behaviour of both the surfactant and the solvent that form the nanodroplets. In the analysis, the emulsions are modeled in the context of Effective Medium Theory to quantitatively determine the dielectric energy storage and loss behaviour.

[1] Antonietti M.,Landfester K., Prog. Polym.Sci. 27, 689 -757(2002).
[2] Baar, C., Buchner, R., Kunz, W., J. physical chem. B 105, 2906-2913 (2001).
[3] Baar, C., Buchner, R., Kunz, W., J. physical chem. B 105, 2914-2922 (2001).
[4] Buchner, R., Barthel, J., Annu. Rep. Prog. Chem. C 97, 349-382 (2001).

Collaborators: M. Antonietti (Max Planck Institute of Colloids and Interfaces, Golm, Germany)

3.1.7 Fourier Transform Infrared Spectroscopy on ferroelectric liquid crystal polymers

F. Kremer, M. Tammer

Time-resolved polarised Fourier Transform Infrared (FTIR) Spectroscopy is employed to analyse the structure and dynamics in ferroelectric liquid crystal (FLC) polymers and elastomers. The specifity of the IR-spectroscopy enables us to study for the different molecular moieties the response to external mechanical end electrical excitations. By that, subtle details of the microscopic motion such as angular excursion, reorientation time, order parameter, asymmetries in the reorientational behaviour or elastomeric memory effects can be unravelled for the system under study.

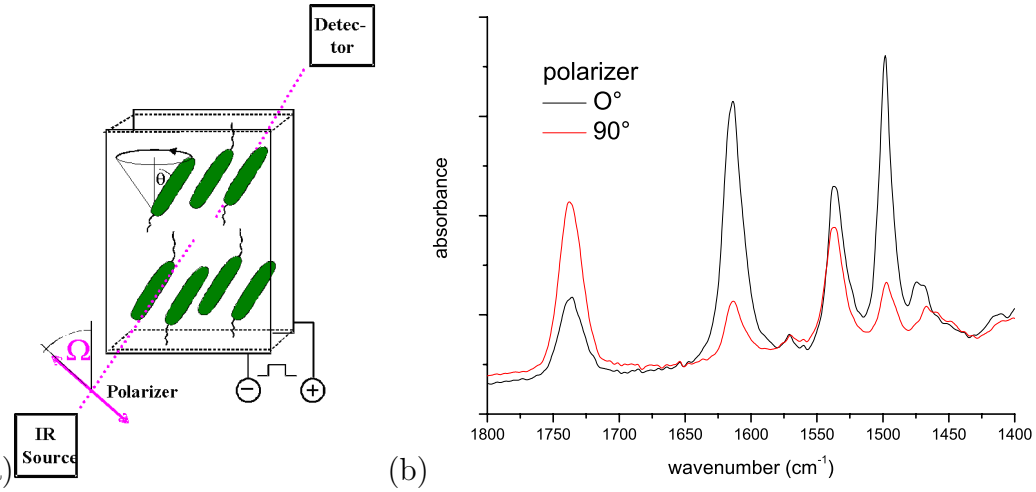

Fig. 1: (a) Setup of the polarized IR Spectroscopy. The liquid crystal is studied in bookshelf geometry: the layer normal of the smectic phase is perpendicular to the surface normal of the cell windows and the IR beam. (b) polarization dependent spectrum

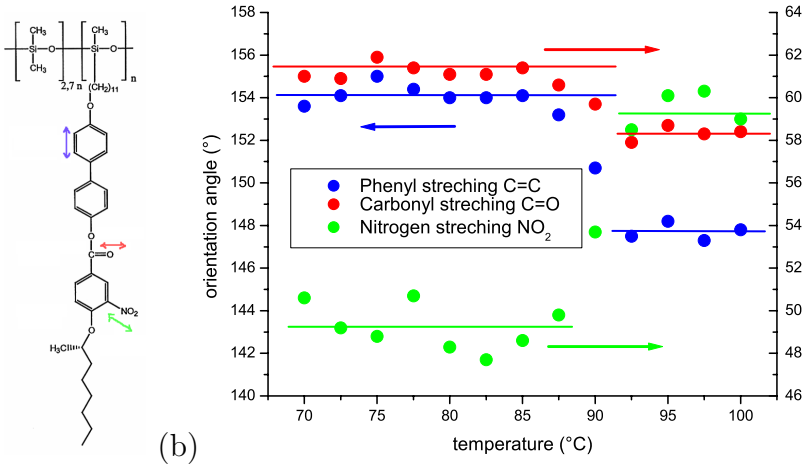

Fig. 2: (a) FLC polymer studied by FTIR. (b) Orientation angle for three different molecular groups of the FLC polymer in dependence of temperature. The change in orientation at the phase transition from SmC* to SmA is studied from these data.

Collaborators: R. Zentel (University of Mainz, Germany), H. Finkelmann (University of Regensburg, Germany)

3.1.8 Optical tweezers as a tool to unfold RNA-aptamers

F. Kremer, M. Salomo, M. Struhalla, J. Reinmuth, W. Skokow

Optical tweezers are commonly used to manipulate microscopic particles, with applications in cell manipulation, colloid research, manipulation of micromachines and studies of the properties of light beams. With their extraordinary resolution in space ($\sim 2\,\mathrm{nm}$) and force ($\sim 1\,\mathrm{pN}$) they became an irreplaceable tool for such purposes.

In our projects we want to use them to study folding and unfolding mechanisms of nucleic acid structures. One project deals with the unfolding of RNA-aptamers. We want to immobilize a single aptamer molecule between two polystyrene particles. One of them is fixed with a femtotip. The other one is hold in the beam by the optical tweezers. To realize the necessary distance between the two colloids the aptamer-RNA was elongated by 500 bases on both ends. The immobilization between the two particles is then realized by DNA/RNA-hybrids (Fig. 1). With the use of this experimental set-up it is possible to apply forces in the range of piconewtons on the folded RNA-sequence. The aim of these experiments is to investigate the behaviour of two aptamers that have specific binding partners, an aptamer that binds to the antibiotic Moenomycin A and a second one that has thrombin as binding partner. We want to investigate the differences in their folding behaviour in absence and presence of their binding partners. So far we have synthesised all necessary components for the pulling experiment (ssDNA handles, RNA aptamers) and are now about to assemble and measure the system.

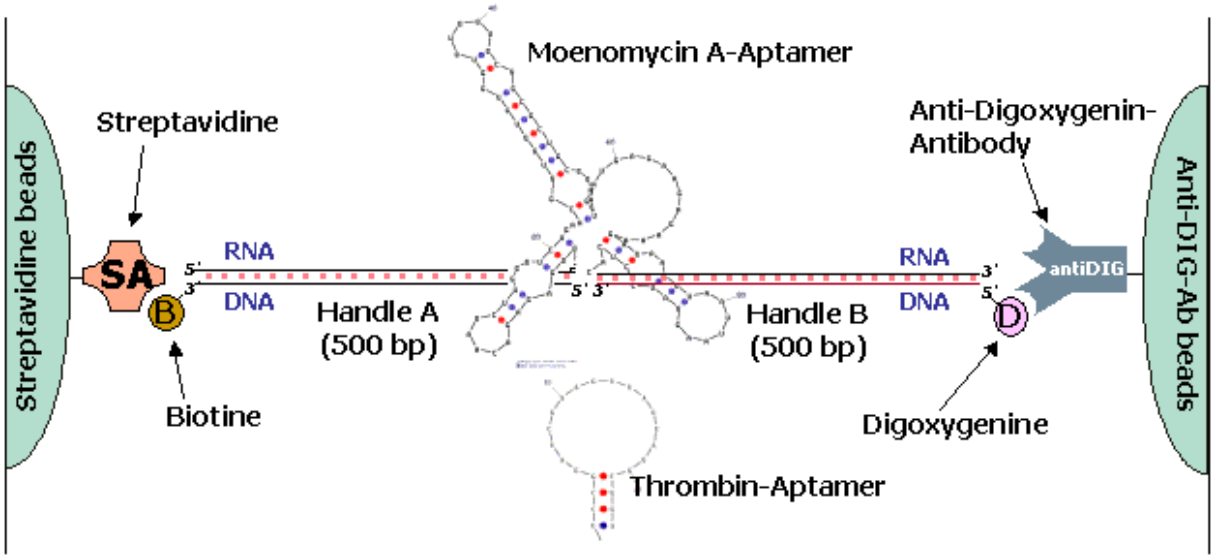

Fig. 1: Schematic representation of the molecule arrangement between the two beads.

[1] J. Liphardt et al., Science 292, 733-737 (2001).

Collaborators: Prof. Dr. U. Hahn (University of Hamburg, Germany), Prof. Dr. A. Beck-Sickinger (University of Leipzig, Germany)

3.1.9 Investigating DNA-binding proteins with optical tweezers

F. Kremer, M. Salomo, M. Struhalla, J. Reinmuth, W. Skokow

Sac7d belongs to a class of small chromosomal proteins identified in the hyperthermophilic archaeon Sulfolobus acidocaldarius. It is extremely stable to heat, acid and chemical agents and binds strongly to the minor groove of DNA, causing a sharp kinking of the DNA helix leading to a shortening of the DNA (Fig. 1a). Our project has the aim to investigate the influence of this DNA-binding protein on a DNA-double helix immobilized between two particles. We want to use the optical tweezers to measure the dimension of shortening. The protein should bind to the DNA every 3 bp leading to a theoretical compaction ratio of ∼1.2. The first aim of our project was to overproduce the sac7d protein. For this purpose we used an E. coli based expression system. The protein purification was done via affinity chromatography. The combination of these two methods enabled us to isolate the protein in sufficient amount with a very high purity. The second step was to establish a suitable experimental setup to measure the shortening of DNA after Sac7d has bound. For that we immobilized a DNA-double helix between two polystyrene particles and we were able to establish a system as shown in Fig. 1b. One particle is fixed by a glass micropipette, the other one is hold in the optical tweezers. Via Streptavidin/Biotin- and Digoxigenin/Anti-Digoxigenin interactions we were able to immobilize a single DNA-molecule between this particles. We immobilized DNA with different lengths (1000 bp - 4000 bp) between the two particles and recorded force extension curves as shown in Fig. 1c.

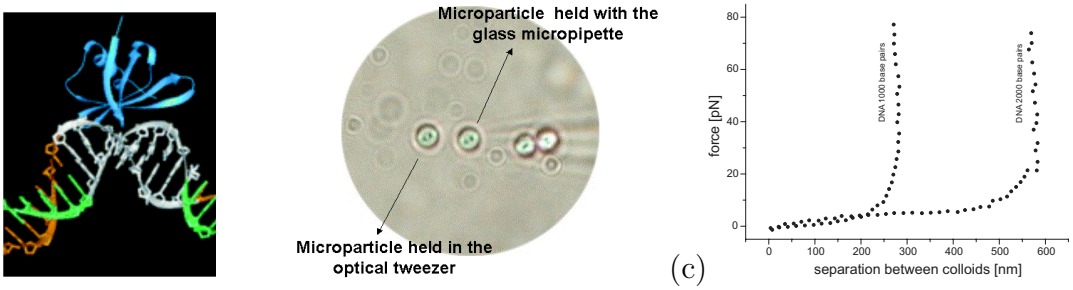

Fig. 1: (a) Model of the binding mechanism of the Sac7d protein (blue) to a DNA helix. (b) Two beads (Ø=2.2 μm) of which one is hold by a femtotip while the other fluctuates in the photonic potential. (c) Force-extension curves for 1000 base pairs (bp) and 2000 bp dsDNA.

[1] H. Robinson et al.; Nature 392, 202-205 (1998).
[2] J.G. McAfee et al.; Bioch. 34, 10063-10077 (1995).
[3] D. Kulms et al.; Biol. Chem. 378, 545-551 (1997).

3.1.10 Nano- and microfluidics using optical tweezers with fast single particle tracking

F. Kremer, K. Kegler

Optical tweezers with fast single particle tracking are microscopic ($\sim$ 1 μm) rheometric tools with nanometer resolution in space and subpico-newton resolution in force. The proposed project has two intentions (i) to contribute to basic questions in colloid- and polymer-research and (ii) to address technological problems of micro- and nanofluidics.In detail the following experiments are planned: 1.) Measurements of the force-distance-dependence between two isolated single colloids of which one is hold by a micropipette (Ø$\sim$ 0.4 μm) and the other by an optical tweezer.

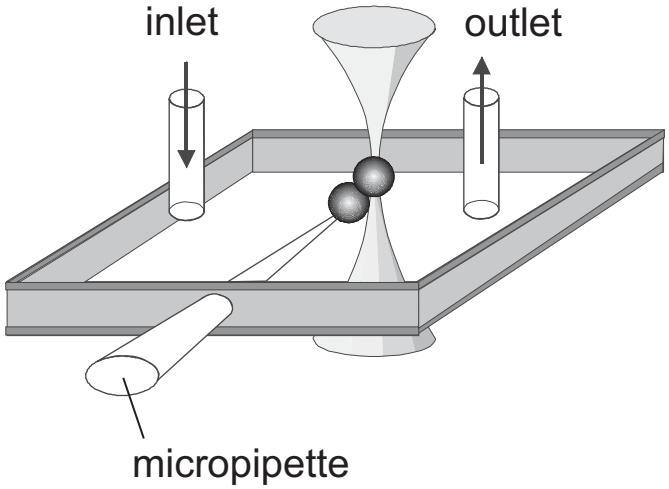

Fig. 1: Scheme of the sample cell to measure forces between two separated colloids.

The separation between the colloids can be varied in nanometer steps. 2.) Measurement of the force-distance-dependence between a *single* colloid and a wall in the steady state and in fluid flow for coated and uncoated surfaces. 3.) Measurement of depletion forces between *single* colloids in the steady state and in flow for polymer solutions of varying concentration and for polymers of different topology. 4.) A fluctuation analysis of the Brownian motion of a colloid in an optical trap enables one to deduce the local tensor of viscosity. By that inhomogeneous microscopic structures like microchannels or living biological systems can be explored. 5.) Measurement of the flow profile of homogeneous and heterogeneous liquids in small ($\sim$ μm) confining geometries like plates with micrometer separation, microchannels, etc. with - and without surface modifications (e.g. hydrophobization).

This project will be part of the DFG-Schwerpunktprogramm "Nano- und Mikrofluide: Von der molekularen Bewegung zur kontinuierlichen Strömung".

3.1.11 Time-resolved in-situ GISAXS measurements of thin films of lamellar diblock copolymers

Ch. M. Papadakis, P. Busch

High molar mass polystyrene-polybutadiene (PS-PB) diblock copolymer thin films have been found to spontaneously form patterned surfaces related to a perpendicular orientation of the lamellae [1,2]. Non-equilibrium structures are notorious in such systems because of the low mobility of the polymers in thin film geometry. Exposure to solvent vapor is therefore frequently used in order to drive the films towards equilibrium. The mechanisms for reorientation have not been elucidated yet, though. By means of Grazing-Incidence Small-Angle X-ray Scattering (GISAXS) the mesoscopic structures within the films can be studied [2]. At low incident angles of the X-ray beam (slightly above the critical angle of total external reflection), a substantial portion of the incident and scattered radiation is reflected by the substrate, resulting in high recorded intensity and low measuring times (a few seconds), which enables time-resolved studies. The intensity due to the substrate reflection can be understood in terms of the distorted-wave Born approximation. Our in-situ studies of a high molar mass PS-PB film during treatment with toluene vapor show that the lamellar orientation changes within minutes but the perpendicular orientation is regained after the solvent is removed (Fig. 1, Ref. 3).

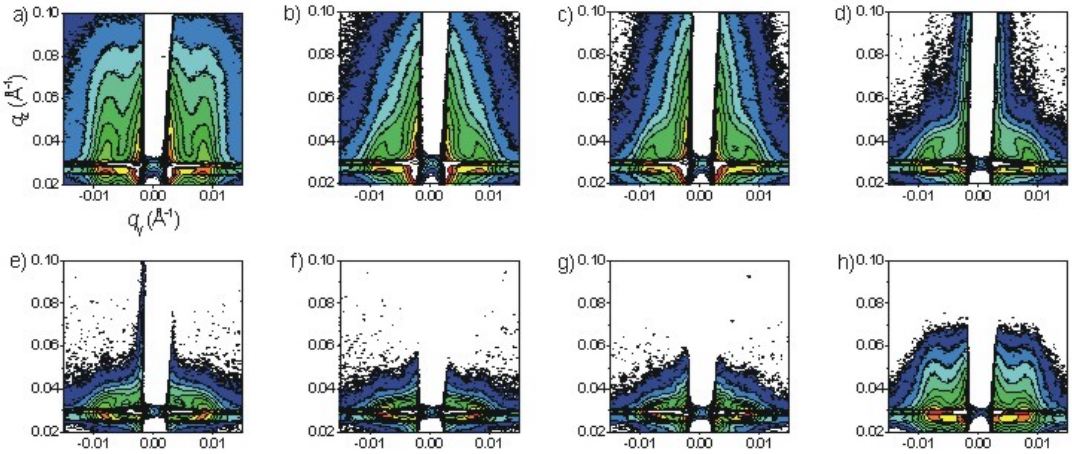

Fig. 1: 2D GISAXS maps of a high molar mass film (183 kg/mol, lamellar thickness 836 Å). (a) In the dry state. (b) 1 min, (c) 2 min, (d) 4 min, (e) 8 min, (f) 17 min, and (g) 33 min after the injection of toluene into the sample chamber. (h) 5 min after removal of toluene. Incident angle = 0.21°. The straight Bragg rods in (a) indicate the presence of perpendicular lamellae, the bending in (b-g) indicates reorientation of the lamellae.

[1] P. Busch, D. Posselt, D.-M. Smilgies, B. Rheinländer, F. Kremer, C.M. Papadakis, Macromolecules 36, 8717 (2003).
[2] P. Busch, D.-M. Smilgies, D. Posselt, F. Kremer, C.M.Papadakis, Macromol. Chem. Phys. 204, F18 (2003), invited contribution.
[3] D.-M. Smilgies, P. Busch, D. Posselt, C.M. Papadakis, Synchr. Rad. News 15, 35 (2002), invited contribution.

Collaborators: Prof. Dr. B. Rheinländer (University of Leipzig), Prof. Dr. D. Posselt (Roskilde University, Denmark), Dr. D. Smilgies (Cornell University, Ithaca, NY, U.S.A)

3.1.12 A model of the GISAXS intensity of thin films of lamellar diblock copolymers in the framework of the DWBA

Ch. M. Papadakis, P. Busch

Block copolymer thin films offer an opportunity for patterning of surfaces on the submicrometer scale. By combining atomic force microscopy with Grazing-Incidence Small-Angle X-ray Scattering (GISAXS), we have investigated the lamellar orientation in thin films of symmetric, lamellae-forming polystyrene-polybutadiene (PS-PB) diblock copolymers [1,2]. GISAXS measurements were performed in dependence of the incident angle α_i. Fig. 1a shows a two-dimensional GISAXS map of a film with lamellae oriented parallel to the substrate surface. Distinct peaks are visible in the vicinity of the beam stop as marked by the arrow. The dependence of the q_z-positions of these peaks on ai cannot be understood in the context of the Born approximation (BA), where only single scattering is considered. We have modeled the scattering within the distorted wave Born approximation (DWBA) which additionally takes into account the refraction of the X-rays by the film surface and the reflection by the substrate. The peak positions expected from this model are in excellent agreement with the experimental data (Fig. 1b).

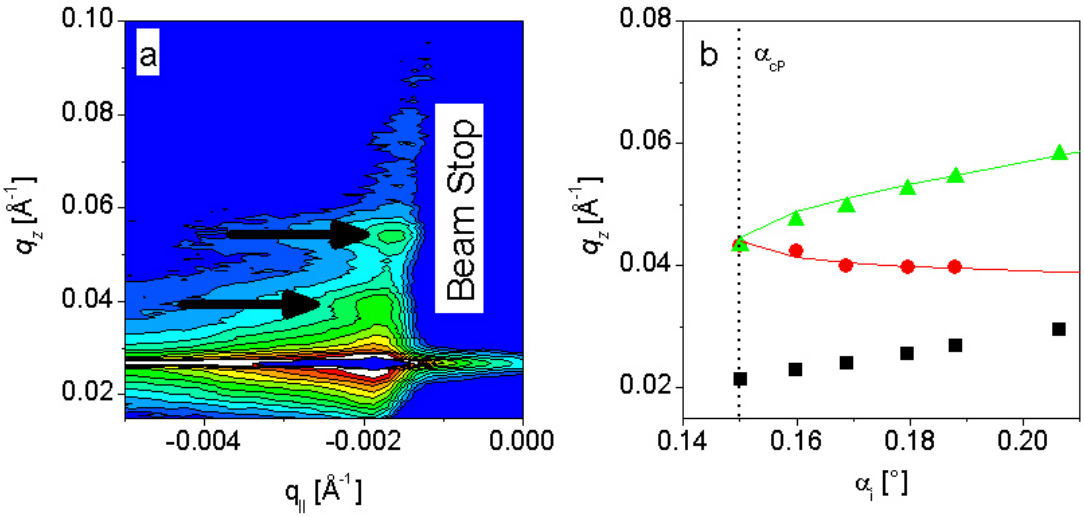

Fig. 1: (a, left) 2D GISAXS map of a thin film of PS-PB having a molar mass of 22.6 kg/mol, a lamellar thickness of 197 ±4 Å and a film thickness of 1750 ±30 Å at α_i = 0.19°. (b, right) Experimental q_z-positions of the specularly reflected beam (squares) and the non-specular peaks in dependence of the incident angle ai (triangles, circles). The solid lines are the positions expected from DWBA theory. The dotted line denotes the critical angle of the polymer film.

[1] P. Busch, D. Posselt, D.-M. Smilgies, B. Rheinländer, F. Kremer and C.M. Papadakis, Macromolecules 36, 8717 (2003).
[2] D.-M. Smilgies, P. Busch, D. Posselt and C.M. Papadakis, Synchr. Rad. News 15, 35 (2002).

Collaborators: Prof. Dr. Bernd Rheinländer (University of Leipzig, Germany), Prof. Dr. Dorthe Posselt (Roskilde University, Denmark), Dr. Detlef Smilgies (Cornell University, Ithaca, NY, U.S.A), Dr. Markus Rauscher (MPI für Metallforschung, Stuttgart, Germany).

3.1.13 Aggregation behavior of amphiphilic diblock copolymers studied using fluorescence correlation spectroscopy and dynamic light scattering

Ch. M. Papadakis, T. B. Bonné

In aqueous solution, amphiphilic block copolymers have been found to spontaneously aggregate into micellar solutions and lyotropic phases reminiscent of the structures encountered in low molar mass surfactants and lipids [1]. The aim of our study is to elucidate the diffusion mechanisms in such systems. Poly(oxazolin) based polymers constitute a very versatile model system. They have the advantage that their architecture (homopolymers, diblock and triblock copolymers) as well as the degree of hydrophobicity of the blocks can readily be varied, and they can be fluorescence labeled. We have used Fluorescence Correlation Spectroscopy (FCS) in order to study the self-diffusion of fluorescence-labeled poly(methyloxazolin)-poly(nonyloxazolin) diblock copolymers in aqueous solution. The fluorescence-labeled polymers were used as tracers in aqueous solutions of otherwise identical, non-labeled polymers. In this way, a large concentration range could be accessed without oversaturating the FCS detector. By identifying the diffusion coefficients of the unimers and the micelles, the critical micelle concentration was identified (Fig. 1). Additional temperature-resolved Dynamic Light Scattering (DLS) experiments showed that dissolution at room temperature results in a metastable state containing very large aggregates. Only after heating to ∼90°C, the micelles assume their equilibrium size of ∼12 nm. Comparison of the hydrodynamic radii obtained using DLS with those from FCS on annealed samples showed that the hydrodynamic radius of the micelles can reliably be determined using FCS (Fig. 1). In the future, we wish to extend our dynamic studies to triblock copolymers as well as to lipopolymers.

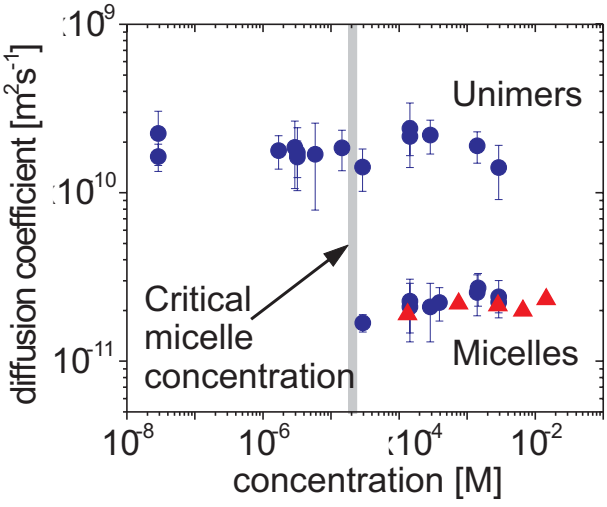

Fig. 1: Concentration dependence of the diffusion coefficients of aqueous solutions of a low molar mass poly(methyloxazoline)-poly-(nonyloxazoline) (PMox-PNox) diblock copolymer (molar mass 4796 g/mol, weight fraction of PMox 56%) with the fluorescence label TRITC attached to the end of the PMox block. The solutions were annealed prior to measurement. Blue symbols: results from FCS, red symbols: results from DLS.

[1] P. Alexandridis, B. Lindman (Eds.), Amphiphilic Block Copolymers: Self-Assembly

and Applications, Elsevier (2000).

Collaborators: Prof. Dr. U. Hahn, Dr. T. Greiner-Stöffele (Fakultät für Biowissenschaften, Pharmazie und Psychologie, Universität Leipzig, Germany), Dr. R. Jordan, DC K. Lüdtke (Fakultät für Chemie, TU München, Germany), Dr. P. Štepánek (Inst. of Macromolecular Chemistry, Prague, Czech Rep.).

3.1.14 Isotropic droplets in freely suspended smectic films

R. Stannarius, H. Schüring

Besides the well-known layer-by-layer thinning, droplet nucleation, as a phase transition phenomena in freely suspended smectic films, came into the focus of interest over the last years. Isotropic inclusions that form in the vincinity of the bulk smectic-isotropic phase transition are investigated my means of reflection microscopy. From their shapes and dynamics in the film plane, interface tensions between smectogens in different phases can be derived. Basing on the assumption of a surface phase transition from the isotropic phase to a smectic surface interphase, a model has been developed that considers the relevant interface tensions and the surface tension of the smectic phase. The latter can be easily determined by use of the earlier established bubble method. Thus, interphase tensions $< 10^{-3}$ N/m between isotropic and smectic phases can be accessed by an analysis of the droplet shapes. An extension of the model to inhomogeneously thick films explains the spontaneous arrangement of droplets at film thickness steps (Fig. 1) as well as the capillary force driven motion of droplets in the direction of the film thickness gradient.

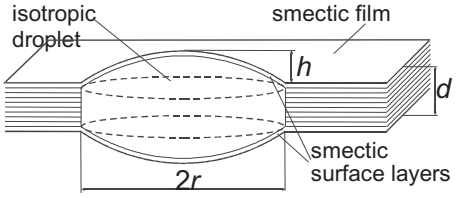

(a)

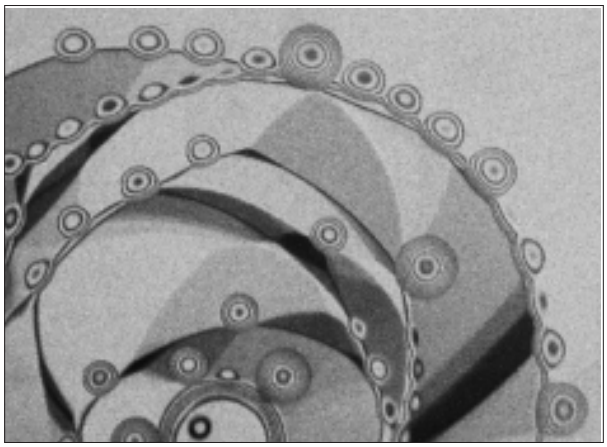

(b)

Fig. 1: (a) Model of an isotropic droplet in a homogeneous smectic film and (b) arrangement of isotropic droplets at film thickness steps, observed by reflection microscopy under monochromatic illumination (λ=630 nm), image size: 260 μm × 190 μm.

[1] H. Schüring, R. Stannarius, Langmuir. 18, 9735 (2002).
[2] H. Schüring, R. Stannarius, Mol. Cryst. Liq. Cryst. (in press).
[3] H. Schüring, PhD thesis, Mechanische und optische Untersuchungen freitragender smektischer Filme, University of Leipzig, 2003.

Collaborators: Prof. Dr. W. Weißflog (MLU Halle, Germany) Prof. Dr. R. Zentel (Universität Mainz, Germany)

3.1.15 Laser diffraction by periodic dynamic patterns in anisotropic fluids

R. Stannarius, T. John, U. Behn

We describe the application of a laser diffraction technique to the study of electroconvection in nematic liquid crystal cells. It allows a real-time quantitative access to pattern wave lengths and amplitudes. The diffraction profile of the spatial periodic pattern is calculated and compared quantitatively to experimental intensity profiles. For small director tilt amplitudes , the phase grating generated in normally incident undeflected light and the first order term correction from light deflection is derived analytically. It yields an dependence of the diffracted intensity I on the amplitude of director deflections. For larger director tilt amplitudes, phase and amplitude modulations of deflection of light in the inhomogeneous director field are calculated numerically. We apply the calculations to the determination of the director deflection and measure growth and decay rates of the dissipative patterns under periodic excitation. Real time analysis of pattern amplitudes under stochastic excitation is demonstrated.

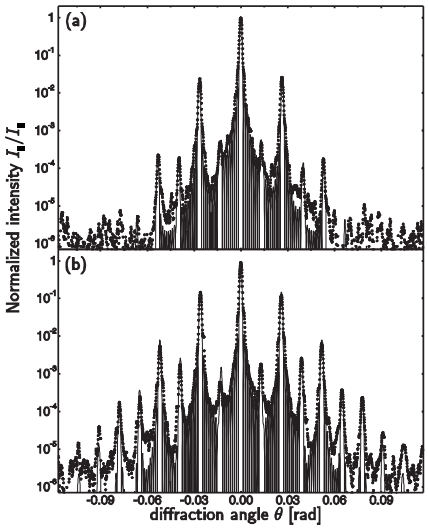

Fig. 1: It is shown the comparison of numerical calculated diffraction profiles (solid line) and measured intensities (dots), normalized to the primary beam intensity. The measured profile at excitation voltage $U = 28.79\,\mathrm{V}$ (a) and $U = 28.90\,\mathrm{V}$ (b) corresponds to the calculation with amplitudes $\phi = 7.4°$ (a) and $\phi = 12.6°$ (b). The pattern wave length $\lambda = 48\mu\mathrm{m}$, cell thickness $48.5\,\mu\mathrm{m}$, critical voltage for onset of electroconvection $U_c = 28.73\,\mathrm{V}$.

[1] H. Amm, U. Behn, T. John, R. Stannarius, Mol. Cryst. Liq. Cryst. 304, 525 (1997).
[2] T. John, R. Stannarius, and U. Behn. Phys. Rev. Lett. 83 749, (1999).
[3] U. Behn, T. John, R. Stannarius, AIP Conf. Proc, 622 381 (2002).
[4] T. John, U. Behn, R. Stannarius, Phys. Rev. E 65 046229 (2002).
[5] T. John, U. Behn, R. Stannarius, Europhys. J. B 35, 267-278 (2003).

Collaboration: Prof. Dr. U. Behn (ITP Leipzig, Germany), Dr. T. Scharf (Neuchatel, Germany)

3.1.16 Funding

Prof. Dr. F. Kremer
Optische Pinzette als mikroskopische Sensoren und Aktuatoren zum Studium der Wechselwirkung zwischen einzelnen Biomolekülen
SMWK-Projekt 7531.50-02-0361-01/11 (2001-2003)

Dr. Ch. M. Papadakis
Strukturbildung in dünnen Filmen aus symmetrischen Diblockcopolymeren
DFG-Projekt, PA 771/1-1 (2001-2003)

Dr. Ch. M. Papadakis
Dynamics of supramolecular aggregates of amphiphilic polymers studied by fluorescence correlation spectroscopy
DFG-Projekt, PA 771/2-1, (2003-2005)

Dr. Ch. M. Papadakis, Dr. I.I. Potemkin (Moscow State University)
Structure formation in thin diblock copolymer films
NATO Collaborative Linkage Grant (2001-2004)

Prof. Dr. U. Behn, Dr. R. Stannarius
Stabilität und statistische Charakterisierung von EHC in Nematen unter stochastischer Anregung
DFG-Projekt, Be 1417/4 (1999-2003)

Dr. R. Stannarius
Flüssige Filamente
DFG-Projekt, Sta 425/14 (2002-2004)

Dr. R. Stannarius
Mechanische Eigenschaften smektischer Elastomere
DFG-Projekt, Sta 425/15 (2002-2005)

3.1.17 Publications

[1] Serghei, A.; F. Kremer
"A novel confinement-induced relaxation process in thin films of cis-polyisoprene"
Phys. Rev. Lett. 91, 165702-1-165702-4 (2003)

[2] Hartmann, L.; F. Kremer, P. Pouret, L. Léger
"Molecular dynamics in grafted layers of poly(dimethylsiloxane) (PDMS)"
J. of Chem.Phys. 118, 6052 (2003)

[3] Doxastakis, M.; D.N. Theodorou, G. Fytas, F. Kremer, R. Faller, F. Müller-Plathe, N. Hadjichristidis
"Chain and local dynamics of polyisoprene as probed by experiments and computer simulations"

J. Chem. Phys. 119, 6883-6894 (2003)

[4] Serghei, A.; F. Kremer, W. Kob
"Chain conformation in thin polymer layers as revealed by simulations of ideal random walks"
EJP E 12, No. 1, 143-146 (2003)

[5] Kremer, F.; L. Hartmann, A. Serghei, P. Pouret, L. Léger
"Molecular dynamics in thin grafted and deposited polymer layers"
Eur. Phys. J. E 12, 139 (2003)

[6] Kremer, F.; A. Huwe, A. Gräser, St. Spange and P. Behrens
"Molecular dynamics in confined space"
Book chapter to "Host-Guest Systems Based on Nanoporous Crystals" Eds. F. Laeri, F. Schüth, U. Simon, M. Wark. Wiley VCH 2003, pp. 379-392

[7] Stannarius, R.; J. Li and W. Weissflog
"A ferroelectric smectic phase formed by achiral straight core mesogens"
Phys. Rev. Lett. 90, 025502 (2003)

[8] Li, J.; R. Stannarius, C. Tolksdorf, R. Zentel
"Hydrogen Bonded Ferroelectric Liquid Crystal Gels in Freely Suspended Film Geometry"
Phys. Chem. Chem. Phys. 5, 916-923 (2003)

[9] John, T.; U. Behn and R. Stannarius
"Laser diffraction by periodic dynamic patterns in anisotropic fluids"
Europhys. J. B 35, 267-278 (2003)

[10] Das, B.; S. Grande, W. Weissflog, A. Eremin, M. W. Schröder, G. Pelzl, S. Diele, and H. Kresse
"Structural and conformational investigations in SmA and different SmC phases of new hockey stick-shaped compounds"
Liquid Crystals 30, 529-539 (2003)

[11] Busch, P.; D. Posselt, D.-M. Smilgies, F. Kremer and C. M. Papadakis
"Diblock copolymer thin films investigated by tapping mode AFM: Molar mass dependence of surface ordering"
Macromolecules 36, 8717-8727 (2003)

[12] Busch, P.; D.-M. Smilgies, D. Posselt, F. Kremer, C. M. Papadakis
"Grazing-incidence small-angle X-ray scattering (GISAXS) - Inner structure and kinetics of thin block copolymer films"
Proceedings of the Makromolekulares Kolloquium Freiburg, Feb. 2003, Macromolecular Chemistry and Physics 204, F18 (2003) (invited contribution)

[13] Das, B.; S. Grande, W. Weissflog, A. Eremin, M.W. Schröder, G. Pelzl, S. Diele,

H. Kresse
"Structural and conformational investigations in SmA and different SmC phases of new hockey-stick shaped compounds"
Liq. Cryst. 30, 529-539 (2003)

in press

Köhler, R.; R. Stannarius, Ch. Tolksdorf and R. Zentel
"Electroclinic effect in free-standing smectic elastomer films"
Appl. Phys.A, accepted for publication (2003)

Weissflog, W.; S. Sokolowski, H. Dehne, B. Das, S. Grande, M.W. Schröder, A. Eremin, S. Diele, G. Pelzl
"Chiral ordering in the nematic and an optically isotropic mesophase of bent-core mesogens with a halogen substituent at the central core"
Liq. Cryst., accepted for publication (2003)

Eremin, A.; H. Nadasi, G. Pelzl, S. Diele, H. Kresse, W. Weissflog, S. Grande
"Paraelectric - antiferroelectric transition in the bent-core liquid-crystalline material PCCP, accepted for publication (2003)

3.2 Physics of Interfaces

3.2.1 Introduction

The highlights in research and education of our group are intimately related to recent progress in the various fields of diffusion measurement, including PFG NMR, interference and IR microscopy. Within the EC-sponsored project TROCAT, under our coordination, nine groups from five countries are jointly exploring the interrelation between molecular diffusion and conversion in heterogeneous catalysis. The so far attained results of both fundamental and industrial relevance were unconceivable without this strong experimental basis within the Magnetic Resonance Centre of our University. We are happy that theses activities shall be continued within a Network of Excellence of the 6th frame programme of the EC (INSIDE-PORES). With the special focus on diffusion in zeolites, we initiated the establishment of an international (British/French/German) research group ("Internationale Forschergruppe"), sponsored by EPSRC, CNRS and DFG. The activities of this group will be of particular benefit for the International Research Training Group ("Europäisches Graduiertenkolleg") dedicated to "Diffusion in Porous Media", which starts to operate in summer term 04 and comprises groups from our institute and from the institutes of Theoretical Physics and of Chemical Technology (Faculty of Chemistry and Mineralogy), together with colleagues of the Universities of Amsterdam, Delft and Eindhoven. We particularly appreciate the presence of Douglas Morris Ruthven, Humboldt - Research - Awardee in 2002, in our group and the numerous attractive projects initiated by his involvement, with the combination of the ZLC techniques and NMR as the most prominent example. The following summaries refer to our contributions to

1. Development of Instrumentation and Technology (Sections 3.2.2–3.2.6)
2. Fundamental Research in Surface Science (Sections 3.2.7–3.2.10)
3. Applications (Sections 3.2.11–3.2.13)

3.2.2 Background gradient suppression in stimulated echo NMR diffusion studies using magic pulsed field gradient ratios

Petrik Galvosas, Frank Stallmach, Jörg Kärger

By evaluating the spin echo attenuation for a generalized 13-interval PFG NMR sequence [1] consisting of pulsed field gradients with four different effective intensities (F^p, G^p, F^r, G^r), magic pulsed field gradient ratios (MPFG) for the prepare (F^p, G^p) and the read $F^r, G^r)$ interval are derived, which suppress the cross term between background field gradients and the pulsed field gradients even in the cases where the background field gradients may change during the z-store interval of the pulse sequence [2]. These MPFG ratios depend only on the timing of the pulsed gradients in the pulse sequence and allow a convenient experimental approach to background gradient suppression in NMR diffusion studies with heterogeneous systems, where the local properties of the (internal) background gradients are often unknown. If the pulsed field gradients are centered in the τ-intervals between the 180° and 90° rf pulses, these two MPFG ratios coincide into one value given by:

$$\eta \equiv \frac{G^p}{F^p} = \frac{G^r}{F^r} = 1 - \frac{8}{1+\frac{1}{3}\frac{\delta^2}{\tau^2}}.$$

Since the width of the pulsed field gradients (δ) is bounded by $0 \leq \delta \leq \tau$, η can only be in the range of $5 \leq -\eta \leq 7$. These theoretical results, which were confirmed experimentally, extend the approach of Sun et al. (J. Magn. Reson. **161**, 168 (2003)), who also introduced a 13-interval type PFG NMR sequence with two asymmetric pulsed magnetic field gradients suitable to suppress unwanted cross terms with spatially dependent background field gradients.

For the experimental realization of such experiments using the proposed magic pulsed field gradient ratios one needs to apply two equal polarity F and G gradients in the prepare interval and two opposite but also equal polarity gradients in the read interval. The figure above shows the necessary intensity ratios of these four gradients on scale, if the pulsed gradients are centered in the τ-intervals and $\delta = \tau/3$.

[1] R.M. Cotts et al., J. Magn. Reson. **83** (1989), 252.
[2] P. Galvosas, F. Stallmach, J. Kärger, J. Magn. Reson. **166** (2004), 164.

3.2.3 A new fiber optical thermometer and its application to process control in strong electric, magnetic and electromagnetic fields

Frank Stallmach, Ulf Roland*
* UFZ - Center for Environmental Research Leipzig-Halle, Dept. of Environmental Technology

A new multi-channel fiber optical thermometer (FOT) system is described which utilizes the temperature dependence of the band gap of a semiconductor (GaAs). Its modular design allows a flexible multi-channel registration and enhances the reliability of the temperature measurement using an innovative sensor concept. The FOT can be easily adapted to a wide range of technical and economical requirements especially concerning the measuring range, number of channels, accuracy and cost per channel. Its measuring principle and design make it a versatile tool for utilization under various conditions critical for conventional temperature measurement devices (strong electric and magnetic fields, radio-wave and microwave applications, continuous process monitoring in environmental technology) [1].

The example below demonstrates the appropriateness and advantages of the FOT system in a very intense static magnetic field in combination with pulsed radio-wave excitation applied in NMR spectroscopy [1]. It shows the increase of the T2 relaxation time distribution of liquid water in sand with decreasing temperature until the water freezes to ice. This shift is controlled by a decreasing influence of the relaxation due to diffusion in internal magnetic field gradients as quantitatively shown in ref. [2].

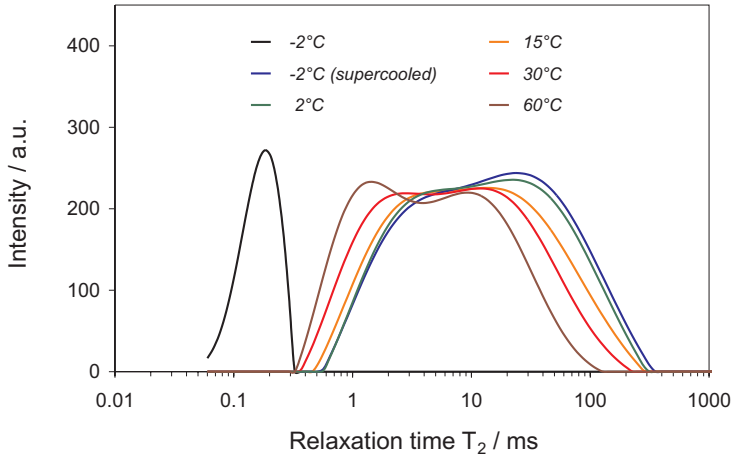

Fig. 1: Distribution of NMR relaxation times T_2 of a humid sand sample (water content approx. 60% of the pore volume) as a function of temperature measured by an FOT placed in the center of the sand/water sample in the NMR coil of the probe inside a 400 MHz NMR spectrometer.

[1] U. Roland, C.P. Renschen, D. Lippik, F. Stallmach, F. Holzer, Sensors Letters **1**, 93 (2003).
[2] F. Stallmach, Habilitation thesis, University of Leipzig (2004).

3.2.4 Application of Interference and FTIR-Microscopy to Investigating Intracrystalline Concentration Profiles in AFI-Type Crystals

Enrico Lehmann, Christian Chmelik, Sergey Vasenkov, Brigitte Staudte, Friedrich Kremer*, Jörg Kärger

* Institute for Experimental Physics I, Physik Anisotroper Fluide

Intracrystalline concentration profiles of water, adsorbed in large crystals of CrAPO–5 and SAPO–5 under equilibrium with water vapor at 1 and 20 mbar, were determined with use of interference and FTIR microscopy [1]. By using both techniques, the high spatial resolution of interference microscopy is complemented by the ability of FTIR spectroscopy to pinpoint adsorbates by their characteristic IR bands. At lower pressure, the profiles reveal highly inhomogeneous distributions of intracrystalline water in both crystal types. This effect is attributed to structural heterogeneity of the crystals. Its possible relation to the progress of the crystal growth process is considered. Under the vapor pressure of 20 mbar, the water molecules are homogeneously distributed over the crystals. In this case, the pore volume is saturated with liquid-like water. The structural heterogeneity has been found to have a low or no influence on the final uptake level of the crystals. The reported results complement our work on studying intracrystalline concentration profiles of methanol in CrAPO–5 zeolite crystals [2].

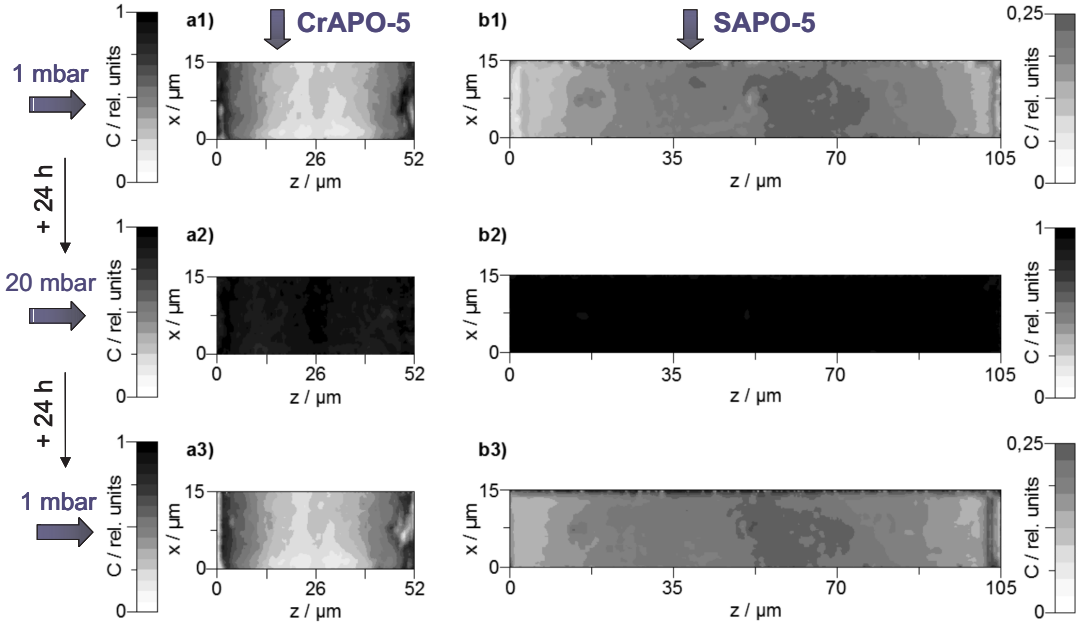

Fig. 1. Intracrystalline concentration profiles of water in the CrAPO-5 (a1, a2, a3) and SAPO-5 (b1, b2, b3) crystals integrated along the y direction under equilibrium with water vapor at 1 mbar (a1, b1, a3, b3) and 20 mbar (a2, b2). The channels run along the z axis. Darker regions correspond to higher concentration integrals.

[1] E. Lehmann, S. Vasenkov, J. Kärger, G. Zadrozna, J. Kornatowski, Ö. Weiss, F. Schüth, J. Phys. Chem. B, **107** (2003), 4685-4687.

[2] E. Lehmann, C. Chmelik, H. Scheidt, S. Vasenkov, B. Staudte, J. Kärger, F. Kremer, G. Zadrozna and J. Kornatowski, J. Am. Chem. Soc. **124** (2002) 8690-8692.

3.2.5 Monitoring Intracrystalline Distributions of Guest Molecules in Ferrierite Crystals by Interference and IR Microscopy

Christian Chmelik, Pavel Kortunov, Enrico Lehmann, Sergey Vasenkov, Jörg Kärger

For theoretical understanding of transport processes, needed for further optimizations and application of new concepts, it is essential to know, how the molecular transport is influenced by various features of zeolite structure (such as pore system, intergrowth effects and transport barriers on surface). The pore structure of ferrierite consists of a network of mutually intersecting channels of two different sizes. Offering in this way two different types of diffusion paths, ferrierite may serve as a model system for "molecular traffic control" (enhanced reactivity as a consequence of different diffusion paths from and to the reactive sites).

The evolution of intracrystalline concentration profiles during molecular uptake or tracer exchange in ferrierite was monitored using Interference (IFM) and FTIR microscopy (IRM) [1]. Non-homogeneous concentration profiles were recorded (also) at sorption equilibrium. This result is attributed to the outer shape of the crystals. From the shape of the profiles during uptake and the uptake or tracer exchange curves for different pressures we conclude that the uptake is controlled by an interplay of intracrystalline diffusion and permeability of the crystal surface, whereby a concentration dependence for both mechanisms has to be assumed.

Quantitative data analysis and monitoring intracrystalline concentration profiles in ferrierite crystals free of surface barriers remains to be a challenging task of our future research.

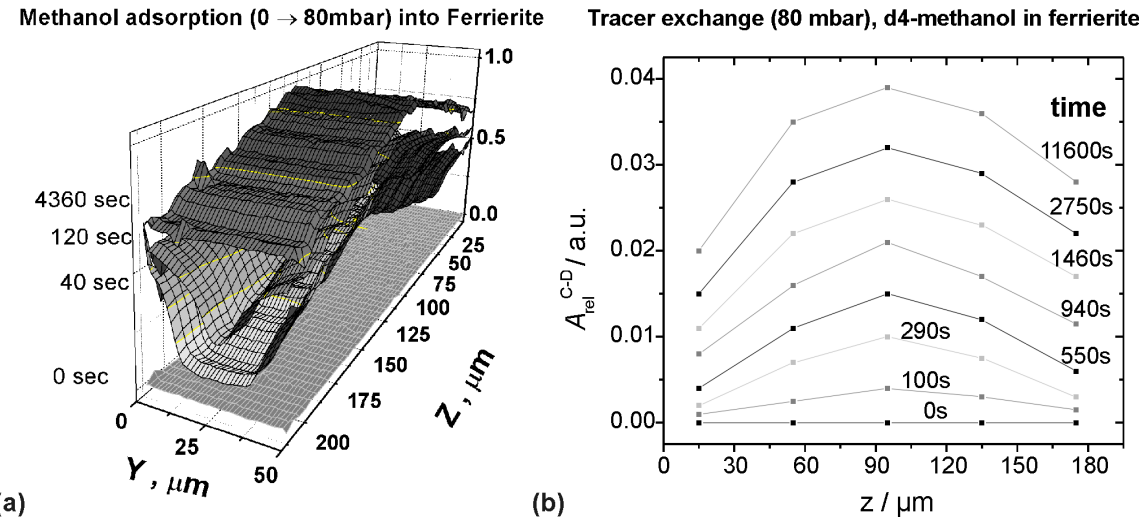

Fig. 1: (a) IFM concentration profiles at different times during uptake (crystal size about $210 \times 50\,\mu\text{m}^2$). The uptake takes place through the channels in y direction (higher concentration at the margins, lower in the middle) and is controlled by an interplay of intracrystalline diffusion and transport barriers on the surface. (b) IRM profiles along z direction for tracer exchange. The inhomogeneous equilibrium profile (also for IFM data) is attributed to the crystal shape, vs. linearly increasing thickness towards the middle.

[1] C. Chmelik, P. Kortunov, E. Lehmann, S. Vasenkov, J. Kärger, Y. Traa, J. Weitkamp, Proceedings of the 16th German Zeolite Conference, Dresden, 2004.

3.2.6 Combining macroscopic and microscopic diffusion studies in zeolites using NMR techniques

Krzyzstof Banas, Federico Brandani, Frank Stallmach, Jörg Kärger , Douglas M. Ruthven
* Department of Chemical Engineering, University of Maine, Orono, Maine, USA

The relation between the diffusivities obtained under equilibrium and non-equilibrium conditions in microporous materials is still an open problem of fundamental research [1]. This work is part of an effort aimed at the establishment of comparative diffusion measurements in zeolites by equilibrium and non-equilibrium techniques. Among the non-equilibrium techniques the Zero Length Column (ZLC) method is widely used for measuring intracrystalline or intraparticle diffusion in zeolite-based adsorbents. It depends on exposing a small sample of adsorbent to an adsorbate at known partial pressure in an inert carrier stream and following the desorption when the sample is purged by pure carrier. By monitoring the decay of the concentration in the fluid phase intracrystalline diffusion coefficients can be determined [2]. In this study the ZLC technique is extended to the case were the decay of the adsorbed phase concentration is observed using NMR.

An adsorption-desorption apparatus compatible with a 400 MHz NMR spectrometer was developed. It operates with nitrogen or helium as inert carrier gas. The column of the adsorbent material is placed in the sensitive region of the superconducting magnet and the rf coil of the NMR spectrometer. In experiment with silicalite-1/isobutane sufficient NMR signal-to-noise ratios are obtained with 25 mg of the zeolite, corresponding to less than 4 mm filling height in the column. Adsorption and desorption of the adsorbate are observed by corresponding intensity changes of the NMR signal. Due to the short transverse relaxation time of isobutane in silicalite ($T_2 = 3$ ms), the CPMG NMR sequence with an interecho spacing of 200 μs was used to monitor the signal intensity and thus the adsorbed isobutane concentration.

The time scales of the adsorption and desorption processes depend on concentration, temperature and crystal shape and are found to be in the range of 5 to 60 minutes. From the desorption branch at a temperature of 90°C the non-equilibrium ZLC NMR measurements yield an intracrystalline diffusion coefficient of 5.2×10^{-13} m^2/s for isobutane in silicalite. This value is in satisfactory agreement with PFG NMR studies of the same column under maximum adsorption that yields a self-diffusion coefficient of 3.1×10^{-13}m^2/s.

Current investigations are focused on the study of the concentration dependence of diffusion coefficients in other adsorbate/adsorbent systems using the ZLC NMR and PFG NMR techniques.

[1] J. Kärger and D.M. Ruthven, *Diffusion in Zeolites and other Microporous Solids*, Wiley & Sons, New York, 1992.
[2] M. Eic and D.M. Ruthven, Zeolites **8**, 40 (1988).

3.2.7 ^{17}O NMR studies of the structure and basic properties of zeolites

Horst Ernst, Dieter Freude, Bernd Knorr, Thomas Loeser, Dagmar Prager, Denis Schneider, Daniel Prochnow

Multiple-quantum magic-angle spinning and double rotation NMR techniques were applied in the high field of 17.6 T to the study of oxygen-17 enriched zeolites A, LSX and sodalites with the ratio Si/Al = 1. A monotonic correlation between the isotropic value of the chemical shift and the Si-O-Al bond angle α (taken from X-ray data) could be found. It was confirmed that individual linear correlations exist between the isotropic 17O chemical shift $\delta(^{17}O)$ and the s-character ρ of the oxygen hybrid orbitals for the hydro- and hydroxysodalites, the zeolites (with Si/Al = 1) Na-A (hydrated) and Na,K-LSX (hydrated, dehydrated). Corresponding linear dependencies can be found if the isotropic chemical shifts $\delta(^{17}O)$ are plotted against the Si-Al-distances in the Si-O-Al bridges. The increase in $\delta(^{17}O)$ by the adsorption of water and cation exchange can be separated from the effect of the bond angle a on the ^{17}O chemical shift.

The dehydration of the zeolites LSX causes ^{17}O NMR chemical shift changes by the superimposed effects of the well-known changes of the Si-O-Al bond angles and the effect of polarization of the framework by the adsorbed water molecules. The total effect is about 8 ppm, whereas the angular corrected effect amounts about 4 ppm. The low field shift due to the adsorption interaction is relatively small (ca. 2.2 ppm) for formic acid.

Ion exchange of the hydrated zeolites generates stronger chemical shift effects. The increase of the basicity of the oxygen framework of the zeolite LSX is reflected by a downfield shift of ca. 10 ppm going from the lithium to the cesium form, and the substitution of sodium by thallium in the zeolite A causes a shift of 34 ppm for the O3 signal.

^{17}O DOR NMR spectra are superior to ^{17}O 3QMAS NMR spectra with respect to the resolution by a factor of two. The application of the FAM2 excitation does not improve resolution or intensity in the ^{17}O 3QMAS NMR spectra. The signal-to-noise ratio of DOR and 3QMAS NMR spectra is comparable, whereas that of 5Q MAS NMR spectra is lower by more than one order of magnitude, and the spectral window is lower by a factor of five. This limits the application of the 5QMAS technique to the ^{17}O NMR. The residual linewidths of the signals in the ^{17}O DOR and ^{17}O 5QMAS NMR are caused by a distribution of the Si-O-Al angles in the zeolites.

3.2.8 Gas diffusion in zeolite beds: PFG NMR evidence for different tortuosity factors in the Knudsen and bulk regimes

Sergey Vasenkov, Oliver Geier, Jörg Kärger

The pulsed field gradient (PFG) NMR technique was applied to study the ethane diffusion in beds of NaX zeolites for displacements, which are orders of magnitude larger than the size of the individual crystals. The experimental results show that the apparent tortuosity factor in the Knudsen regime may be significantly larger than that in the bulk regime for one and the same porous medium [1]. The observed difference between the tortuosity factors in the bulk and Knudsen regimes may have its origin in the different influence of the geometrical details of the pore surface of the intercrystalline space on diffusion in these two regimes. Most recent MC studies of the effect of surface roughness on self- and transport diffusion in porous systems show that for the same mean pore size the self-diffusion coefficients in the Knudsen regime may vary in a broad range (up to one order of magnitude) depending on surface roughness [2]. The detailed explanation of the differences between the apparent tortuosity factors in the bulk and Knudsen regimes remains to be the subject of future research.

[1] S. Vasenkov, O. Geier, J. Kärger, Gas diffusion in zeolite beds: PFG NMR evidence for different tortuosity factors in the Knudsen and bulk regimes, Eur Phys J E 2003, **12**, s01 009 (2003).
[2] K. Malek, M.-O. Coppens. Effects of Surface Roughness on Self- and Transport Diffusion in Porous Media in the Knudsen Regime, Phys. Rev. Lett. **87**, 125505 (2001).

3.2.9 Desorption of particle mixtures into vacuum from a quadratic lattice with Molecular-Traffic-Control character

Peter Bräuer, Andreas Brzank, Jörg Kärger

The possibility of reactivity enhancement by molecular traffic control (MTC) was rationalized by dynamic Monte Carlo simulations in a network of single-file systems under a stationary regime [1]. It was clarified under which conditions the superiority of the MTC system versus the reference (REF) system is maintained. It turns out that the MTC system becomes progressively beneficial over the REF system with increasing file lengths between the intersection points. Thus, the benefit of the MTC system is found to be purchased by (i) stronger transport inhibition and (ii) a reduced density of active sites (since in the model considered the sites in the channel segments - being accessible by only one type of molecules - had to be required to be inactive for molecular conversion). Now it is of great interest, which behavior the molecules show in the case, if they can be expand into the vacuum from a quadratic lattice consisting of α- and β-channels with different hop probabilities P_B^α of the product molecules in the α-channels [2]. The figure shows the profiles of the particles A (first line), B (second line) and of their sum (third line) on the lattice after 50 elementary desorption time steps for the hop probabilities $P_B^\alpha = 0$ (the so-called hard MTC system), $P_B^\alpha = 0.3$ (a so-called soft MTC system) and $P_B^\alpha = 1$ (the REF system). In the case of the REF system one can observe normal symmetrical diffusion behavior of the molecules. In the case of the MTC system (especially pronounced at its hard form) the transport inhibition of the particles B in the α-channels is correlated with the diffusion of the particle A in the α-channels (the diffusivity is smaller than in the REF system) as well as with the diffusion of the B molecules in β-channels (the diffusion is faster). This leads to a more pronounced diffusion anisotropy than expected.

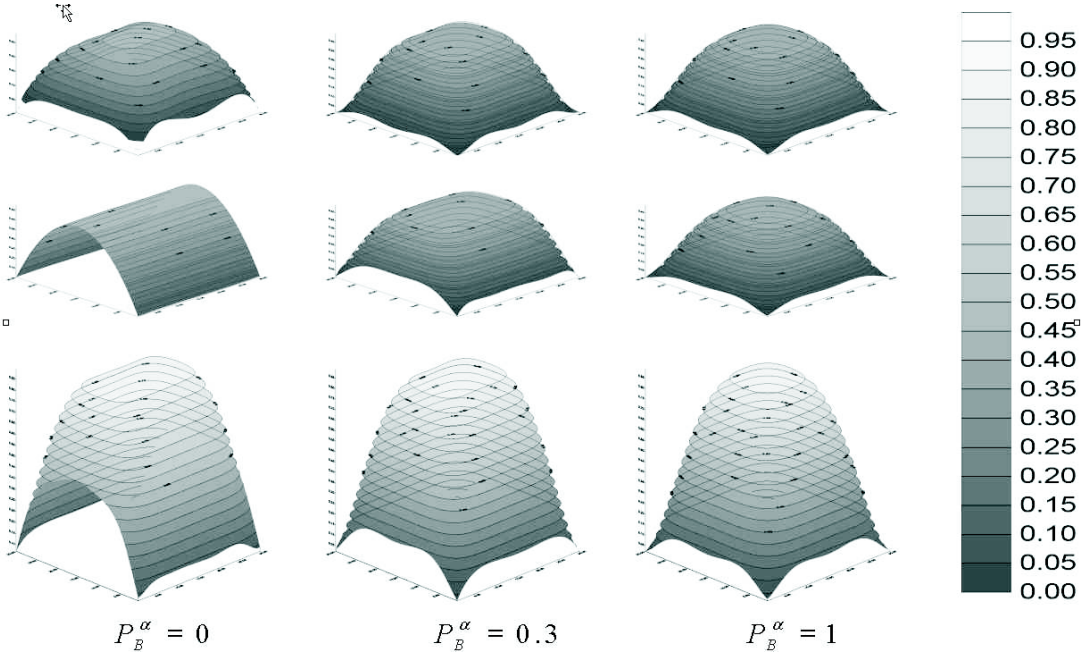

[1] Bräuer, P., Brzank, A., Kärger, J.: "Adsorption and Reaction in Single-File Networks", J. Phys. Chem. B 2003, **107**, 1821 - 1831.
[2] Bräuer, P., Brzank, A., Kärger, J.: in preparation.

3.2.10 Comicellisation of Diblock and Triblock Copolymers in a Selective Solvent. Pulsed Field Gradient NMR and Light Scattering Investigations

Stefan Gröger, Frank Stallmach, Jörg Kärger, Dieter Geschke* und Cestmír Konák**
* Institute of Experimental Physics I, Polymer Physics
** Institute of Macromolecular Chemistry, Academy of Sciences of the Czech Republic, Prague

Comicellisation of diblock polystyrene-block-hydrogenated polyisoprene and triblock polystyrene-block-hydrogenated polybutadiene-block-polystyrene copolymers was investigated by pulsed field gradient NMR and dynamic light scattering (DLS) methods at 25°C in decane [1]. The equilibrium concentrations of triblock unimer in solutions were evaluated from normalised attenuation functions obtained by pulsed-field gradient NMR.

Previous dynamic light scattering experiments with the diblock copolymer polystyrene-polyisoprene and the triblock copolymer polystyrene-polybutadiene-polystyrene mixtures dissolved in n-decane revealed that the micelles formed by the diblocks were significantly affected by the, essentially molecularly dissolved, triblocks [2]. This finding was confirmed in this study by self-diffusion measurements using our pulsed field gradient NMR technique. This agreement is of particular relevance since PFG NMR is able to record the diffusion paths of the proton-containing molecules with uniform sensitivity, determined by the number of protons per particle, while in DLS the contribution of large agglomerates is overemphasised. Thus, PFG NMR is a more suitable method for investigation of self-association processes in multi-component (co)polymer systems than light scattering methods.

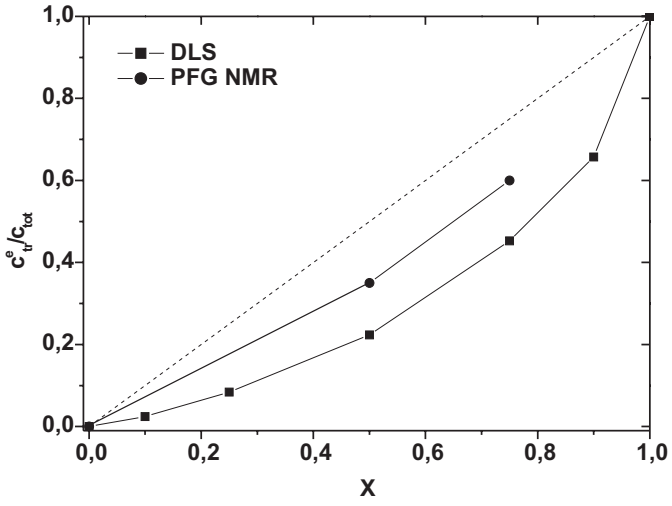

Fig. 1: Normalized equilibrium weight concentration of PS-HPB-PS triblock copolymer, c^e_{tr}/c_{tot}, plotted as a function of X; obtained from spin echo attenuation curves measured by PFG NMR, calculated from apparent molecular weights of (co)micelles measured by DLS. The dashed line corresponds to a mixture of hypothetical non-interacting particles.

[1] St. Gröger, D. Geschke, J. Kärger, F. Stallmach, C. Konk, Macromolecules Rapide Communications, in press.
[2] C. Konák, M. Helmstedt, Macromolecules **36**, 4603 (2003).

3.2.11 Transport optimization of FCC catalysts in the framework of the EC Project 'TROCAT'

Pavel Kortunov, Sergey Vasenkov, Dieter Freude, Jörg Kärger

In this project, our intention is to find the routes of the production of fluid catalytic cracking (FCC) catalysts, which lead to improved catalytic performance due to optimization of the transport of reactants and products in these materials. Recent progress in the area of the pulsed field gradient technique of nuclear magnetic resonance (PFG NMR) has made possible the direct observation of molecular migration (diffusion) in microporous catalysts. In the TROCAT project this technique is used to overcome one of the main shortcomings in the optimization of FCC catalysts, i.e. the lack of the optimization with respect to the transport properties. Investigations of the transport properties of the samples were complemented by the characterization of their catalytic and structural properties, by special syntheses and by molecular modelling performed by our partners in the University of Athens, CEPSA (Madrid), Grace (Worms), the Heyrovsky Institute Prague, SINTEF (Oslo) and the Stuttgart University.

Our data suggest that for relatively small molecules ($\sim C_{10}$) the rate of molecular exchange between the catalyst particles and their surroundings may be influenced to a great extent by the intracrystalline diffusivity (i.e. diffusivity in zeolite crystals). At the same time, for large molecules this rate is primarily determined by the intraparticle diffusion coefficient (i.e. diffusivity in catalyst particles) and to a much smaller extent by the intracrystalline diffusivity. In response to this result the study of the correlations between such particle properties as macroporosity and the macropore size distribution, which affect the intraparticle diffusivities, on one hand, and the catalytic performance of these particles, on the other hand, has been carried out. To this end several catalyst samples containing the same amounts of the same zeolite Y but having different intraparticle morphology were manufactured and investigated. The molecular simulations have been performed in order to help to understand an influence of the morphology of catalyst particles on the intraparticle transport properties. The results obtained show that the samples with higher catalytic activity also reveal larger intraparticle diffusivity. The catalyst optimization route leading to higher intraparticle diffusivities is considered to be especially promising at this point. The high potentials of this route are demonstrated by the preparation of the new catalyst samples GRACE 4 and GRACE 5 showing better catalytic performance than the reference GRACE 1 sample.

3.2.12 PFG NMR Studies in Industrial Catalysts

Frank Stallmach, Stefan Gröger, Ulrich Müller*
* BASF AG, Ludwigshafen, Germany

Pulsed field gradient nuclear magnetic resonance (PFG NMR) is a versatile tool to study transport processes of fluids and gases in porous materials. It monitors averaged molecular displacements (r.m.s. displacements) and the self-diffusion coefficients of the guest molecules on time scales, which – depending of the nuclear relaxation times – typically range from a few milliseconds up to seconds. PFG NMR may be used to determine geometric pore structure parameters or to clarify the transport mechanisms of the guest molecules in the porous materials.

During the past years we developed and successfully applied a PFG NMR method to selectively measure the tortuosity of the transport pores in formulated catalyst particles [1]. It is based on measurements of liquid saturated catalyst particles. It monitors the time-dependence of the self-diffusion of the liquid molecules in the transport pores of the catalyst and compares it to the corresponding data in the bulk liquid. Results obtained on formulated catalysts for synthesis of propylenoxid (based on a titanium zeolite with MFI structure) and propane dehydration (based on platinum loaded zirconium oxid) [2] are reported.

For the ZrO-based catalysts, PFG NMR studies of adsorbed propane and propene contributed to the clarification of the transport process responsible for diffusional transport under conditions in the reactor. Based on the experimental data for propane and propene self-diffusion, the above mentioned PFG NMR studies of the tortuosity, mercury porosimetry and adsorption isotherms, a comprehensive model was developed which predicts the diffusion in the transport pores without any unknown, hidden parameters.

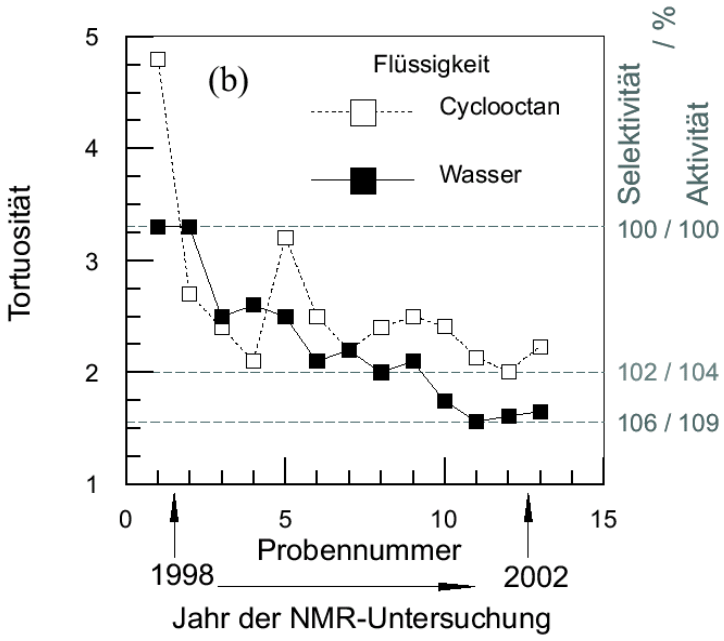

Fig. 1: Tortuosity of formulated catalyst samples as measured by PFG NMR using water and cyclooctane as probe molecules, respectively. During the fife years period of development of the catalyst, the tortuosity decreased and the catalytic properties like selectivity and activity increased [1,2].

[1] F. Stallmach, Habilitation thesis, University of Leipzig (2004).
[2] U. Müller, R. Senk, W. Hader, P. Rudolf, N. Rieber, Shaped body and method for producing the same, Internationales Patent, WO 02/085513 A2, PCT/EP 02/02278 (2002).

3.2.13 *In situ* Studies of the Mechanism of Heterogeneously Catalyzed Reactions by Laser -Supported High-Temperature MAS NMR

Horst Ernst, Dieter Freude, Johanna Kanellopoulos, Toralf Mildner, Dagmar Prager, Denis Schneider

Surface sites capable of donating protons or accepting electrons from adsorbed molecules are essential for heterogeneous catalysis. Magic-angle-spinning nuclear magnetic resonance spectroscopy (MAS NMR) has been successfully applied to the study of the interaction between acid sites in zeolites and base molecules and to the catalytic conversion of organic molecules. The in situ technique became the most important tool for such studies. A new technique making use of a laser beam makes it possible to switch from room temperature, at which the reaction is too slow to be measured, to temperatures up to 800 K, at which the reaction takes place within a few seconds.

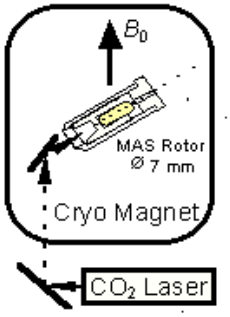

(a)

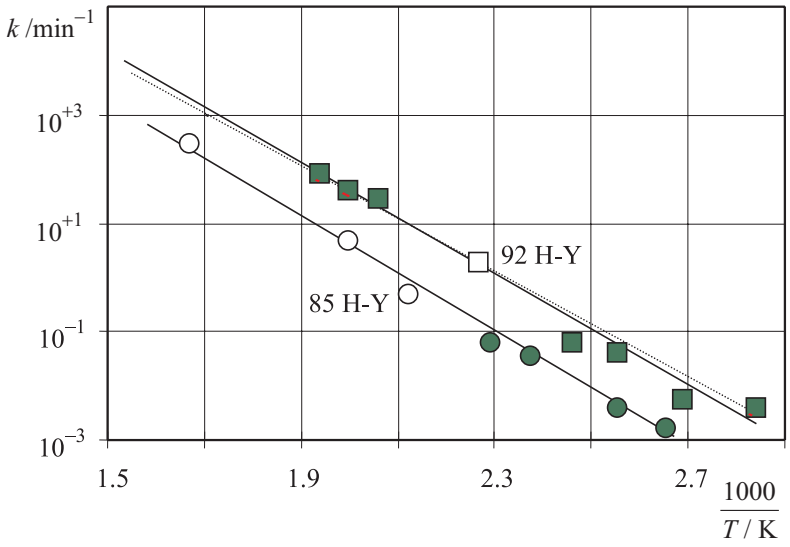

(b)

Fig. 1: (a) Experimental set-up, (b) Arrhenius plot of the H-D and H-H exchange rates for benzene molecules in the zeolites 85 H-Y and 92 H-Y. The values which are marked by open or full circles and squares were measured by laser heating or conventional heating, respectively.

Activation energies of the proton transfer have been obtained under the assumption of a constant value of the pre-exponential factor in the Arrhenius plot to 102 kJ mol^{-1} for zeolite 85 H-Y (Si/Al = 2.4) and 93 kJ mol^{-1} for zeolite 92 H-Y (Si/Al = 3.1). In this case, the variation of the Si/Al ratio, which causes a change of the deprotonation energy of the bridging hydroxyl groups, can explain the differences of the exchange rate. However, a variation of the pre-exponential factor by steric effects like the existence of non-framework aluminum species cannot be excluded.

3.2.14 Funding

Prof. Dr. D. Freude, Dr. H. Ernst
Characterization of elementary steps of the crystallisation of zeolites in porous glasses by in situ MAS NMR
DFG-Projekt FR 902 / 6-2

Prof. Dr. D. Freude, Prof. Dr. D. Michel
DOR and multi-quantum MAS NMR for high field NMR studies of quadrupole nuclei on solids
DFG-Projekt FR 902 / 9-2

Prof. Dr. D. Freude, Dr. H. Ernst
Untersuchung der Protonen-Beweglichkeit in H-Zeolithen mit SFG NMR und MAS NMR im Temperaturbereich bis 800 K.
DFG-Projekt FR 902 / 12-1

Prof. Dr. J. Kärger
Permeation of monomers in nanoporous host/guest-systems / Schwerpunktprogramm "Nanoporöse Materialien"
DFG-Projekt Ka 953/13-1 und 13-2

Prof. Dr. J. Kärger
Molecular diffusion in nanoporous materials
DFG-CNRS-Project Ka953/14-1, Ka953/14-2

Prof. Dr. J. Kärger
Reaktion und Diffusion in Single-File Netzwerken: Computersimulationen und statistisch-thermodynamische Untersuchungen.
DFG-Projekt KA 953/15-1

Prof. Dr. J. Kärger, Dr. F. Stallmach
Fourier-Transform-PFG-NMR mit starken Feldgradientenimpulsen zur selektiven Selbstdiffusionsmessung.
DFG-Projekt KA 953/16-1

Prof. Dr. J. Kärger
Wasserbilanz in Hochleistungsbeton.
DFG-Projekt KA 953/17-1

Prof. Dr. J. Kärger
Studying Zeolitic Diffusion by Interference and IR Microscopy. DFG-Projekt KA 953/18-1 within the International Research Group "Diffusion in Zeolites"

Prof. Dr. J. Kärger
Development of new ceramics
EC-Project GRD1-1999-11207

Prof. Dr. J. Kärger
New dealumination routes to produce transport-optimised catalysts for crude oil conversion
EC-Project GRD2-2000-30364

Prof. Dr. J. Kärger, Dr. F. Stallmach
Diffusion optimation of microporous membranes and particle batches
EC-Project HPMD-CT-2000-00029

Prof. Dr. J. Kärger, Dr. F. Stallmach
PFG NMR investigations on technical catalysts
BASF AG

Dr. F. Stallmach, Prof. Dr. J. Kärger
NMR and MRI studies of aquifer rock
UFZ Halle-Leipzig GmbH

3.2.15 Organizational Duties

Participation in committees

Jörg Kärger
Ombudsman of Leipzig University
Membership in the Programme Committee "Magnetic Resonance in Porous Media" (Ulm 2002, Paris 2004), "Fundamentals of Adsorption" (Serona, Arizona, USA, 2004), International Zeolite Conference (Capetown 2004) and in the permanent DECHEMA committees "Zeolites" and "Adsorption"

Reviewing and refereeing duties

J. Kärger
Membership in Editorial Boards:
Microporous and Mesoporous Materials (European Editor)
Diffusion Fundamentals (Online Journal, Editor)
Adsorption
Referee: Phys. Rev., Phys. Rev. Lett., Europhys. Lett., J. Chem. Phys., J. Phys. Chem., Langmuir, Micropor. Mesopor. Mat., PCCP, J. Magn. Res.
Project Reviewer: Deutsche Forschungsgemeinschaft, National Science Foundation (USA)

D. Freude
Project Reviewer: Deutsche Forschungsgemeinschaft
Membership in Editorial Boards: Solid State NMR
Diffusion Fundamentals (Online Journal, Editor)
Referee: Chem. Phys. Lett., J. Chem. Phys., J. Phys. Chem., J. Magn. Res., Solid State NMR

B. Staudte
Referee: Micropor. Mesopor. Mat.

S. Vasenkov
Referee: J. Am. Chem. Soc., Micropor. Mesopor. Mat.

F. Stallmach
Referee: J. Magn. Res., Micropor. Mesopor. Mat., Phys. Rev. Lett.

3.2.16 External cooperations

Academic

Acad Sci Czech Republ, Inst Macromol Chem, Czech Republic
Prof. Konak, Prof. Stepanek

Acad Sci Czech Republ, Heyrovsky-Inst. Phys. Chem., Czech Republic
Dr. Kocirik, Dr. Zikanova

Delft University, Inst.Chem. Tech., Delft, Niederlande
Prof. Kapteijn

Institut de Recherches sur la Catalyse, CNRS, Villeurbanne, France
Dr. Jobic

Institut Francais du Petrole, Malmaison, France
Dr. Methivier

FZ Jülich GmbH, Forschungszentrum, Festkörperforschung/Theorie, Jülich, Germany
Dr. Schütz

Max Planck Institut für Kohlenforschung, Mülheim, Germany
Dr. Schmidt, Prof. Schüth

Max Planck Institut für Metallforschung, Stuttgart, Germany
Dr. Majer

Russian Acad Sci, Boreskov Inst Catalysis, Siberian Branch, Novosibirsk, Russia
Dr. Stepanov

TU München, Lehrstuhl Technische Chemie 2, Germany
Dr. Kornatowski, Prof. Lercher

Universit di Sassari, Dipartimento Chimica, Sassari, Italy
Prof. Demontis, Prof. Suffritti

Universiät Eindhoven, Schuit Institute, Eindhoven, Niederlande

Prof. van Santen

Universität Erlangen Nürnberg, Dept Chem Engn, Erlangen, Germany
Prof. Emig, Prof. Schwieger

Universität Hannover, Dept Phys.Chem, Hannover, Germany
Prof. Caro, Prof. Heitjans

Universität Leipzig, Institut für Analytische Chemie, Leipzig, Germany
Prof. Berger

Universität Leipzig, Institut für Technische Chemie, Leipzig, Germany
Prof. Einicke, Prof. Papp

Universität Leipzig, Institut für Medizinische Physik und Biophysik, Leipzig, Germany
Prof. Arnold, Prof. Gründer

Universität Leipzig, Instiut für Pharmazeutische Technolgie, Leipzig, Germany
Prof. Süß

Universität Leipzig, Wilhelm Ostwald Institut für Physikalische & Theoretische Chemie, Leipzig, Germany
Dr. Hunger, Dr. Knoll

Universität Regensburg, Institut Biophysik & Physikalische Biochemie, Regensburg, Germany
Prof. Brunner

Universität Stuttgart, Institut für Technische Chemie, Stuttgart, Germany
Prof. Hunger, Prof. Weitkamp

University Athens, Dept Chem. Engn., Athens, Greece
Prof. Theodorou

University of Maine, Dept. Chem. Engin., USA
Prof. Ruthven

Industry

Air Prod & Chem Inc, Allentown
Dr. Coe, Dr. Zielinski

BASF, Ludwigshafen
Dr. Müller

Cepsa, Madrid
Dr. Perez

Grace, Worms
Dr. McElhiney

Resonance Instruments Ltd., Witney, UK
J. McKendry

SINTEF, Oslo
Prof. Stöcker

Tricat, Bitterfeld
Dr. Tufar

WITEGA, Berlin
Dr. Lutz

3.2.17 Publications

Journals

Bräuer P., Brzank A., Kärger J.:
Adsorption and reaction in single-file networks.
J. Phys. Chem. B 107 (2003)1821-1831.

Bräuer, P., Fritzsche, S., Kärger, J., Schütz, G.:
Diffusion in Channels and Channel Networks in Molecules in Interaction with Surfaces and Interfaces
Haberlandt, R., Michel, D., Pöppl, A., Stannarius, R. (Editors), Springer (Lecture Notes in Physics)

Fritzsche S., Kärger J.:
Memory effects in correlated anisotropic diffusion.
Europhys. Lett. 63 (2003) 465-471.

Fritzsche S., Kärger J.:
Tracing memory effects in correlated diffusion anisotropy in MFI-type zeolites by MD simulation.
J. Phys. Chem. B 107 (2003) 3515-3521.

Fritzsche S., Wolfsberg M., Haberlandt R.:
The importance of various degrees of freedom in the theoretical study of the diffusion of methane in silicalite-1.
Chem. Phys. 289 (2003): 321-333.

Geier O., Vasenkov S., Freude D., Kärger J.:
PFG NMR observation of an extremely strong dependence of the ammonia self-diffusivity on its loading in H-ZSM-5.

J. Catal. 213 (2003) 321-323.

Jobic H., Paoli H., Methivier A., Ehlers G., Kärger J., Krause C.:
Diffusion of n-hexane in 5A zeolite studied by the neutron spin-echo and pulsed-field gradient NMR techniques.
Micropor. Mesopor. Mater. 59 (2003) 113-121.

Kärger J.:
Measurement of diffusion in zeolites - A never ending challenge?
Adsorption 9 (2003) 29-35.

Kärger J.:
Diffusion under Confinement
Sitzungsberichte der Sächsischen Akademie der Wissenschaften zu Leipzig 128 (6) 5-43.

Kärger J., Stallamach F., Vasenkov S.:
Structure-mobility relations of molecular diffusion in nanoporous materials.
Magn. Reson. Imaging 21 (2003) 185-191.

Krause C., Stallmach F., Honicke D., Spange S., Kärger J.:
A surprising drop of the diffusivities of benzene in a mesoporous material of type MCM-41 at medium pore filling factors.
Adsorption 9 (2003) 235-241.

Lehmann E., Vasenkov S., Kärger J., Zadrozna G., Kornatowski J., Weiss Ö., Schüth F.:
Inhomogeneous Distribution of Water Adsorbed under Low Pressure in CrAPO-5 and SAPO-5: An Interference Microscopy Study.
J. Phys. Chem. B 107 (2003) 4685-4687.

Lehmann E., Vasenkov S., Kärger J., Zadrozna G., Kornatowski J.:
Intracrystalline monitoring of molecular uptake into the one-dimensional channels of the AFI-type crystals using interference microscopy
J. Chem. Phys. 118 (2003) 6129-6132.

Loeser T., Freude D., Mabande G. T. P., Schwieger W.:
O-17 NMR studies of sodalites.
Chem. Phy. Lett.370 (2003) 32-38.

Naji L., Schiller J., Kaufmann J., Stallmach F., Kärger J., Arnold K.:
The gel-forming behaviour of dextran in the presence of KCl: a quantitative C-13 and pulsed field gradient (PFG) NMR study
Biophys. Chem. 104 (2003) 131-140.

Pampel A., Kärger J., Michel D.:
Lateral diffusion of a transmembrane peptide in lipid bilayers studied by pulsed field gradient NMR in combination with magic angle sample spinning.

Chem. Phys. Lett. 379 (2003) 555-561.

Pimenov G.G., Opanasyuk O.A., Skirda V.D., Kärger J.:
NMR detection of phase transition in a ZSM-5 silicalite caused by the adsorbed hexane and decane molecules.
Colloid J. 65 (2003) 60-64.

Roland, U., Renschen, C.P., Lippik, D., Stallmach, F., Holzer, F.
A New Fiber Optical Thermometer and Its Application for Process Control in Strong Electric, Magnetic and Electromagnetic Fields
Sensor Lett. 1 (2003) 93-98

Stallmach F., Kärger J.:
Abstracts of a number of invited lectures and contributed presentations - Pore structure of aquifer sediments studied by PFG NMR and MRI.
Magn. Reson. Imaging 21 (2003) 415-419.

Stallmach F., Kärger J.:
Using NMR to measure fractal dimensions - Reply.
Phys. Rev. Lett. 90 (2003) art. no. 039602.

Vasenkov S., Geier O., Kärger J.:
Gas diffusion in zeolite beds: PFG NMR evidence for different tortuosity factors in the Knudsen and bulk regimes.
Eur. Phys. J. E 12 (2003) 35-38.

Vartapetyan, R. Sh., Khozina, E.V., Chalykh, A.E., Skirda, V., Feldstein, M.M., Kärger, J., Geschke, D.:
Molecular Mobility in a Poly(ethylene glycol)-Poly(vinyl pyrrolidone) Blends: Study by the Pulsed Gradient NMR Techniques.
Colloid J. 65 (2003) 684-690

Book sections

Kärger, J.; Vasenkov, S.; Auerbach, S. M.
Diffusion in Zeolites
In Handbook of Zeolite Science and Technology, S. M. Auerbach, K. A. Carrado P. K. Dutta, (Editors) Marcel-Dekker Inc., New York, 2003, pp. 341-423

Kärger, J.; Vasenkov, S.:
Probing Host Structures by Monitoring Guest Distributions. In Host-Guest Systems Based on Nanoporous Crystals
Laeri, F. , Schüth, F., Wark, M. (Editors) WILEY-VCH, Weinheim, 2003, pp.255-279

in press

Geier, O., Snurr, R.Q., Stallmach, F. Kärger, J.
Boundary effects of molecular diffusion in nanoporous materials: A pulsed field gradient nuclear magnetic resonance study
J. Chem. Phys.

Galvosas, P., Stallmach, F., Kärger, J.:
Background gradient suppression in stimulated echo NMR diffusion studies using magic pulsed field gradient ratios
J. Magn. Reson.

Gröger, S., Geschke, D. Kärger, J. Stallmach, F. Konák, C.:
Comicellisation Investigated by Pulsed-Field-Gradient Nuclear Magnetic Resonance
Macromol. Rapid Comm.

Valiullin, R., Kortunov, P., Kärger, J., Tinoshenko, V.:
Concentration-dependent self-diffusion of liquids in nanopores: a nuclear magnetic resonance study
J. Chem. Phys.

Kärger, J., Papadakis, C.M., Stallmach, F.:
Structure-Mobility Relations of Molecular Diffusion in Interface Systems
Haberlandt, R., Michel, D., Pöppl, A., Stannarius, R. (Editors), Springer (Lecture Notes in Physics)

Conference contributions, Talks, Posters

(inv. T.: invited Talks, T: talks, P: posters)

S. Gröger, P. Galvosas, F. Stallmach, J. Kärge
An Improved Method for the Measurement of Low Self-diffusion Coefficients of Mixtures Adsorbed in Zeolites by FT PFG NMR
(KV8), 15. Deutsche Zeolith-Tagung , Kaiserslautern, 5.–7. März 2003 (T)

J. Kärger, P. Heitjans
Leitung der "Sommerakademie der Studienstiftung des deutschen Volkes *Diffusion*" 01.09.2003 – 12.09.2003

J. Kärger and S. Vasenkov
PFG NMR Diffusion Studies of Nanoporous Materials
NATO summer school 'Fluid Transport in Nanoporous Materials' (France, June 16–27, 2003) (inv. T)

J. Kärger and S. Vasenkov
Structure-Related Anomalous Diffusion in Zeolites
NATO summer school 'Fluid Transport in Nanoporous Materials' (France, June 16–27, 2003) (inv. T)

J. Kärger
Struktur- Beweglichkeitsbeziehungen bei der Diffusion in nanoporösen Materialien"
Kolloquium im Institut für Physikalische Chemie und Theoretische Chemie Technische Universität Braunschweig, 23. Mai 2003 (inv. T)

J. Kärger
Structure - Dependent Molecular Diffusion in Nanoporous Materials
Kolloquium, Ludwig - Maximilians - Universität München, Center for NanoSciences München, 28.11.2003 (inv. T)

J. Kärger
PFG NMR Diffusion Studies
Pre-Conference School of the Indo-Pacific Catalysis Association (IPCAT-3) Taipei, Taiwan, November 13–15, 2003 (inv. T)

J. Kärger
Structure - Mobility Relations in Zeolitic Diffusion
The Third Conference of the Indo-Pacific Catalysis Association (IPCAT-3), Taipei, Taiwan, November 16–18, 2003 (inv. T)

S. Fritzsche, A. Schüring, S. Vasenkov, J. Kärger
Correlated Anisotropic Diffusion
85th Bunsen-Colloquium on Atomic Transport in Solids: Theory and Experiments", Rauischholzhausen/Gießen, 31.10.03 (P)

3.2.18 Graduations

PhD

Geier, Oliver Marcel
Die Diffusion unter dem Einfluß der zeolithischen Realstruktur
17.03.2003

Prochnow, Daniel
Festkörper-NMR-Untersuchungen an Phosphat-Materialien
23.06.2003

Postdoctoral lecture qualification (Habilitation)

Vasenkov, Sergey
Struktur-Beweglichkeits-Beziehungen bei der anomalen Diffusion in nanoporösen Materialien
11.08.2003

Diploma

Brzank, Andreas
Molecular Traffic Control in single-file Netzwerken
30.09.2003

Schneider, Denis
NMR-Untersuchungen an Protonenleitern
13.10.2003

3.2.19 Guests

Prof. Dr. Douglas M. Ruthven
University of Maine, since July 2003

Dr. Taro Ito
Sapporo, Juni 2003

Dr. Krysztof Banas
University of Krakov
as a Marie-Curie Fellow of the EC

Dr. Federico Brandani
University of Maine
as a Marie-Curie Fellow of the EC

Dr. Rustem Valiullin
University of Kazan
as an Alexander von Humdoldt fellow

3.2.20 Awards

Dr. Petrik Galvosas
FDI-Förderpreis Leipzig

3.3 Polymer Physics

3.3.1 Space charge distribution in conjugated polymers

D. Geschke, F. Feller, U. Weber

The decay of space charge in conjugated polymers due to detrapping from deep traps after the turn-off of an external bias has been investigated. A novel experiment was introduced which allows measuring of time resolved laser intensity modulation method (LIMM) spectra with a resolution of about 1 second. For this pyroelectric current transients have been recorded at different temperatures from 220 to 360 K. The data have been analysed assuming detrapping of charge carriers from single energy trap levels to a Gaussian distribution of transport levels to be the predominating process of the space charge decay. In poly[2-methoxy,5-(2'-ethyl-hexyloxy)-p-phenylene-vinylene] (MEH-PPV) hole trapping was found with a trap depth of $E_\mathrm{t} = 0.6\,\mathrm{eV}$ and a trap density $N_\mathrm{t} > 2 \times 10^{21}\,\mathrm{m}^{-3}$. In poly(2,5-pyridinediyl) (PPY) both, electron and hole trapping was observed and the analysis of the decays yield $E_\mathrm{t} = 0.55\,\mathrm{eV}$ and $N_\mathrm{t} > 10^{21}\ \mathrm{m}^{-3}$. No deep trapping could be observed in poly (9,9-dioctylfluorene) (PFO) confirming the high chemical purity of this polymer.

References:
Feller, F., Geschke, D., Monkman, A. P. Polymer 43 (2002) 4011-4016
Feller, F., Rothe, C., Tammer, M., Geschke, D., Monkman, A. P. Journal of Applied Physics 91 (2002) 9225-9231
Feller, F., Geschke, D., Monkman, A. P. J. Phys.: Condens. Matter 14 (2002) 8455-8462
Feller, F., Geschke, D., Monkman, A. P. Polymer International 51 (2002) 1184-1189

In cooperation with:
A. P. Monkman, "Organic Electroactive Materials" Group, Department of Physics, University of Durham, UK
J. Honerkamp, "Statistical Data Analysis" Group, Freiburg Materials Research Center, Freiburg, Germany

Financial support: DFG Ge 718 / 7-1

3.3.2 Funding

Raumladungsverteilung in konjugierten Polymeren
Prof. Dr. D. Geschke
DFG-Projekt Ge 718 / 7-1 (2001-2003)

3.3.3 Publications

Li, J., Stannarius, R., Tolksdorf, C., Zentel, R.
Hydrogen bonded ferroelectric liquid crystal gels in freely suspended film geometry
Phys. Chem. Chem. Phys. 5 (2003) 916-923

Feller, F., Geschke, D., Monkman, A. P.
Decay of space charge in conjugated polymers measured using pyroelectric current transients
Journal of Applied Physics 93 (2003) 2884-2889

Bender, M., Holstein, P., Geschke, D.
Observation of echoes in reorientation processes of nematic liquid crystals
Journal of Magnetic Resonance 164 (2003) 35-43

Vartapetyan, R. Sh., Khozina, E. V., Chalykh, A. E., Skirda, V. D., Feldstein, M. M., Kärger, J., and Geschke, D.
Molecular Mobility in a Poly(ethylene glycol)-Poly(vinyl pyrrolidone) Blends: Study by the Pulsed Gradient NMR Techniques
Colloid Journal 65 (2003) 684-690

3.3.4 Graduations

PhD

M. Sc. Frank Feller
Raumladungsverteilung in konjugierten Polymeren
14.04.2003

3.3.5 Visitors

Prof. Dr. C. Konak
(Visiting Professor of the AvH Foundation)
Czech Academy of Sciences, Institute of Macromolecular Chemistry, Prague

3.4 Soft Matter Physics

3.4.1 General Scientific Goals - Polymers and Membranes in Cells

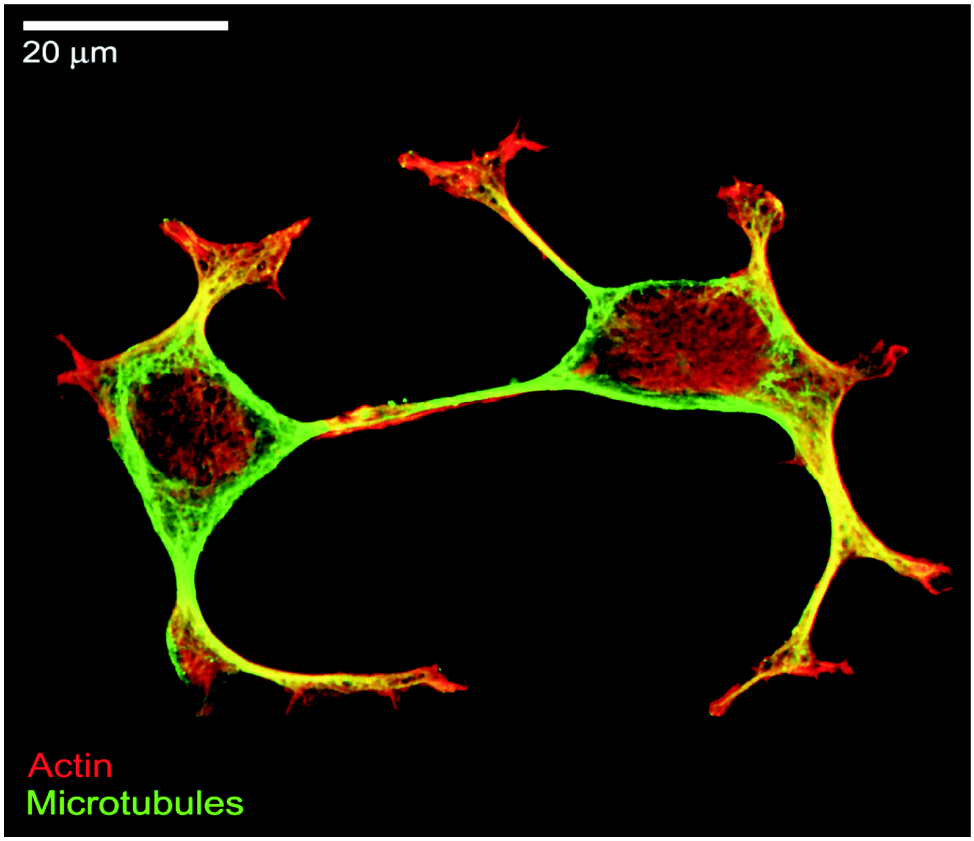

Fig. 1: Cytoskeleton (i.e. intracellular polymer networks) of two neuronal cells. Actin filaments are shown in red and microtubles are shown in green.

Studies of soft matter physics on the scale of nanometers to tens of microns, i.e., on the scale of proteins and cells, in complex multifunctional biological matter - often far from equilibrium and frequently behaving in a highly nonlinear manner - are the next big challenge for physics. Our research group is based on the idea that a complete understanding of molecular and cell biological systems calls forth a new type of fundamental physics, biological physics, which can describe biological soft matter with active elements and which is adaptive to multipurpose. Over the last decade there has been tremendous progress in molecular biology. Nevertheless, this progress will only impact the design and development of new materials if a novel combination of nanosciences and soft matter physics is developed - bridging biology and engineering. This synergetic research in physics, chemistry, bioengineering and biology simultaneously advances our fundamental knowledge-base and provides novel applications in biomedicine and materials science.

The need for novel soft matter physics is exemplified in the actin cytoskeleton, an active network of protein filaments and molecular machines found in biological cells, and the plasma membrane, a complex liquid crystal material made out a wide variety of lipids and proteins. In contrast to well-described, conventional materials the actin cytoskeleton

and the plasma membrane are not a static materials they actively change in response to various cellular functions (e.g. cell motility), conversely mechanical stimuli applied to them directly feedback into cell function (e.g. mechanotransduction). Our division's specific goal is to unravel the biological physics of the actin cytoskeleton and the plasma membrane. This complex soft matter with its active responses unmatched in the inanimate world and with its multiple functions requires an integrated approach which *in vitro* investigates the motions and interactions of actin filaments, molecular motors, and lipids on a single molecule level and *in vivo* measures the collective properties on a cellular level. This guiding principle allowed us over the last years to identify the following key projects described in the next sections, which clearly illustrate the unparalleled, fundamentally new properties of the actin cytoskeleton and the plasma membrane.

The technical strength of our group lies in the synergetic and unique combination of methods which allows us the study of the actin cytoskeleton and the plasma membrane from a level of individual molecules *in vitro* to *in vivo* studies of the cellular actin cytoskeleton with techniques which integrate novel microrheological techniques, optical nanomanipulation, multiphoton microscopy, single particle tracking in Langmuir monolayers and molecular biology. We have pioneered the study of the polymer dynamics of individual actin filaments in actin networks (e.g. direct visualization of reptation in actin networks). For the first time we succeeded in visualizing the motions of single molecule in lipid monolayers. We have developed a unique tool box to measure the viscoelastic properties of individual cells locally by AFM-based microrheology as well as globally with a new laser trap, the optical stretcher. These two techniques complement each other by allowing us to obtain very detailed information from single cells as well as to screen large numbers of cells. The AFM-based technique also allows us for the first time to measure the forces that enable a motile cell to move forward. Furthermore, we have developed novel approaches to use laser light to manipulate cells without touching them as we have demonstrated with the optical stretcher and the optical neuron guidance.

(a) 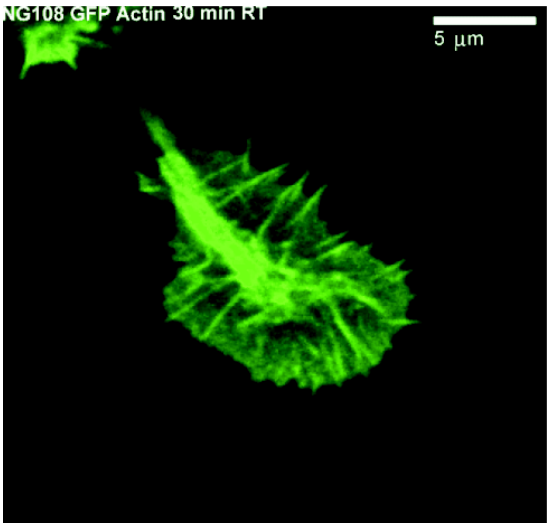

(b) 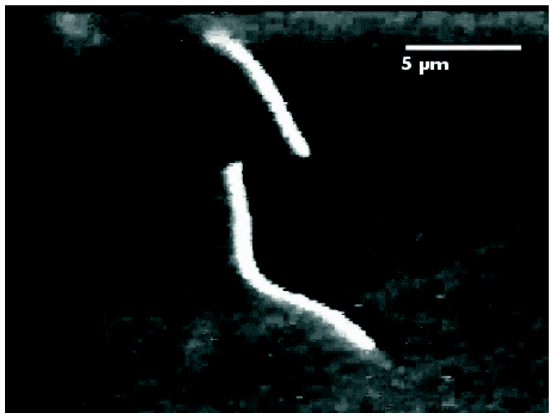

Fig. 2: Actin cytoskeleton of biological cells. (a) Actin cytoskeleton of a neuronal growth cone visualized by transfection with GFP-actin. (b) Single actin filaments *in vitro*.

3.4.2 Active Polymer Dynamics in Cells

David Smith, Vanessa Bell, Brian Gentry, Josef Käs

The molecular motor myosin II has not only the well-known force generating functions in structures such as muscle cells; it can fluidize entangled actin networks by superseding reptation dynamics with myosin-induced filament sliding. This illustrates how molecular motors can overcome conventional polymer dynamics and generate an active material with a new switchable viscoelastic behavior. Up to 40% of a cell's energy (i.e. ATP) turnover fuel this active, energy-dissipating states of the actin cytoskeleton illustrating the importance for a cell's material properties

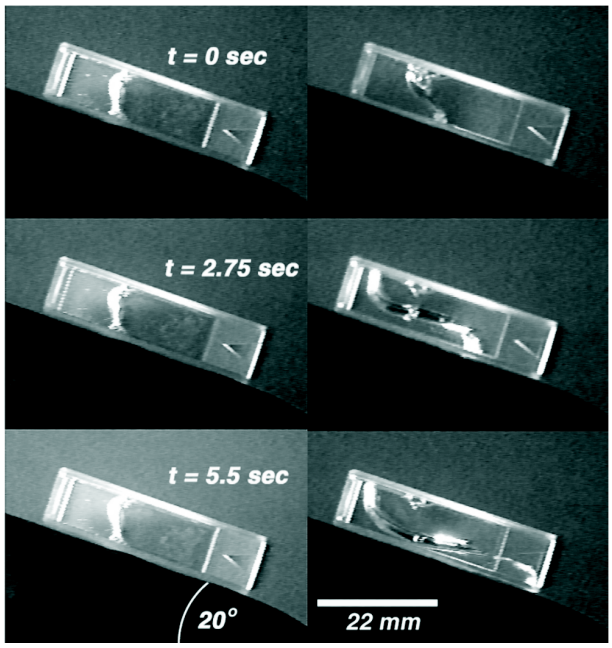

Fig. 3: Comparison of the flow properties of actin networks with inactive (left side) or active (right side) myosin dispersed in them. Under ADP conditions with inactive myosin the samples gelated and behaved like an elastic solid. In the presence of ATP or when caged ATP was released the active motors caused fluid-like flow properties.

As a subsequent step we will build a biomimetic copy of the lamellipodium, one of the most dynamic parts of the actin cytoskeleton, and characterize its rheologic properties. For this purpose, we will use a specially functionalized spherical microfluidic chamber that promotes actin polymerization at its outer border and actin depolymerization towards the center of the chamber. In this fashion, the reconstituted actin network in the sample chamber displays the same retrograde flow found in cells. The outside coating also cause an orientation of the actin filament's plus ends and of the fork-shaped ends of Arp 2/3 towards the outer rim of the microfluidic chamber. Rheology will be performed by our AFM-technique and by two bead microrheology.

Publications: 1) D. Humphrey, C. Duggan, D. Saha, D. Smith and J. Käs, Active fluidization of polymer networks through molecular motors, Nature, 416 413- 416 (2002) For background see also: 2) J. Käs, H. Strey and E. Sackmann, Direct imaging of reptation for semiflexible actin filaments, Nature, 368, 226-229 (1994)

3.4.3 Molecular Motors and Entropic State of Polymer Networks

David Smith, Vanessa Bell, Brian Gentry, Josef Käs

Besides the well known functions in contractility and transport molecular motors also influence the spatial organization of actin filaments and microtubules. We found that with increasing myosin-to-filament ratio the isotropic actin mesh continuously transforms first into a network of filament bundles which then orders into a pattern of asters and at even higher concentrations of the motor myosin to highly condensed actin coagulates. These assemblies drastically depend on motor activity. Although fully active myosin minifilaments randomize, i.e. disorder, actin networks, ATP-depletion, which drastically slows down motor function and makes the minifilaments to crosslinkers, cause the association of supramolecular actin filament assemblies. In contrast, Dr. Surrey's and Dr. Nedelec's group at the EMBL in Heidelberg have seen that active motor constructs caused aster formation and ordering in microtubule networks whereas inactive motors resulted in the decay of this ordered structures. Nevertheless, both results clearly illustrate that molecular motor activity impacts the spatial organization of the cytoskeleton.

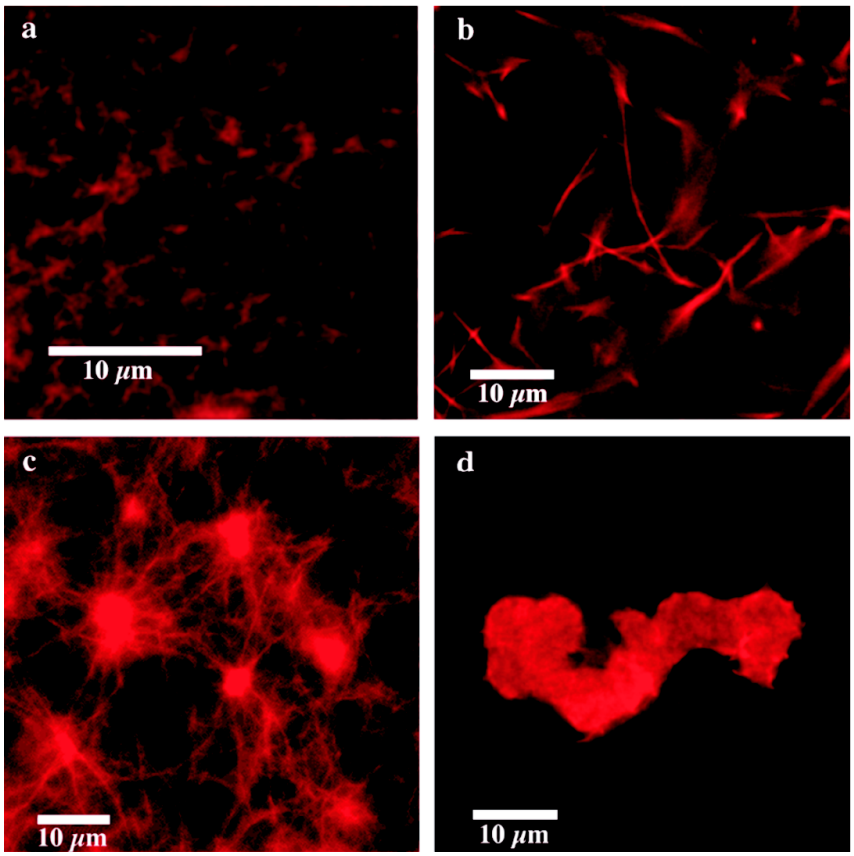

Fig. 4: Fluorescence pictures of spatial patterns formed in actin-myosin networks at different motor concentrations after ATP is used up: a) random mesh at 10 motors/ filament, b) network of actin bundles at 10^2 motors/ filament, c) asters at 10^3 motors/filament, d) strongly condensed phase at 10^4 motors/filament.

In usual polymer systems order is frequently controlled by temperature as illustrated by thermotropic liquid crystals. Temperature is a fixed parameter in biological cells. Thus, motor activity may be an alternative variable - not known in conventional material science - to control order and disorder. However, in the light of the contrasting effects observed for microtubules and actin a fundamental understanding can be only found in collaboration between the Leipzig and the Heidelberg group considering the differences and common of the two biopolymer systems. Here also the collaboration with Dr. Amblard from Dr. Joanny's laboratory at the Institute Curie will be of great help. He has recently shown that the fragment S1 of the protein myosin, the active subunit of myosin minifilaments, increases the kinetic energy, i.e. the effective temperature, of an actin network when the fragment is activated.

Publications:
1) A.L. Lin, B.A. Mann, G. Torres-Oviedo, B. Lincoln, J. Käs, H.L. Swinney, Localization and extinction of bacterial populations under inhomogeneous growth conditions, Biophys. J., in press (2004)
2) D. Smith, D. Humphrey, C. Duggan and Josef Käs, Molecular motor induced order disorder transitions in polymer networks, Nature, submitted (2003)
For background see also:
3) Nedelec, F.J., Surrey, T., Maggs, A.C. and Leibler, S. Self-organization of microtubules and motors, Nature 389, 305-308 (1997)

3.4.4 AFM-based Microrheology

Kristian Franze, Jens Gerdelmann, Bernd Kohlstrunk, Andreas Reichenbach, Thomas Arendt, Wirtz, Josef Käs

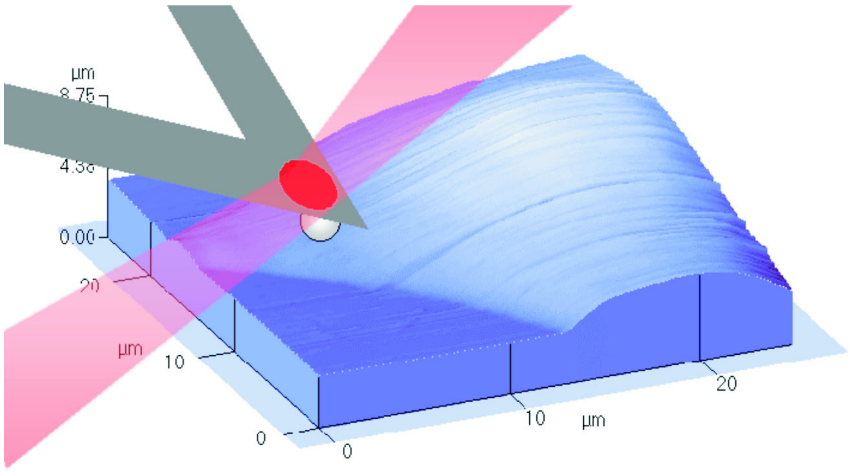

Fig. 5: An AFM cantilever with a polystyrene bead of well-defined diameter is used as a scanning tip to probe the viscoelastic and active responses of cells to deformation forces. The entire AFM is mounted on an inverted microscope equipped for fluorescence and phase contrast microscopy. The AFM is equipped with a temperature controlled wet-cell to assure stable physiologic conditions for the cells.

Atomic Force Microscopy (AFM) measurements of cell elasticity have been only of a qualitative nature due to the complex, nonlinear deformation by standard AFM tips, hydrodynamic contributions of the cantilever, and deviations from the Hertz model caused by finite sample thickness. Our new AFM-based microrheology allows us precise quantitative measurements of the spatial distribution of a cell's viscoelastic behavior (i.e. complex shear modulus and Poisson ratio) and adhesive state. In particular, the active lamellipodial regions of a cell show a viscoelastic signature similar to actin networks *in vitro*. Thus, dynamic measurements of the viscoelastic changes will provide an understanding of the actin-based active processes underlying cell motility, which will ultimately provide a template for the design of active polymeric materials.

A particular focus of our microrheological studies have been questions related to biomedical topics. These questions relevant to biomedicine are to what extent Alzheimer disease causes a weakening in the structural strength of neuronal cells, whether drugs that soften lung epithelial cells can reduce the risk of respiratory distress syndrome, and whether structural defects in Miller cells are the cause of retinoschisis.

Publications:
1) S. Park, R. Cardenas, J. Käs, and C.K. Shih, Correlation between local viscoelasticity and motility of fibroblasts, Biophys. J., submitted (2003)
2) R. Mahaffy, S. Park, E. Gerde, J. Käs, and C.K. Shih, Quantitative analysis of the viscoelastic properties of thin regions of fibroblasts using atomic force microscopy, Biophys. J., 86, 1777-1793 (2004)
For background see also:
3) R. Mahaffy, C.K. Shih, F.C, MacKintosh, and J. Käs, Scanning probe-based, frequency-dependent microrheology of polymer gels and biological cells, Phys. Rev. Lett., 85(4), 880-883 (2000)

3.4.5 Mechanotransduction

Jens Gerdelmann, Timo Betz, Bernd Kohlstrunk, Hubert Wirtz, Thomas Arendt, Josef Käs

One of the most exciting results in cytoskeletal research of the last ten years was that the cytoskeleton is not only involved in cell motility and mitosis by actively organizing the cell, but also senses the cell's mechanical environment and reacts to changes. For this process the term mechanotransduction has been coined. Since the lung is an active organ subjected to various mechanical forces, all cells of the lung have been implicated in mechanotransduction events. A single mechanical stretch of alveolar type II epithelial cells causes a transient increase in cytosolic Ca^{2+} mobilized from intracellular stores and followed by a sustained increased pulmonary surfactant secretion. The specific mechanisms how the mechanical stimuli are transmitted throughout mechanotransduction are not understood. The alveolar type II cells are particularly well suited to study the transduction process since the response is immediate and not an indirect change in gene expression. Furthermore, we study to what extent changes in mechanotransduction are involved in the progression of Alzheimer disease.

AFM-based microrheology will provide a spatial map of the viscoelastic constants of alveolar cells to determine a characteristic dissipation length, which limits the intracellular

transmission of mechanical stimuli. By using the same AFM-techniques our laboratory has recently demonstrated that growing neurons retract when opposed to a threshold stress equaling their mechanical strength. For the alveolar cells, the threshold stress for intracellular Ca^{2+}-release and the cellular areas which respond preferred to mechanical stimulation will be determined. These data, which will precisely characterize the initial stimuli in mechanotransduction events, will provide a fundamental understanding how the cytoskeleton as an active polymer network can function as a delicate mechanical sensor.

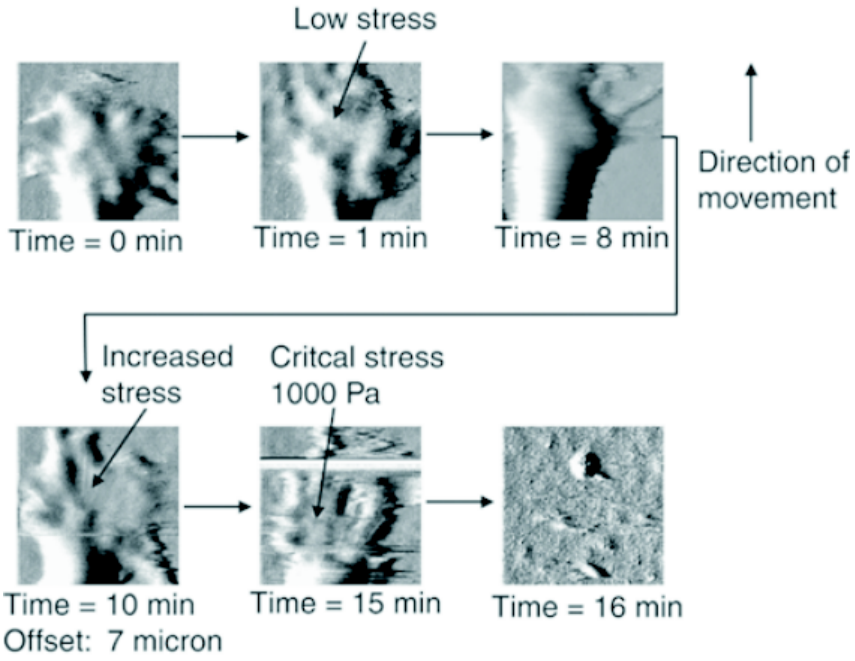

Fig. 6: Time series of a PC12 cell undergoing a critical force measurement by AFM. The first two images demonstrate the negligible effect of the imaging forces on the forward extension of the growth cone (size $\approx 5\,\mu$m). Following this, a low force was applied at a single point. Again, no effect was observed on the forward motion of the growth cone, which then moved out of the current imaging range. After the necessary offset, a higher force was applied and resulted in a significant change in the growth cone shape with some withdrawal. At even higher forces the growth cone retracted from view. The critical force corresponds to an approximate deforming stress on the growth cone of approximately 900 Pa. This withdrawal stress was verified on another cell with a value of approximately 1000 Pa. With time, the flat growth cone reformed, thus, demonstrating that although the stresses forced a withdrawal, critical damage was avoided.

Publications:
1) M. Lakadamyali, J. Bayer, R.E. Mahaffy, N.L. Peffly, C.K. Shih, and J. Käs, Local mechanosensing by neuronal growth cones, Nature, submitted (2003)
For background see also:
2) H. R. Wirtz et al, Calcium Mobilization and Exocytosis After One Mechanical Stretch of Lung Epithelial Cells, 250, 1266-1269, Science, 1990

3.4.6 Forces in Cell Motility

Claudia Brunner, Michael Gögler, Allen Ehrlicher, Bernd Kohlstrunk, Josef Käs

Cell motility is a fundamental objective in many disciplines, such as cell biology, developmental biology, neuroscience, biomedicine and biophysics. Mechanisms of force generation in cells, involving actin polymerization or molecular motors, have been described in various models, but experimental data on measured forces hardly exist. Here we present a direct *in vivo* measurement of the forward force generated by a fish epithelial keratocyte. We attached a polystyrene bead to a cantilever-tip of an atomic force microscope (AFM), positioned it in front of a cell, and pushed it slightly onto the plastic surface of the Petri dish. The cell crawls underneath the bead and pushes therefore the cantilever up. The forward force is calculated by the detected upward force using a simple "wedge model". The results might indicate different force mechanisms between the front of the lamellipodium and regions near the cell body.

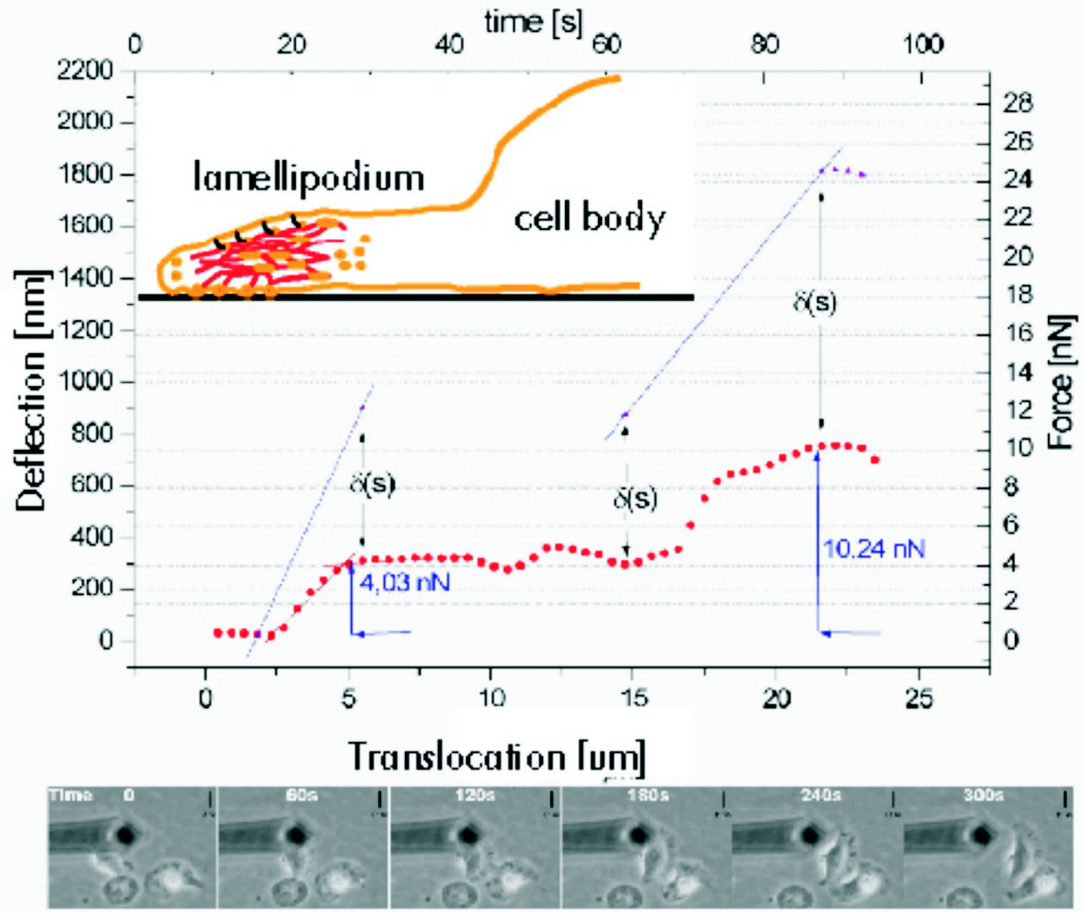

Fig. 7: Force exerted by a cell on an AFM-cantilever.

Publications:
1) C. Brunner, M. Gögler, A. Ehrlicher, and J. Käs, Propulsive forces of fast moving cells, Nature, in preparation (2004)

3.4.7 Optical Deformability as a Cell Marker

Falk Wottawah, Stefan Schinkinger, Bryan Lincoln, Susanne Ebert, Frank Sauer, Maren Romeyke Frank Emmrich, Anderas Reichenbach, Torsten Remmerbach, Jochen Guck

To fully comprehend the role the multifunctional viscoelastic properties of the actin cytoskeleton have for cells it is essential to measure the variability of cell elasticity within and between cell lines. This requires high throughput measurements, which cannot be provided by relatively slow techniques such as our AFM technique (the scans provide precise local data, but need time). To accurately measure the variability of the elasticity of whole cells within and between cell lines we have devised and built an optical tool with an unprecedented force range (pN – nN) to stretch single cells between two laser beams, the optical stretcher. By using a microfluidic setup for the optical stretcher, samples with many cells can easily be handled similar to a flow cytometer. Our results show that cells actively respond to deforming stresses and that optical deformability is a precise cell marker, which allows diagnosing diseases such as cancer in which the cytoskeleton dedifferentiates. Our finding that the elasticity of the actin cytoskeleton is a tightly regulated cellular parameter illustrates the importance of the viscoelastic properties for a cell's state. Already samples of 50 cells are sufficient to obtain statistically significant results. Due to the high sensitivity of this technique the optical stretcher can uniquely distinguish different stages of the progression of cancer as demonstrated for breast cancer. A commercial microfluidic optical stretcher is currently being developed together with a Dresden based company, Gesim.

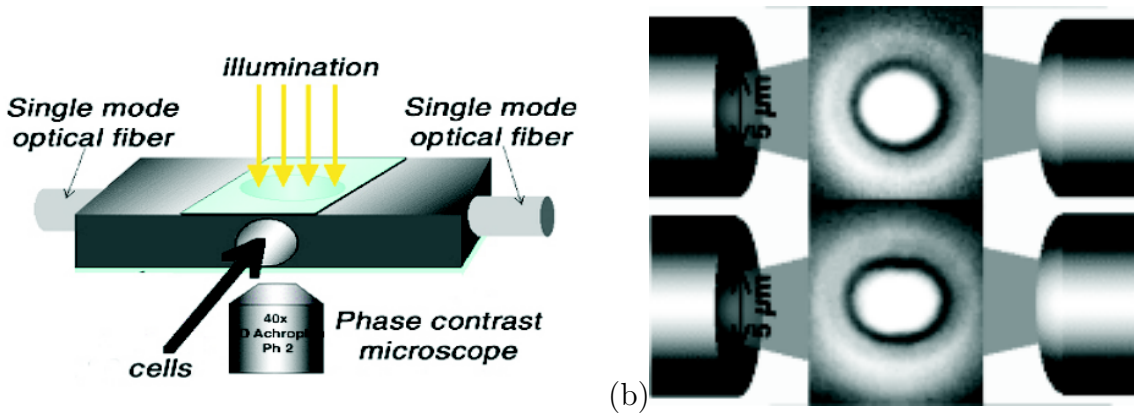

Fig. 8: The optical stretcher. The upper part shows the microfabricated flow chamber. The lower two pictures show the two laser beams stretching a fibroblast (diameter ≈ 30 μm) in phase contrast. Between the upper and the lower picture of the trapped cell, the laser power has been increased from 10 mW to 800 mW. The optical fibers, not drawn to scale, are 150 μm away from the cell. This distance was chosen so that the beam, diverging slightly from a 5 mm waist, illuminates the entire cell.

Publications:

1) J. Guck, H.M. Erickson, R. Ananthakrishnan, D. Mitchell, B. Lincoln, S. Schinkinger, F. Wottawah, M. Romeyke, J. Käs, S. Ulvick, C. Bilby, Optical Deformability as Inherent Cell Marker for Malignant Transformation and Metastatic Competence, Biophys. J., submitted

For background see also:
3) J. Guck, R. Ananthakrishnan, T.J. Moon, C.C. Cunningham and J. Käs, Optical deformability of soft dielectric materials, Phys. Rev. Lett., 84(23), 5451-5454 (2000)
3) J. Guck, R. Ananthakrishnan, T.J. Moon, C.C. Cunningham and J. Käs, The Optical Stretcher - A Novel, noninvasive tool to manipulate biological materials, Biophys. J., 81 767-784 (2001)

3.4.8 Biomolecular Machines Based on Active Viscoelasticity

Karla Müller, Revathi Ananthakrishnan, Maren Romeyke, Mireille Martin, Falk Wottawah, Stefan Schinkinger,Attila Tarnok, Josef Käs

Due to their inherent elastic properties it is common in materials science that polymers are used to generate well-defined mechanical properties. In cells a fundamental aspect is added to providing structural support. The cytoskeleton is an active structure participating in and responding to cell function. As a general rule, changes in the functioning of a cell are mirrored in cytoskeletal changes. During malignant transformation the cytoskeleton gets less pronounced and more disordered. In cancer metastasis the cytoskeleton transforms from a structural material, to an active machine, which propels a metastatic cell through viscoelastic changes. Thus, precise measurements and a fundamental understanding of the dynamic viscoelastic properties are central to understand the cytoskeleton as a guide for new active materials. For this purpose we measure cell elasticity as a function of cytoskeletal composition and of cellular motility. In particular, we consider the clearly visible active responses of the cytoskeleton to deforming stresses.

To determine the dependence of cell elasticity on the cytoskeletal composition we transfect cells with oncogenes to induce changes in the molecular composition of the cytoskeleton. Using the optical stretcher to measure whole cell elasticity we particularly pick transfected clones which represent the entire spectrum of achievable cell elasticities. The elasticity data are then correlated with cytoskeletal architecture and composition by Western blotting, RNA microarrays and multiphoton microscopy. The cytoskeleton is a complex polymeric compound material which strain hardens, behaves highly nonlinear and can actively respond to deformations. The cytoskeletal transformation to an active cellular machine which is the driving force in cancer metastasis is exemplified when MCF-7 cells, a breast tumor cell line, are treated with phorbolester and become motile. We monitor the time course of the phorbolester-induced cytoskeletal changes by cell elasticity measurements with the optical stretcher, which identifies time points of significant change in cytoskeletal elasticity, and correlate this data with expression data of cytoskeletal proteins obtained by RNA microarrays. Since we assume that these points represent the key molecular events in the development to an actively advancing cell we use our AFM-based microrheology to obtain a temporal and spatial map of the viscoelastic changes in the lamellipodial region, i.e. leading edge of the cell, at these characteristic points. Despite there is great knowledge about the proteins of the cytoskeleton multiple models for cell motility have been proposed. Recent experiments in the Joanny lab at the Institute Curie have shown that cell motility is solely based on the active material properties of the cytoskeleton. Nevertheless, the cytoskeleton is highly redundant. Our experiments have the advantage that they correlate viscoelasticity with molecular architecture and they monitor the changes from a non-motile to a motile cell. This allows us to extract the

key elements which allow the cytoskeleton to become an active machine which advances through viscoelastic changes. These data will be cross-fertilized by Dr. Joanny's theoretical work. He currently develops a model of cell motility based on an active viscoelastic material. An experimental proven model of cell motility will be the ideal basis to develop active biomimetic materials.

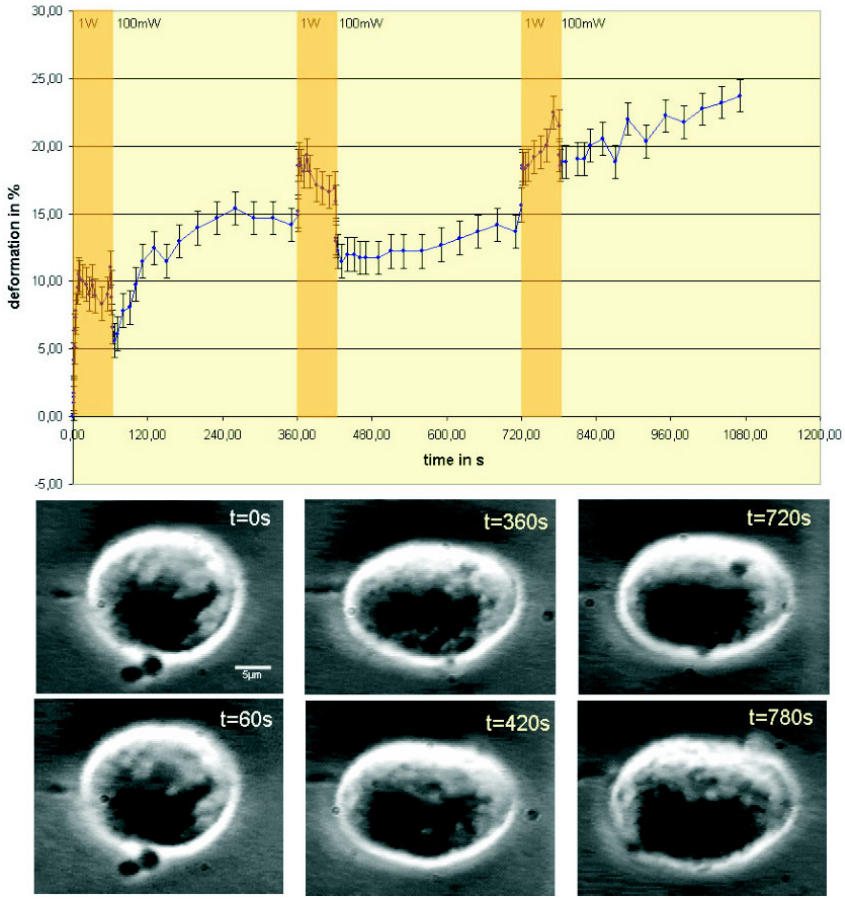

Fig. 9: Active response of a fibroblast to the mechanical stress exerted by the optical stretcher.

Publications:
1) R. Ananthakrishnan, J. Guck, F. Wottawah, S. Schinkinger, Estimating the Contribution of Actin Networks to the Elastic Strength of Fibroblasts, Biophys. J., in press
2) F. Wottawah, S. Schinkinger, B. Lincoln, R. Ananthakrishnan, M Romeyke, J. Guck, J. Käs, Optical Rheology of Biological Cells, Phys. Rev. Lett., submitted

3.4.9 Optically Guided Neuronal Growth

Allen Ehrlicher, Timo Betz, Daniel Koch, Bjoern Stuhrmann, Michael Goegler, Elke Westphal, Mark Raizen, Thomas Arendt, Bigl, Josef Käs

Understanding and controlling neuronal growth are fundamental objectives in biophysics, neuroscience, and biomedicine, and are vital for the formation of neural circuits

in vitro, as well as nerve regeneration *in vivo*. The growth cone is a complex molecular machine, which is regulated by an intricate interplay of gene expression and signal transduction events. These complicated molecular instructions are translated by the cytoskeleton into mechanical forces and active morphological changes by mechanisms, which are not fully understood.

We have developed a laser-based method to guide neuronal growth cones, which has been reported in PNAS [A. Ehrlicher et al. Guiding neuronal growth with light, PNAS, 99, 16024, (2002)]. Optical forces control the direction and speed taken by an actively extending growth cone, as well as induce bifurcations of a growth cone. More recently, we have seen that it is also possible to optically arrest growth cones and induce cell-cell contacts between growth cones and other soma. Since laser-generated forces (e.g. optical gradient forces) predominantly influence larger macromolecular ensembles, we assume that the laser manipulates the cytoskeleton and that interactions with signaling molecules are unlikely. The primary goals in this proposal are to identify the fundamental processes underlying optical guidance, as well as to illuminate further the cytoskeletons role in growth cone movement, branching, and the early stages of synaptogenesis. Moreover, we have a new investigative tool to research the active cytoskeletal processes in growth cone motility.

To understand the optomolecular basis of laser-directed neuronal growth and to elucidate the cytoskeletal basis of growth cone motility, we propose the following six hypothetical mechanisms, which we believe to be the most plausible in optical guidance: 1) optical gradient forces biasing intracellular diffusion; 2) biased thermal ratchets at the lamellipodial leading edge; 3) hindered retrograde flow of the actin network; 4) stresses inducing Ca^{2+}-release; 5) optical gradient forces directing filopodia (which are important for growth cone steering); 6) intracellular reactions influenced by local laser heating. From these hypotheses, we will identify the relative importance of each in optical guidance through a series of decisive experiments and in turn we will clarify their relevance in cytoskeletal dynamics.

Since the cytoskeletal machinery is responsible for all morphological changes of the growth cone, a second series of experiments will examine directed arrest, bifurcation, and cell-cell contacts. These experiments will investigate to what extent optically induced bifurcations and growth cone-soma contacts show changes of the cytoskeleton similar to cytoskeletal maturation found in neuronal branching and synaptogenesis.

Our two optical guidance setups are based on optical tweezers. In optical guidance the laser interacts with intracellular processes, while in optical tweezers cellular structures are mechanically moved. Inspired by promising preliminary results, we will conduct our experiments with primary embryonic rat neurons, which are supplied by our collaborator Prof. Arendt at the Paul-Flechsig Institute for Brain Research. In parallel, we will use cell lines transfected with GFP-actin and YFP-tubulin to visualize the distributions of these two essential cytoskeletal components during optical guidance. To investigate the above mentioned hypotheses further, we will apply techniques well established in our lab, such as multiphoton/confocal microscopy and atomic force microscopy.

In the long term, as we learn more about our system and improve our guidance techniques, we will return our knowledge to the scientific community in the form of a novel non-invasive laser-based tool for controlling neuronal growth and network formation. Moreover, our results on optomolecular interactions will provide a better understanding how cytoskeletal dynamics morphologically change the growth cone.

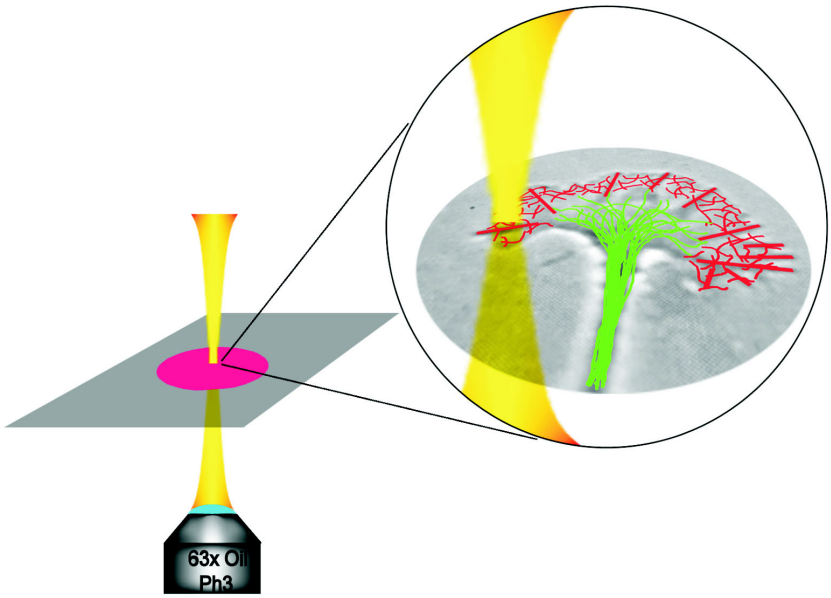

Fig. 10: Experimental setup for the optical guidance of growing neurons. A laser spot ($\varnothing$= 2 – 16 μm, power = 20 – 120 mW, λ = 800 nm) was placed with partial overlap in front of an actively extending growth cone. The overlap area was chosen in the direction of the preferred growth and to cover the actin cortex, which directly underlies the plasma membrane and drives the advancement of the leading edge of the nerve.

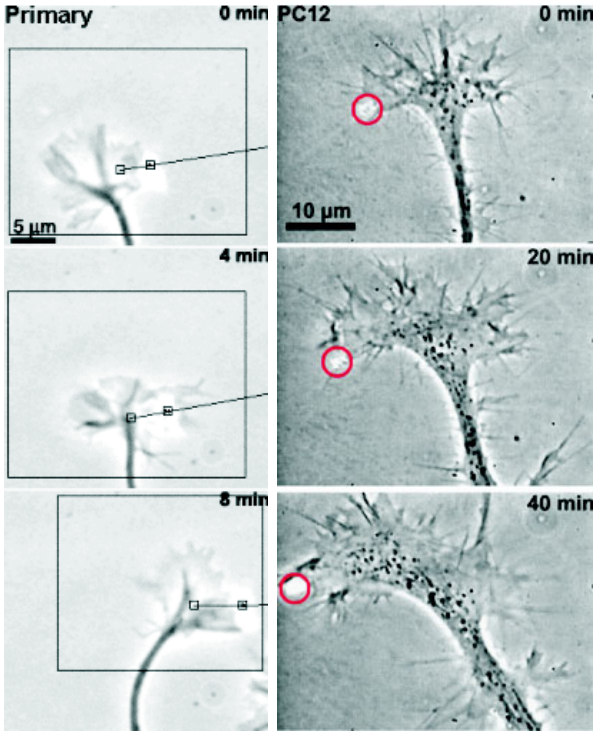

Fig. 11: Optically guided turns of growth cones. Left side: Guided growth of a primary embryonic rat cortical neuron. The square over the bright spot indicates the position of the laser. The black line displays the desired optical guiding path. Right side: Guidance of a PC12 growth cone. The circle indicates the position of the laser.

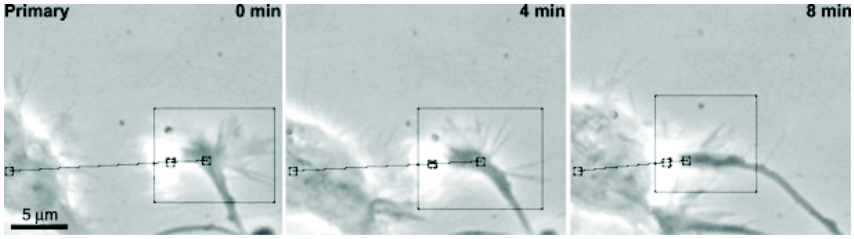

Fig. 12: Optically induced cell-cell contact. The growth cone of a primary rat cortical neuron was guided towards and put in contact with the soma of another primary cell.

Publications:
1) A. Ehrlicher, T. Betz, B. Stuhrmann, D. Koch, V. Milner, M. Raizen and J. Käs, Guiding neuronal growth with light, PNAS, 99(25) 16024-16028 (2002)
For background see also:
2) E. J. Furnish, W. Zhou, C.C. Cunningham, J. Käs, and C.E. Schmidt, Increased actin severing via gelsolin overexpression enhances neurite outgrowth, FEBS Lett., 508 282 - 286 (2001)

3.4.10 Signal Transduction Investigated by Nano-probes

Florian Rückerl, Doug Martin, Martin Forstner, Undine Dietrich, Carsten Selle

In inhomogeneous 2-dimensional lipid monolayers with spatial domain structures (i.e. obstacles) that can vary between nanometers and tens of microns the Brownian dynamics of nano-probes (quantum dots and polystyrene beads) is studied by single particle tracking. We specifically investigate the impact of dipole-dipole interactions between the probe particle and lipid domains dispersed in a more fluid lipid matrix on local diffusion. Our initial results indicate sharp transitions with increasing interaction strength between extensive 2-dimensional diffusion among the domains of the monolayer and 1-dimensional diffusion along the domain boundaries. In the transition regime 1- and 2-dimensional diffusion behavior recurrently interchanges. Monte Carlo simulations predict that in the long term limit this recurrent changes result in 2-dimensional normal diffusion with a drastically decreased effective diffusion coefficient. However, it is also conceivable that in future experiments subdiffusive behavior will be observed in the transition regime. Since the radial dependence of dipole-dipole interactions can change conditional on domain size and shape the diffusive behavior will critically depend on the 2-dimensional topography of the monolayer. In synopsis, we plan to investigate how dipole-dipole interactions in inhomogeneous films influence diffusive transport by controlling interchange between transient events of localized 1-dimensional diffusion and extensive 2-dimensional diffusion. This knowledge is a potential tool to enhance diffusion-limited biochemical reactions.

Inspired by observations of a wide variety of diffusive behaviors in cell membranes - including spatially and temporally varying behavior and anomalous diffusion - diffusive transport in lipid monolayers and bilayers has become of a broad scientific interest. From a biological perspective specific lipid raft mixtures have been implicated in the control of the diffusive behavior and of the potential landscape in lipid films. By and large, theoretical work proposes that lipid domains as confining structures drastically slow down

diffusive transport to a degree that anomalous diffusion can occur. Nonetheless, this poses very specific conditions on the confining structures. Diffusion in a random maze remains normal. However, if these confining random boundaries become attractive for the Brownian driven probe particle the impediment of diffusive transport is more drastic and depending on the specific attractive potential subdiffusion can arise. Since lipid domains as well as membrane proteins exhibit dipole moments we have chosen to investigate the basic Brownian dynamics of a probe particle in a confining landscape that has through dipole-dipole interactions attractive boundaries.

The study of the fundamental Brownian dynamics in inhomogeneous lipid systems requires the ability to follow the track of Brownian particles over a broad range of time (0.01 – 1000 s) and length (10^{-7} – 10^{-2} m) scales and to control and vary the state of the inhomogeneous landscape. For this purpose we developed a technique that allows us to perform single particle tracking experiments on Langmuir monolayers overcoming previous problems with the vibrational sensitivity and monolayer drift (M. Forstner, J. Käs and D. Martin, Single lipid diffusion in Langmuir monolayers, Langmuir, 17(3), 567-570 (2001)). In addition, our novel data analysis allowed us to demonstrate that previous reports of subdiffusion in cell and model membranes were only apparent due to an artifact caused by even small noise levels (D. Martin, M. Forstner and J. Käs, Apparent subdiffusion inherent to single particle tracking, Biophys. J., 83 2109-2117 (2002)). More recent improvements permit the simultaneous visualization of the Brownian dynamic of individual particles and of the surrounding inhomogeneous landscape (M. Forstner, D. Martin, A.M. Navar, and J. Käs, Simultaneous single-particle tracking and visualization of domain structures on lipid monolayers, Langmuir, 19, 4876-4879 (2003)). This approach allowed us to demonstrate that in the liquid-crystalline coexistence regime of DMPE-monolayers probe particles switch between periods of 2-dimensional diffusion in the fluid phase and phases of 1-dimensional diffusion along the liquid-crystalline domain boundaries (D. Martin, M. Forstner and J. Käs, Dipole-dipole induced transitions in the dimensionality of diffusion, PRL, submitted).

As probe particles we will use quantum dots and fluorescent beads (a few hundred nanometers in diameter) since they provide the possibility to visualize simultaneously the landscape (i.e. domains) of the monolayer by fluorescent techniques. They will be either directly immersed in the monolayer or coupled to lipids by antibodies or peptides. As monolayers we will use single lipids or fatty acids which are well known systems to form domains in the liquid-crystalline coexistence regime. We will use systems where the domains solely exhibit a net dipole moment (e.g. DMPE, DPPC) as well as systems where the molecules of the monolayer are also charged (e.g. DMPA). The use of the different lipids and fatty acids in conjunction with the direct control of the monolayer density allows us to choose domain size, shape, and topology. The detailed tracks of the probe particles enable us to analyze diffusion on a wide range of length and time scales. The density distribution of the probe particle with respect to the domain boundaries provides measurements of the energy landscape the particle feels. These experimental efforts will be complemented by extensive Monte Carlo simulations. We have already developed the required algorithms and software (D. Martin, M. Forstner and J. Käs, Dipole-dipole induced transitions in the dimensionality of diffusion, PRL, submitted).

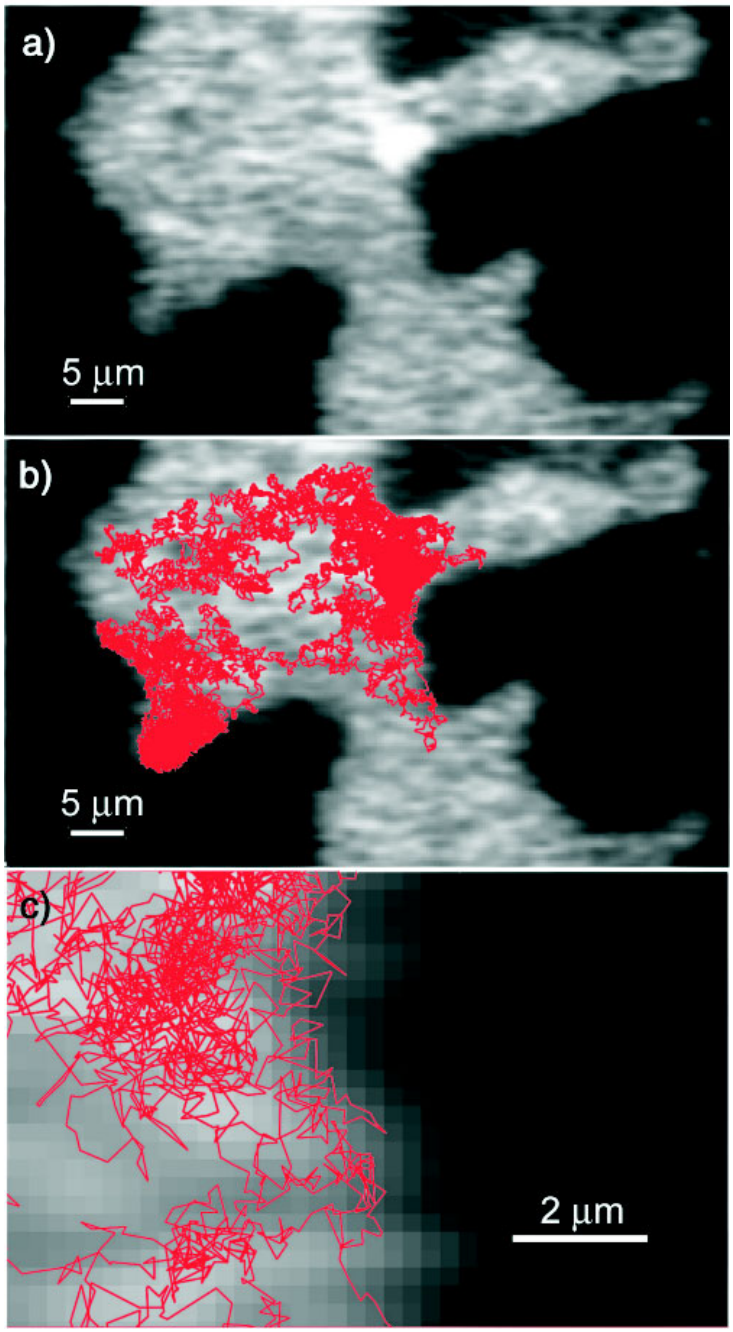

Fig. 13: 200 nm fluorescent polystyrene bead (bright spot marked by the arrow) at the boundary of the liquid expanded (light grey) and the liquid condensed phase (dark grey) of a DMPE lipid monolayer at a surface pressure of 16.0 ± 0.5 mN/m. (b) Overlay of the bead's random walk on the monolayer picture. (c) Magnification of a portion of the random walk close to the domain boundary.

It is one of the foremost properties of nature to be fare from equilibrium. Consequently, this means that energy dissipating states stabilize ordered states. Thus, we will explore to what extend the reaction-diffusion system formed by the lipid PIP2, the protein MARCKS, and the enzymes protein kinase C and phospatase constitutes under ATP-hydrolysis a nonlinear pattern forming system. Since the phase space is large and it is practically im-

possible to find the right pattern forming conditions by trial-and-error our efforts will be closely guided by theoretical modelling. Since PIP2 is a quintessential second messenger in cells these findings would be of key relevance for cell biology.

Already in 1952 the British mathematician Alan Turing predicted that reaction-diffusion systems can form nonlinear patterns. Despite of the nonequilibrium state of nature reports about nonlinear pattern forming systems in biology remain sparse. Considering the eminent importance of PIP2 for signal transduction in cells the finding that the MARCKS-PIP2 system is a nonlinear pattern forming system could have profound implications, e.g. instabilities could serve as fast switches in cell signaling.

Nonlinear pattern forming reaction-diffusion systems are typically studied in steady state reactors. This is practically impossible when we use Langmuir monolayers since a steady supply of biochemical reactants would induce turbulent flows (note: also vesicular systems do not allow a steady state exchange of the reactant lipids). Nevertheless, the monolayers offer a large observation space which is necessary to determine the wavelengths of the occurring patterns. Furthermore, the large monolayer surface and the extensive subphase will provide large enough reservoirs to reach a quasi steady state, which should allow us to observe pattern formation for sufficient long times.

Publications: 1) D. Martin, M. Forstner and J. Käs, Attractive interactions between membrane structures and single particles drastically impact lateral diffusion, Phys. Rev. Lett., submitted 2) D. Martin, M. Forstner and J. Käs, Apparent subdiffusion inherent to single particel tracking, Biophys. J., 83 2109-2117 (2002) For background see also: 3) M. Forstner, D. Martin, A.M. Navar, and J. Käs, Simultaneous single-particle tracking and visualization of domain structures on lipid monolayers, Langmuir, 19, 4876 - 4879 (2003) 4) M. Forstner, J. Käs and D. Martin, Single lipid diffusion in Langmuir monolayers, Langmuir, 17(3), 567-570 (2001)

3.4.11 Interaction of Functionalized Nanoparticles with β-Amyloid Peptides

Herbert Schmiedel, Wolfgang Härtig

The general purpose of the project is the explanation of the structure and the physicochemical properties of nanoparticles acting as carriers of active ingredients in the treatment of neurodegenerative deseases such as Alzheimer disease (AD). One hallmark of brains in AD is the appearance of extracellular plaques consisting of amyloid-beta-peptide aggregates (Aβ, usually comprising 40 – 42 amino acids). Polymer nanoparticles coated with various agents (see e.g. /1/) were shown to penetrate the blood-brain barrier and might interact with the Aβ plaques. Coated nanoparticles will be chosen for the *in vitro* interactions between Aβ- aggregates and some of their specific ligands. This study will include nanoparticles surface-labelled with: 1. b-sheet breaking low-molecular-mass substances, 2. Aβ-specific antibodies and 3. Aβ itself (with appropriate spacers). In addition, several types of biotinylated nanoparticles will be developed as well-characterized model polymers. We will then investigate their interactions with streptavidin and subsequently between streptavidin-ensheathed nanoparticles with biotinylated Aβ-peptides or biotinylated antibodies directed against Aβ.Due to the interdisciplinary character of the project largely different methods can be applied to study the interaction of functionalized nanoparticles with Aβ-aggregates. SANS /2/ (Small Angle Neutron Scattering)

measurements will be performed to derive the structure of the active layers coating the nanoparticles. QELS (Quasi Elastic Light Scattering) and ITC (Isothermic Titration Calorimetry) measurements will be used to support the SANS results /3/. The distribution of the nanoparticles and its relevant Aβ-targeted compounds in animal tissues will be studied by light and electron microscopy including multiple fluorescence labelling and confocal laser scanning. First electron microscopic data on the delivery of the Aβ-binding model compound thioflavin-T after injection of nanoparticles with encapsulated thioflavin into the hippocampus of mice were recently published. /4/. Nanoparticles optimized by the physico-chemical methods mentioned above should be tested for drug targeting in animal models and might result in carriers for medical applications.

/1/ B.-R. Paulke, W. Härtig, G. Brückner. Synthesis of nanoparticles for brain cell labelling *in vivo*. Acta Polymerica 43 (1992) 288-291.
/2/ H. Schmiedel, P. Jörchel, M. Kiselev, G. Klose. Determination of structural parameters and hydration of unilamellar POPC/C12E4 vesicles at high water excess from neutron scattering curves unsing a novel method of evaluation. J. Phys. Chem. B 105 (2001) 111-117.
/3/ R. Wang, H. Schmiedel, B.-R. Paulke. Isothermal Titration Calorimetric Studies of Surfactant Interactions with negatively charged, 'hairy' Latex Nanoparticles. Colloid & Polymer Science (2004) in press.
/4/ W. Härtig, B.-R. Paulke, C. Varga, J. Seeger, T. Harkany, J. Kacza. Electron microscopic analysis of nanoparticles delivering thioflavin-T after intrahippocampal injection in mouse: implications for targeting β-amyloid in Alzheimer's disease. Neurosci. Lett. 338 (2003) 174-176.

3.4.12 Funding

Alexander von Humboldt Foundation, Euro 2.0 Mio, 2002 - 2005, "Molecular structure and function of biopolymer networks, characterized by novel laser trapping tools, nanorheology and single polymer microscopy"

Private Donation, Ms. Marianne Duda, Euro 40,000.-

Handelskammer Leipzig, Euro 8,000.-

Wechselwirkung beschichteter Nanopartikel mit Amyloid-Peptiden Interaction of functionalized nanoparticles with b-amyloid peptides
Prof. H. Schmiedel (jointly with Dr. W. Härtig, Paul-Flechsig-Institut für Hirnforschung)
BMBF, 03DUO3LE (from 1/2003, within Bereich Neutronenstreuung)

3.4.13 Organizational duties

J.A. Käs
Beirat des Physikzentrums in Bad Honnef
Advisory committee for soft matter physics, NASA, USA
Prize committee, "Freundlichste Auslaenderbehörde", Alexander von Humboldt Foundation

Reviewing and Refereeing Duties
Journal review: Nature, Physical Review Letters, Physical Review E, Biophysical Journal, Biophysica and Biochemica Acta, Biochemistry, Proceedings of the National Academy of Science, European Biophysical Journal, Langmuir, Journal of Cell Biology Grant review: National Science Foundation, Div. of Materials

Research; National Science Foundation, Div. of Cellular Organization; National Science Foundation, Div. of Computational Biology; National Science Foundation, Div. of Physics, Special Programs; Deutsche Forschungs Gesellschaft, Alexander von Humboldt Foundation, Deutsche Studienstiftung, Centre National de Reserche, Israel Science Foundation

3.4.14 External Cooperations

Academic

Prof. Dr. Michel Follen, MD Anderson Cancer Center, Houston, Texas

Prof. Dr. Harry Swinney, Center for Nonlinear Dynamics, Austin, Texas

Prof. Dr. Ken Shih, University of Texas at Austin

Prof. Dr. Mark Raizen, University of Texas at Austin

Prof. Jean-Francois Joanny, Institute Curie, Paris

Prof. Dr. Jacques Prost, ESPCI, Paris

Prof. Dr. Marie-France Carlier, Cea Saclay, France

Prof. Dr. Robert Austin, Princeton

Prof. Dr. Walter Zimmermann, University of Saarbruecken

Prof. Dr. Reinhardt Lipowsky, MPI for Colloids, Golm

Prof. Dr. Frank Juelicher, MPI for Complex Systems, Dresden

Dr. Markus Bär, MPI for Complex Systems, Dresden

Dr. Silvio May, MPI for Complex Systems, Dresden

Dr. Kurt Andersen, MPI for Cell Biology, Dresden

Industry

Nimbus GmbH, Leipzig

jpk Instruments, Berlin

EuroPhoton GmbH, Berlin

Evotec GmbH, Berlin

Gesim GmbH, Dresden

Euroderm, GmbH, Leipzig

3.4.15 Publications

Journals

1) M. Forstner, D. Martin, A.M. Navar, and J. Käs, Simultaneous single-particle tracking and visualization of domain structures on lipid monolayers, Langmuir, 19, 4876 - 4879 (2003)

2) R. Mahaffy, C.K. Shih, F.C. MacKintosh, and J. Käs, Quantitative analysis of the viscoelastic properties of thin regions of fibroblasts using atomic force microscopy, Biophys. J., 86, 1777-1793 (2004)

submitted, in press

3) A.L. Lin, B.A. Mann, G. Torres-Oviedo, B. Lincoln, J. Käs, H.L. Swinney, Localization and extinction of bacterial populations under inhomogeneous growth conditions, Biophys. J., in press (2004)

4) R. Ananthakrishnan, J. Guck, F. Wottawah, S. Schinkinger, Estimating the Contribution of Actin Networks to the Elastic Strength of Fibroblasts, Biophys. J., in press

5) F. Wottawah, S. Schinkinger, B. Lincoln, R. Ananthakrishnan, M Romeyke, J. Guck, J. Käs, Optical Rheology of Biological Cells, Phys. Rev. Lett., submitted

6) J. Guck, H.M. Erickson, R. Ananthakrishnan, D. Mitchell, B. Lincoln, S. Schinkinger, F. Wottawah, M. Romeyke, J. Käs, S. Ulvick, C. Bilby, Optical Deformability as Inherent Cell Marker for Malignant Transformation and Metastatic Competence, Biophys. J., submitted

7) D. Martin, M. Forstner and J. Käs, Attractive interactions between membrane structures and single particles drastically impact lateral diffusion, Phys. Rev. Lett., submitted

8) S. Park, R. Cardenas, J. Käs, and C.K. Shih, Correlation between local viscoelasticity and motility of fibroblasts, Biophys. J., submitted (2003)

9) M. Lakadamyali, J. Bayer, R.E. Mahaffy, N.L. Peffly, C.K. Shih, and J. Käs, Local mechanosensing by neuronal growth cones, Nature, submitted (2003)

10) R. Wang, H. Schmiedel, B.-R. Paulke. Isothermal Titration Calorimetric Studies of Surfactant Interactions with negatively charged, 'hairy' Latex Nanoparticles. Colloid & Polymer Science (2004) in press.

Invited Talks

Josef Käs
15.1.2003 - Colloquium, MPI for Math. in the Sciences, Leipzig
Dynamics of actin filaments

24.1.2003 - Biophysics colloquium, EMBL, Heidelberg
The physics of the actin cytoskeleton

26.02.-10.03.2003 - APS-meeting Austin, Texas
Molecular Motors Fluidze Polymer Networks

17.3.2003 - Seminar, MPI for Complex Systems, Dresden
The physics of the actin cytoskeleton

19.3-22.3.2003 - Meco, Universität Saarbrücken
Polymers in Cells: A journey from fundamental polymer physics to cancer diagnosis and neuronal growth

23.4.2003 - Rotary Club, Leipzig
Manipulating Cells without Touching Them

12.05.-13.05.2003 - Soft Matters, MPI for Colloids, Golm
Polymers in Cells: A journey from fundamental polymer physics to cancer diagnosis and neuronal growth

17.5.2003 - Campus03, Universität Leipzig
Laser - berührungslose Finger für biologische Zellen

05.06. 2003 - Biophysics colloquium, Universität Heidelberg
Polymers in Cells: A journey from fundamental polymer physics to cancer diagnosis and neuronal growth

10.6.2003 - Physics colloquium, Otto-von-Guericke-Universität, Magdeburg
Polymers in Cells: A journey from fundamental polymer physics to cancer diagnosis and neuronal growth

03.07. 2003 - Biology colloquium, Universität Rostock
The actin cytoskeleton: A journey from fundamental polymer physics to cancer diagnosis

and neuronal growth

04.09.-11.09.2003 - Advanced Immunological Techniques, Epona Ungarn
Manipulating Cells without Touching Them: Laser-based Analysis and Control of Eukaryotic Cells

20.10.-24.10.2003, Cell, MPI for Complex Systems, Dresden
Polymers in Cells: A journey from fundamental polymer physics to cancer diagnosis and neuronal growth

06.11.2003 - Physics colloquium, Martin-Luther-Universität Halle-Wittenberg
Polymers in Cells: A journey from fundamental polymer physics to cancer diagnosis and neuronal growth

14.11.2003 - Nanoscience colloquium, Ludwigs-Maximillian Universität, München
Polymers in Cells: A journey from fundamental polymer physics to cancer diagnosis and neuronal growth

18.-21.11.2003, Soft Matter Days, KFA Jülich
Polymers in Cells: A journey from fundamental polymer physics to cancer diagnosis and neuronal growth

09.12.2003 - Physics colloquium, Universität Stuttgart
Polymers in Cells: A journey from fundamental polymer physics to cancer diagnosis and neuronal growth

Jochen Guck

25.02.2003
Jochen Guck, "Stretching Cells with Light", Symposium "Cancer and Photonics", Heidelberg

04.03.2003
Jochen Guck, "Stretching Cells with Light", American Physical Society Meeting, Austin, U.S.A.

05.03.2003
Jochen Guck, "Stretching Cells with Light", Biophysical Society Meeting, San Antonio, U.S.A.

31.03.2003
Jochen Guck, "Stretching Cells with Light", Seminar Biologische Physik, Max- Planck-Institut für die Physik komplexer Systeme, Dresden

22.05.2003
Jochen Guck, "Stretching Cells with Light", Theorie-Seminar, Hahn-Meitner-Institut

Berlin

26.05.2003
Jochen Guck, "Stretching Cells with Light", Seminar Nichtlineare Dynamik, Universität Magdeburg

24.06.2003
Jochen Guck, "Stretching Cells with Light", Seminar, Arbeitsgruppe von Marie- France Carlier, C.N.R.S., Gif-sur-Yvette, Frankreich

25.06.2003
Jochen Guck, "Stretching Cells with Light", Kolloquium, Institut Curie, Paris, Frankreich

Conference Contributions

(p: poster, t: talk)

16.01.2003
"Bio-Optical Neuron Guidance & Growth Cone Motility", Seminarvortrag, Universität Leipzig

23.01.2003
"Optical Cell Guiding", Michael Gögler, Seminarvortrag, Universität Leipzig

02.03.2003
"Self Assembly and Spatial Structure in Actin Networks", Brian Gentry, Biophysical Society Annual Meeting, San Antonio, Texas, USA p

04.03. 2003
"Mimicking temperature through molecular machines", David M. Smith, Biophysical Society Meeting, San Antonio, Texas, USA

04.03.2003
"Guiding neuronal growth with light", Timo Betz, Annual Meeting of the Biophysical Society, San Antonio, Texas, USA

04.03.2003
"Self Assembly and Spatial Structure in Actin Networks", Brian Gentry, APS Annual Meeting, Austin, Texas, USA

06.03.2003
"Order-disorder-transitions in polymer networks through molecular motors", David M. Smith, American Physical Society Annual Meeting, Austin, Texas, USA

01.-05.03.2003
"The viscoelasticity of the cytoskeleton", Stefan Schinkinger et al., Biophysical Society Meeting, San Antonio, Texas, USA

01.-05.03.2003
"Mechanical properties of murine Müller cells", Kristian Franze, Neurobiology Conference, Göttingen

12.05.2003
"Vesicles in the Optical Stretcher", Frank Sauer, Max-Planck-Institut Potsdam/Golm

07.05.2003
"Guiding neuronal growth with light", Allen Ehrlicher, American Physical Society, session on Neurobiological Physics

12.-13.05.2003
"Optical guidance of growth cones" und "Guiding cells with light", Allen Ehrlicher et al., Soft Matters 2003 Bilateral Symposium, MPI for Colloids and Interfaces, Golm

13.05.2003
"Order-disorder-transitions in polymer networks through molecular motors", David M. Smith, Soft Matters 2003, MPI-KG, Potsdam/ Golm

14.-16.05.2003
"Characterization of cellular growth in 3D polymer scaffolds", Susanne Ebert, Konferenz "Interface Biology of Implants", Universität Rostock

17.05.2003
"Optical cell guidance", Allen Ehrlicher et al., Tag der Universität Leipzig "Campus 2003", Innenstadt Leipzig (Filmvorführung)

21.05.2003
"Stretching cells with light", S. Schinkinger et al., 2. Biotechnologietag, Universität Leipzig

21.05.2003
"Guiding cells with light", Allen Ehrlicher et al., 2. Biotechnologietag an der Universität Leipzig, Biotechnologisch-Biomedizinisches Zentrum, Leipzig

21.05.2003
"Mechanical properties of Müller cells", Kristian Franze, 2. Biotechnologietag, Leipzig,

03.-06.09.2003
"Mechanical properties of Müller cells", Kristian Franze, Euroglia 2003, Berlin

12.-15.06.2003
"Bio-optical neuron guidance", Daniel Koch et al., 29th Göttingen Neurobiology Conference 2003

12.-15.06.2003

"Biomechanical properties of Müller cells", Kristian Franze, Neurobiology Conference, Göttingen

24.09.2003
"Mechanical & Optical Properties of Müller cells", Kristian Franze, Paul-Flechsig-Institut, Leipzig

28.-30.09.2003
"Isothermal Titration Calorimetric Studies (ITC) of Ionic Surfactant Interactions with Charged Latex Nanoparticles", R. Wang, 42th Biennial Meeting of the Germany Colloid Society in conjunction with Bayreuth Polymer Symposium 2003, Bayreuth

21.10.2003
"Optical guidance of growth cones", Timo Betz, Workshop and Seminar "Motion, sensation and self-organization in living cells", Dresden

24.10.2003
"Pressure on neurodegeneration", Jens Gerdelmann et al., 2nd Research Festival for Life Sciences 2003

24.10.2003
"Bio-optical neuron guidance", Allen Ehrlicher et al., 2. Research-Festival 2003, Max-Bürger-Forschungszentrum, Interdisziplinäres Zentrum für Klinische Forschung (IZKF), Leipzig

24.10.2003
"Electron microscopic analysis of nanoparticles delivering thioflafin-T after intrahippocampal injection in mouse: Implications for targeting beta-amyloid *in vivo*", W. Härtig et al., 2nd Leipzig Research Festival for Life Sciences, Leipzig

24.10.2003
"ITC Study of Interaction between Surfactant and Charged Latex Particle", R. Wang, 2nd Leipzig Research Festival for Life Sciences, Leipzig

24.10.2003
"Mechanical properties of Müller cells", Kristian Franze, Leipzig Research Festival for Life Sciences, Leipzig

06.11.2003
"Mechanical & Optical Properties of Müller cells", Kristian Franze, Abt. Physik weicher Materie, Universität Leipzig

13.11.2003
"Vesicles in the Optical Strecher", Frank Sauer, Seminarvortrag, Universität Leipzig

4

Institute for Experimental Physics II

4.1 Nuclear Solid State Physics

4.1.1 The high-energy ion nanoprobe LIPSION

T. Butz, D. Lehmann, H. N. da Luz, Ch. Meinecke, F. Menzel, T. Reinert, D. Spemann, W. Tröger, J. Vogt

The high-energy ion nanoprobe LIPSION at the University of Leipzig has been operational since October, 1998 (Fig. 1). Its magnetic quadrupole lens system, arranged as a separated Russian quadruplet, was developed by the Microanalytical Research Centre (MARC), Melbourne and has a symmetrical demagnification factor of about 130. The single-ended 3 MV SINGLETRON^{TM} accelerator (High Voltage Engineering Europa B.V.) supplies H^+ and He^+ ion beams with a beam brightness of approximately 20 A·rad^{-2}m^{-2}eV^{-1}. Due to this high brightness, the excellent optical properties of the focusing system of the nanoprobe and the suppression of mechanical vibrations by founding the bed-plates of accelerator and probe in greater depths separately from the surroundings, lateral resolutions below 100 nm for the low current mode (STIM) and 300 nm at a current of 10 pA (PIXE) were achieved routinely. A beam diameter of 41 nm was achieved. The UHV experimental chamber is equipped with electron, X-ray, and particle detectors to detect simultaneously the emitted secondary electrons (Ion Induced Secondary Electron Emission, SE), the characteristic X-rays (Particle Induced X-Ray Emission, PIXE), as well as the backscattered ions (Rutherford Backscattering Spectrometry, RBS) and - in case of thin samples - the transmitted ions (Scanning Transmission Ion Microscopy, STIM, and Scanning Transmission Ion Micro-Tomography, STIM-T). A newly installed optical microscope allows sample positioning and inspection during measurement. The magnetic scanning system moves the focused beam across the sample within a scan field of adjustable extent. The data collection system MPSYS (MARC Melbourne) collects and stores the spectra of the several techniques at any beam position (Total Quantitative Analysis, TQA). In addition, optional windows can be set in the spectra for real-time elemental mapping. The pictures are viewed and printed as two-dimensional colour-coded intensity distributions.
The installation of an active compensation system of stray magnetic fields using Helmholtz-coils (see Fig. 1) yields compensation factor in excess of 100 and proved very useful. The installation of an irradiation platform designed for single ion bombardment of living cells

allows first patterned irradiations and hit verification tests.

Fig. 1: LIPSION laboratory.

Current work in nuclear nanoprobe performance is focused on:

1. installation of a new target chamber with a UHV-x,y,z-translation stage and eucentric goniometer; the chamber can also be converted into a new irradiation platform for living cells with microscope access from the rear.

2. replacement of the old data acquisition system by the new MicroDAS MARC (Melbourne)

3. computer controlled ion beam writing

Accelerator Statistics 2003:

operating hours: 1500 h
maintenance and conditioning: 90 h

4.1.2 Ion beam micromachining

F. Menzel, D. Spemann, J. Vogt, J. Lenzner, H. Herrenberger, T. Butz

Within the framework of the research group "Architecture of nano- and microdimensional building blocks" (FOR 522) first micromachining experiments were performed. Micromachining allows to create structures e.g. for microoptical and micromechanical applications in photoresist via direct proton beam writing and subsequent etching. In the first experiments simple structures (Fig. 2a) were produced in SU-8 resist in order to study the effect off different ion fluence on the quality of the structures. Figure 2b shows that the edge precision which can be obtained with the existing target chamber is better than 200 nm. A new target chamber equipped with a very precise sample manipulation

stage is currently under construction and will allow to produce structures with even better edge definition. Furthermore, a dedicated beam scanning system for micromachining of arbitrarily shaped structures is under development.

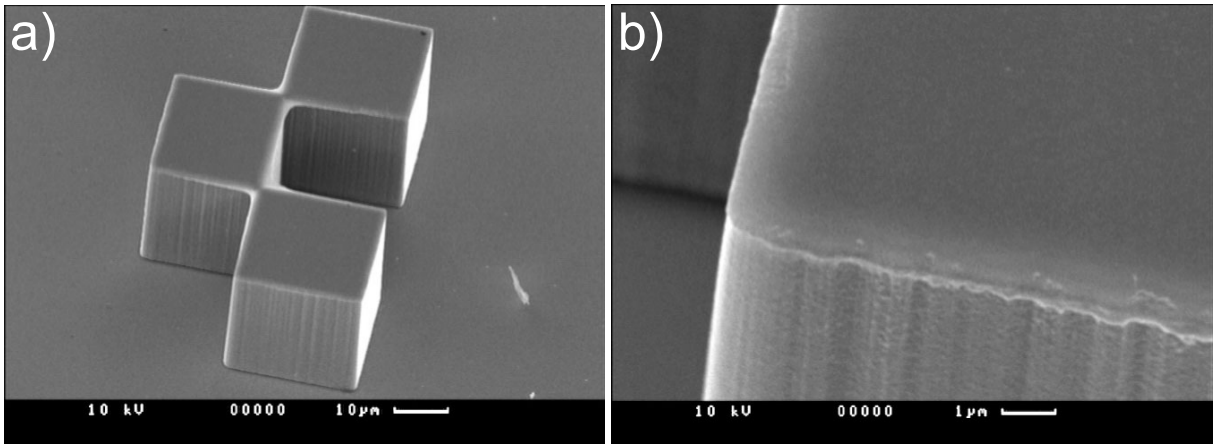

Fig. 2: (a) REM image of a structure produced in SU-8 by direct proton beam micromachining and (b) of the bottom left edge of the same structure. The edge precision is better than 200 nm.

4.1.3 Analysis of ZnO-microwhiskers and RBS-simulation of microstructures

Ch. Meinecke, J. Vogt, T. Butz

Within the framework of the DFG project "Architecture of nano- and microdimensional building blocks" we will investigate nanoscopic structures with the method of ion beam analysis µPIXE. In cooperation with the Semiconductor Physics group (HLP) we analysed the composition of microdimensional ZnO-whiskers, which were produced in the HLP group. Therefore the ion beam was focused down to below 1 µm to resolve the microdimensional ZnO-whisker. Due to this high spatial resolution it was possible to determine the elemental composition of the ZnO-microwhisker.
Figure 3 (left) shows the PIXE-map for zinc. The scan area was approx. 19 µm × 19 µm; Figure 3 (right) shows the REM-picture of the same zinc whisker.

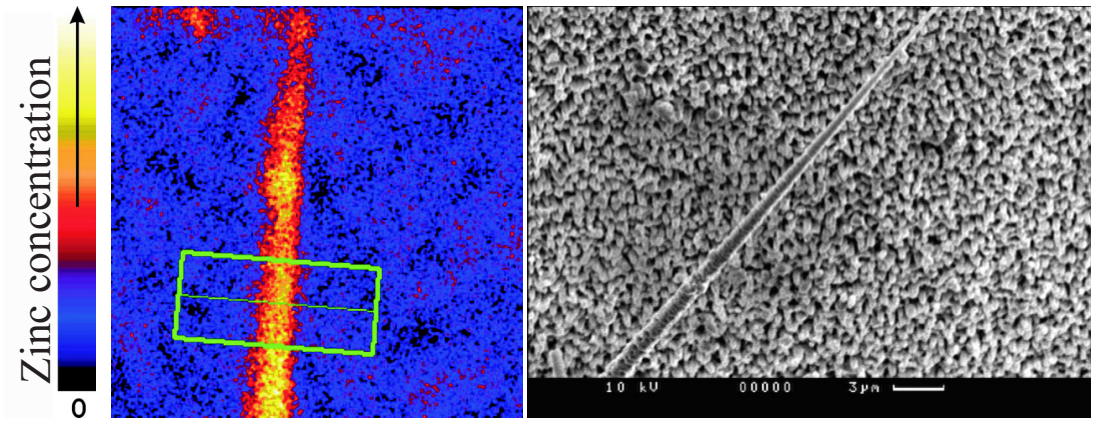

Fig. 3: Lateral distribution of zinc (*left*) and a REM-picture of the same ZnO-microwhisker.

Figure 4 shows the distribution of the elemental concentrations of various elements across the traverse, which is approx. 9 µm long, indicated in figure 3 (left). The detection of gold is no surprise because gold dots were used to initiate the whisker growth. However we found that this sample includes contaminations of other elements, so that the preparation setup has to be improved.

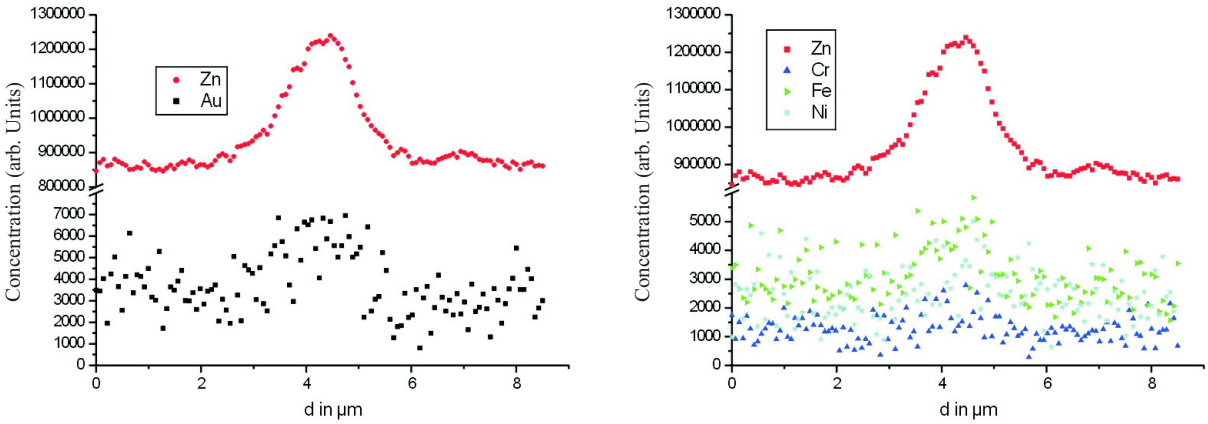

Fig. 4: Elemental distribution along the line scan, indicated in the left part of Fig. 3.

Furthermore we develop simulations for three-dimensional RBS-analysis. First, we simulated RBS-spectra of a gold coated glass rod with a diameter of 2 µm. Experiments with the new faceted RBS-detector are in preparation.

4.1.4 Ion beam analysis of epitaxial (Mg, Cd)$_x$Zn$_{1-x}$O and ZnO:(Li, Al, Ga, Sb) thin films grown on c-plane sapphire

D. Spemann, E.M. Kaidashev, M. Lorenz, J. Vogt, T. Butz

ZnO thin films, nominally undoped, doped with Li, Al, Ga, and Sb and alloyed with Mg and Cd grown epitaxially on c-plane sapphire by pulsed laser deposition (PLD) were investigated. In order to correlate the optical and electrical properties, e.g. the band gap energy and carrier concentration, to the elemental composition, the films were analysed by Rutherford Backscattering Spectrometry (RBS), Particle Induced X-ray Emission (PIXE), and Particle Induced γ-ray Emission (PIGE) using He^+ and H^+ ion beams. It was found that the element transfer from the PLD target to the film differs significantly for the individual doping and alloying elements, with concentration ratios between film and target ranging from approx. 4% for Li and Cd to approx. 400% for Ga. In general, the films exhibited a metal to oxygen ratio of 1:1, only the ZnO:Li films were slightly oxygen deficient.
Furthermore, the crystalline quality of the films was investigated using ion channeling. The nominally undoped ZnO films which were deposited with low-temperature interlayers in order to reduce the lateral stress showed a normalized minimum RBS yield of χ_{min}=3.3% under channeling conditions, a value which underlines the high crystal quality. Whereas the incorporation of isovalent alloying atoms into the ZnO films leads to a slight degradation of the crystalline quality only, doping degrades the crystalline quality remarkably, even at low dopant concentrations (see Fig. 5). This indicates that the

dopant atoms do not reside on regular Zn lattice sites (for one ZnO:Li film this could be proved by the Li-RBS yield under channeling conditions) and/or that the incorporation of a dopant atom leads to a locally strained lattice around the atom, possibly associated with a trapped defect or impurity atom. Both crystalline distortions lead to an increased backscattering yield under channeling conditions.

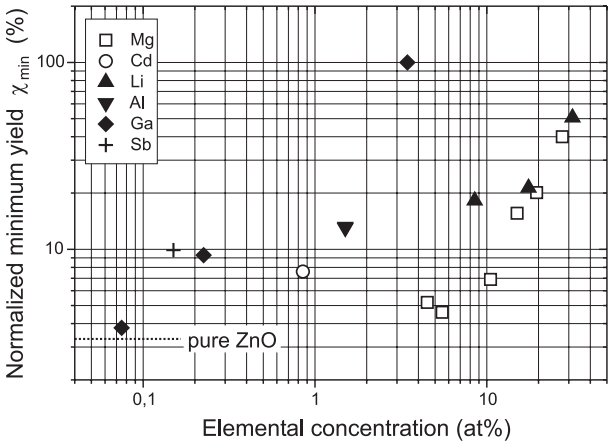

Fig. 5: Normalized minimum yield $\chi_{\min}$ from ZnO-based films doped or alloyed with various elements at different concentrations. In general, the crystalline quality degrades with increasing concentration, but to a different extent for doping and alloying elements. Whereas alloying (Mg and Cd) leads to a slight degradation of the crystalline quality only, the incorporation of doping atoms (Li, Al, Ga, and Sb) results in a significant degradation of the crystalline quality, even at low dopant concentrations.

4.1.5 Ion beam analysis of CIGS solar cells on polyimide foil

D. Spemann, K. Otte, M. Lorenz, T. Butz

Solar cells based on Cu(In,Ga)Se_2 (CIGS) absorber layers are one of the most promising thin film solar materials and stand on the edge of a profitable industrial realization. Photovoltaic conversion efficiencies of up to 19.2% have been achieved. Mechanically flexible thin film solar cells based on CIS absorbers deposited on polyimide foils by the Solarion company were investigated in the ion beam laboratory LIPSION of the University of Leipzig by means of Rutherford Backscattering Spectrometry (RBS) and Particle Induced X-ray Emission (PIXE) using high energy broad ion beams and microbeams. From these measurements the composition of the absorber as well as the lateral homogeneity and the film thicknesses of the individual layers could be determined under some reasonable assumptions. For the first time, quantitative depth profiling of the individual elements was performed by microPIXE measurements on a bevelled section of a CIS solar cell consisting of the following layers: polyimide / Mo / CIS / CdS / ZnO (see Fig. 6). The bevelled section was prepared at the Leibniz-Institute for Surface Modification (IOM) Leipzig using ion beam etching with 500 eV nitrogen ions. The depth profiling is performed using the K-X-ray lines of the elements Mo, Cu, In, Se, Cd, and Zn.

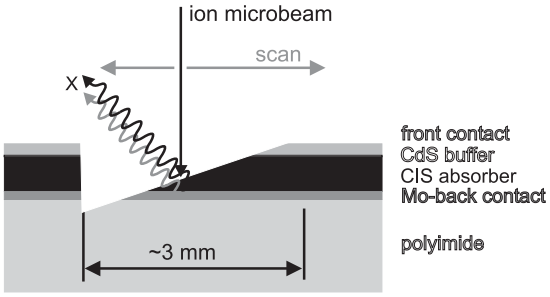

Fig. 6: Schematic of a bevelled section of a CIS solar cell.

Figure 7a shows the normalized X-ray yields from selected elements normalized to the values observed on the non-etched part of the solar cell. The observed yields from Cu, In, and Se were used to calculate the composition of the CIS absorber as a function of depth (Fig. 7b). For this purpose, the measured yields were compared with theoretical ones calculated from GeoPIXE II in order to correct for the varying thickness of the CIS absorber. The depth profiling by PIXE yielded no significant concentration-depth-gradients of Cu, In, and Se in the CIS absorber layer within the experimental errors, contrary to the SNMS depth profiling which was applied on the same samples for comparison. The values at a thickness of 0.01 mg/cm^2, i.e. the remaining 20 nm of the absorber after ion beam etching, should not be considered significant as they are very likely influenced by the ion beam etching. Furthermore, both PIXE and SNMS show a remarkable amount of Cd from the CdS buffer layer in the underlying absorber and the Mo / CIS-interface. The diffusion-like profile of Cd(S) within the absorber results most probably from the fact that the CdS covers the surface of the CIS crystallites accessible to it in the polycrystalline absorber. In addition, diffusion of Cd(S) may either (i) occur naturally in CIS or (ii) is promoted by the ion sputtering used in SNMS and for the preparation of the bevelled section. The possibility of Cd diffusion into the CIS absorber layer has to be taken into consideration carefully for the future optimization of the deposition processes.

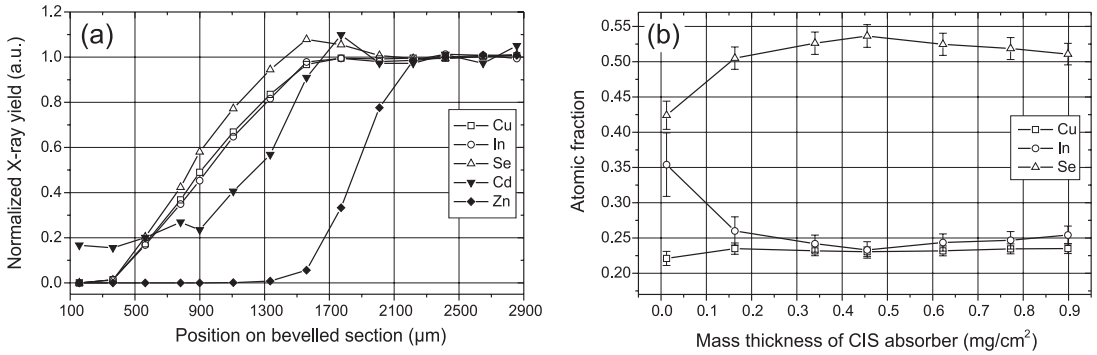

Fig. 7: (a) Normalized K-line X-ray yields extracted along bevelled section. (b) Composition of the CIS absorber as a function of depth.

4.1.6 Ferromagnetism in highly oriented pyrolytic graphite induced by proton irradiation

D. Spemann, K.-H. Han, P. Esquinazi, R. Höhne, A. Setzer, T. Butz

Ferromagnetic ordering in highly oriented pyrolytic graphite samples was created by high energy proton irradiation using broad ion beams and microbeams. Simultaneously, the impurity content was checked using Particle Induced X-ray Emission (PIXE). Due to the excellent sensitivity of better than 0.5 μg/g of PIXE for metallic impurities like Fe, it was possible to exclude the possibility of metallic impurities as a cause of the observed ferromagnetism. This work was done in close co-operation with the Superconductivity and Magnetism group (SUM). For more details see the reports of SUM.

4.1.7 Skin as a barrier to ultra-fine particles

F. Menzel, T. Reinert, E. Ahmed Mohamed, U. Anderegg *), M. Sticherling *), J. Vogt, T. Butz

*) Klinik und Poliklinik für Dermatologie, Universität Leipzig

Micronised TiO_2 particles used in sunscreens as physical UV filters are suspected to pass through the horny *stratum corneum* into vital skin layers via intercellular channels, hair follicles, and sweat glands. However, this penetration is undesirable because of its possible impact on human health. For example, the particles can activate the immune system and accumulations of these particles in the skin can decrease the threshold for allergies [1]. The function of the *stratum corneum* as a barrier against dermal uptake of ultrafine particles was the subject of several investigations which came to different conclusions concerning the penetration depth of the particles [2,3]. Most of these studies used the method of tape stripping which is relatively imprecise in comparison with the spatially resolved methods of ion beam analysis PIXE, RBS, ERDA, STIM and SEI we carried out on freeze dried cross sections of porcine skin which was exposed to different TiO_2 containing formulations.

These investigations concentrate on the influence of different kinds of pretreatment procedures, e.g. wetting the skin and removing the *stratum corneum*, and of different TiO_2 containing formulations on the barrier function of skin.

For the evaluation of the RBS data the hydrogen content of the sample material must be known. For this purpose a new method for the determination of the hydrogen content was developed which uses a recursive fitting algorithm of ERDA and RBS data.

The skin layers were identified by their different contents of phosphorus, sulfur, chlorine, potassium and calcium determined with PIXE (see Fig. 8). The concentration of titanium and its penetration depth was also determined with this method.

These investigations show that most of the applied TiO_2 remained on the skin surface or penetrated just into the *stratum corneum*. A close inspection of the traverses indicats that a small amount of the TiO_2 penetrates into the vital *startum granulosum*. But no indications for a penetration into deeper skin layers were found up to now.

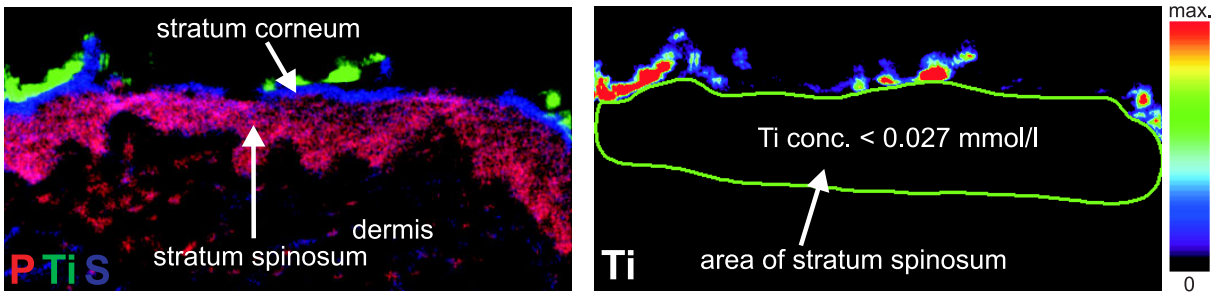

Fig. 8: Three element image of phosphorus, titanium and sulphur (left) and map of titanium distribution with marked region of interest (right) of pig skin exposed to TiO_2 containing polyacrylatgel after water application (424 µm × 193 µm).

[1] B. Granum, P.I. Gaarder, E.-C. Groeng, R.-B. Leikvold, E. Namork and M. Løvik, Toxicology Letters 115 (2001) 171-181.
[2] F. Pflücker, V. Wendel, H. Hohenberg, E. Gärtner, T. Will, S. Pfeiffer, R. Wepf and H. Gers-Barlag, Skin Pharmacol Appl Skin Physiol 14 (2001) 92-97.
[3] M.-H. Tan, C. A. Commens, L. Burnett and P.J. Snitch, Australasian Journal of Dermatology 37 (1996) 185-187

4.1.8 Hit precision for targeted bombardment of living cells with single ions

T. Reinert, A. Fiedler, J. Škopek, J. Tanner, J. Vogt, T. Butz

It was often stated that the advantages of scanned focused ion beams for radiobiological applications are easily lost due to formidable difficulties arising from the horizontal configuration of the microprobes and the need of a beam exit window [1,2]. Despite these restrictions we try to overcome these difficulties in taking advantage of our system. Currently we are developing our existing horizontal nuclear microprobe for radiobiological applications. Our key objective is the investigation of the cellular response to targeted irradiation with light ions (H^+, He^+), especially the radiation induced bystander effect [3]. This effect is, in short, the radiation related response of non-irradiated cells neighboring an irradiated cell. For these studies a precise targeting on the cells is mandatory. Furthermore, the measurement of the number and energy loss of the ionising particles within the cell determines precisely the applied dose. The next challenging step is to precisely determine and to target on selected positions for the irradiation within the cells, e.g. to distinguish between the cytoplasm and the cell nucleus or even between smaller structures within the cell. Therefore, we developed an irradiation platform for living cells at the high-energy ion nanoprobe laboratory LIPSION. The platform enables the irradiation of living cells in a mini-Petri dish with as little medium as possible in a vertical position and the detection and energy loss measurement of the transmitted projectile ions. Technically, our primary concern is to increase the hit accuracy to below 1 µm. Therefore, we use thin Si_3N_4 windows as beam exit and in the Petri dish bottom. Scientifically, our studies started with adhesion, survival, and sedentariness tests with endothelial cells and first patterned irradiation experiments.

In order to determine the hit accuracy, tests on CR-39 with different patterns were performed. The CR-39 foil was glued onto the bottom of the mini-Petri dish and irradi-

ated through the exit window. Since the protons of 2.25 MeV cannot penetrate the thick CR-39 foil we could not detect single events. Therefore, we set up the beam intensity to about 3000 protons per second. At each target position the beam gate was opened for 1 ms enabling the passage of three protons on average. We wrote a 10 × 10 dot pattern and the word "LIPSION" with dots separated by 2 µm (Fig. 9, left). The statistical analysis of the hit positions revealed a hit accuracy significantly better than 0.5 µm. Using a Monte-Carlo simulation code (program code `SRIM`) we calculated for 2.25 MeV protons through 100 nm Si_3N_4 and 100 µm air a lateral straggling of theoretically less than 0.2 µm. Our high hit accuracy would enable us to write the small word "ION" into a cell nucleus (Fig. 9, right) if the target recognition would be of similar precision. However, in some cases large angle scattering occurred. Additional tests with four spots, each having about 1000 protons, showed in total eight hits between 2.5 µm and 5 µm away from the targeted position which is 0.2 % of the total number of ions only.

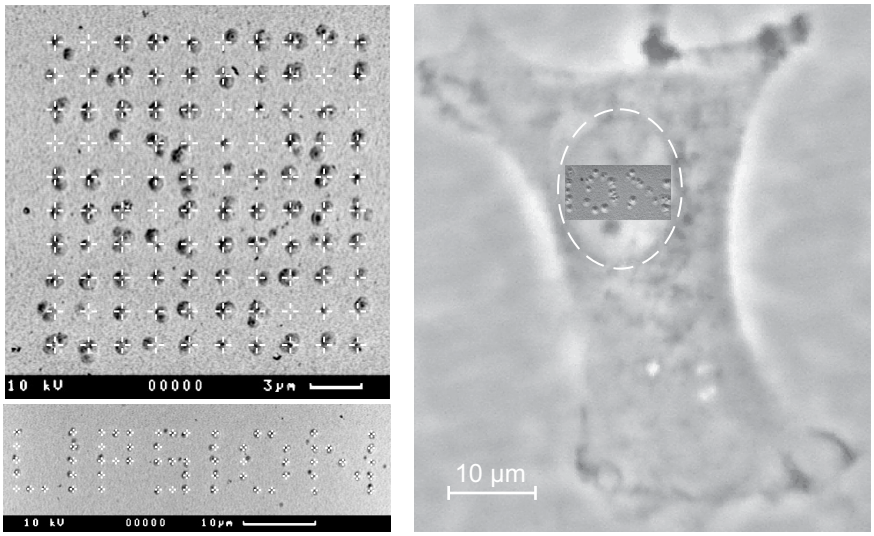

Fig. 9: *Left*: Hit verification tests on CR-39 (ca. 3000 protons per second, 1 ms beam gate per position): The pattern was drawn with dots separated by 2 µm. The target position markers (white crosses) have a size of 1 µm. The REM images reveal a hit accuracy significantly better than 0.5 µm; *Right*: The REM image of J. Lenzner of the word "ION" from a 1 µm spaced "LIPSION" on CR-39 was overlaid to the microscopic image of an epithelial cell right on top of the nucleus of the cell (dashed oval).

First irradiation experiment of living cells were carried out with 2.25 MeV protons homogeneously distributed in different patterns and number of protons over the cells [4]. Thus, we applied a dose up to 2 Gy to the cells. We checked for survival at different times after irradiation. Surprisingly, the cell survival was not affected significantly; the doubling time seemed to be slightly lower. The pattern of the irradiation could not be recognized in the cell cultures after irradiation.

[1] B.E. Fischer, M. Cholewa, H. Noguchi, Nucl. Instr. and Meth. B 181 (2001) 60.
[2] M. Folkard, K.M. Prise, B. Vojnovic, S. Gilchrist, G. Schettino, O.V. Belyakov, A. Ozols, B.D. Michael, Nucl. Instr. and Meth. B 181 (2001) 426.
[3] J. Österreicher, K.M. Prise, B.D. Michael, J. Vogt, T. Butz, J. Tanner, Strahlenther. Onkol. No. 2 (2003) 69.
[4] A. Fiedler, J. Škopek, T. Reinert, J. Tanner, J. Vogt, J. Österreicher, L. Navratil, T. Butz, Radiat. Res. 161 (1) (2004) 95.

4.1.9 Perineuronal nets potentially protect against metal ion-induced oxidative stress: A nuclear microscopy study in human and rat brain

M. Morawski*), T. Reinert, G. Brückner, W. Meyer-Klaucke**), F. E. Wagner***), T. Butz, Th. Arendt*), W. Tröger
*) Paul-Flechsig-Institut für Hirnforschung, Universität Leipzig
**) EBML Outstation Hamburg, Universität Leipzig
***) Physik Department E15, TU München

A specialized form of extracellular matrix termed perineuronal nets (PN) consisting of large aggregating chondroitin-sulfate proteoglycans, with hyaluronan and aggrecan as main components, surrounds subpopulations of neurons. Due to their glycosaminoglycan components, these PN form highly charged structures in the direct microenvironment of neurons and thus might be involved in local ion homeostasis. Through their polyanionic character, PN might also potentially be able to scavenge and bind redox-active iron and reduce the local oxidative potential in the neuronal microenvironment, thus providing some neuroprotection to net-associated neurons. The quantity and distribution of iron-charged PNs of the extracellular matrix in the human and rat cortex, the subiculum of the hippocampal formation, and the red nucleus was measured using the powerful combination of Particle-Induced X-ray Emission (PIXE), Extended X-ray Absorption Fine Structure (EXAFS), and Mössbauer spectroscopy. PIXE was used to localize and quantify the bound iron. The binding affinity-constant (K_D) was calculated using the Michaelis-Menten equation. EXAFS and Mössbauer spectroscopy were performed to give information on the chemical state and form of the PN bound iron as well as on the chemical surrounding of the iron. These studies reveal that the iron is bound to the PNs as Fe(III) in oxygen containing iron clusters. The EXAFS as well as the Mössbauer data show no significant differences between the different net containing brain areas.

The results show that the PN ensheathed neurons accumulate up to 4,6 fold more iron than any other extra cellular matrix structures depending on the applied Fe concentration in the investigated brain areas with local amount maxima of 480mmol/l Fe at PNs. The affinity-constants K_D range depending on the analysed brain area from 2,2 mmol/l to 6,3 mmol/l.

These data suggest that PNs potentially protect the ensheated neurons by binding pathologically increased free iron thereby possibly preventing the formation of iron-induced formation of free radicals. Vulnerability studies on neurons influenced by free radical formation are under way.

4.1.10 Quantitative subcellular elemental analysis of parkinsonian and healthy human brain tissue

Ch. Meinecke, M. Morawski*), T. Reinert, Th. Arendt*), T. Butz
*) Paul-Flechsig-Institut für Hirnforschung, Universität Leipzig

In cooperation with the Paul-Flechsig-Institute for brain research we investigated the correlation between the distribution and concentration of trace elements (especially iron) in the brain and neurodegenerative diseases (Parkinson's and Alzheimer's disease).

Potentially discussed as a trigger of neurodegenerative diseases is the oxidative stress induced by metal ions (e.g. Fe, Al, Cu and Zn). Therefore, we analysed the elemental concentrations (especially the iron concentration) in sections of the human *substantia nigra* using μPIXE (PIXE - particle induced X-ray emission). The advantage of PIXE is the quantification of the elemental concentrations with a high spatial resolution. For these investigations we used a scanning proton beam focussed down to below 1 μm. Thus it was possible to determine the iron concentration qualitatively. Histochemical analysis did not provide such a quantification of the elemental concentration.
For the first time we have investigated the intra- and extraneuronal elemental concentrations (P, S, Ca, Fe, Cu, Ni, Zn) of the human *substantia nigra pars compacta* versus *pars reticulata* with detection limits in the range of 50 μmol/l (equivalent to $3,7$ μg/g). Thus, we could compare the iron concentration in human brain sections of healthy and parkinsonian brain tissue. Clear differences in the iron concentration and distribution could be disclosed (see Fig. 10).

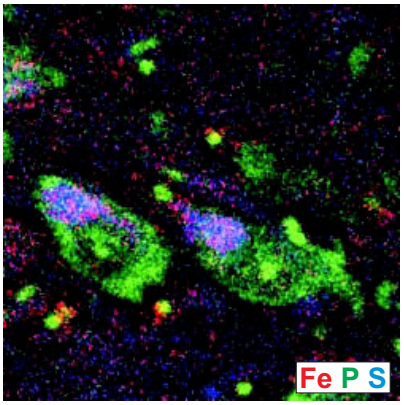

Fig. 10: Three element image showing the lateral distribution of phosphorus (green), iron (red), and sulphur (blue). The size of the scan area was 108 μm × 108 μm. Displayed is a melanin rich neuron. The melanin is characterized by an higher concentration of iron and sulphur (red an blue overlaid yields violet).

4.1.11 Metal Stoichiometries in Metalloproteins

H. N. da Luz, A. Vogel*), O. Schilling*), W. Meyer-Klaucke*), D. Spemann, W. Tröger
*) EBML Outstation Hamburg, Universität Leipzig

The use of proton induced X-ray emission (PIXE) allows to use the known sulphur content of a protein sample as an internal standard to determine the metal to protein ratio. The protein sulphur content is derived from the known protein amino acid sequence (cysteine and methionine residues). The PIXE measurements were performed at the LIPSION microprobe facility with a 2.25 MeV scanning proton beam. The scanning mode with a focused proton beam of low current has the following advantages compared with the use of a broad beam PIXE analysis (i.e., beam diameter of approximately 1 mm):

1. the spatial resolution reveals any sample inhomogeneities and allows to identify external contaminations of the sample or the supporting foil

2. the low currents in combination with the scanning reduce drastically the heating and the evaporation of volatile elements of the sample.

In order to check the latter, each scan was individually analysed and no significant loss of sulphur or metal ions was observed. Sorting and spatial mapping of the PIXE events also assured that the spatial distribution of the elements was uniform over the measured area of the sample. The protein samples are deposited in 1 µl drops on a 0.9 µm thick polyethylene terephthalate (PET) foil stretched on an aluminum sample holder. The protein concentration was about 1 µM. STIM (Scanning Transmission Ion Microscopy) together with the TRIM code for Monte Carlo simulation are used to derive the thickness of the protein samples which is important for calculating correctly the X-ray emission yields and the self absorption of X-rays by the sample, especially the characteristic K lines from sulphur. We explored the limits of the metal stoichiometry determination of this techniques with test samples containing inorganic dissolved copper salts embedded in an organic polymer matrix. These tests lead to a successful application of the PIXE method together with EXAFS measurement for elucidating the protein to metal stoichiometry and the geometric structure of the Zn site in the ZiPD protein, which is associated with certain types of cancer (see Fig. 11).

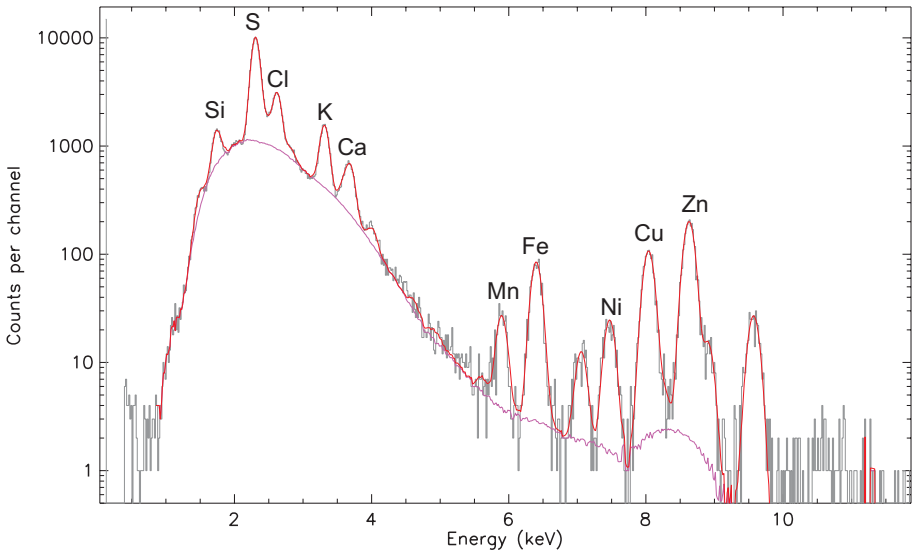

Fig. 11: The PIXE spectrum of a mutant of the ZiPD protein. The areas of the peaks are used to determine the relative concentration of the elements in the sample.

4.1.12 TDPAC-Laboratory

W. Tröger, S. Friedemann, F. Heinrich, T. Butz

Nuclear probes are used to study the interaction of metals with biological macromolecules like, e.g., DNA and proteins. Many life processes are based on such interactions. The structure and dynamics of metal sites in biomolecules are important in determining the functional efficiency of these macromolecules. In order to study those metal sites close to physiological conditions a highly sensitive spectroscopic method is required, like Time Differential Perturbed Angular Correlation (TDPAC). Here, a radioactive atom is placed at the site of interest and by correlating the emitted γ-quanta in space and on a nanosecond time scale local structural information is provided. These investigations allow a deeper insight into the detoxification processes, switches, adaptivity and rigidity of metal sites in electron transfer proteins, and also the development of new radiopharmaceuticals in cancer therapy. Two modern 6-detector-TDPAC spectrometer are installed permanently at the Solid State Physics Lab of the ISOLDE on-line isotope separator at CERN. This outstation of the Leipzig TDPAC Laboratory is dedicated for TDPAC experiments with rather short-lived TDPAC isotopes, like ^{111m}Cd or ^{199m}Hg, ^{204m}Pb with half-lifes less than 70 minutes.

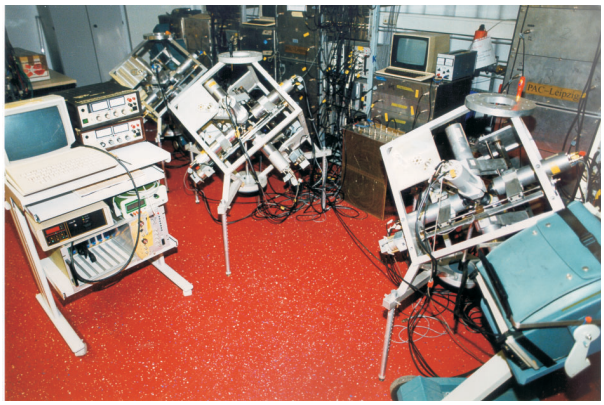

Fig. 12: View of the TDPAC laboratory with three modern TDPAC-Cameras ("silver cubes").

4.1.13 ^{204m}Pb: A new isomeric TDPAC probe

W. Tröger, S. Friedemann, F. Heinrich

Recently, the lead isotope ^{204m}Pb ($t_{1/2}$ = 67 min) became available for TDPAC measurements at the online separator ISOLDE at CERN, Geneva (TDPAC - Time Differential Perturbed Angular Correlation). This isotope is well suited for dynamic studies due to the long life time of the intermediate state (τ_N= 382 ns), which allows an excellent frequency resolution. In first experiments the NQIs of a large number of inorganic ^{204m}Pb(II)-compounds has been determined (e.g. see Fig. 12). These compounds serve as model compounds for life sciences. Additional first experiments on biological molecules have been performed, e.g. of the type-II metal binding site in Azurin (see Fig. 13) and of a lead binding catalytic DNA which might serve as a metal sensor.

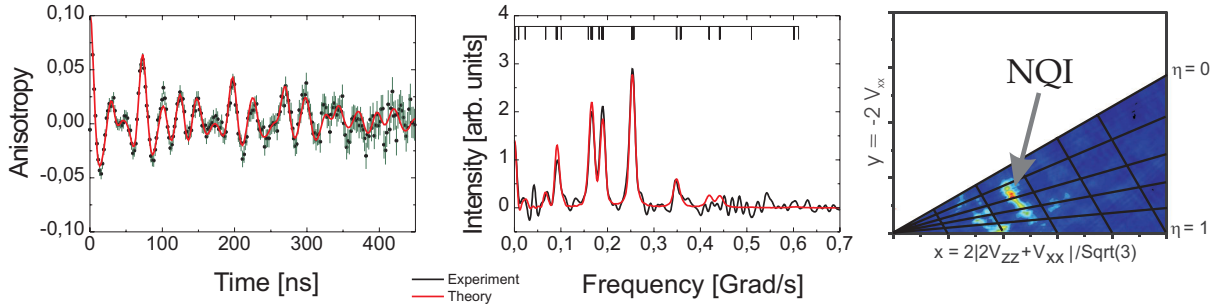

Fig. 12: Left: The TDPAC spectrum of $Pb_3(PO_4)_2$, a model compound for biological molecules. A single NQI, i.e. only one binding site of the Pb, was observed. Middle: Cosine Transform of the TDPAC spectrum. Right: Czjzek plot

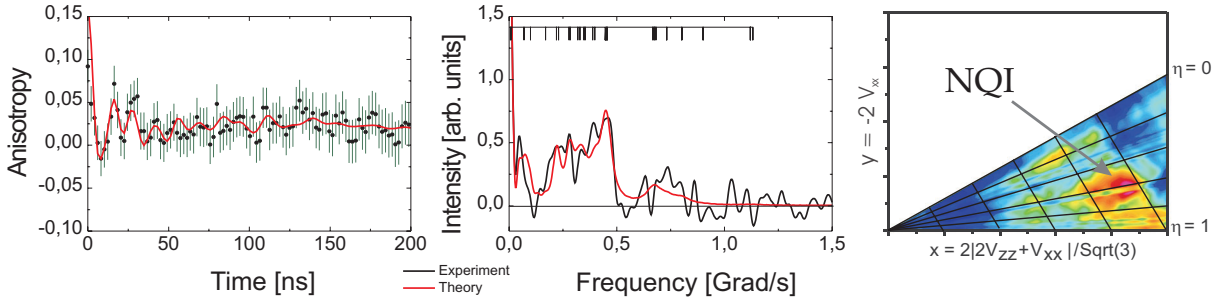

Fig. 13: Left: First TDPAC spectrum of Pb-Azurin (wt). A large line broadening can be observed which is not yet completely understood. Middle: Cosine Transform of the TDPAC spectrum. Right: Czjzek plot

Besides the ^{204m}Pb isotope production at ISOLDE much effort was spent to optimize the production of this isotope at the ISL facility (ISL - Ionenstrahllabor) at the Hahn-Meitner-Institute in Berlin. There, a lead target is irradiated with protons to produce ^{204}Bi ($t_{1/2}$ = 11,4 h) which is used for a ^{204}Bi/^{204m}Pb generator. We developed a special target holder for the Pb irradiation which reduces drastically the production of unwanted radioisotopes in the lead target as well as in the target holder. Furthermore, the separation of ^{204m}Pb from ^{204}Bi in the ion exchanger column was significantly improved by the use of a High Performance Liquid Chromatography unit.

4.1.14 Radioactive Metal Probes as Diagnostic Tools in Biomolecules

F. Heinrich, W.Tröger, T. Butz

The small blue copper proteins like azurin (Az), stellacyanin (Sc) and plastocyanin (Pc) act as electron transfer proteins. All contain one copper atom in the reactive centre, called type-1 Cu for its spectroscopic properties. In order to carry out studies of electron transfer in proteins, it is desirable to adsorb protein monolayers onto atomically flat surfaces which can be used as electrodes. 1T-TaS_2 and MoS_2 single crystals with atomically flat surfaces, grown by iodine vapour transport, are easily prepared with dimensions of several mm in diameter and 10 - 30 µm in thickness. Atomic Force Microscopy (AFM) studies revealed that a monolayer of Sc could be absorbed onto the flat surface of a MoS_2.

Further studies by time differential perturbed angular correlation (TDPAC) spectroscopy will be performed to check whether this absorption occurred without a denaturation of the protein or a distortion of the metal centre. In case the MoS_2 surface is a biocompatible electrode, the TDPAC studies on the electron transfer process will be started.

4.1.15 Ab initio Calculations of the Electric Field Gradient in Molecules

F. Heinrich, W. Tröger

Electric field gradients (EFG) at the nucleus of a nuclear probe can be measured via the nuclear quadrupole interaction by various methods, e.g. NMR or time differential perturbed angular correlation spectroscopy (TDPAC). Usually, the interpretation of the experimental data is done by comparison of the experimental EFG with well-known EFGs of model compounds. Ab initio calculations of the EFG represent an alternative to validate proposed chemical geometries of metal binding sites.

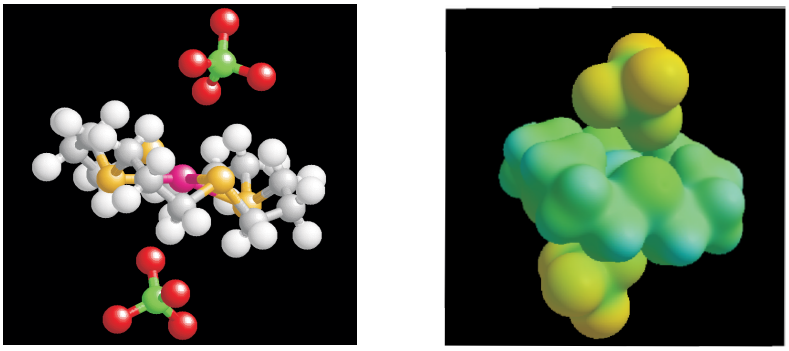

Fig. 14: Cd-16S4-$(ClO_4)_2$ - crown ether structure and iso-surface of the electron density. The Coulomb-potential is shown as a color field.

Our investigations are focused on the calculation of EFGs of molecules of different families as mercaptides, thio-crown ethers (see Fig. 14) and metal centers of blue copper proteins. We successfully reproduced EFGs in small and medium-sized molecules as mercaptides and thio-crown ethers. These calculations are the basis to calculate EFGs in macromolecules and to solve remaining problems of ligand coordination in metal centers of proteins.

4.1.16 TDPAC-Solid State Physics: High T_c Superconductors, Colossal Magnetoresistive Oxides, Semiconductors

J.G. Correia*), J.P. Araujo*), V.S. Ameral*), F. Heinrich, T. Butz, W. Tröger
*) Institute of Nuclear Technology, Sacavém, Portugal

In the framework of international cooperations we perform local studies on relevant structural problems of High Tc Superconductors (HTSC) and Colossal Magnetoresistive Oxides (CMO) by doping these with suitable radioactive isotopes for Perturbed Angular Correlations (TDPAC) and Emission Channeling (EC). In the case of the CMO the

measurement of the nuclear quadrupole interaction (NQI) in insulators and conducting samples provides information on the coupling between the local structure and chemical doping (by oxygen and metal vacancies), magnetic and electric properties. The hyperfine magnetic field is also useful to probe magnetic ordering of Mn ions in the CMO family of manganites. The main issue addressed was the characterization of local deformations in manganites, due to polaronic mechanisms, using appropriate radioactive ions, to study the effects of charge ordering and phase separation on a local scale. In the case of HTSC the characterization of the order/disorder of Hg in planes of the HTSC family $Hg_1Ba_2R_{n-1}Cu_nO_{2n+2+\delta}$ due to to the oxygen defect plays an major role. We implemented *ab initio* calculations of the electronic densities and the electric field gradients (EFG) in these compounds to interprete the TDPAC data. This illustrates Fig. 15 showing that the doping with oxygen leads to two inequivalent Hg sites. The proposed position of O_δ is based on the corresponding EFG calculations.

Furthermore, we studied the lattice location of rare earth and transition metals in III-nitride conductors, the II-VI semiconductor ZnO by the EC technique and performed TDPAC studies in order to elucidate the structure of defects in these materials.

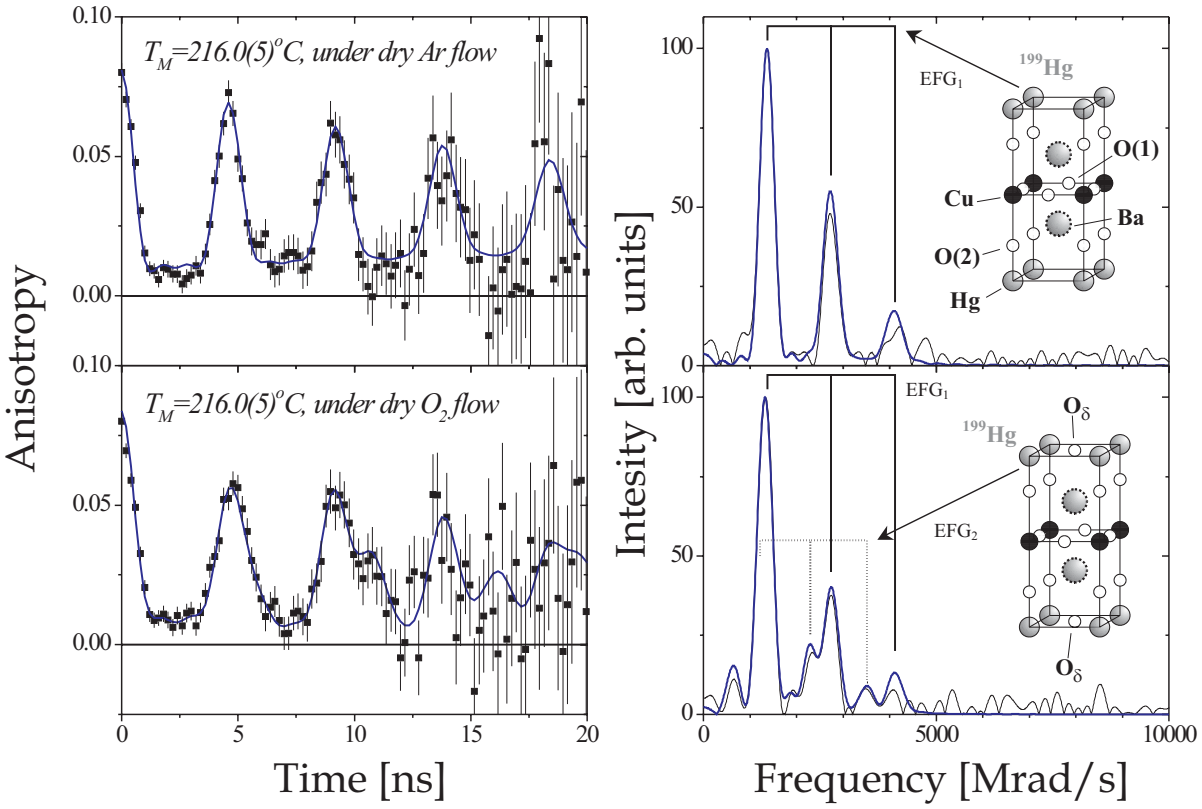

Fig. 15: Left: The TDPAC signal of $Hg_1Ba_2R_{n-1}Cu_nO_{2n+2+\delta}$ at different oxygen stoichiometries. Right: Fourier transforms of the TDPAC signal and proposed configurations.

4.1.17 An Update on the Mercury(II) Binding to Metallothioneins

W. Tröger, F. Heinrich, À. Leiva-Presa*), M. Capdevila*), P. Gonzàlez-Duarte*)
*) Universitat Autonoma de Barcelona, Spain

Metallothioneins (MT) are ubiquitous, cysteine-rich proteins of low molecular weight which bind d^{10} metal ions such as Zn(II), Cd(II), Cu(I) and Hg(II) in metal-thiolate clusters. They play an important role in the metabolism and in the modulation of the essential trace element zinc and copper and in the binding of toxic heavy metals. The latter suggests also the involvement in cellular detoxification mechanisms. Several 3D structures have been solved for mammalian $Me(II)_7$-MT, containing Zn(II) and/or Cd(II) ions. These metal ions are tetrahedrally coordinated by both bridging and terminal thiolates in cluster structures. We studied the Hg(II) binding in these molecules by optical absorption spectroscopy and by time differential perturbed angular correlation (TDPAC) spectroscopy. The former gives information on the stoichiometry and degree of folding of the Hg(II)-MT species present in solution, and the latter has recently been used successfully to elucidate the primary coordination sphere of Hg(II) ions in soluble $Hg(SCys)_n$ species at physiological concentrations. The overall results provide information on the variables affecting the Hg/protein stoichiometries and structures of the species formed as well as on the evolution of the coordination geometry about Hg(II) at increasing Hg/MT molar ratios. The titration of MT with different amounts of Hg revealed that MT can bind up to 18 Hg(II) ions per MT molecule. Furthermore, there is a significant shift from lower to higher frequencies for higher Hg(II) contents. From TDPAC studies with model compounds we can assign certain frequency intervals to coordination numbers. Whereas 4-fold Hg(II) co-ordinations dominate in Hg_7-MT, Hg_{18}-MT forms mainly 3-and 2-fold Hg(II) co-ordinations (see figure 16).

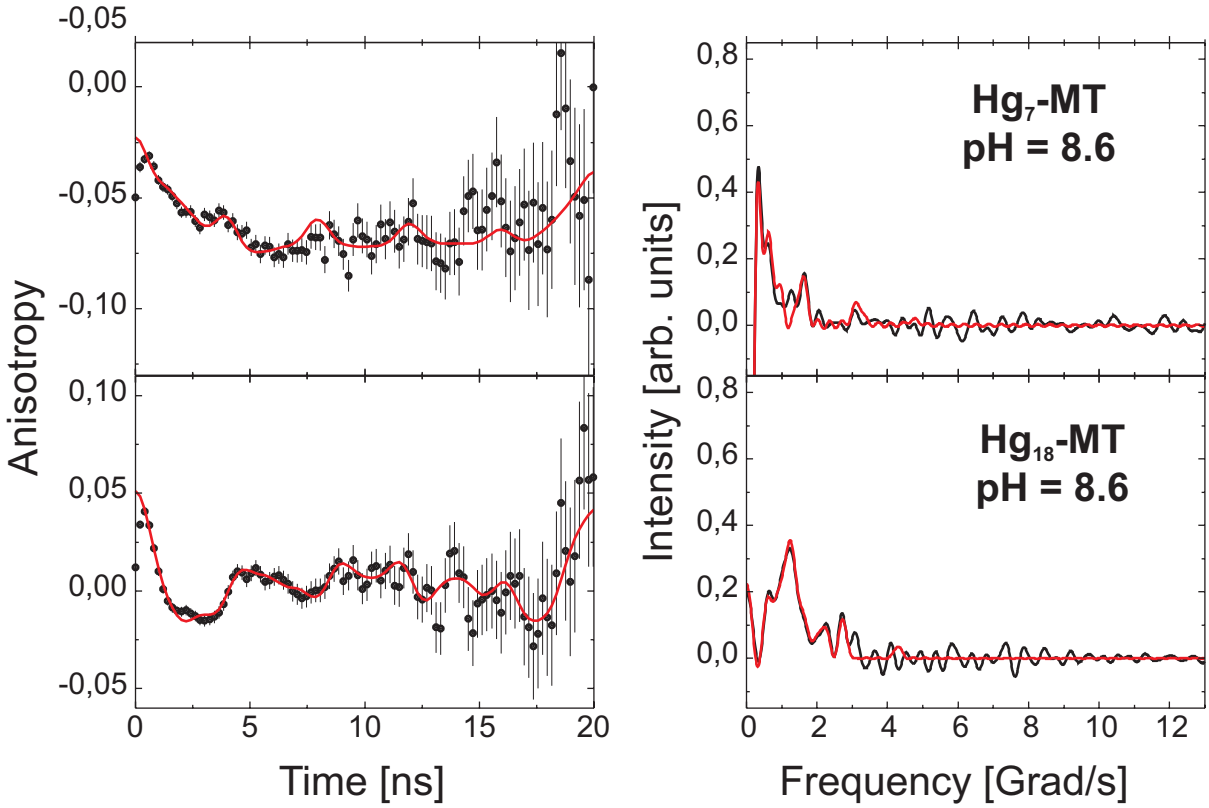

Figure 16: TDPAC spectra (left) and the cosine transforms of the TDPAC-spectra of Hg_7-MT (top) and Hg_{18}-MT (bottom). The shift from lower to higher frequencies indicates the change of 4-fold Hg(II) co-ordinations to co-ordinations with lower coordination numbers.

4.1.18 Funding

3D-Ionenstrahlanalytik zur morphologischen und stofflichen Charakterisierung nano- und mikrodimensionaler Strukturbauelemente und "Ionenstrahl-Micromachining"
Prof. T.Butz
DFG Bu 594/19-1
within Forschergruppe FOR 522
Architecture of nano- and microdimensional building blocks

Verbundprojekt: Wachstumskern INNOCIS "Kostengünstige, flexible CIS-Photovoltaik"; Teilprojekt: "Elektronische und optische Eigenschaften, in-situ-Ramanstreuung, in-situ-Ellipsometrie und Ionenstrahlanalytik von flexiblen CU-(In, Ga)-(Se, S)-Dünnfilmsolarzellen"
Prof. Grundmann
BMBF, 03 WKI 09

Single Ion Bombardment of Living Cells
Prof. T. Butz
Marie Curie-Development Host Fellowship, HPMD-CT-2000-00028

NANODERM – Quality of Skin as barrier to ultra-fine particles
Prof. T. Butz
EU-Project, QLK4-CT-02678

Koordinationstudien mit TDPAC an makrozyklischen AG-Kronen und -Käfigen: Molekulare Integrität von ^{111} Ag-Radiopharmaka
Priv.-Doz. Dr. W. Tröger
Deutsche Forschungsgemeinschaft, Tr327/5-2

Radioactive Metal Probes as Diagnostic Tools in Biomolecules
Priv.-Doz. Dr. W. Tröger
Deutsche Forschungsgemeinschaft, Tr327/8-1

4.1.19 Organizational Duties

T. Butz
Member of the committees "Forschung mit nuklearen Sonden und Ionenstrahlen" (BMBF), and " International Symposium on Nuclear Quadrupole Interactions"
Vorsitzender des wissenschaftlichen Beirates des Instituts für Oberflächenmodifizierung e.V., Leipzig
Vertrauensdozent der Studienstiftung des deutschen Volkes
Reviewer; DFG, Studienstiftung des deutschen Volkes, The University of Melbourne
Referee: J. of Physics C, Phys. Rev. B, Radiochim. Acta, Phys. Rev. Lett., J. Biol. Inorg. Chem.

W. Tröger
Referee: Hyperfine Interactions, Z. Naturforsch. A

T. Reinert
Referee: Nucl. Instr. and Meth. Phys. Res. B

D. Spemann
Referee: Nucl. Instr. and Meth. Phys. Res. B

F. Menzel
Referee: Nucl. Instr. and Meth. Phys. Res. B

4.1.20 External Cooperation

Academic

CENBG, Bordeaux, Prof. PH. Moretto
CERN, Genf, ISOLDE Collaboration
Chalmers Technical Highschool, Göteborg
CSIRO, Exploration and Mining, Sydney, Dr. C. Ryan
EMBL Outstation Hamburg, Dr. W. Meyer-Klauke, Dr. A. Vogel, O. Schilling
FRM, Garching, Prof. E. Wagner, Dr. U. Wagner
FU Berlin, Prof. U. Abram
Gray Cancer Institute, London, Prof. B.Michael
GSI Darmstadt, Dr. D. Dobrev, Dr. B. Fischer
HMI, Berlin, Dr. D. Alber, Dr. H. Haas
IIF Leipzig, K. Franke
INFN-LNL, Legnaro-Padova, Prof. P. Mittner
Institute of Physics, Kraków
Institute of Nuclear Technology, Sacavém, Dr. T. Pinheiro
IOM Leipzig, Dr. K. Zimmer, Dr. J. Gerlach
KVL, Kopenhagen, Prof. R. Bauer, Dr. E. Danielsen, Dr. L. Hemmingsen
Massenseperator-Kollaboration Bonn-Göttingen
MLU Halle-Wittenberg, Dr. J. Tanner
MPI für Biochemie, Martinsried, Prof. R. Huber, Dr. A Messerschmidt
MPI für Mikrostrukturphysik, Halle/S., Dr. J. Heitmann
MPI für Polymerforschung, Mainz, Prof. W. Knoll
Panjab University, Dr. P. Sidhu
Paul-Flechsig-Institut, Prof. T. Arendt, M. Morawski
Prähistorische Staatssammmlung München, Dr. R. Gebhard
PSI Villigen, Schweiz, Prof P.A. Schubiger
The University of Melbourne, Microanalytical Research Centre
TU Wien, Prof. K. Schwarz, Prof. P. Blaha
Universidade de Aveiro, Portugal, Prof. V.S. Amaral
Universitat Autonoma de Barcelona, Dr. Á. Leiva-Presa, Dr. M.Capdevila, Prof. P. González-Duarte
Université de Montreal, Prof. S. Roorda
Universität Leipzig, Prof. R. Hoffmann
Universität Mainz, Dr. H. Decker

Universität Zürich, Prof. Vašak, Dr. P. Faller, Prof. R. Alberto
Universitätskliniken Leipzig, PD Dr. G. Hildebrandt, Prof. M. Sticherling
University of Illinois, Prof. Y. Lu, J. Liu

Industry

Fa. Hille & Müller, Dr. W. Olberding
Solarion GmbH
Dr. E. Zschau, Self-employed expert in materials research

4.1.21 Publications

Journals

Infrared dielectric functions and phonon modes of high-quality ZnO films
N. Ashkenov, B.N. Mbenkum, C. Bundesmann, V. Riede, M. Lorenz, D. Spemann, E.M. Kaidashev, A. Kasic, M. Schubert, M. Grundmann, G. Wagner, H. Neumann, V. Darakchieva, H. Arwin, B. Monemar
J. Appl. Phys. 93(1), 126 (2003)

Dielectric functions (1 to 5 eV) of wurtzite $Mg_xZn_{1-x}O$ ($x \leq 0.29$) thin films
R. Schmidt, B. Rheinländer, M. Schubert, D. Spemann, T. Butz, J. Lenzner, E.M. Kaidashev, M. Lorenz, A. Rahm, H.C. Semmelhack, M. Grundmann
Appl. Phys. Lett. 82(14), 2260 (2003)

Active Compensation of Stray Magnetic Fields at LIPSION
D. Spemann, T. Reinert, J. Vogt, J. Wassermann, T. Butz
Nucl. Instr. Meth. B 210, 79 (2003)

Evidence for Intrinsic Weak Ferromagnetism in a C60 Polymer by PIXE and MFM
D. Spemann, K.-H. Han, R. Höhne, T. Makarova, P. Esquinazi, T. Butz
Nucl. Instr. Meth. B 210, 531 (2003)

Observation of Intrinsic Magnetic Domains in C60 Polymer
K.-H. Han, D. Spemann, R. Höhne, A. Setzer, T. Makarova, P. Esquinazi, T. Butz
Carbon 41, 785 (2003)
Addendum: Observation of Intrinsic Magnetic Domains in C60 Polymer
Carbon 41, 2427 (2003)

Quantitative Microanalysis of Perineuronal Nets in Brain Tissue
T. Reinert, M. Morawski, Th. Arendt, T. Butz
Nucl. Instr. Meth. B 210, 395 (2003)

Dielectric properties of Fe-doped $Ba_xTi_{1-x}O_3$ thin films on polycrystalline substrates at temperatures between $-35\,°C$ to $+85\,°C$.
M. Lorenz, H. Hochmuth, M. Schallner, R. Heidinger, D. Spemann, M. Grundmann
Solid-State Electronics 47, 2199 (2003)

Optical and electrical properties of epitaxial (Mg, Cd)$_x$Zn$_{1-x}$O, ZnO, and ZnO:(Ga, Al) thin films on c-plane sapphire grown by pulsed laser deposition
M. Lorenz, E.M. Kaidashev, H. von Wenckstern, V. Riede, C. Bundesmann, D. Spemann, G. Benndorf, H. Hochmuth, A. Rahm, H.-C. Semmelhack, M. Grundmann
Solid-State Electronics 47, 2205 (2003)

Radiation-Induced Bystander Effects
J. Österreicher, K.M. Prise, B.D. Michael, J. Vogt, T. Butz, J.M. Tanner
Strahlenter. Onkol. 179, 69 (2003)

Ferromagnetic spots in graphite produced by proton irradiation.
K.-H. Han, D. Spemann, P. Esquinazi, R. Höhne, V. Riede, T. Butz
Adv. Mater. 15(20), 1719 (2003)

Raman scattering in ZnO thin films doped with Fe, Sb, Al, Ga, and Li
C. Bundesmann, N. Ashkenov, M. Schubert, D. Spemann, T. Butz, E.M. Kaidashev, M. Lorenz, M. Grundmann
Appl. Phys. Lett. 83(10), 1974 (2003)

Beta1-Integrin and IL-1alpha expression as bystander effect of medium from irradiated cells: the pilot study
J. Österreicher, J. Škopek, J. Jahns, G. Hildebrandt, J. Psutka, Z. Vilasova, J.M. Tanner, J. Vogt, T. Butz
Acta Histochem. 105(3), 223 (2003)

Fission of actinides using a tabletop laser
H. Schwoerer, F. Ewald, R. Sauerbrey, J. Galy, J. Magill, V. Rondinella, R. Schenkel, T. Butz
Europhys. Lett. 61, 47 (2003)

On nuclear quadrupole interaction "families"
T. Butz
Hyperfine Int. 151/152, 49 (2003)

Induced Magnetic Ordering by Proton Irradiation in Graphite
P. Esquinazi, D. Spemann, R. Höhne, A. Setzer, K.-H. Han, T. Butz
Phys. Rev. Lett. 91(22), 227201 (2003)

In Press

Surface characterization of backside-etched transparent dielectrics
R. Böhme, D. Spemann, K. Zimmer
Thin Solid Films

Magnetic signals of proton irradiated spots created on highly oriented pyrolithic graphite

surface
K.-H. Han, D. Spemann, P. Esquinazi, R. Höhne, V. Riede, T. Butz
J. Magn. Magn. Mater.

Magnetism of pure, disordered carbon films prepared by pulsed laser deposition
R.Höhne, K.-H. Han, P. Esquinazi, A. Setzer, H. Semmelhack, D. Spemann, T. Butz
J. Magn. Magn. Mater.

Magnetic carbon: An explicit evidence on ferromagnetism induced by proton irradiation
P. Esquinazi, R. Höhne, K.-H. Han, A. Setzer, D. Spemann, T. Butz
Carbon

Ion beam analysis of epitaxial (Mg, Cd)$_x$Zn$_{1-x}$O and ZnO:(Li, Al, Ga, Sb) thin films grown on c-plane sapphire
D. Spemann, E.M. Kaidashev, M. Lorenz, J. Vogt, T. Butz
Nucl. Instr. Meth. B

Ion beam analysis of functional layers for Cu(In,Ga)Se$_2$ solar cells deposited on polymer foils
D. Spemann, R. Deltschew, M. Lorenz, T. Butz
Nucl. Instr. Meth. B

Ferromagnetic microstructures in highly oriented pyrolytic graphite created by high energy proton irradiation
D. Spemann, K.-H. Han, P. Esquinazi, R. Höhne, T. Butz
Nucl. Instr. Meth. B

Single ion bombardment of living cells at LIPSION
T. Reinert, A. Fiedler, J. Škopek, J. Tanner, J. Vogt, T. Butz
Nucl. Instr. Meth. B

Investigations of percutaneous uptake of ultrafine TiO$_2$ particles at the high energy ion nanoprobe LIPSION
F. Menzel, T. Reinert, J. Vogt, T. Butz
Nucl. Instr. Meth. B

Lattice parameter and elastic constants of cubic Zn$_{1-x}$Mn$_x$Se epilayers grown by molecular-beam epitaxy.
M. Hetterich, B. Daniel, C. Klingshirn, P. Pfundstein, D. Litvinov, D. Gerthsen, K. Eichhorn, D. Spemann.
phys. stat. sol. (c)

Pulsed laser deposition of Fe-, Cu-, and Fe, Cu-doped ZnO thin films.
E. Guzmán, H. Hochmuth, M. Lorenz, H. von Wenckstern, A. Rahm, E.M. Kaidashev, M. Ziese, A. Setzer, P. Esquinazi, A. Pöppl, D. Spemann, R. Pickenhain, H. Schmidt, M. Grundmann.

Annalen der Physik

Annual Reports

T. Butz (Editor)
NFP - Scientific Activities.
In: M. Grundmann (Ed.)
The Physics Institutes of Universität Leipzig, Report 2002, ISBN 3-934178-25-1 (2003)

Conference Contributions

Introduction to ion beam nano-analytics (inv. T.)
T. Butz
14. Edgar-Lüscher-Seminar, Serneus (Schweiz), 06.02.2003

Ion microscopy and micro-tomography (T)
T. Reinert
14. Edgar-Lüscher-Seminar, Serneus (Schweiz), 06.02.2003

First irradiation experiments with living cells at LIPSION (T)
A. Fiedler, J. Škopek, T. Reinert, J. Tanner, J. Vogt, J. Österreicher, L. Navratil, T. Butz
6^{th} Intl. Workshop "Microbeam Probes of Cellular Radiation Response", Oxford, 23.03.–29.03.03

Dielectric properties of Fe-doped $Ba_xSr_{1-x}TiO_3$ thin films on polycrystalline substrates at temperatures between -35 and $+85\,°C$. (P)
M. Lorenz, H. Hochmuth, M. Schallner, R. Heidinger, D. Spemann, M. Grundmann.
Frühjahrstagung der DPG, Dresden, 24.–28.03.2003.

Optische Übergänge und Brechungsindices von $Mg_xZn_{1-x}O$. (P)
R. Schmidt-Grund, B. Rheinländer, M. Schubert, E.M. Kaidashev, M. Lorenz, D. Spemann, G. Wagner, A. Rahm, C.M. Herzinger, M. Grundmann.
Frühjahrstagung der DPG, Dresden, 24.–28.03.2003.

Molekularstrahlepitaxie, Charakterisierung und Kompositionseichung von $Zn_{1-x}Mn_xSe$-Schichten. (P)
B. Daniel, J. Kvietkova, M. Hetterich, H. Priller, J. Lupaca-Schomber, C. Klingshirn, D. Spemann, M. Schubert, N. Ashkenov, P. Pfundstein, D. Gerthsen, K. Eichhorn.
Frühjahrstagung der DPG, Dresden, 24.–28.03.2003.

Pulsed laser deposition of high quality epitaxial ZnO, $(Mg, Cd)_xZn_{1-x}O$, and ZnO:(Ga, Al) thin films on c-, a-, and r-plane sapphire. (P)
M. Lorenz, E.M. Kaidashev, H. Hochmuth, D. Spemann, V. Riede, C. Bundesmann, H. von Wenckstern, A. Rahm, G. Benndorf, M. Grundmann.
Frühjahrstagung der DPG, Dresden, 24.–28.03.2003.

Magnetic Carbon: Observation of Intrinsic Magnetic Domains in C60 Polymer. (P)

K.-H. Han, D. Spemann, R. Höhne, A. Setzer, T. Makarova, P. Esquinazi, T. Butz.
Frühjahrstagung der DPG, Dresden, 24.–28.03.2003.

Investigations of percutaneous uptake of ultrafine TiO_2 particles at the high energy ion nanoprobe LIPSION. (P)
F. Menzel, T. Reinert, J. Vogt, T. Butz
16th Int. Conf. on Ion Beam Analysis, Albuquerque, N.M., USA, 29.06.–04.07.2003.

Single Ion Bombardment of living cells at LIPSION (T)
T. Reinert, A. Fiedler, J. Škopek, J. Tanner, J. Vogt, T. Butz
16th Int. Conf. on Ion Beam Analysis, Albuquerque, N.M., USA, 29.06.–04.07.2003.

Ion beam analysis of epitaxial (Mg, Cd)$_x$Zn$_{1-x}$O and ZnO:(Li, Al, Ga, Sb) thin films grown on c-plane sapphire. (P)
D. Spemann, E.M. Kaidashev, M. Lorenz, J. Vogt, T. Butz.
16th Int. Conf. on Ion Beam Analysis, Albuquerque, N.M., USA, 29.06.–04.07.2003.

Ion beam analysis of functional layers for Cu(In,Ga)Se_2 solar cells deposited on polymer foils.(P)
D. Spemann, R. Deltschew, M. Lorenz, T. Butz.
16th Int. Conf. on Ion Beam Analysis, Albuquerque, N.M., USA, 29.06.–04.07.2003.

Ferromagnetic microstructures in highly oriented pyrolytic graphite created by high energy proton irradiation.(P)
D. Spemann, K.-H. Han, P. Esquinazi, R. Höhne, T. Butz.
16th Int. Conf. on Ion Beam Analysis, Albuquerque, N.M., USA, 29.06.–04.07.2003.

Surface characterization of backside-etched transparent dielectrics. (P)
R. Böhme, D. Spemann, K. Zimmer.
E-MRS Spring Meeting 2003, Strasbourg, France, 10.–13.06.2003.

Pulsed laser deposition of Fe-, Cu-, and Fe, Cu-doped ZnO thin films. (P)
E. Guzmán, H. Hochmuth, M. Lorenz, H. von Wenckstern, E.M. Kaidashev, M. Ziese, P. Esquinazi, A. Pöppel, A. Rahm, D. Spemann, R. Pickenhain, H. Schmidt, M. Grundmann.
10. International Workshop on Oxide Electronics, Augsburg, 11.–13.09.2003.

Ion beam analysis of $CuInSe_2$ solar cells deposited on polyimide foils. (P)
D. Spemann, K. Otte, M. Lorenz, T. Butz.
12. Tagung Festkörperanalytik, Wien, Österreich, 22.–24.09.2003.

Erzeugung ferromagnetischer Mikrostrukturen in HOPG mittels Protonenbeschuss. (T)
D. Spemann, K.-H. Han, P. Esquinazi, R. Höhne, T. Butz.
Arbeitstreffen FSI 2003, Berlin, 30.09.–01.10.2003.

Ab initio DFT calculations of electric field gradients in molecules. (T)
F. Heinrich, W. Tröger.

Arbeitstreffen FSI 2003, Berlin, 30.09.–01.10.2003.

Proton induced magnetism in graphite. (T)
D. Spemann, T. Butz, K.-H. Han, P. Esquinazi, R. Höhne.
Granzer Workshop 2003, GSI Darmstadt, 10.11.–11.11.2003.

4.1.22 Graduations

Diploma Theses

Ch. Meinecke
Bestimmung der intra- und extraneuronalen Eisenkonzentration im Gehirn mittels Ionenstrahlanalytik
Diplomarbeit, Universität Leipzig (2003).

4.1.23 Guests

Dipl.-Biol. M. Morawski (Paul-Flechsig-Institut für Hirnforschung), 10 weeks
Prof. Dr. X. Ni (Shanghai Institute of Nuclear Physics, China), 2 months
Dr. W. Meyer-Klaucke, Dipl.-Biol. O. Schilling (EBML Outstation Hamburg), 1 week

4.2 Physics of Dielectric Solids

4.2.1 New NMR Equipment

G. Klotzsche, D. Michel

(a) 

(b) 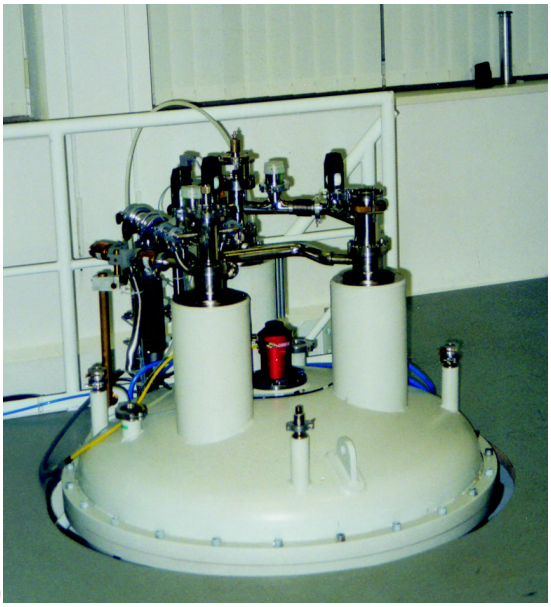

Fig. 1: 17.64 T magnet of the AVANCE 750 at the lower level of the lab (a) and at the upper level (b).

For our NMR based research several spectrometers with superconducting wide bore (89 mm) magnets are available covering a magnetic field range from 2.35 T to 17.62 T (corresponding to proton resonance frequencies between 100 and 750 MHz). The installation of the new high-field solid-state NMR spectrometer "AVANCE 750" in a wide-bore magnet provides, in combination with a 400 MHz AVANCE NMR-spectrometer excellent possibilities for fundamental and applied research. Various groups in Leipzig, Berlin, Jena, Regensburg and others colleagues are involved in the measuring regime. Both spectrometers of the AVANCE-series of Bruker Biospin (Karlsruhe) are equipped with a comparable modern electronics enabling applications of advanced pulse techniques, like shaped pulses and back-to-back pulses important for solid-state NMR applications. All NMR spectrometers are suitable for experiments on solid-state matter as well as for investigations at systems with restricted mobility (e.g. interface systems, biological membranes). We now have possibilities to measure with very strong (more than 1000 W) radio-frequency fields at any desired form in 2 or more channels simultaneously. Magic Angle Spinning (MAS) up to 32 kHz is possible to simplify powder patterns, but we can also orient and rotate stepwise single crystals using goniometer probeheads. Typical solid state NMR-measurements

using broad band excitation may be performed in a wide temperature region from 4.2 K to about 800 K.

For more details please contact Dipl.-Phys. Gert Klotzsche and Dr. André Pampel. klotzsch@physik.uni-leipzig.de, anpa@physik.uni-leipzig.de

4.2.2 Size Effects of Doped Perovskite Nanoparticles Observed by Means of Electron Paramagnetic Resonance (EPR)

E. Erdem, R. Böttcher, H.-C. Semmelhack, H.-J. Gläsel*, E. Hartmann*
* Leibniz-Institut für Oberflächenmodifizierung, 04318 Leipzig, Germany

The continuous studies of size effects on ferroelectric properties of oxide perovskites since the fifties have obtained great impetus in recent years. Curie temperature, electrical polarization, coercive field, switching time etc. potentially depend on particle size or, more generally, correlation size. Whereas X-ray diffraction (XRD) technique bases on coherent scattering at extended crystallographic planes and is, therefore, insensitive to subtle structural short-range changes in perovskite nanocrystallites, the EPR method sensitively probes small changes of the local symmetry at the particular crystal sites. Therefore, the main field of our research is the application of multi-frequency EPR to the perovskitic nanocrystallites doped by 3d ions. Ultrafine powders are prepared from a monomeric metal-organic precursor through combined-solid state polymerization and pyrolysis (CPP) [1]. This particular route enables not only the adjustment of the mean particle size but also the incorporation of paramagnetic metal ions. Before the EPR measurements, CPP-prepared oxide perovskite nanopowders were carefully characterized by various methods (TGA, DSC, FT-Raman, XRD, SEM and EDX).

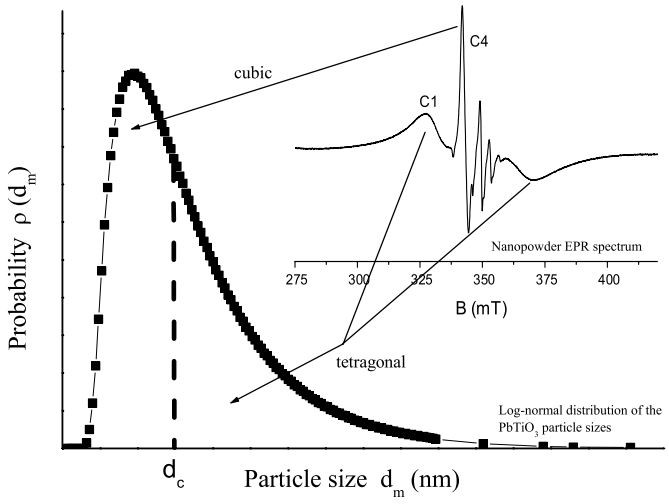

Fig. 1: Powder EPR spectrum of nanocrystalline $PbTiO_3$. The spectrum can be explained by the log-normal distribution of the particle sizes. Particle with sizes less than the critical size d_c generate the cubic spectrum C4.

Recently, we extended our investigations on Cr^{3+} doped $PbTiO_3$ nanopowder samples with varying mean particle size. EPR spectra were taken at room temperature using the Bruker spectrometers ESP 380, EMX and ELEXSYS E 600 in the X (9.5 GHz),

Q (34.2 GHz) and W (94.1 GHz) band measurements, respectively [2]. With the aid of a well approved simulation program the parameters of the axial spin-Hamiltonian: $\hat{H} = \beta \hat{S} g B + D[\hat{S}_z^2 - S(S+1)/3]$ of the Cr^{3+} centres ($S = 3/2$) from the powder spectra were deduced. Note that the D parameter is distributed due to the changes of the lattice parameters in the nanocrystalline $PbTiO_3$ samples. The mean fine structure parameters D and the widths ΔD of the distribution reveal a pronounced size dependence. The superposition model by Newman was applied to translate the fine structure data into local displacements inside the distorted oxygen octahedra of the $PbTiO_3$ lattice [2]. When going to nanopowder samples with mean particle size below a critical value, other than the center C1 are no longer detectable (Fig. 1). Instead, a new one (C4) appears, testifying a pronounced size effect.

[1] E. Erdem, R. Böttcher, H.-C. Semmelhack, H.-J. Gläsel, E. Hartmann and D. Hirsch J. Mater. Sci. 38 (2003) 3211-3217.
[2] E. Erdem, R. Böttcher, H.-C. Semmelhack, H.-J. Gläsel and E. Hartmann phys. stat. sol. b 239 (2003) R7-9.

4.2.3 Size Effects of Perovskite Nanoparticles Observed by Means of Nuclear Magnetic Resonance (NMR)

G. Klotzsche, D. Michel

In addition to the EPR measurements of doped perovskite nanoparticles by Böttcher et al., the properties of $BaTiO_3$ powders were investigated by means of NMR spectroscopy. The advantage is that these studies may be performed on natural local probes, e.g. ^{137}Ba nuclear spins. The NMR method sensitively allows to study small changes of the local symmetry at the Ba site and to elucidate collective properties such as structural phase transitions. The NMR spec-trum of ^{137}Ba nuclei is predominantly influenced by nuclear quadrupolar interaction. The tensor of the quadrupolar interaction derived is proportional to the tensor of the electric field gradient which is very sensitive to local structure and dynamics. NMR powder spectra of the central line transitions ($m = +1/2 \Leftrightarrow m = -1/2$) were measured and simulated using second order perturbation theory of the quadrupolar interaction to estimate the quadrupolar coupling constant e^2qQ/h. Typical spectra for the various phases are shown in the Fig. 1.

In nanoparticles (i.e. samples with an average grain size in the range between $25\,\text{nm} \leq d_\text{m} \leq 250\,\text{nm}$), a distribution of the quadrupolar constant e^2qQ/h was found owing to distributions of the electric field gradient within the grain and additionally of the grain size in the sample. The studies are especially sensitive when they are performed in the tetragonal phase. The simulation of the NMR spectra is consistent with a structural model for a grain in which a only weakly distorted tetragonal core is surrounded by a highly distorted shell where the local symmetry is no more tetragonal. In agreement with the model, the spectra were simulated assuming two values of the quadrupolar constant e^2qQ/h and respective values $\Delta(e^2qQ/h)$ for the width of distribution. The thickness of the shell does not depend on the grain size. Hence, in small grains the spectra are dominated by the influence of the highly distorted shells and in very small grains a tetragonal center cannot be found.

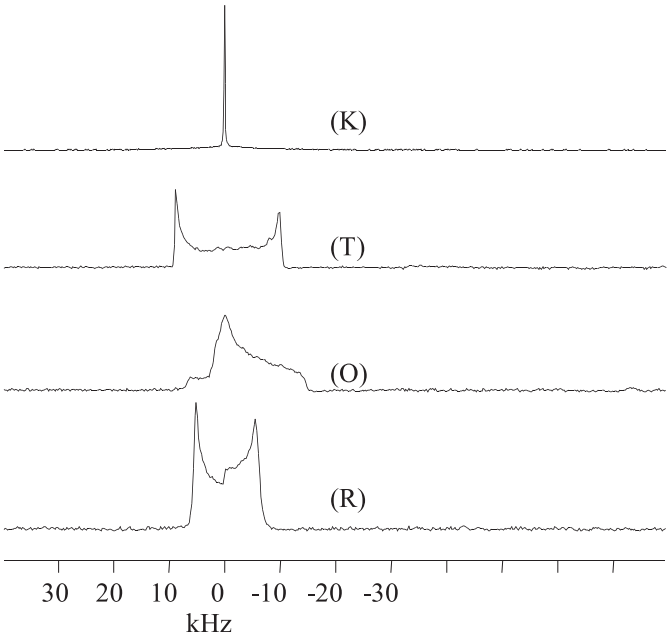

Fig. 1: ^{137}Ba NMR spectra of microcrystalline $BaTiO_3$ powder, prepared from single crystals, at various temperatures. Resonance frequency: 55.6 MHz (d.c. magnetic field of 11.7 T). Temperatures: (R) rhombohedral phase at 160 K, (O) orthorhombic phase at 260 K, (T) tetragonal phase at 293 K and (K) cubic phase at 416 K.

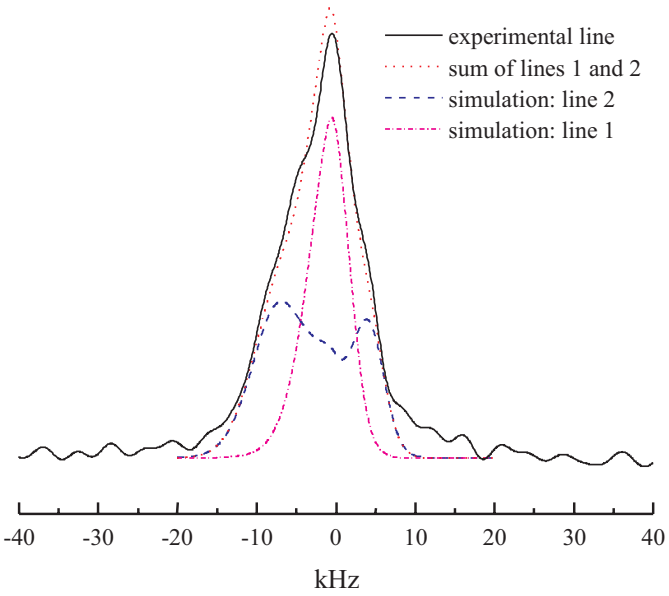

Fig. 2: NMR powder pattern of nanosized $BaTiO_3$, mean grain diameter 75 nm, $B_0 = 11.744$ T, $T = 300$ K. Line 1 corresponds to ^{137}Ba nuclei in a highly distorted surrounding ("shell", $\Delta(e^2qQ/h) = 1$ MHz). Line 2 corresponds to ^{137}Ba nuclei in a weakly distorted surrounding ("tetragonal core", $\Delta(e^2qQ/h) = 0.5$ MHz)

4.2.4 Copper-Doped Hexagonal Barium Titanate Ceramics

H. T. Langhammer*, T. Müller*, R. Böttcher, V. Mueller*, H.-P. Abicht*
*Fachbereich Physik, Martin-Luther-Universität, Halle-Wittenberg

The crystallographic phase, microstructure and dielectric properties of $BaTiO_3$ + 0.02 BaO + x CuO ceramics are studied at various Cu-doping level ($0 \leq x \leq 0.02$). It is confirmed by electron paramagnetic resonance that Cu^{2+}_{Ti} occupies Ti lattice-sites. Tetragonal and hexagonal phase coexist at room temperature for $x \geq 0.003$ (air-sintered, 1400°C). The portion of tetragonal phase decreases with x, leading to a decrease and broadening of the dielectric anomaly at the Curie temperature. Although, as compared to other 3d transition dopants (e.g., Mn), the hexagonal phase is stabilized at room temperature at smaller Cu-concentration, the tetragonal phase does not vanish completely even at higher doping level. Grains with exaggerated, plate-like shape (mean grain size $> 100\,\mu$m) are attributed to the hexagonal phase. We suggest that Jahn-Teller distortion due to the d^9 electron configuration of Cu^{2+}_{Ti} represents the driving force for the cubic-hexagonal transition.

4.2.5 Synthesis and Characterisation of One Dimensional Ferroelectrics with Perovskite Structure

R. Böttcher, E. Hartmann*
*Leibniz-Institut of Oberflächenmodifizierung Leipzig

Advances toward nanoscale electroncis have created interest in the effects of particle size on the properties of oxidic perovskite substance (ABO_3). These materials are employed for their dielectric, piezoelectric, eletrostrictive, pyroelectric, and electro-optic properties. Understanding how the crystal structure and the state of polarization are influenced by particle size is important to the performance of these ferroelectric materials in many applications. Our work aims to understand how nanoscaling influences the ferroelectric properties and to determine the critical size where a ferroelectric nanostructure no longer behaves like the bulk material. This project in the frame of the Forschergruppe 522 focuses on the synthesis and characterisation of perovskite nanotubes made by template method. Masked Whatman anodics membranes (200 nm pores) served as templates and are dipped into a solution of monomeric metallo-organic precusor from barium (lead) oxide, titanicum (IV) isopropoxide and methacrylic acid. After calciming the templates are removed and the powder sample of the nanotubes are characterized. Crystallographic characterization is performed with X-ray diffraction (XRD), electron microscopy and FT-Raman spectroscopy. EPR investigations of paramagnetic 3d-ions incorporated into the perovskite lattice at Ti-sites and dielectric measurements in a broad frequency band give a deep insight in the change of the dielectric properties of nanotubes in dependence of the aspect ratio.

4.2.6 Q-Band Pulsed ENDOR Spectrometer for the Study of Transition Metal Ion Complexes in Solids

J. Hoentsch, Yu. Rosentzweig*, K. Köhler**, M. Gutjahr, A. Pöppl, G. Völkel, R. Böttcher
*Laboratory of Magnetic Resonance, Kazan State University, Russian Federation
**Anorganisch-chemisches Institut, Technische Universität München, Germany

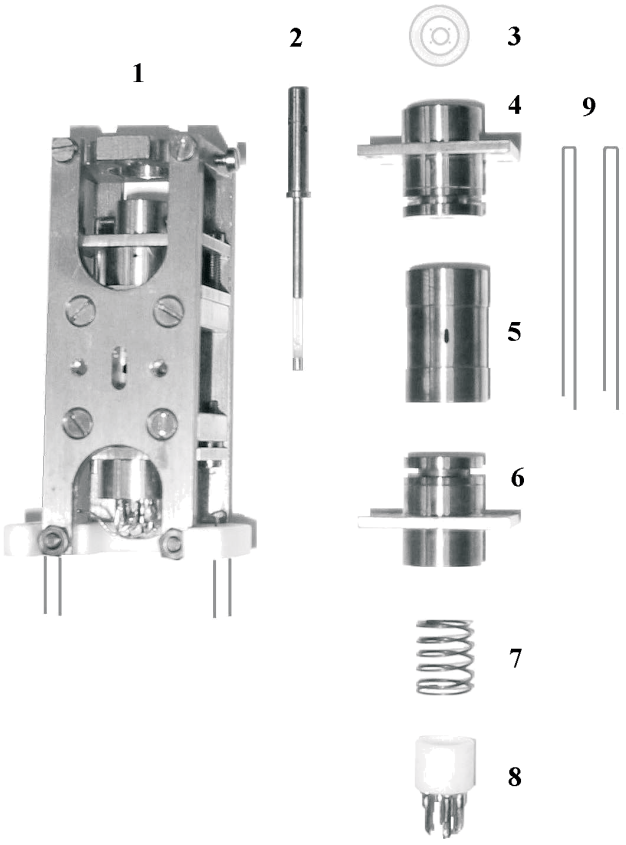

Pulsed ENDOR spectroscopy at Q-band (34 GHz) offers a good compromise between the experimental setups at conventional X-band or W-band frequencies. The orientation-selection in ENDOR spectra of disordered systems is already superior to X-band experiments without serious interference by g strain effects. Furthermore, Q-band mw components are still compa-rable in costs and performance with X-band components and conventional magnets can be used. Surprisingly, only a few pulsed EPR spectrometers operating in the intermediate mw frequency range between X- and W-band have been described so far. In our group a pulsed ENDOR spectrometer operating at Q band frequencies (35 GHz) for studies of transition metal ion complexes in the temperature range between 4.2 K and 297 K was designed. Specific features of the spectrometer are a microwave IMPATT generator, a home-built cavity, and a commercial BRUKER magnet system which allow the construction of a pulse spec-trometer at relatively low costs. The most mw components implemented were designed in Magnetic Radiospectroscopy and Quantum Electronics Laboratory of Kazan State University. In our experimental setup a gunn diode serves as the main mw source. Its microwave output power of 70 mW is

divided into two parts for the pulse forming and the reference arm by a direction coupler (DR, 7 dB). The pulse mw IMPATT generator delivers a train of three pulses with lengths of 50–200 ns with a maximum output power of about 6 W at a repetition rate of 5 kHz. It is controlled by the three digital delay generators and generates the mw pulses for the Davies or Mims ENDOR experiments as well as for the electron spin relaxation time measurement. The echo signals and the mw power reflected at the resonator input are directed via the circulator (CIRC) to the preamplifier (LNA, $F = 4$ dB, gain = 29 dB), protected by the switch SPST1 and the limiter LIM. The detection is based on a balanced mixer. The echo and the reference signal are mixed to yield the video signal which is amplified by the video amplifier (VA, gain = 18 dB) and directed into a boxcar integrator. A home-made TE011 cavity with a quality factor $Q_0 \approx 1000$, tunable from 34.6 GHz to 35.4 GHz is used as ENDOR probe head (see figure).

With the slightly over-coupled cavity the two pulse echo of our test sample (diamond doped with nitrogen) is developed to the maximum for mw $\pi/2$ and π pulses with lengths of 60 ns and 120 ns at an incident mw power of 6 W. For ENDOR experiments the radio frequency (RF) field is injected with a pair of hairpin loops of two turns each inside the cavity. Standard Davies and Mims ENDOR sequences have been implemented. The performance of the spectrometer is demonstrated for a broad radio frequency range by ^{1}H, ^{14}N, ^{31}P, ^{133}Cs, and ^{207}Pb pulsed ENDOR experiments of Cu^{2+}, Cr^{5+}, and V^{4+} transition metal ion complexes in both single crystals and disordered materials.

4.2.7 Characterization of Heterogeneous Catalysts by EPR Spectroscopy

A. Pöppl, V. Umamaheswari, M. Gutjahr, N. Vijayasarathi

A major research topic of our group is the study of active surface sites in heterogeneous catalysts by electron paramagnetic resonance (EPR) spectroscopy. To apply ESR methods to such systems the catalytically active sites have to be either paramagnetic species by themselves (e.g. paramagnetic transition metal ions) or paraprobe molecules have to be adsorbed on the studied diamagnetic surface sites (eg. acid centers and transition metal ion species).

The first approach has been used to characterize the immobilization of catalytically active V(IV) complexes on various solid surface supports (SiO_2, Al_2O_3, AlF_3). The grafting of tetrakis(dimethylamido)-vanadium(IV) precursor complexes and the subsequent exchange of the dimethylamido ligands by phosphorous and vanadium(V) containing ligands was studied in detail by a combined application of several EPR techniques at low temperatures. Besides continuous wave multifrequency EPR spectroscopy at X, Q, and, W band pulsed electron nuclear double resonance (ENDOR) as well as hyperfine sublevel correlation (HYSCORE) spectroscopy have been used to measure the weak superhyperfine (shf) interactions between the unpaired electron spin at the metal ion and the nuclear spins in the ligand molecules (^{1}H, ^{14}N, ^{31}P, ^{51}V) or in the surface support (^{27}Al, ^{19}F). These shf interactions are the key information in the structural analysis of such immobilized paramagnetic transition metal ion complexes. Alternatively, nitric oxide (NO) and di-tert-butyl nitroxide (DTBN) probe molecules were employed to characterize Lewis acid sites and Cu(I) cations in various zeolite materials. The geometrical and electronic structures of the resulting adsorption complexes with alkali and transition metal cations

could be again determined by a combined application of advanced EPR methods.

An attractive example for the application of modern EPR methods for the study of surface sites in microporous materials is the invetigation of the adsorption of DTBN in Cs exchanged Y zeolites. ^{133}Cs HYSCORE spectroscopy has been employed to characterize the structure of adsorption complexes of DTBN with cesium cations in zeolite CsNaY. The experimental ^{133}Cs HYSCORE data proved the direct coordination of the adsorbed DTBN molecules to the Cs^+ ions and revealed unambiguously the existence of two different types of adsorption complexes. Evaluation of the orientation selective ^{133}Cs HYSCORE spectra provided the ^{133}Cs hyperfine coupling tensors and thus information about the geometrical structure of those complexes (Fig. 1). For one type of adsorption complexes a complex geometry was obtained where the Cs^+ ion is located within the molecular mirror plane of the DTBN radical with an oxygen - cesium cation bond length of 0.25 nm (complex structure A). For this complex the isotropic Cs hyper-fine coupling was found to be negative. The second Cs^+-DTBN complex is characterized by a bent structure (complex structure B). With an isotropic ^{133}Cs hyperfine coupling of 9 MHz the unpaired electron spin density in this Cs^+-DTBN complex localized at the Cs ion was determined as 0.36%.

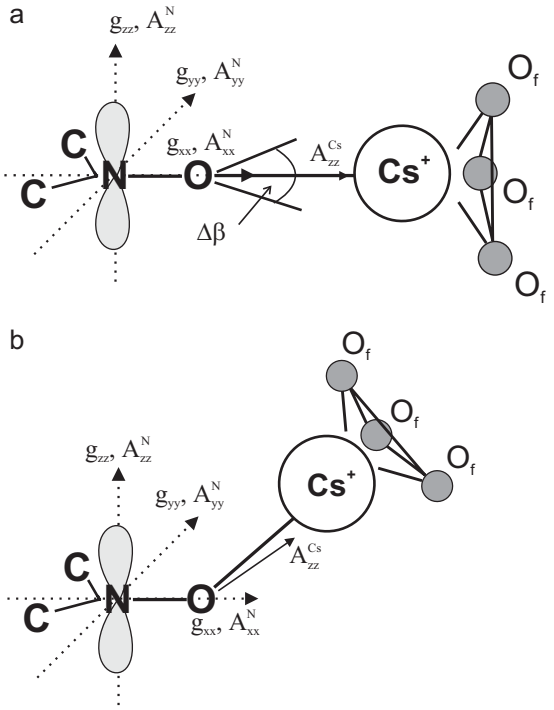

Fig. 1: Structural models of the DTBN-Cs^+ adsorption complexes zeolite CsNaY (with the frame-work oxygen of the zeolite indicated by O_f): (a) complex geometry A with a bond length $R_{O-Cs} = 0.25$ nm and $\beta_{bond} = 180° \pm 25°$; (b) complex structure B with $R_{O-Cs} = 0.21$ nm and $\beta_{bond} = 137° \pm 25°$.

[1] K. M. Neyman, D. I.. Ganyushin, V. A. Nasluzov, N. Rösch, A. Pöppl, M. Hartmann: Electronic g values of Na^+-NO and Cu^+-NO complexes in zeolites: Analysis using relativistic density functional methods, Phys. Chem. Chem. Phys. 5 (2003) 2429-2434.
[2] M. Gutjahr, R. Böttcher, A. Pöppl: ^{133}Cesium HYSCORE Investigation of the Di-tert-butyl Nitroxide — Cs^+ Adsorption Complex in CsNaY Zeolite, J. Phys. Chem. B 107 (2003) 13117-13122.

4.2.8 MAS-NMR Studies on Model Membranes: Lipid Bilayers Containing Membrane Peptides

A. Pampel, D. Michel

Part of the research program of our group is also the investigation of so called "soft-matter" or "semi-solid matter", especially of systems in liquid-crystalline phases as drug delivery systems and models for biological membranes. We are applying a multidisciplinary approach using mainly Solid State NMR spectroscopy to reveal structural and dynamical aspects of such systems. NMR spectroscopy has definite advantages over diffraction techniques in the structure elucidation of liquid-crystalline structures, which exhibit very low short-range order. These advantages, however, are frequently offset by resonance broadening mechanisms, which are caused by the anisotropic NMR parameters. Therefore, for this research we are using methods, which have been developed for the High-resolution NMR spectroscopy of solids. Main parts of our activities include the application, the development and the optimization of methods of High-resolution MAS techniques for the investigation of lipid bilayers containing membrane peptides. Current research projects include investigations of models of biological membranes with the main focus is on the determination of structure and dynamical behavior of molecules within membranes, e.g. peptides and proteins. In cooperation with the Institute of Biochemistry (Prof. A.G. Beck-Sickinger) we are investigating structural aspects of the membrane binding of the neuropeptide Y. As a novel technique for investigation of such system we have introduced the combination of Pulsed Field Gradient NMR and HR MAS NMR spectroscopy. The PFG MAS technique allows the determination of diffusion coefficients, even in a complicated environment like a membrane, which contains many components. Recently, we were successful in determining the diffusion coefficient of all membrane components of membranes containing lipids, water and a membrane peptide. [1]

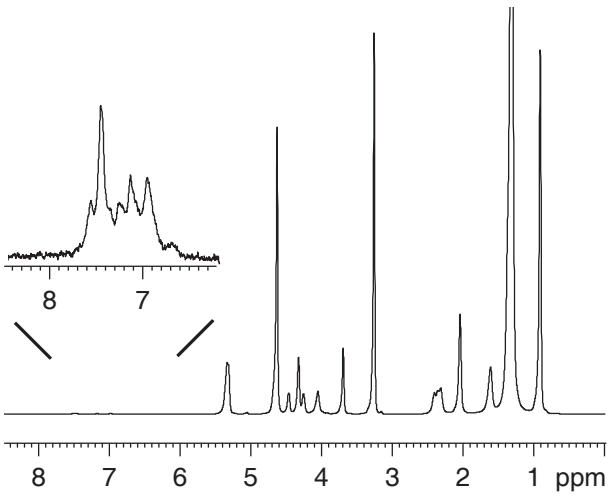

Fig. 1: ^{1}H MAS NMR spectrum of a lipid membrane composed of POPC, the peptide WALP16, and water, which was observed using the 750 MHz spectrometer (see above).

The inset shows the magnified region of the rather small signals of the aromatic rings of WALP16, which becomes detectable by the use of the high magnetic field.

The high resolution obtained allows the observation of the diffusion of all membrane components simultaneously.

Currently, we are focusing on further development of the PFG MAS method, especially on improvements of the theoretical description of the experiments.

[1] Pampel, A., J. Kärger and D. Michel, Lateral diffusion of a transmembrane peptide in lipid bilayers studied by pulsed field gradient NMR in combination with magic angle sample spinning, Chem. Phys. Lett., 2003. 379(5-6): p. 555-561.

4.2.9 Matrix Materials for Studies of Molecules in Confined Geometry

W. Böhlmann, D. Michel, S. Mulla-Osman

Zeolites and mesoporous molecular sieves have highly-ordered micro- and mesopores, which are suitable for many applications such as molecular sieving, cation exchange, catalyst, and quantum confinement of guest compounds. Furthermore, the study of mass transport and diffusion is particularly important in the understanding of catalytic processes.

Well-known MCM-41 and a further ordered mesoporous materials (OMM) of the SBA-type were prepared, which were of great interest as matrix materials in the last years. The OMM mentioned have uniform pore diameters and a hexagonal or cubic ordered pores, which makes them ideally suited as templates for preparing various inorganic nanowires/arrays and nanostructures. Besides the adsorption of different organic molecules the introduction of inorganic functional nanoparticles gives novel inorganic host-guest nanocomposites with specific optical, electronic and magnetic properties. Besides these aspects, it is known that molecules in confined geometry have another phase transition behavior as in the bulk state. Recently it could demonstrate that the freezing point temperature is reduced inversely proportional to the mean pore diameter when liquids are confined within small pores.

We studied the dynamic behavior of long chain molecules like n-dodecane and n-undecylamine in two different porous materials (MCM-41 and zeolite NaX) using several NMR methods [1]. NMR measurements were performed over a wide temperature range to characterize the behavior of molecules confined in the porous material. Moreover, recent advances in experimental techniques led to an additional increase in the resolution of ^{1}H NMR spectra and, in particular, allowed the observation of high-resolution ^{1}H MAS NMR spectra of adsorbed molecules. ^{13}C MAS and ^{13}C CP/MAS NMR studies are more sensitive to get information about the dynamics of the adsorbed molecules at low temperatures and and to study structural details. Independent of the host system used, both n-dodecane and n-undecylamine reveal a reduced melting-freezing transition temperature which lies about 60 K below that for the bulk liquids.

[1] W. Böhlmann, S. Mulla-Osman, and D. Michel, 1H and 13C NMR Studies of Long Chain Hydrocarbons Adsorbed on MCM-41 and Zeolite NaX, Stud. Surf. Sci. Cat., 2004, in press

4.2.10 NMR and Dielectric Investigations on Ethylene Glycol Molecules Sorbed in Zeolites

Özlen F. Erdem, Dieter Michel

Glass forming molecule ethylene glycol (EG) molecules are adsorbed in various types of zeolites (NaX, ZSM-5, sodalite) which possess different diameters of their internal cages. The aim of this study is to characterize the physical and chemical properties of the molecules in confined geometry and to study especially the reorientational and translational dynamics of the adsorbed molecules. In a first step of the studies, high-resolution ^{1}H, ^{13}C and CP MAS NMR spectroscopy was used to investigate the behavior of the adsorbed molecules for different pore filling degrees (or loadings). An important question is to determine the loading of the pores with high accuracy and to characterize the molecules in the internal holes besides those adsorbed on the external surfaces. This was possible by means of the ^{1}H NMR shifts.

Temperature dependent ^{1}H NMR measurements show clear differences between samples where the amount of adsorbed EG molecules in NaX zeolites corresponds to a complete or smaller filling of the cages (so-called normal loading, pore filling factor $\Theta \leq 1$) and "over-loaded" ones with a filling factor of $\Theta > 1$. Typical NMR spectra are shown in Fig. 1.

A pore filling factor $\Theta = 1$ corresponds to 10 EG molecules per large cavity (supercage) of NaX zeolites. In the present stage of the work, the task is to understand the typical changes in the NMR line shape on going from the range with $\Theta \leq 1$ to "overloaded" samples in terms of conformational changes of the adsorbed molecules under the influence of confinement. Moreover, it can be shown that frequency dependent ^{1}H NMR spin lattice relaxation time measurements allow us to characterize the state of adsorbed molecules in terms of molecular mobility and determine the correlation times of the thermal motion and their activation energies. In a next step the latter measurements will be compared with the results of dielectric measurements in order to understand whether an Arrhenius type behavior or Vogel-Fulcher type relaxation rates occur.

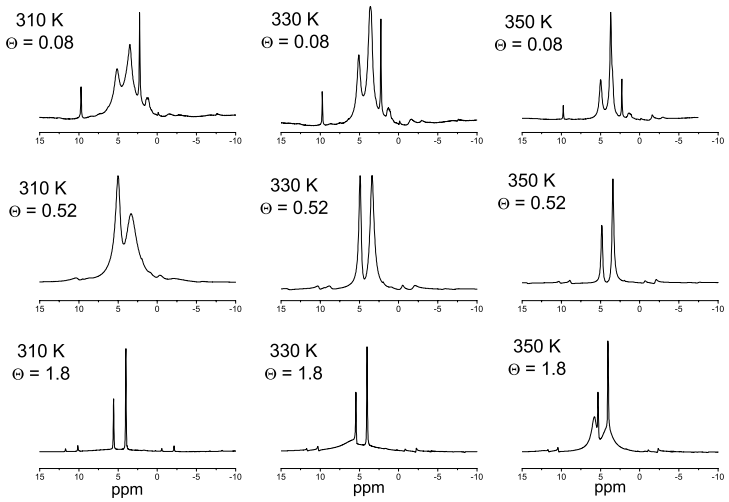

Fig. 1: ^{1}H MAS NMR spectra for ethylene glycol in NaX with different loading degrees, at temperatures of 310, 330 and 350 K.

4.2.11 Study of dynamics and structure of incommensurately modulated crystals by means of nuclear magnetic resonance spectroscopy

D. Michel, A. Taye
in close co-operation with Professor Jörn Petersson, University of Saarland, Saarbrücken

A large number of crystals, such as bis(4-chlorophenyl)sulphone ($[(ClC_6H_4)_2SO_2]$, abbreviated as BCPS), exhibit a phase transition from a high temperature normal phase into a one-dimensionally structurally incommensurately (IC) modulated phases, where a local property is modulated with a period which is not an integral multiple of the paraelectric unit cell edge. Consequently the translational periodicity is lost, and the crystallographic sites are no longer equivalent. With reference to the intention of the present work this fact has two important consequences. First, any static and local physical property shows a typical distribution. This is sometimes expressed by stating that the whole crystal may be looked upon as the elementary cell. Second, the initial phase of the modulation wave is arbitrary and the IC structure is continuously degenerate with respect to a phase shift. Thus, special low energy excitations termed phasons are present in IC systems. Quadrupolar perturbed nuclear magnetic resonance (NMR) has been proved to be an accurate and sensitive tool for investigating IC phases [1]. The static part of the electric field gradient (EFG) is a local physical property whose components are distributed in a characteristic manner because of the structurally incommensurate modulation. Accordingly, a spectrum of NMR frequencies occurs which shows edge singularities as a typical feature (Fig. 1).

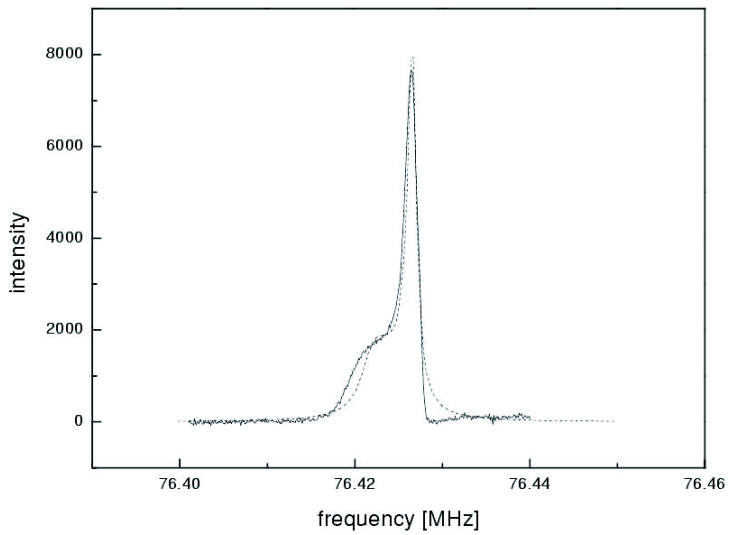

Fig. 1: Comparison of the calculated and the experimental ^{35}Cl NMR spectra in the IC phase at the temperature $T = 148.25\,\mathrm{K}$. The simulations reflect quite well the features of the experimental ^{35}Cl NMR spectra.

Moreover, the NMR spin-lattice relaxation rates, $1/T_1$, allow special insights into the phason and amplitudon dynamics in the IC phase of BCPS below $T_\mathrm{i} \approx 150\,\mathrm{K}$ and about the collective dynamics in the critical range above T_i. The simulation of the ^{35}Cl NMR

line shape in the IC-Phase of high quality BCPS single crystals performed and the interpretation of the critical contribution to $1/T_1$ achieved are in complete agreement with the general theoretical predictions for systems with IC phases:
a) The asymmetric frequency distribution with edge singularities very close to the N-IC phase transition below T_i (Fig. 1) is a clear indication that large-scale fluctuations of the modulation wave ("floating") do not occur [2].
b) The critical behavior above T_i is in good agreement with the predictions of the 3d XY model and with the results of the renormalization group theory [3].
c) The behavior of $1/T_1$ in the IC phase below T_i is consistent with the predictions of the dominant role of phason and amplitudon fluctuations [3].
d) The broad temperature range for the critical dynamics above T_i which is in contradiction to the Ginzburg-Landau criterion, can be completely understood on the basis of an extended renormalization scheme [4].

[1] F. Decker, and J. Petersson, Phys. Rev. B 61, 8993 (2000)
[2] A. Taye and D Michel, physica status solidi. (b), (2004), in press
[3] A. Taye, D. Michel, and J. Petersson, Phys. Rev. B, (2004), in press; A. Taye, D. Michel, J. Petersson, 35Cl nuclear magnetic resonance study of critical fluctuations in bis(4-chlorophenyl)sulphone [(ClC6H4)2SO2], Phys. Rev. B 66 (2002) 174102-1-7
[4] J. M. Wesselinowa, D. Michel, H. Braeter, N. M. Plakida, J. Petersson, and G. Völkel, Phys. Rev. B 68, 224109 (2003).

4.2.12 The Low-Temperature Phase of Chromium Doped Dimethylammonium Gallium Sulfate Hexahydrate (DMAGaS) Studied by Electron Paramagnetic Resonance

G. Völkel, R. Böttcher, D. Michel, Z. Czapla*
*University of Wroclaw, Institute of Experimental Physics

Dimethylammonium gallium sulfate hexahydrate (DMAGaS) and dimethylammonium aluminum sulfate hexahydrate (DMAAS) are isomorphous and ferroelastic at room temperature. Both they show an order-disorder type transition into a ferroelectric phase but only DMAGaS exhibits a further first-order transition into a low temperature non-ferroelectric phase. We investigated the electron paramagnetic resonance (EPR) of chromium doped DMAGaS giving insight into the peculiar reorientation order of the polar dimethylammonium ions on a microscopic level. We found that the low-temperature phase of DMAGaS below 115 K shows a sequence of commensurate and incommensurate phases. Below 60 K the crystal becomes antiferroelectric [1]. This unusual phase sequence can be well explained by means of a Landau approach using a great number of sublattice polarizations and more generally by the semimicroscopic extended DIFFOUR model [2].

[1] G. Völkel, R. Böttcher,D. Michel, Z. Czapla, Ferroelectrics 268, 181 (2002).
[2] G. H. F. van Raaij, K. J. H. van Bemmel, T. Janssen Phys. Rev. B 62, 3751 (2000).

4.2.13 Order-disorder of TMA ions and phase transitions in tetramethylammonium cadmium chlorid (TMCC) studied by NMR

D. Michel, S. Mulla-Osman, G. Völkel, Z. Czapla*
*University of Wroclaw, Institute of Experimental Physics, 50204 Wroclaw, Poland

TMCC belong to the isostructural family of tetramethylammonium (TMA) haloids, $(CH_3)_4NMX_3$, with the bivalent metals M = Mn, Ni, Cd, Cu, V and the halogen atoms X = Cl, Br, I, have attracted much attention because of their one-dimensional type structure. They are built up from infinite chains of MX_6 octahedra. The space between the chains is occupied by the $(CH_3)_4N^+$ [TMA] cations. ^{14}N and ^{1}H NMR measurements enable to study the ordering of TMA ions in relation to the phase transition from the high-temperature hexagonal phase I (space group $P6_3/m$, $Z = 2$ formula units) to a ferroelastic phase II ($P2_1/m$) of TMCC. The results are discussed on the base of theoretical predictions about the orientational order of the TMA groups in the well-known contribution of Braud et al. [1].

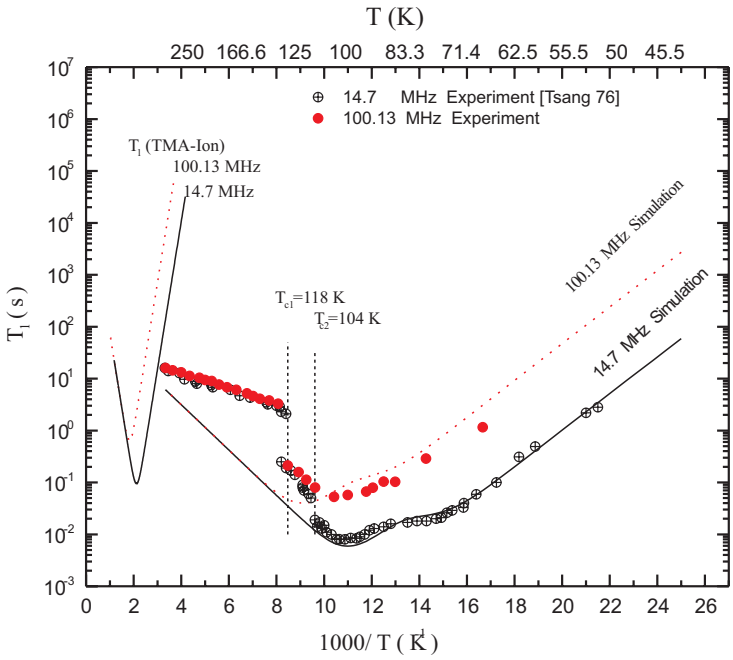

Fig. 1: ^{1}H-NMR spin-lattice relaxation time for TMCC single crystals. The red points (•) represent our measurements at the resonance frequency of $\nu = 100.13$ MHz. Previous maesurements (⊕) from Tsang et al. [6] were run at 14.7 MHz.

In our previous ^{35}Cl NMR investigations [2, 3] which are also essential for the interpretation of XRD measurements [4], we have found a twin domain structure in the ferroelastic phase II. The measured saturated rotational angle between the epitaxially grown domains of $\Theta_{exp} = 4°$ is in a very good agreement with the theoretical value of $\Theta_s = 3.5°$ calculated from the ferroelastic strain tensor. The sequence of the structural phase transitions in this crystal family was previously described in the framework of the Landau theory [1]. To proof these predictions, ^{14}N NMR and ^{1}H NMR spin-lattice relaxation time measurements were run [5]. The temperature dependence of the ^{14}N quadrupole coupling tensors

in the various phases of TMCC crystals can be explained on the base of a pseudo spin model. This treatment also explains the two-component order parameter h in the ferroelastic phase II the amount of which can be directly derived from the NMR spectra. Thus, the results presented provide a detailed proof of the theoretical predictions in [1]. With respect to this pseudo-spin operator analysis two different sorts of CH_3 groups are present in phase II. Even this conclusion is nicely supported by further ^{1}H NMR spin-lattice relaxation studies on TMCC at different fields B_0 (see Fig. 1) which are based on a previous paper by Tsang and Utton [6]. In the range $1000/T < 4$ a contribution to the relaxation time is expected owing to the isotropic reorientation of the TMA ions. In the simulation shown here, the activation energies were taken from Ref. [7]. Besides the overall tumbling of the whole TMA ion, the reorientation of the CH_3 groups about their C-N axes gives a significant contribution to T_1. In the phase III of TMCC, below 104 K, the contribution of two different types of methyl groups can be seen, which directly supports the prediction of the pseudo-spin theory which was developed for the whole important crystal family showing the quasi-one dimensional ordering behavior.

[1] M. N. Braud M N, M. Couzi and N. B. Chanh, J. Phys.: Condens. Matter 2, 8243 (1990).
[2] S. Mulla-Osman, D. Michel, G. Völkel and Z. Czapla, phys. status solidi 219, 9 (2000), "Investigation of the ferroelastic domain structure of TMCC by means of nuclear magnetic resonance spectroscopy".
[3] S. Mulla-Osman, D. Michel, G. Völkel, I. Peral and G. Madariaga, ^{35}Cl-NMR studies of the domain structure of tetramethyl-ammonium cadmium chloride (TMCC) at lower temperatures, J. Phys.: Condens. Matter 13, 1119 (2001).
[4] I. Peral, G. Madariaga, A. Perez-Etxebarria and T. Breczewski, Acta Cryst. B 56, 215 (2000).
[5] S. Mulla-Osman, D. Michel, Z. Czapla, phys. status solidi (b) 256, 173 (2003), "^{14}N-NMR study of the domain structure of tetramethylammonium cadmium chloride (TMCC)".
[6] T. Tsang, D. B.Utton, J Chem Phys. 64, 3780 (1976).
[7] S. Albert, H. S. Gutowsky, J. A. Ripmeester, J Chem. Phys. 56, 3672 (1972)

4.2.14 Advanced Signal Processing for Magnetic Resonance

D. Michel, A. Pampel

Quantitation of time domain data is a very useful tool for the estimation of spectral parameters in magnetic resonance spectroscopy (MRS) and for applications in magnetic resonance imaging (MRI).

This work was part of a European Project (with participants from the Belgium, France, Germany, Greece, The Netherlands and Spain) in which a program system for Medical Magnetic Resonance Imaging and Spectroscopy is developed with a special "Magnetic Resonance User Interface (MRUI)". The co-ordinator of this EU project was Prof. Dirk Van Ormondt, Technische Universiteit Delft (NL).

Software development is one of the goals of the EU Project, "Advanced Signal Processing for Medical Magnetic Resonance Imaging and Spectroscopy", formerly in the Human Capital and Mobility Networks programme (HCM , CHRX-CT94-0432, 1994-1997) and

later in the programme Training and Mobility of Researchers (TMR, FMRX-CT97-0160, 1997-2001).

The Advanced Time Domain Signal Processing Package includes
-Black box quantitation based on Singular Value Decomposition (SVD)
-Non Linear Least Squares quantitation (NLLS)
-Preprocessing algorithms
-Error estimation: Cramér-Rao lower bounds

Details are available in:
http://azur.univ-lyon1.fr/TMR/tmr.html
(see also <Dr. Danielle Graveron>)
http://www.mrui.uab.es/mrui/mruiHomePage.html
(see also <Dr. Miguel Cabanas>)

The programme system is freely accessible and is already used world wide.

4.2.15 Melting-freezing phase transition of gallium embedded in porous glasses

D. Michel
in close co-operation with
B. F. Borisov*, E. V. Charnaya*, D. Yaskov*, C. Tien**, C. S. Wur**, and Yu. A. Kumzerov***
*Institute of Physics, St. Petersburg State University, St. Petersburg, 198904, Russia
**Department of Physics, National Cheng Kung University, Tainan, 701 Taiwan
***A.F.Ioffe Physico-Technical Institute RAS, St.Petersburg, 194021, Russia

The main topics of this work include
- the study of phase transitions in confined geometry, in particular melting and freezing of metallic gallium nanoparticles within porous matrices;
- the influence of size effects on the mobility in confined liquids, e.g. the mobility of melted metallic gallium in pores;
- the effect of confinement on electronic properties of metals which may be sensitively studied by means of alterations of the Knight shift for gallium within pores.

Samples of porous glasses (with pore diameter of 3.5 to 200 nm) and synthetic opals (regular spheres of silica) were used as matrices.

The melting-freezing phase transition of gallium confined within Vycor glass was studied by NMR and acoustic techniques. A pronounced depression of the freezing and melting phase transition temperatures and a hysteresis in the melting-freezing processes were found and discussed. NMR studies on liquid confined gallium revealed a noticeable decrease in the Knight shift and a drastic acceleration in gallium spin-lattice relaxation. These changes depend on the size and the geometry of the pores. The relaxation measurements were used to estimate the thermal correlation times of the Ga atoms in the confined geometry and to relate them with atomic diffusion.

4.2.16 An exactly soluble model for distortive structural phase transitions in a crystal with a single defect

H. Braeter, D. Michel

An exactly soluble three-dimensional spherical-like model [Physica A 321 (2003) 543-564] is considered to describe the distortive structural phase transition of a crystal with a single defect. The defect can be incorporated in the vibrations of all other particles only if the attractive single site potential of the defect is less than a certain critical value. No local distortions can appear above the phase transition temperature T_C of the perfect host crystal. Above the critical value of its attractive single-site potential, the defect does not participate in the motions of the host. But a local mode may appear above T_C, which only condenses if the critical value is reached. The local mode can only soften at the phase transition temperature of the perfect system. All critical exponents of the model with a single defect are the same as the critical exponents of the perfect lattice.

4.2.17 Funding

Strukturaufklärung der Tieftemperaturphase des Dimethylammoniumgalliumsulfat (DMA-GaS) und der Untersuchung des Ordnungs-Unordnungs-Verhalten der Dimethylammoni-umgruppen mit Hilfe der EPR-Spektroskopie
Investigation of the low-temperature phase in demethylammoium gallium sulfate (DMAGaS) and the order disorder behaviour of the dimethylammonium groups (DMA) by means of EPR
R. Böttcher, D. Michel: DFG, Bo 1080/7

Strukturaufklärung nanokristalliner Ferroelektika mit Perowoskitstruktur durch Hochfeld-EPR-Spektroskopie
Investigation of nanocrystalline ferroelectrics with pervoskite structure by means of high-field-EPR spectroscopy
(im Rahmen des Schwerpunktprogrammes 1051)
R. Böttcher: DFG, Bo 1080/6-3

Synthese und Charakterisierung eindimensionaler Ferroelektrika mit Perowskitstruktur
Synthesis and characterisation of one dimensional ferroelectrics with perovskite structure
(im Rahmen der Forschergruppe 522)
R. Böttcher, E. Hartmann: DFG Bo 1080/8-1

Hochfeld-ESR Spektroskopie von monomerem und dimerem Stickstoffoxid-Komplexen in Zeolithen
High field EPR spectroscopy of monomer and dimer nitric oxide complexes in zeolites
(im Rahmen des Schwerpunktprogrammes 1051)
A. Pöppl, M. Hartmann: DFG: PO 426/2-3

Synthese und Strukturaufklärung von Vanadium-Phosphat-Systemen mittels ENDOR-und ESEEM-Spektroskopie
Synthesis and determination of the structure of vanadium-phosphate systems by means

of ENDOR and ESEEM spectroscopy
A. Pöppl, K. Köhler: DFG, PO 426/3-1

Experimental proof of the predictions of renormalization theory on the critical exponents in systems with incommensurately structurally modulated phases
D. Michel: DFG Mi 390/

Advanced Signal Processing for Medical Magnetic Resonance Imaging and Spectroscopy
D. Michel (mit A. Pampel)
(EU, programme TMR: Contract No. ERBFMRXCT970160)

High-Resolution NMR Spectrometer with a Proton Resonance Frequency of 750 MHz
D. Michel: DFG, Mi 390/5-3

Phase transitions in metals and ferroelectrics embedded into porous glasses and other porous matrices.
D. Michel, E. V. Charnaya: DAAD, Leonhard-Euler programme

NMR studies of short-chain surfactants in a heavy water solutions
D. Michel, V. I. Chizhik: DAAD, Leonhard-Euler programme

4.2.18 External cooperations

Leibniz-Institut für Oberflächenmodifizierung - IOM Leipzig (Dr. E. Hartmann)

Universität Kaiserslautern, Fachbereich Chemie, Technische Chemie (Dr. M. Hartmann)

Technische Universität München, Anorganisch-chemisches Institut (Prof. K. Köhler)

The Weizmann Institute of Science, Department of Physical Chemistry, Rehovot, Israel (Prof. D. Goldfarb)

Vilnius University, Radiophysics Department (Dr. J. Banys)

Wroclaw University, Institute of Experimental Physics (Prof. Z. Czapla)

University of Opole, Institute of Mathematics (Prof. V. A. Stephanovich)

Max-Delbrück-Center for Molecular Medicine (Dr. R. Reszka)

Universität des Saarlandes, Saarbrücken (Prof. J. Petersson et al.)

St. Petersburg State University (Prof. E. V. Charnaya, Prof. B. N. Novikov, Prof. V. I. Chizhik)

Ioffe Institute St. Petersburg (Prof. J. A. Kumzerov)

Kirensky Institute of Physics of the Sibirian Branch of the Russian Academy of Sciences, Krasnoyarsk (Prof. I. P. Aleksandrova, Dr. J. Ivanov)

A. Mickiewicz University of Poznan (Prof. S. Jurga)

Universität Leipzig, Fakultät für Biowissenschaften, Pharmazie und Psychologie (Prof. A. Beck-Sickinger)

Martin-Luther-Universität Halle-Wittenberg: Department of Physics (Dr. H. T. Langhammer, Prof. Dr. H. Schneider, Prof. Dr. H. Beige)
School of Pharmacy, Institute for Pharmaceutics (Prof. R. H. H. Neubert, Prof. Dr. S. Wartewig)

4.2.19 Publications

Journals

G. Völkel, R. Böttcher, D. Michel, Z. Czapla
Low-temperature phase of chromium-doped dimethylammonium gallium sulfate hexahydrate studied by electron paramagnetic resonance
Phys. Rev. B 67 (2003) 024111-1 - 14

S. Mulla-Osman, D. Michel, Z. Czapla
^{14}N NMR study of the domain structure of tetramethylammonium cadmium chloride (TMCC)
phys. Stat. Sol. (b) 236 No. 1 (2003) 173-181

H. Trommer, S. Wartewig, R. Böttcher, A. Pöppl, J. Hoentsch, J.H. Ozegowski, R. H.H. Neubert
The effects of hyaluronan and ist fragments on lipid models exposed to UV irradiation
Int.Journal of Pharmaceutics 254 (2003) 223-234

K. M. Neyman, D. I. Ganyushin , V. A. Nasluzov, N. Rösch, A. Pöppl, M. Hartmann
Electronic g values of Na^+-NO and Cu^+-NO complexes in zeolites: Analysis using a relativistic density functional method
Phys. Chem. Chem. Phys. 5 (2003) 2429-2434

H. Braeter, D. Michel
An exactly soluble model for distortive structural phase transitions in a crystal with a single defect
physica A 321 (2003) 543 - 564

E. Erdem, R. Böttcher, H.-C.Semmelhack, H.-J. Gläsel, E. Hartmann
Multi-frequency EPR study of Cr3+ doped lead titanate (PbTiO3) nanopowders
Phys: Stat: Sol: (b) 239 (2003) R7-R9

E. Erdem, R. Böttcher, H.-C. Semmelhack, H.-J. Gläsel, E. Hartmann, D. Hirsch

Preparation of lead titanate ultrafine powders from combined polymerisation and pyrolysis route
J. Mat. Sci. 38 (2003) 3211-3217

H. T. Langhammer, T. Müller, R. Böttcher, H.-P. Abicht
Crystal structure and related properties of copper-doped barium titanate ceramics
Solid State Science 5 (2003) 965-971

A. Pampel, J. Kärger, D. Michel
Lateral diffusion of a transmembrane peptide in lipid bilayers studied by pulsed field gradient NMR in combination with magic angle sample spinning
Chem. Phys. Lett. 379 (2003) 555 - 561

E. V. Charnaya, D. Michel, C. Tien, Yu. A. Kumzerov, D. Yaskov
The Knight shift in liquid gallium confined within porous glasses and opals
J. Phys.: Condens. Matt. 15 (2003) 5469 - 5477

D. Michel, A. Pampel, J. Roland
Investigation of conformational changes of organic molecules sorbed in zeolites by proton magnetic resonance spectroscopy
J. Chem. Phys. 119 (2003) 9242-9250

M. Gutjahr, R. Böttcher, A. Pöppl
133Cesium HYSCORE Investigation of the Di-tert-Butyl Nitroxide-Cs+ Adsorption Complex in CsNaY Zeolite
J. Phys. Chem. B 107 (2003) 13117-13122

O. Klepel, A. Loubentsov, W. Böhlmann, H. Papp
Oligomerization as an important step and side reaction for skeletal isomerization of linear butenes on H-ZSM-
Appl. Catalysis A: General 255 (2003) 349-354

J. Hoentsch, Yu. Rosentzweig, D. Heinhold, K. Köhler, M. Gutjahr, A. Pöppl, G. Völkel, R. Böttcher
A Q-Band Pulsed ENDOR Spectrometer for the Study of Transition Metal Ion Complexes in Solids
Appl. Magn. Reson. 25 (2003) 249-259

J. M. Wesselinowa, D. Michel, H. Braeter, N. M. Plakida, J. Petersson, G. Völkel
Width of the critical region at incommensurate phase transitions
Phys. Rev. B, 68 (2003) 224109-1 - 224109-5

J. Petersson, D. Michel
Obituary Professor Dr. Horst Müser (1925 - 2003)
Ferroelectrics 297 (2003) 1 - 2

Conference contributions

Talks

"Characterization of Active Sites in Zeolites by Means of EPR Spectroscopy", A. Pöppl, M. Gutjahr, T. Rudolf, V. Umamaheswari, 45th Rocky Mountain Conference on Analytical Chem-istry", Denver, 2003

"High-field CW-EPR Studies of Chromium-doped PbTiO3 nanopowders", E. Erdem, R. Böt-tcher, Statement Colloquium of the priority program High Field EPR in Biology, Chemistry and Physics, 21-24.09.2003, Hirschegg /Austria

"Size Effects in Chromium-doped PbTiO3 nanopowders", E. Erdem, R. Böttcher, SFB Collo-quium, Technical University of Darmstadt, 03.12.2003

"NMR and Acoustic Studies of the Melting-Freezing Phase Transition for Gallium in Porous Glasses", E.V.Charnaya, B.F.Borisov, D.Yaskov, D.Michel, C.Tien, Yu.A.Kumzerov, DPG-Jahrestagung in Dresden 24.–28. 3. 2002, Arbeitskreis Festkörperphysik

"Domänenstruktur und Mechanismus der Phasenübergänge in TMCC-Kristallen", D. Michel, S. Mulla-Osman, G. Völkel, Z. Czapla, DPG-Jahrestagung in Dresden 24. bis 28. März 2002, Arbeitskreis Festkörperphysik

"35Cl NMR study of critical fluctuations in bis(4-chlorophenyl)sulphone [(ClC6H4)2SO2]", A. Taye, D. Michel, J. Petersson, DPG-Jahrestagung in Dresden 24. bis 28. März 2002, Arbeits-kreis Festkörperphysik

"Dielectric properties of a DMAGaS/DMAAS mixed crystal", J. Banys, G. Völkel, R. Bött-cher, D. Michel, Z. Czapla, DPG-Jahrestagung in Dresden 24. bis 28. März 2002, Arbeits-kreis Festkörperphysik

"Study of Order and Disorder of TMA ions in Tetramethylammonium (TMA) Cadmium Chlorid Type Solids by NMR", Dieter Michel, invited talk, RAMIS 03, Poznan, April 24 -26, 2003, Vortrag am 24th April, 1000 -1045 h

"Proton Conductivity as Studied by 2D Exchange NMR", Dieter Michel, Invited Lecture AMPERE XI NMR SCHOOL in Zakopane, June 1 - 6, 2003

"Order-disorder of TMA ions and phase transitions in tetramethylammonium calcium chlorid (TMCC) studied by NMR", Dieter Michel, Samir Mulla-Osman, Georg Völkel, Zbigniew Czapla, 10th European Meeting on Ferroelectricity (EMF10), Cambridge, August 3 - 8, 2003

"NMR and acoustic studies of metallic gallium embedded into porous glasses and artificial opals", D.Michel, B.F.Borisov, E.V.Charnaya, C.Tien, D.Yaskov,Yu.A.Kumzerov, invited lecture, 5. Specialized Colloque AMPERE 2003, Portoro, Slovenia, September 8 - 12, 2003

"Magnetische Resonanzmethoden zum Studium von Ordnungs- und Unordnungsphänomenen in Ferroelektrika", D. Michel, Vortrag zum Heraeus-Ferienkurs "Ferroelektrika - Intelligente Materialien für Aktoren, Sensoren und Speicher", MLU Halle, 22. 09.2003

D. Michel, Kolloquiumsvortrag, 20.11.03, MLU Halle, Fachbereich Physik, anläßlich des Festkolloquiums anläßlich des 65. Geburtstags von Prof. Dr. Horst Schneider,

Posters

"ESR SPECTROSCOPY OF CU(I)-NO ADSORPTION COMPLEXES IN ZEOLITES", A. Pöppl, V. Umamaheswari, M. Hartmann, Christoph Freysoldt, Joachim Reinhold, 5th Meeting of the European Federation of EPR Groups, Lisbon, 2003

"A COST-EFFICIENT Q-BAND PULSED ENDOR SPECTROMETER FOR THE STUDY OF TRANSITION METAL ION COMPLEXES IN SOLIDS", J. Hoentsch, Yu. Rosentzweig, K. Köhler, M. Gutjahr, A. Pöppl, G. Völkel, R. Böttcher, 5th Meeting of the European Federa-tion of EPR Groups, Lisbon, 2003

"Preparation of lead titanate ultrafine powders from combined polymerisation and pyrolysis route", E. Erdem, R. Böttcher, H.-C. Semmelhack, H.-J. Gläsel, E. Hartmann, D. Hirsch, Spring Meeting of the Condensed Matter Division of the German Physics Society, Dresden, 24-28.03.2003

"Multi-frequency EPR study of Cr3+ doped lead titanate (PbTiO3) nanopowders", E. Erdem, R. Böttcher, H.-C. Semmelhack, H.-J. Gläsel, E. Hartmann, 5th Meeting of the European Fed-eration of EPR Groups, Lisbon, 2003

"EPR study of Cr3+ doped lead titanate", E. Erdem, R. Böttcher, H.-C. Semmelhack, H.J. Gläsel, E. Hartmann, 25th Discussion Meeting of GDCh, , Leipzig, 2003

"Synthesis and Characterization of Ferroelectric Nanopowders", E. Erdem, R. Böttcher, H.J. Gläsel, E. Hartmann, International Nanotechnology Symposium- nanofair 03, Dresden, 2003

"The Low-Temperature Phase of Chromium Doped Dimethylammonium Gallium Sulfate Hexahydrate (DMAGaS) Studied by Electron Paramagnetic Resonance", G. Völkel, R. Böttcher, D. Michel, Z. Czapla, DPG-Jahrestagung in Dresden 24. bis 28. März 2002, Arbeitskreis Festkörperphysik

"Critical dynamics in BCPS at the N-IC phase transitions", D. Michel, J. Petersson, A. Taye 10th European Meeting on Ferroelectricity (EMF10), Cambridge, August 3 - 8, 2003

"^{1}H NMR Spectroscopy of Molecules Adsorbed in Porous Media ", D. Michel, A. Pampel, J. Roland, 5th Specialized Colloque AMPERE 2003, Portoro, Slovenia, September 8 - 12, 2003

"Critical dynamics at N-IC phase transitions", D. Michel, J. Petersson, A. Taye, 5th Special-ized Colloque AMPERE 2003, Portoro, Slovenia, September 8 - 12, 2003

"Proton NMR spectroscopy at very high magnetic fields", D. Michel, A. Pampel, Alpine NMR Conference, 14 th to 18 th Sept 2003, Chamonix, France

4.2.20 Guests

A large number of guests have visited our group in 2003 about which we cannot report here in detail. This includes also numerous guests from abroad, e.g. from Israel, France, Lithuania, Poland, Syria, Vietnam, Russian Federation (St. Petersburg, Kazan), and the United States.

4.3 Semiconductor Physics

4.3.1 Introduction

In 2003 we have enjoyed tremendous progress in our activities in the fields of ZnO and related compounds and self-assembled nanostructures. Our efforts related to nanostructures are supported now within the Forschergruppe 522 *Architecture of nano- and micro-dimensional building blocks* (based in Leipzig[1]). With funding in the framework of Forschergruppe 404 *Oxide interfaces* (based in Halle/Saale[2]) heterostructures are investigated, in particular CdZnO/MgZnO quantum wells, oxide Bragg mirrors and ferroelectric ZnO/$BaTiO_3$/ZnO structures. The work regarding magnetic ZnO-based alloys is performed in the 'Nachwuchsgruppe' (Young Research Team) *Nano-Spintronics*[3], lead by Dr. Heidemarie Schmidt. We enjoy a fruitful collaboration with the Superconductivity and Magnetism group with regard to the magnetic properties of transition metal doped ZnO and Schottky contacts on GaAs including ferromagnetic metals.

We have fabricated and investigated $Mg_xZn_{1-x}O$ alloys now in the complete range $0 \leq x \leq 1$. $Mn_xZn_{1-x}O$ thin films with a few percent Mn have been found to be ferromagnetic at room temperature. Next year will see increased efforts in the study of $Cd_xZn_{1-x}O$ and alloys including other transition metals.

ZnO nanowhiskers have been fabricated using thermal growth and pulsed laser deposition. First results have in the meantime also been achieved for the growth of ZnO-based alloy wires, such that we are close to our goal to grow nanowire heterostructures.

We enjoy close collaboration with the Institute of Anorganic Chemistry, in particular with our colleague Dr. Volker Gottschalch, who is fabricating excellent III-V material using MOVPE, such as boron and nitrogen alloyed InGaAs, and GaAs-based nanostructures, such as nanowhiskers and scrolls.

Using empirical pseudopotentials we have successfully modelled the band structures of group-V nitrides, also with the 'new' small InN band gap. Excellent agreement has been found between our theoretical and experimental data for the UV dielectric function of ZnO.

We gratefully acknowledge the arrival of equipment in the framework of the 'HbfG-Verfahren' to characterize semiconductors and semiconductor devices on the wafer level with optical and electrical methods. Also we could expand the cathodoluminescence set-up with a 1 m monochromator for high spectral resolution studies of single nanowires.

A significant amount of time was invested in coordinating the application for a Network of Excellence in the 6th framework programm of the EC in the field of self-assembled semiconductor nanostructures. We have now taken all necessary steps and look forward to receiving the contract and starting the network SANDiE with 28 European partners in June 2004.

Please look through the following abstracts to learn about some more details of our research and publications. Links to the papers can mostly be found on our WWW site[4].

M. Grundmann

[1] www.uni-leipzig.de/∼for522
[2] www.physik.uni-halle.de/FG/fg_main.html
[3] www.uni-leipzig.de/∼nse
[4] www.uni-leipzig.de/∼hlp

4.3.2 ZnO nanowire arrays on sapphire grown by high-pressure pulsed laser deposition

M. Lorenz, E. M. Kaidashev, A. Rahm, T. Nobis, H. Hochmuth, J. Lenzner, M. Grundmann

Flexible control of the diameter and the shape of ZnO nanowires is achieved using high-pressure pulsed laser deposition. A few monolayers of gold are required to initiate the nucleation of well aligned ZnO nanowire arrays on a-plane and c-plane sapphire. The wire diameter was varied between 50 and 3,000 nm. Cathodoluminescence spectra taken on single ZnO nanopillars show detailed bound (FWHM (I_6) = 1.5 meV at T = 8 K) and free exciton peak features similar to MOCVD grown nanowires [1, 2, 3].

Figure 1 shows a scheme of the multi-target high-pressure PLD chamber designed for ZnO nanowires and heterostructures. The main part of the chamber is a T-shape quartz tube with outer diameter of 30 mm. The flexibility of the proposed PLD process concerning size and shape of the ZnO nanostructures is demonstrated in Figs. 2b and 3, respectively. Fig. 2b shows the effect of the target to substrate distance in the high-pressure PLD system on the diameter of the ZnO nanowires. Fig. 3a shows the effect of substrate covering with gold using a mask with 100 μm holes. The growth of free standing ZnO nanowires is clearly limited to the gold coated substrate region thus illustrating the importance of gold for the nanowire nucleation process. On the substrate areas not covered with gold only a thin ZnO layer is found, as shown in Fig. 3a and b. Figure 3b-f shows main shapes of PLD grown ZnO nanowires, with increasing structural complexity. Thus, we demonstrate the flexibility of high-pressure PLD to grow ZnO nano- and microstructures in a wide morphology range [2, 3].

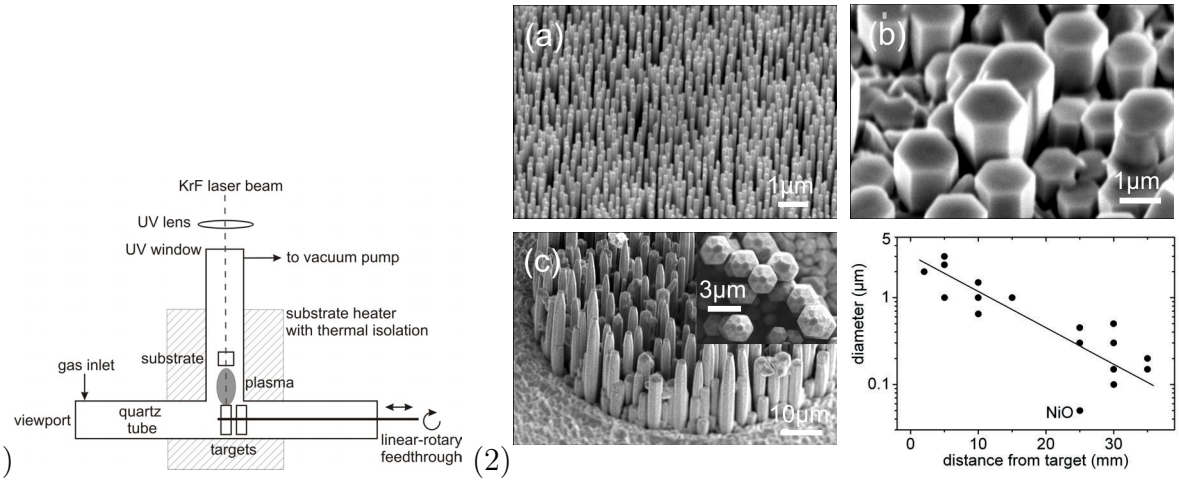

Fig. 1: Scheme of high-pressure PLD chamber for nano-heterostructures consisting of a T-shape quartz tube. Fig. 2: Increasing size of ZnO nanowires for decreasing target to substrate distance during PLD growth: (a) nanowire diameter 100–150 nm at 30 mm distance, (b) 1,000 nm diameter at 10 mm distance, and (c) 2,500 nm diameter at 5 mm distance, *inset* shows top view. The label NiO indicates a NiO nucleation layer instead of gold.

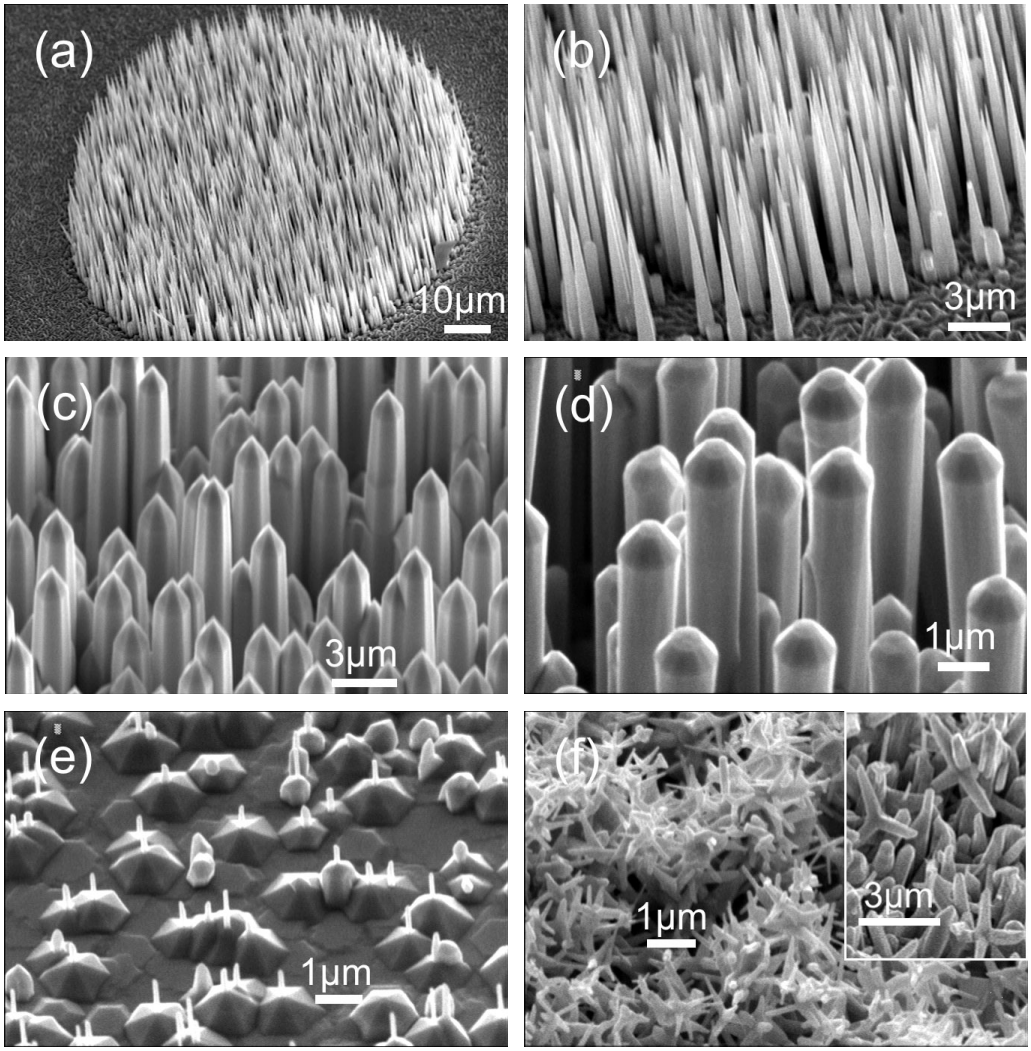

Fig. 3: Typical shapes of ZnO nanostructures on sapphire for different PLD growth conditions: (a) nanowire growth limited to monolayer gold nucleation film with 100 μm diameter, (b) needle-like structures, preferably grown on a-plane sapphire upon reduced plasma density, (c) hexagonal nanocrystals with top of high index planes on c-plane sapphire, grown upon slightly reduced Ar pressure of 50 instead of 100 mbar, and (d) nanocrystals with polygon cross section and top cap, grown by successive ablation from a ZnO and a ZnO:Zn target. Dot-like (e) and branched tripod-like (f) structures have been grown using a CeO_2 buffer layer.

This work is supported by the DFG within the framework of FOR 522 (Gr 1011/11-1), and by BMBF Wachstumskern INNOCIS under Grant No. 03WKI09.

[1] M. Lorenz, J. Lenzner, E. M. Kaidashev, H. Hochmuth, M. Grundmann, Ann. Phys. **13**, 39 (2004).
[2] T. Nobis, E. M. Kaidashev, A. Rahm, M. Lorenz, J. Lenzner, M. Grundmann, Nano Letters (2004) in press.
[3] M. Lorenz, E. M. Kaidashev, A. Rahm, T. Nobis, H. Hochmuth, J. Lenzner, M. Grundmann, unpublished

4.3.3 Spatially resolved optical properties of single ZnO microcrystals

Th. Nobis, A. Rahm, M. Grundmann

We investigate the local optical properties of zinc oxide micro- and nanostructures using spatially resolved cathodoluminescence (CL) imaging. For each digitally controlled scan position of the electron beam of a scanning electron microscope (SEM) a complete CL spectrum is recorded in the spectral region of interest.

A top view SEM image of the investigated hexagonal micropillars is given in Fig. 1a. At room temperature those pillars exhibit two broad luminescence bands, the first around 3.23 eV (UV) according to radiative recombination of free excitons, the second at 2.3 eV (VIS) attributed to deep levels such as oxygen or zinc vacancies. When mapping the average intensity ratio of both luminescence bands the spatial distribution of deep levels can be visualized as depicted in Fig. 1b. Apparently, UV emission is extremely enhanced at all the pillars' centers (bright regions) whereas VIS emission is suppressed there. When approaching the border of the pillars, the intensity ratio decreases below 0.1 and green emission dominates (dark regions) indicating an increasing influence of deep defects.

To reveal reasons for the enhanced UV luminescence intensity highly resolved low temperature CL point spectra have been collected shown in Fig. 1c. The spectrum from the border of the pillar at point B shows a dominating narrow donor bound exciton line at 3.3607 eV (I_6, FWHM = 1.6 meV), indicating a neutral aluminium donor [1]. In comparison to point B, at point A the CL intensity is about 20 times greater, but the spectral maximum is shifted by a few meV to a lower energy of 3.3575 eV in association with a line broadening of about a factor of 6.

These results indicate the local concentration and accumulation of aluminium at the center of the studied ZnO pillars, since that would explain both the increased donor bound exciton emission *and* the broadened line shape. Strain effects have been observed on pillars clamped by others and result in a continuously shifted I_6-peak that remains sharp. Whether the Al accumulation is caused by diffusion from the Al_2O_3 substrate or due to other processes is one question of further investigations. For a detailed discussion see [2].

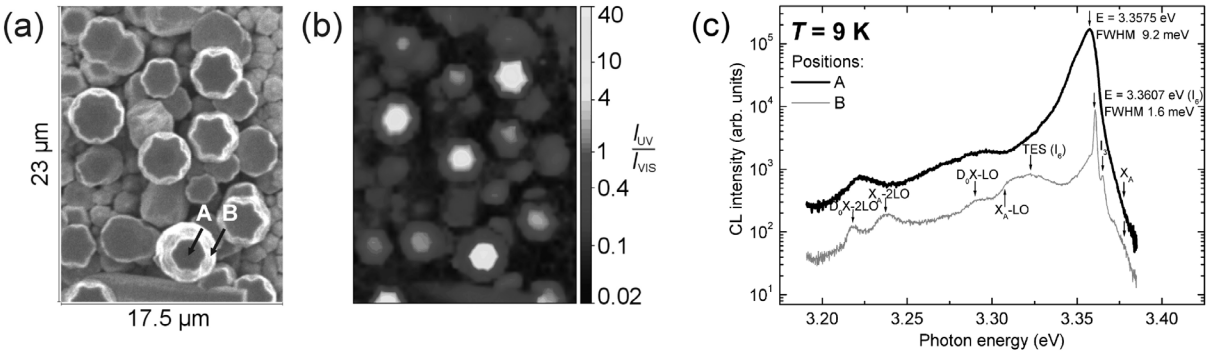

Fig. 1: (a) SEM-image (top view) of ZnO micropillars grown by PLD. (b) Spatial map of the UV-VIS-intensity ratio using a logarithmic scale. (c) Local CL spectra at $T = 9$ K for the positions A and B as indicated in (a).

[1] B.K. Meyer et. al., phys. stat. sol. (b) 241, 231 (2004)
[2] Th. Nobis et. al., Nano Letters (2004), in press

4.3.4 MOVPE-growth of $A^{III}B^{V}$-nanowhiskers

J. Bauer*, H. Herrnberger*, V. Gottschalch*, G. Wagner*, J. Lenzner, M. Grundmann
* Department of Inorganic Chemistry, Semiconductor Chemistry Group, University of Leipzig

The worldwide interest in semiconductor technology concentrates on the formation of nanoscaled building blocks to make electronic devices faster and more efficient. New effects in these materials (e.g. quantum confinement of electrons in low-dimensional structures) lead to new applications in optoelectronics.

We investigate the growth of free-standing column-shaped $A^{III}B^{V}$ -nanocrystallites with metal-organic vapor phase epitaxy. The well-known growth mechanism of silicon whiskers is described by the 'vapor-liquid-solid'-process [1]. According to this basic concept, we evaporated thin gold films on cleaned GaAs $(\bar{1}\bar{1}\bar{1})$ As-substrates. We found, that the gold layer is built up of small clusters at low deposition rates (Fig. 1).

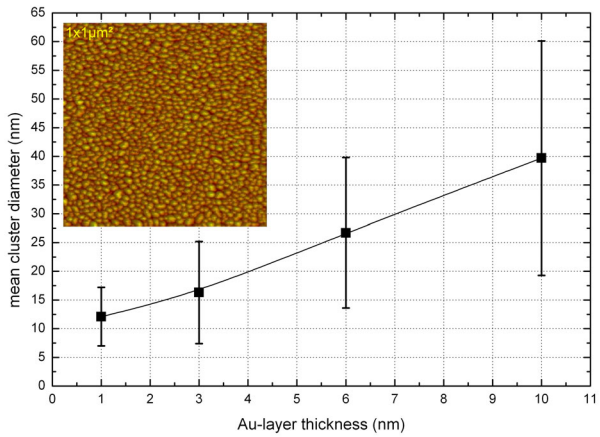

Fig. 1: At low deposition rates of the gold evaporation process the deported layer consists of self-assembled gold-nanoclusters (*inset*: $1\,\mu m^2$ AFM-picture of a 6 nm thick gold film on GaAs $(\bar{1}\bar{1}\bar{1})_{As}$-substrate). With increasing layer thickness the clusters lump together and the cluster size distribution increases.

The whisker diameter depends directly on the size of the gold clusters. Annealing measurements showed a coarsening of the cluster size distribution. To accomplish the most homogeneous diameter distribution we disclaimed any additional annealing step in the growth procedure. According to Fig. 1 the whisker diameter can be tuned due to the gold film thickness. In that way, we reached dense fields of GaAs-whiskers with diameters less than 50 nm (Fig. 2).

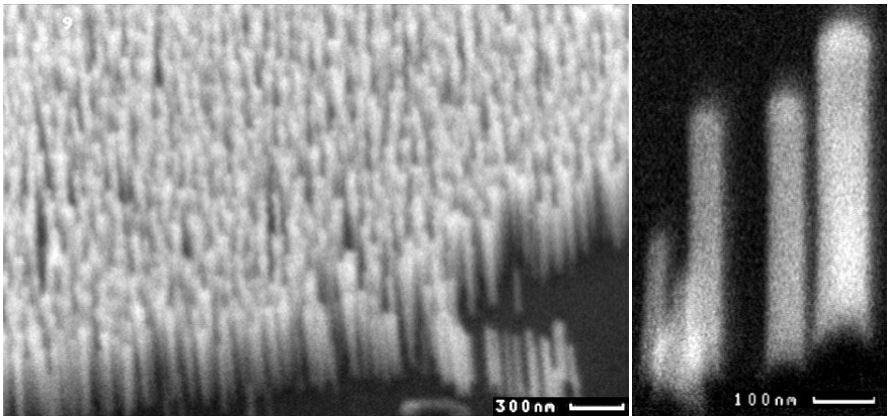

Fig. 2: MOVPE-grown narrow organized GaAs-nanowhiskers perpendicular to the substrate using TMGa and AsH_3 at 480°C. The GaAs $(\bar{1}\bar{1}\bar{1})_{As}$-substrate was covered with an 1 nm thick gold film.

[1] Givargizov et al., J. Cryst. Growth 31, 20 (1975)

4.3.5 Preparation of $A^{III}B^{V}$ nanotubes from epitaxial thin films

O. Lühn*, V. Gottschalch*, H. Herrnberger*, J. Lenzner
* Department of Inorganic Chemistry, Semiconductor Chemistry Group, University of Leipzig

The method of self-rolling nanotubes from strained semiconductor heterostructures was first introduced by Prinz et al. and enables to build nanotubes of various length and radii [1]. By etching a sacrificial AlAs layer, a moment of force develops. Continuum strain relaxation theory predicts the ⟨100⟩-directions as preferred winding directions in the cubic zinc blende structures (see next section).

Strained heterostructure bilayers of $B_xGa_{1-x}As/In_yGa_{1-y}As$ ($0.02 < x < 0.04; 0.16 < y < 0.23$) of different thicknesses (10 nm–20 nm) with AlAs as the sacrificial layer were grown on (100) oriented GaAs with low-pressure MOVPE.

Material selective etching of $Al_{0.35}Ga_{0.65}As$ and AlAs resulted in a preferred etching direction which is the ⟨100⟩ (Fig. 1) and resembles the preferred direction of rolling up. This SEM picture shows the resulting square of $Al_{0.35}Ga_{0.65}As$; the formed planes of the crystal are 100 equivalent. The sacrificial layer was etched with a solution of citric acid:hydrogen peroxide. Similar results were obtained for AlAs.

Knowing the preferred etching behavior we can conclude that tubes form, in agreement with strain relaxation theory, preferentially along the etch front in ⟨100⟩ direction (Fig. 2a) and helices along the ⟨110⟩ direction (Fig. 2b).

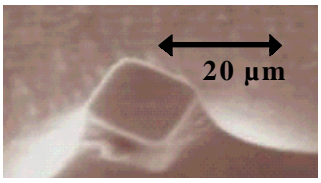

Fig.1: Etched square.

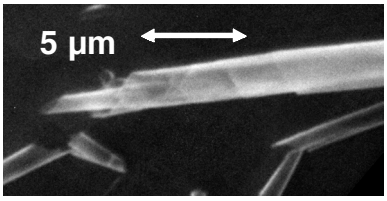

Fig.2a: Tube along ⟨100⟩.

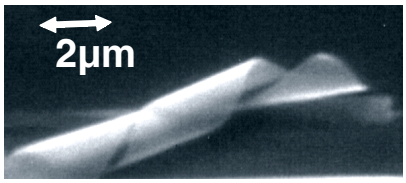

Fig.2b: Helix along ⟨110⟩

The influence of lateral etch rates on the rolling process is shown in figure 3. Photolithography was used to define the starting conditions of the roll-up process (Fig.4). We prepared squares of different sizes by depositing a photoresist on the crystal surface and etched them down to the substrate. Afterwards the rolling process was initiated by etching the sacrificial AlAs layer.

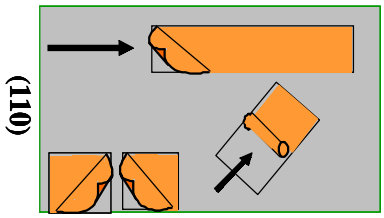

Fig.3: Overview directional rolling.

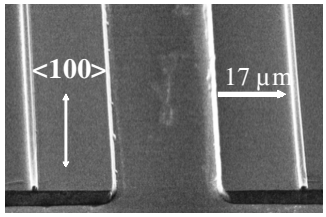

Fig.4: Formed tubes along ⟨100⟩.

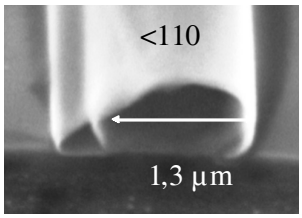

Fig.5: Broken tube along ⟨110⟩

Tubes roll up along the ⟨100⟩ direction from the starting edges (Fig. 4). By rolling up along ⟨110⟩ the tubes break along the cleavage plane (Fig. 5) which lies in the axis of the rolled-up tube.

[1] Prinz et al., Physica E 6, 828 (2000).

4.3.6 Theory of strained nanoscroll heterostructures

M. Grundmann

Nanoscrolls are a novel type of nanostructure, cylindrically or spirally rolled, strain-engineered semiconductor films which have been reported first in [1]. The strain is built in by pseudomorphic growth of materials lattice mismatched to the substrate. For sufficiently large strain, small sheet thickness d and great length L of the sheet, the strain relaxation leads to spirally rolled structures with many windings. Various novel applications like pipes or nanocoils have been envisioned for such structures.

We model the strain relaxation in nanoscrolls made up from semiconductor multilayers using continuum elasticity theory [2]. The scroll strain energy E

$$E = \frac{C_{11}-C_{12}}{2C_{11}}\left(C_{11}(\epsilon_t+\epsilon_y)^2 + C_{12}(\epsilon_t^2+\epsilon_y^2)\right) + (2C_{44}-C_{11}+C_{12})\left(\frac{\epsilon_t-\epsilon_y}{2}\right)^2 \sin^2(2\phi)$$

depends on the winding direction ϕ (azimuthal angle with respect to [100]) due to the cubic symmetry of the semiconductors. ϵ_t and ϵ_y denote the strains in the tangential direction and along the cylinder axis, respectively. Therefore also the bending radius of the scroll depends on ϕ. $\langle 100\rangle$ is predicted the preferred winding direction (Fig. 1a) in agreement with experiment which shows that narrow sheets form curls with winding along $\langle 100\rangle$ (Fig. 1b and previous section). The inclusion of anharmonic strain (third order elastic coefficients) leads to a small decrease of the scroll radius [2].

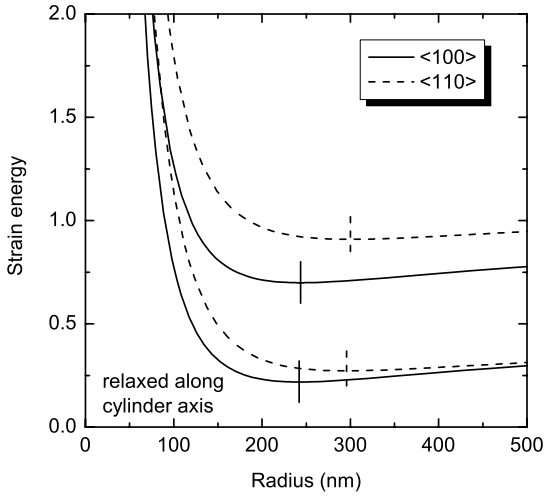

(a)

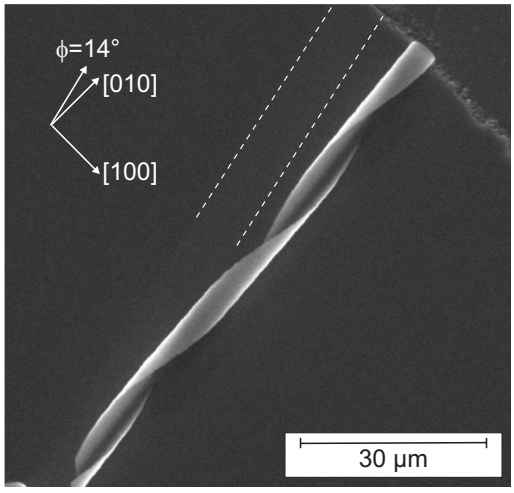

(b)

Fig. 1: (a) Strain energy (in units of the strain energy of the flat pseudomorphic layers) of a scroll of a 4-layer SiGe structure (three layers of $Si_{0.3}Ge_{0.7}$, $Si_{0.6}Ge_{0.4}$ and $Si_{0.8}Ge_{0.2}$, each 3 nm thick and a 1 nm Si cap) as a function of radius for winding directions along $\langle 100\rangle$ and $\langle 110\rangle$. Top (bottom) curves without (with complete) strain relaxation along the cylinder axis. Vertical lines indicate the positions of the respective energy minima. From [2]. (b) SEM image of curled InGaAs/GaAs nanoscroll rolled $\phi = 14°$ off $\langle 100\rangle$. The stripe from which the film was rolled off is indicated by white dashed lines. From [3].

[1] V.Y. Prinz, V.A. Seleznev, A.K. Gutakovsky, Proc. 24th Int. Conf. on the Physics of Semiconductors, Israel, 1998, p. Th3-D5.
[2] M. Grundmann, Appl. Phys. Lett. 83, 2444 (2003).
[3] S. Mendach, University of Hamburg, private communication.

4.3.7 Pulsed laser deposition of undoped and doped ZnO thin films and multilayers

M. Lorenz, H. Hochmuth, H. von Wenckstern, E. M. Kaidashev, R. Schmidt-Grund, G. Ramm, M. Grundmann

Epitaxy of undoped and doped ZnO thin films by means of pulsed laser deposition is established now as a flexible, fast and cost effective growth technique for high-quality material for numerous research activities and applications. These include:

1. Undoped ZnO thin films with high electron mobility at 300 K [1].
2. ZnO-MgO Bragg resonator multilayer structures, see Fig. 1 (and Sect. 4.3.12).
3. ZnO-MgO thin films for determination of optical constants by spectroscopic ellipsometry [2] and structural analysis in cooperation with Prof. A. Krost, University of Magdeburg.
4. Attempts for p-type conducting ZnO thin films by doping with N, Ga, Li, Sb, P [3] (see Sect. 4.3.10).
5. Ferromagnetic ZnO thin films by doping with Fe, Mn, Ni in cooperation with BMBF young scientists group 'Nano-Spintronics' (Dr. H. Schmidt) (see Sect. 4.3.8).
6. ZnO thin films with high and laterally homogeneous luminescence yield at room temperature for innovative detector applications, in cooperation with ElMul Technologies Ltd., Yavne, Israel.

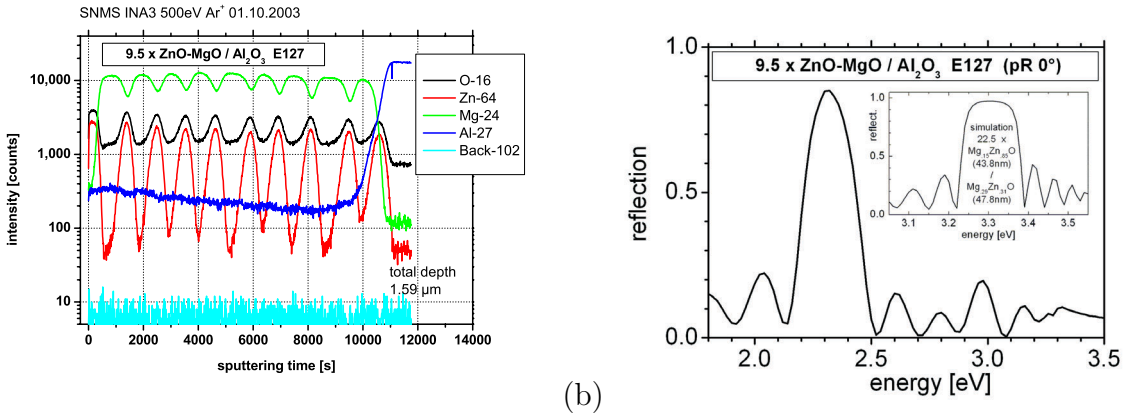

(a) (b)

Fig. 1: (a) SNMS concentration depth profile of a 9.5 pair ZnO-MgO Bragg multilayer on sapphire. (b) Spectral reflectivity of the 9.5 pair Bragg resonator which is analyzed in (a). *Inset* shows simulation of a 22.5 pair MgZnO-MgZnO resonator.

This work was supported by BMBF Wachstumskern INNOCIS under Grant No. 03WKI09, and by DFG SPP 1136.

[1] E. M. Kaidashev, M. Lorenz, H. von Wenckstern, A. Rahm, H.-C. Semmelhack, K.-H. Han, G. Benndorf, C. Bundesmann, H. Hochmuth, M. Grundmann, Appl. Phys. Lett. **82**, 3901 (2003).
[2] R. Schmidt, B. Rheinländer, M. Schubert, D. Spemann, T. Butz, J. Lenzner, E. M. Kaidashev, M. Lorenz, M. Grundmann, Appl. Phys. Lett. **82**, 2260 (2003).
[3] C. Bundesmann, N. Ashkenov, M. Schubert, D. Spemann, T. Butz, E. M. Kaidashev, M. Lorenz, M. Grundmann, Appl. Phys. Lett. **83**, 1974 (2003)

4.3.8 Mn-doped ZnO films for spintronics

Heidemarie Schmidt*, Erick Guzmán*, Mariana Diaconu*, A. Setzer**, P. Esquinazi**, H. v. Wenckstern, G. Benndorf, H. Hochmuth, M. Lorenz, M. Grundmann
* BMBF-Nachwuchsgruppe 'Nano-Spinelektronik' **Superconductivity and Magnetism Group

By incorporating 3d transition metals [1] into a semiconductor one obtains alloyed or hybrid materials for new devices based on spin manipulation, for example spin-transistors and magneto-optical sensors. The saturation magnetization (measured by SQUID) of pulsed laser deposited $Zn_{1-x}Mn_xO$ thin films on sapphire substrates with $x = 0.04$ amounts to 0.065 emu g^{-1} and 0.02 emu g^{-1} at 10 K and at room temperature, respectively. The structural, electrical, and magnetic properties of the $Zn_{1-x}Mn_xO$ thin films strongly depend on the PLD target preparation, oxygen partial pressure, and growth temperature. As can be seen from the AFM and SQUID measurements on $Zn_{0.96}Mn_{0.04}O$ and $Zn_{0.94}Zn_{0.06}O$ room temperature ferromagnetism seems to be favored by formation of a larger crystallites.

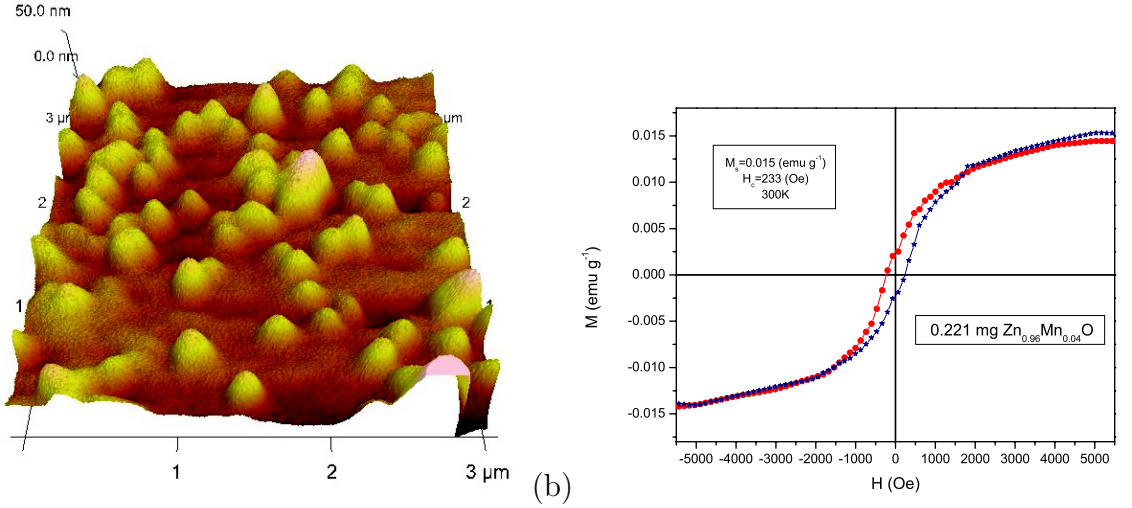

That corresponds to the observation that ferromagnetism in ZnMnO nanostructures shows higher coercivity field strength than in ZnMnO thin films [2]. As already known from unintentionally doped, naturally n-type ZnO where the oxygen partial pressure also suppresses the formation of intrinsic donor impurities (V_O, Zn_i, Zn_O), the n-type conductivity in ZnMnO thin films is tuned from $n = 10^{18}$ cm^{-3} to highly compensated for a pressure ranging from 0.0001 mbar to 0.3 mbar, respectively. The free charge carrier tunability and also the occurrence of an additional very efficient luminescence transition M_1 at low temperatures which reflects intrinsic properties of Mn in ZnO [3] do not sensitively depend on the Mn content. In contrast to the band gap shift of isoelectronically doped ZnMgO or ZnCdO, the D^0X and D^0X-LO optical transitions are unshifted in ZnMnO. The M_1 and D^0X PL intensity depend linearly on the photoluminescence excitation intensity (for $D < 80$ W/cm^2).

[1] E. Guzmán et al., Ann. Phys. 13, 57 (2004).
[2] V.A. L. Roy et al., Appl. Phys. Lett. 84, 756 (2004).
[3] P. Dahan and V. Fleurov, J. Phys.: Cond. Matter 6, 101 (1994).

4.3.9 Homogeneous Schottky contacts on ZnO

H. v. Wenckstern, G. Biehne, J. Lenzner, R. Pickenhain, H. Hochmuth, M. Lorenz, M. Grundmann

The II-VI semiconductor ZnO is a promising material for the realization of different classes of devices as for instance emitters or detectors in the ultra-violet range. Metal-semiconductor-metal (MSM) photodiodes have very fast response times and are therefore suitable structures for the realization of high speed detectors. MSM photodiodes are made up of two Schottky contacts (SC) that are opposingly connected. The quality of the SC's strongly influences the performance of the device. Up to now, SC's on ZnO do not fulfill requirements as low leakage currents, small ideality factors, and reproducibility necessary for device application. We have investigated the homogeneity of SC's on ZnO by means of electron beam induced current measurements in dependence on the surface preparation prior to the evaporation of the contact metal. Wet chemical etching methods and a treatment in N_2O plasma were used. We found that the induced current is homogeneous for contacts treated in the N_2O plasma as depicted in Fig. 1a. Reflection high energy electron diffraction measurements showed that the surface is not roughening due to this procedure [1]. In contrary, EBIC images of wet chemically etched samples revealed lateral variations of the induced current signal (Fig. 1b). The bright spots and the bright veined structure correspond to regions where higher currents are induced. A spot of the inhomogeneous contact was imaged with higher magnification.

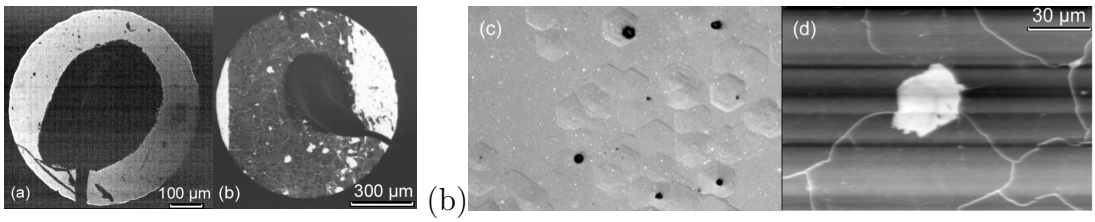

Fig. 1: (a) EBIC image of homogeneous SC. (b) EBIC image of inhomogeneous SC. (c) SEM image showing etch pits. (d) EBIC image of the same surface spot.

Fig. 1c is a secondary electron microscopy (SEM) image showing etch pits resulting from the etching procedure. Fig. 1d is an EBIC image of the same surface spot. A comparison of the two figures implies that the veined structure in the EBIC image does not correlate with the etch pits visible in Fig. 1c. Within the bright spot in the middle of Fig. 1d there is only a small variation in the induced current signal. This might be due to etch pit induced surface steps since there are hexagonal grooves at the same surface patch in Fig. 1c. Overall the effect of the etch pits is negligible compared to the large regions showing almost no induced current signal. The origin of these dark regions is under further investigation but remains up to now unclear. In conclusion, the treatment of ZnO in a N_2O plasma prior to the deposition of the contact metal results in homogeneous SC's and is therefore preferred to chemical etching.

[1] H. von Wenckstern, E. M. Kaidashev, M. Lorenz, H. Hochmuth, G. Biehne, J. Lenzner, V. Gottschalch, R. Pickenhain, M. Grundmann, Appl. Phys. Lett. 84, 79 (2003).

4.3.10 Acceptor incorporation in ZnO thin films

H. v. Wenckstern, S. Heitsch, E. M. Kaidashev, M. Lorenz, G. Benndorf, M. Grundmann

Zinc oxide is a transparent semiconductor with a band gap of 3.44 eV at T=2 K and a high exciton binding energy of approximately 60 meV. Therefore, it is a promising material for effective excitonic devices working in the UV spectral range. ZnO thin films doped with lithium and nitrogen or antimony have been investigated by means of photoluminescence and Hall measurements. The films were grown on a-plane or c-plane sapphire by pulsed laser deposition.

The Li and N doped samples were realized by sputtering a ZnO-target containing 5% Li_3N. The films show n-type conduction. Photoluminescence was excited by the 325 nm line of a He-Cd laser with a maximum power density of 80 W/cm^2 and measured at temperatures between 2K and 300K. The luminescence spectra of ZnO:Li,N samples show a donor-acceptor-pair (DAP) transition at ∼3.25 eV which could be identified on the basis of temperature dependent measurements (Fig. 1a). The involved acceptor can be assigned to the nitrogen acceptor at an oxygen site. Assuming the involved donor to be an effective-mass donor with a binding energy of about 65 meV (as determined from Hall measurements at nominally undoped ZnO thin films), the acceptor binding energy of nitrogen in ZnO may be approximated to be ∼130 meV. Sb-doped samples were produced using ZnO-targets containing 0.5% or 5% Sb. The first have a free electron concentration of about 10^{17} cm^{-3} the latter from 5×10^{18} to 5×10^{19} cm^{-3}. Annealing the samples in flowing nitrogen at 800°C does not change the electron concentration of the samples with lower Sb-content but the electron concentration of the higher doped samples decreases by a factor of 10. Such an annealed sample showing a clear drop in the electron concentration was investigated by photoluminescence spectroscopy. In the corresponding low-temperature spectrum a donor-acceptor-pair transition can be found at ∼3.24 eV (Fig. 1b). Following the above mentioned procedure, the antimony acceptor in ZnO can be approximated to have a binding energy of ∼140 meV. In conclusion, we were able to incorporate acceptors in ZnO. Photoluminescence measurements show DAP-transitions from which the acceptor binding energies of N and Sb were approximated to be ∼130 and ∼140 meV, respectively.

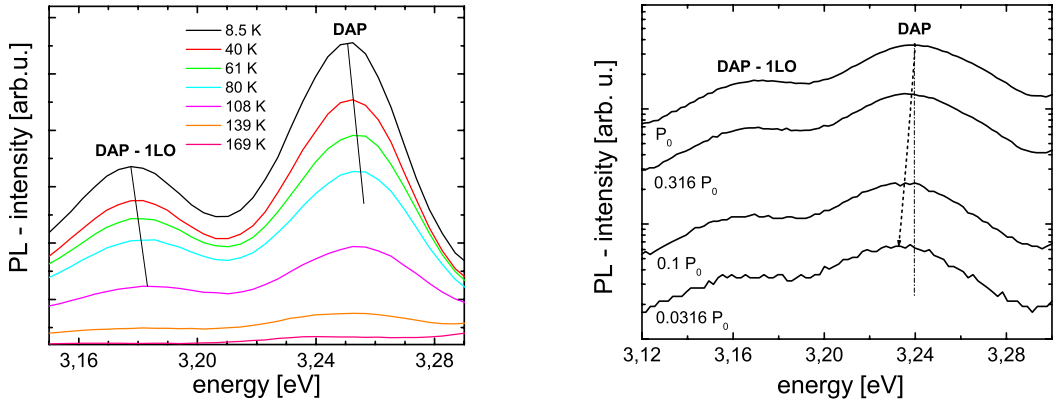

(a) (b)

Fig. 1: (a) Temperature dependence of the DAP line and its first phonon replica of ZnO:Li,N, (b) dependence on the excitation power of the DAP line and its first phonon replica of ZnO:Sb at 2 K.

4.3.11 VUV ellipsometry and band-structure of MgZnO

R. Schmidt-Grund, D. Fritsch, M. Schubert, B. Rheinländer, H. Schmidt,
E. M. Kaidashev, M. Lorenz, C. M. Herzinger*, and M. Grundmann
* J.A. Woollam Co., Inc., Lincoln, NE 68508, U.S.A

For ternary wurtzite $Mg_xZn_{1-x}O$ films, optical properties were determined using spectroscopic ellipsometry and the band-structure was obtained from empirical pseudopotential calculations (EPM). The $Mg_xZn_{1-x}O$ ($0 \leq x \leq 0.53$) layers with a thickness of typically 1 μm have been deposited by pulsed laser deposition on sapphire substrates. For the a-plane ZnO layer, the spectra of the dielectric functions for the polarization parallel and perpendicular to the c-axis show a series of transitions which named here E_1 - E_6. These can be assigned to critical point transitions in the band structure obtained by empirical pseudopotential calculations (Fig. 1).

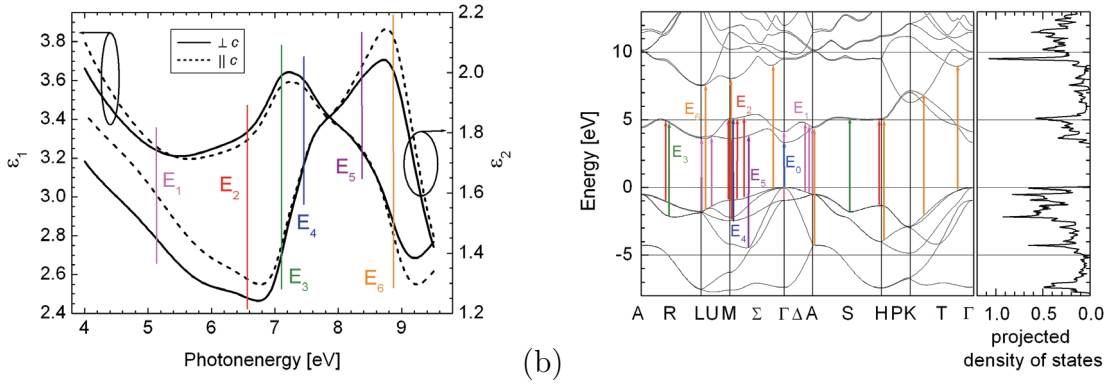

(a) (b)

Fig. 1: (a) Real (ϵ_1) and imaginary (ϵ_2) part of the dielectric functions of ZnO. The energies of the observed transitions are indicated by *vertical lines*. (b) Band-structure of ZnO. The experimentally observed transitions are assigned to vertical electronic band-to-band transitions within the calculated band-structure are indicated by *vertical bars*.

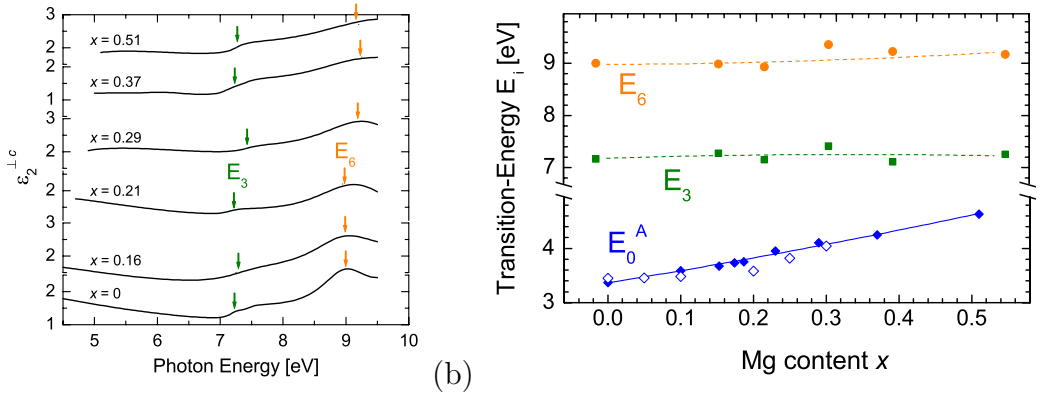

(a) (b)

Fig. 2: (a) Imaginary part of the dielectric function ϵ_2 of $Mg_xZn_{1-x}O$. The energies of the observed transitions are indicated by *arrows*. (b) Band-to-band transition energies determined by ellipsometry (*filled symbols*) and calculated by EPM for T=0 K (*open symbols*). The lines at the E_3 and E_6 transitions are intended to guide to the eye.

For the c-plane $Mg_xZn_{1-x}O$ layers, the dielectric functions for the polarization perpendicular to the wurtzite c-axis was determined. Only two transitions named E_3 and E_6 are observable. The energies of E_3 and E_6 are only slightly blue-shifted by the cation sub-

stitution of Zn by Mg. The fundamental gap energy E_0 [1] shows a significant blue-shift with increasing Mg content which is comparable with theoretical results (Fig. 2).

[1] R. Schmidt et al., Appl. Phys. Lett. **82**, 2260 (2003).
[2] R. Schmidt-Grund et al., Thin Solid Films 455-456, pp. 500-504 (2004).

4.3.12 $Mg_xZn_{1-x}O$ alloys for UV-Bragg-reflectors

A. Carstens, R. Schmidt-Grund, H. Hochmuth, B. Rheinländer, D. Spemann, A. Rahm, M. Lorenz und M. Grundmann

For Bragg resonators in opto-electronic devices based on ZnO, the alloy system $Mg_xZn_{1-x}O$ is a well appropriate candidate. Single $Mg_xZn_{1-x}O$ layers with $x = 0 \ldots 1$ were deposited by means of Pulsed Laser Deposition (PLD) on c-plane sapphire. The layer thicknesses range from 100 nm to 400 nm. The Mg-mole fractions x have been deduced from Rutherford backscattering (RBS) data. In order to design Bragg reflectors, the refractive indices of both reflector materials have to be known. The refractive index spectrum for a given mole fraction $x > 0.5$ was evaluated from the fit of a Cauchy refractive-index model to the spectra in the ellipsometric parameters for the respective transparency range. The ellipsometric parameters were measured in the photon energy range $E = (0.75 - -4.50)$ eV. The band gaps were estimated from transmissivity and reflectivity spectroscopy. The refractive indices for a device-relevant energy $E = 3.4$ eV are given in Fig. 1a. Considering the refractive index spectrum for $x < 0.5$ [1], the materials for the Bragg reflectors should comprise the mole fraction range $x = 0.2 - 1.0$. Because layers with $x < 0.4$ are of wurtzite type and for $x > 0.6$ of rocksalt type, the layer stack of the Bragg reflector should consist of an alternating series of layers of both types. We have shown that such a layer sequence can be deposited successfully and a grown ZnO-MgO Bragg reflector works well. On the basis of all these results the simulation of a realistic version of ZnMgO Bragg reflectors is demonstrated in Fig. 1b. Applying 15 layer pairs with x=0.2 and 1.0 the reflectivity surmounts values of 0.9.

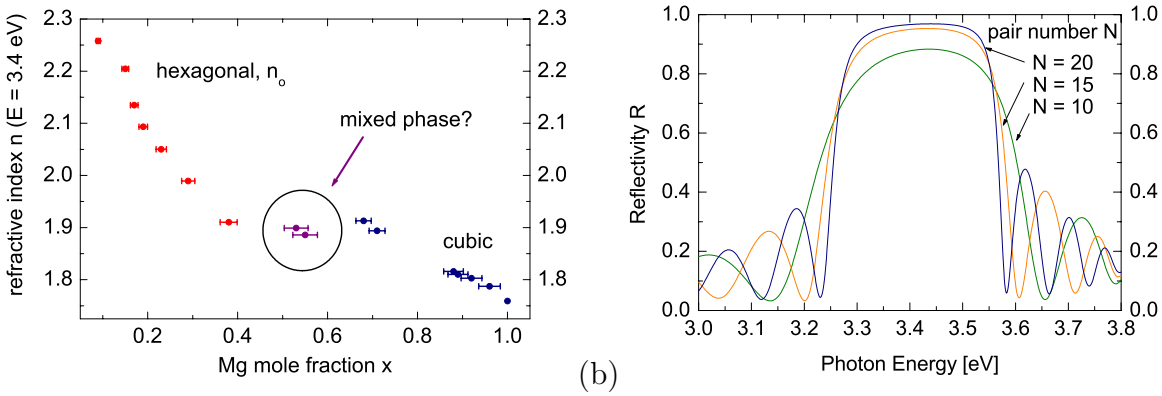

Fig. 1: (a) Experimental values for the refractive index (at fixed photon energy E=3.4 eV) of $Mg_xZn_{1-x}O$ compounds for various Mg content. (b) Simulated reflection for a Bragg stack with $x = 0.2$ and $x = 1.0$ for various number of pairs N as labelled.

[1] R. Schmidt et al., Appl. Phys. Lett. **82**, 2260 (2003).

4.3.13 Band dispersion relations of zincblende and wurtzite InN

D. Fritsch, H. Schmidt, M. Grundmann

Until recently the band gap of wurtzite InN (α-InN) was believed to be in the 1.9 to 2.1 eV energy range. New experiments on high-quality α-InN samples reveal a downward correction of the fundamental band gap by approximately 1 eV. Based on the also re-examined zincblende (β-InN) band gap of 0.59 eV [1], we reinvestigated the electronic properties of α- and β-InN by means of the Empirical Pseudopotential Method (EPM) using transferable model potental parameters [2]. The success of this approach has been demonstrated by investigating the group-III nitrides AlN, GaN, and InN where the Al, Ga, In, and N model potentials have been the same for both zinc-blende and wurtzite crystals [3,4]. The small β-InN band gap of 0.59 eV has been obtained with the transferable N potential parameters from [3] and by only changing the In potential parameters. Then the band structure of α-InN has been calculated with the transferable In and N model potential parameters. The α-InN band gap of 0.82 eV agrees very well with the 0.81 eV proposed by Bechstedt and Furthmüller [1] and lies in the experimentally determined energy range from 0.7 to 0.9 eV. The band structures of InN in both crystal structures are shown in Fig. 1.

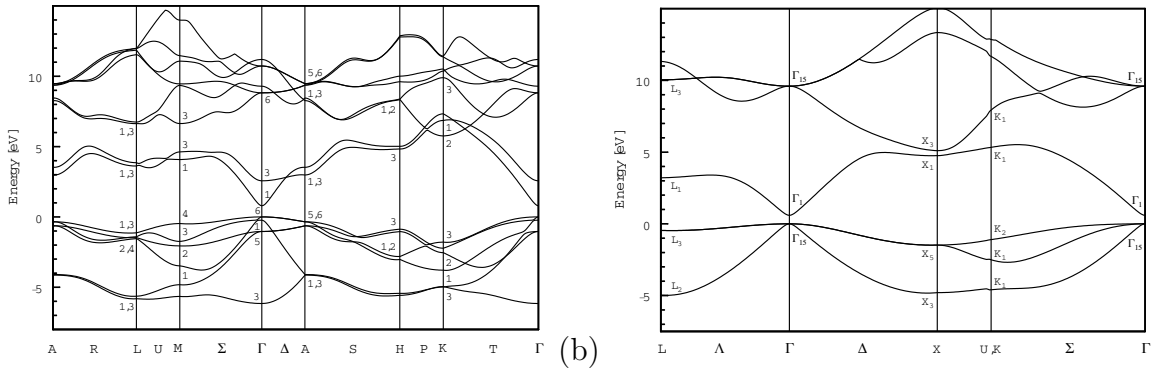

Fig. 1: (a) Band dispersion of α-InN along high symmetry lines in the Brillouin zone. (b) Band dispersion of β-InN along high symmetry lines in the Brillouin zone.

Comparing our band structure data with recent experiments using spectroscopic ellipsometry [5] we were able to assign critical-point transition energies to eigenenergies at different points in the Brillouin zone.

Furthermore, investigating the band structures using k·p-methods we determined a complete set of Luttinger and Luttinger-like parameters for β- and α-InN, respectively, which are necessary to obtain the valence band effective masses. Our obtained α-InN electron effective mass of 0.066 m_0 agrees well with the only known experimentally determined value of 0.07 m_0 [6].

[1] F. Bechstedt and J. Furthmüller, J. Cryst. Growth **246**, 315 (2002).
[2] D. Fritsch, H. Schmidt, and M. Grundmann, Phys. Rev. B **69**, 1652XX (2004), in press.
[3] D. Fritsch, H. Schmidt, and M. Grundmann, Phys. Rev. B **67**, 235205 (2003).
[4] H. Schmidt and G. Böhm, Phys. Rev. B **67**, 245306 (2003).
[5] A. Kasic *et al.*, submitted to Phys. Rev. B.
[6] J. Wu *et al.*, Phys. Rev. B **66**, 201403 (2002).

4.3.14 Investigation of ZnO band structure using empirical pseudopotentials taking into account spin-orbit interaction

D. Fritsch, H. Schmidt, M. Grundmann

We investigate the band structure of ZnO and its ternary compounds Zn(Mg, Cd)O [1] which became the focus of new optoelectronic devices in the green, blue and ultraviolet region by means of the Empirical Pseudopotential Method (EPM) and transferable model potentials. In order to obtain the Zn, Mg, Cd, and O EPM model potential parameters from a set of experimentally determined low-temperature transition energies of several binary II-VI compounds in zinc-blende structure (ZnS, ZnSe, CdS), rocksalt structure (CdO, MgO), and wurtzite structure (ZnO, ZnS) with partially large spin-orbit interactions, one cannot include the spin-orbit interaction by perturbation theory. For example, the spin-orbit splitting energy which increases with increasing anion mass for ZnSe and ZnTe is in the order of magnitude of the band gap energy (Fig. 1a).

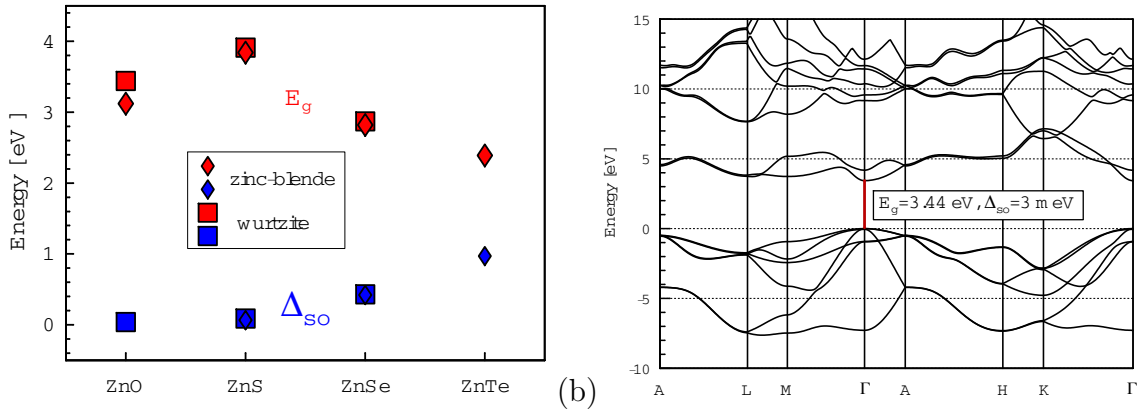

Fig. 1: (a) Band gap (upper symbols, red) and spin-orbit splitting (lower symbols, blue) energies of binary wurtzite Zinc compounds. (b) Band dispersion of wurtzite ZnO along high symmetric lines in the Brillouin zone.

It should be noted that by including the spin-orbit interaction in the Hamiltonian not only the valence band splitting but also other material parameters as Luttinger and Luttinger-like parameters can be directly obtained from the calculated band structure, i.e., the perturbation theoretical k×p-approach can be circumvented. As an example for the successful implementation of spin-orbit interaction into our band structure code the calculated low-temperature band dispersion of wurtzite ZnO where the spin-orbit interaction energy at the Γ-point amounts to −3 meV is shown in Fig. 1b.

[1] R. Schmidt-Grund, B. Rheinländer, M. Schubert, D. Fritsch, H. Schmidt, A. Rahm, R.M. Kaidashev, M. Lorenz, C.M. Herzinger, and M. Grundmann, ThP F52 (ICPS-3) and Thin Solid Films, in press (2004).

4.3.15 Luminescence spectroscopy and transmission electron microscopy of ZnO thin films

S. Heitsch, W. Czakai, G. Wagner, G. Benndorf, H. Hochmuth, M. Lorenz, M. Grundmann

Zinc oxide thin films grown by pulsed laser deposition on *a*-plane sapphire and Si(111), respectively, have been investigated by means of photoluminescence spectroscopy (PL) and transmission electron microscopy (TEM).

Photoluminescence was excited by the 325 nm line of a He-Cd laser with a maximum power density of 80 W/cm^2 and measured at 2 K. The PL measurements (Fig. 1) show two recombination lines of donor-bound excitons (D^0X_1, D^0X_2), which can be observed in both types of structure. Although the peaks are broader in the PL-spectrum of the ZnO thin film on Si(111), it can be clearly seen, that the energetic positions of the two peaks are the same for both structures. As the origin of the the D^0X_1-Peak Meyer et al. [1] proposed the recombination of an exciton bound to the aluminum donor in ZnO.

In ZnO thin films grown on silicon substrates a donor-acceptor-pair transition (DAP) can be observed which is not present in ZnO films grown on sapphire. This indicates that more impurities are present in ZnO grown on Si(111). The DBX-Peak in the PL-spectra is due to the recombination of excitons bound to structural defects [1]. In the films grown on Si substrates this peak has a much higher relative intensity and is broader than in ZnO films grown on sapphire, which indicates that during the growth of ZnO thin films on Si more structural defects are induced.

This interpretation is also supported by TEM images of a ZnO thin film grown on Si(111) (Fig. 2). In contrast to the thin films on sapphire, the films on Si consist of azimuthally twisted pillars which are grown together, i.e. they are polycrystalline.

In conclusion, ZnO thin films on silicon (111) and on sapphire, respectively, show mainly the same emission characteristics. However, more defects are incorporated in ZnO thin films grown on silicon (111).

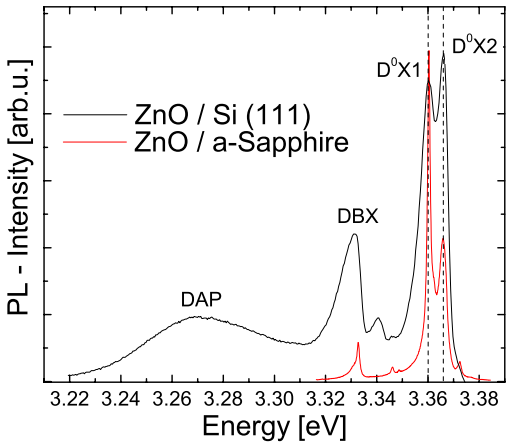

Fig. 1: Photoluminescence spectra of ZnO thin films grown on a-sapphire and silicon (111), respectively.

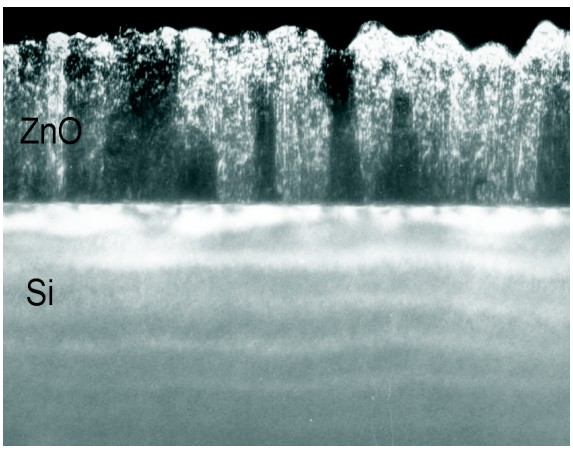

Fig. 2: TEM weak beam image of a polycrystalline ZnO film grown on (111) silicon.

[1] B.K. Meyer, H. Alves, D.M. Hofmann, W. Kriegseis, D. Forster, F. Bertram, J. Christen, A. Hoffmann, M. Straßburg, M. Dworzak, U. Haboeck, A. V. Rodina, phys. stat. sol. (b) **241** (2), 231 (2004)

4.3.16 Dielectric properties of $Ba_xSr_{1-x}TiO_3$ gradient thin films grown by combinatorial PLD

M. Lorenz, H. Hochmuth, G. Ramm, H. M. Christen*, M. Grundmann
* CMSD, Oak Ridge National Laboratory, TN, U.S.A.

Ferroelectric thin films can be applied as varactors, phase shifters, dynamic RAMs and optical waveguide devices. To overcome the undesirable temperature dependence of the dielectric constant ε_r and to reduce the loss tangent of $Ba_xSr_{1-x}TiO_3$ (BSTO) thin films, adjustment of x and doping with Fe, Mg, Y, Ti, Zr has been examined [1, 2]. In addition, BSTO films with linear Sr, Ba concentration depth gradients have been deposited by a continuous compositional-spread PLD approach at ORNL [3]. Substrate was a Pt-covered, Al_2O_3 - based ceramic suitable for microwave applications. The Ba and Sr content was varied linearly during film growth from x=0.5 near the substrate to x =0.85 near the top electrode, as shown by the SNMS depth profile and the plot of the Sr/(Sr+Ba) ratio in figure 1. The relative dielectric constant and its temperature and DC bias dependence (figure 1 right) was determined at 1 kHz using capacitance measurements [1, 2]. Compared to homogeneous films without variable composition profile, the gradient BSTO films show reduced temperature dependence of ε_r, as expected from the superposition of the dielectric properties of the BSTO film slices with different Ba and Sr content.

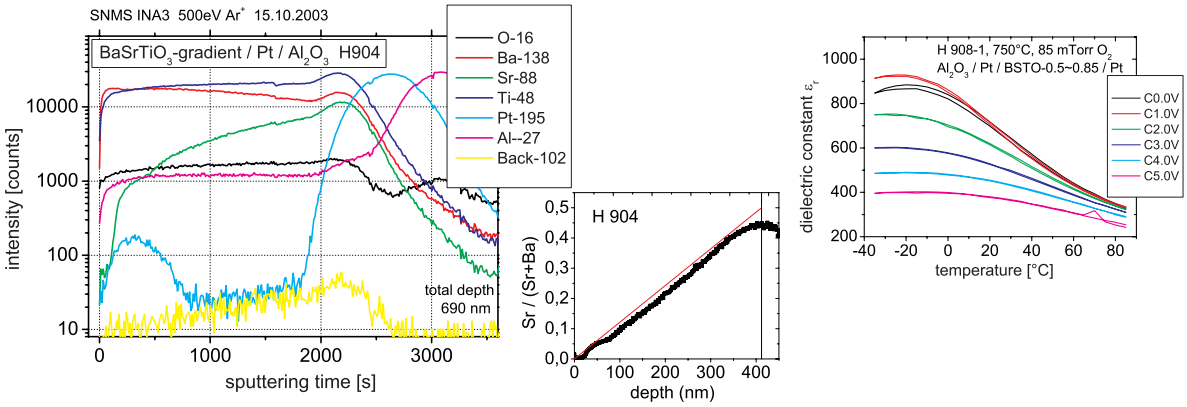

Fig. 1: SNMS depth profile of a gradient BSTO thin film with Pt top and bottom electrode, deposited by combinatorial PLD approach at ORNL (*left*), with plot of relative change of Sr/(Sr+Ba) ratio calculated from the SNMS depth profile (*center*), and dielectric constant of a gradient BSTO film in dependence on DC bias and temperature (*right*).

This work was supported by BMBF Leitprojekt "Supraleiter und neuartige Keramiken für die Kommunikationstechnik der Zukunft", TP FKZ 13N8158.

[1] M. Lorenz, H. Hochmuth, M. Schallner, R. Heidinger, D. Spemann, M. Grundmann, Solid State Electron. **47**, 2199 (2003).
[2] M. Lorenz, Schlussbericht des BMBF-Vorhabens FKZ 13N8158, 01.07.2001-30.06.2003.
[3] H. M. Christen, in ORNL-CMSD progress report No. ORNL-6969 (2002) p 76.

4.3.17 Intrinsic carbon doping of (AlGa)As

V. Gottschalch*, G. Leibiger*, G. Benndorf, H. Herrnberger*
* Department of Inorganic Chemistry, Semiconductor Chemistry Group, University of Leipzig

The intrinsic carbon doping of GaAs and (AlGa)As during MOVPE allows the growth of well-defined doping profiles with high hole concentrations [1]. We have studied the intrinsic carbon doping of GaAs-contact and (AlGa)As-cladding layers in (InGa)As double-quantum well laser diodes ($\lambda \sim 1.17\,\mu$m) for typical growth temperatures between 500 and 650°C and using the precursors TMGa, TMAl, AsH_3, and TBAs. Epitaxial layers were characterized with high-resolution x-ray diffraction (XRD), Hall-measurements, photoluminescence (PL), spectroscopic ellipsometry (SE), and transmission electron microscopy (TEM).

For GaAs we obtained a maximum hole concentration of $3 \times 10^{19}\,\mathrm{cm}^{-3}$ using TBAs. The carbon concentrations obtained using XRD (lattice mismatch of GaAs:C samples) are in good agreement with the hole concentrations obtained with Hall-measurements, PL (band-gap shrinkage) and infrared-SE. Figure 1a shows the dependence of the hole (or carbon) concentration, and of the room temperature mobility, as a function of the III/V ratio for growth temperature of 540°C. The x-ray diffraction curves for AlAs-samples of different carbon concentration (variation of the V/III ratio) are summarized in Fig. 1b.

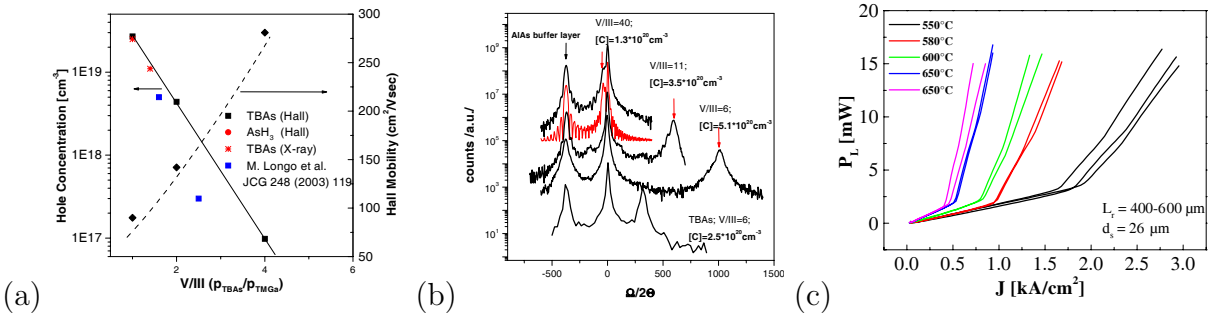

Fig. 1: (a) Dependence of hole concentration and Hall mobility on the V/III ratio for GaAs. (b) Influence on the carbon incorporation on the lattice mismatch of AlAs:C samples grown by various V/III ratios. (c) L-J-characteristics of 1.17 μm laser diodes with carbon doped (AlGa)As cladding layers for different growth temperatures and C-concentrations.

A maximum hole concentration of $4 \times 10^{20}\,\mathrm{cm}^{-3}$ has been measured for $Al_{0.60}Ga_{0.40}As$ at a growth temperature of 540°C. A reduction of V/III-ratio and growth temperature and an increase of the Al-composition resulted in an increase of the carbon concentration.

Additionally, we have grown laser structures with (GaIn)As/GaAs double quantum wells as active regions sandwiched between carbon- and Si-doped (AlGa)As layers. The grown (GaIn)As/GaAs double quantum wells structures were fabricated into oxide stripe lasers with different stripe widths and cavity lengths. The growth temperature of the p-cladding layers was variied in the range of 540 to 650°C (Fig. 1c). The best laser characteristics was obtain using growth temperature of 650°C and a V/III ratio of 17.

[1] T. F. Kuech, J. M. Redwing, J. Cryst. Growth 145, 382 (1994).

4.3.18 Doping of (InGa)(NAs) and (BGaIn)As

G. Leibiger*, C. Krahmer*, V. Gottschalch*, G. Benndorf
* Department of Inorganic Chemistry, Semiconductor Chemistry Group, University of Leipzig

(In,Ga)(NAs) alloys have attained great attention in the past few years due to the rapid decrease of the band-gap energy with increasing nitrogen concentration in combination with the possibility of lattice matched growth on GaAs substrates. The latter holds also for the new (BGaIn)As material system which offers new opportunities in strain- and band-gap engineering. Both systems are of interest for application as absorption layers in tandem solar cells for which systematic doping studies are a prerequisite. In this work, we have investigated the Si- and Zn-doping of lattice matched $B_{0.027}Ga_{0.913}In_{0.06}As$- and $In_{0.047}Ga_{0.953}N_{0.016}As_{0.0984}$-layers using metalorganic vapor phase epitaxy (MOVPE) with disilane and diethylzinc as doping precursors. Epitaxial layers were characterized with high-resolution x-ray diffraction (HRXRD), photoluminescence (PL), Hall-measurements, infrared spectroscopic ellipsometry (IR-SE) and transmission electron microscopy (TEM).

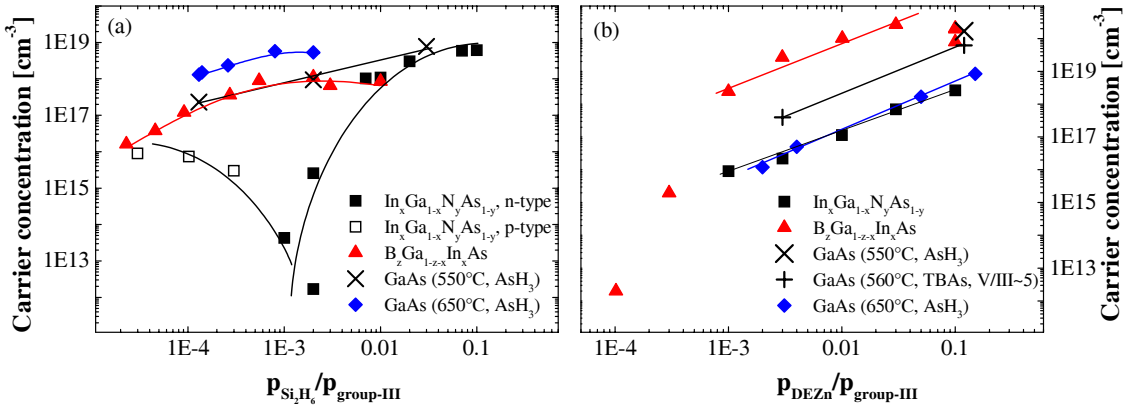

Fig. 1: Free carrier concentration of as-grown Si-doped (a) and Zn-doped (b) $In_{0.047}Ga_{0.953}N_{0.016}As_{0.0984}$- (*squares*) and $B_{0.027}Ga_{0.913}In_{0.06}As$-layers (*triangles*) depending on the ratio of the partial pressure of disilane (a) or DEZn (b) to the partial pressures of all group-III precursors. All lines are shown to guide the eye.

The p-type $In_{0.047}Ga_{0.953}N_{0.016}As_{0.0984}$ layers become show n-type conduction for $p_{Si}/p_{group-III}$-values above 10^{-3} and a maximum electron concentration of $\sim 6 \times 10^{18}\,cm^{-3}$ is reached (Fig. 1a). In comparison, the saturation value for the electron concentration in $B_{0.027}Ga_{0.913}In_{0.06}As$:Si is clearly reduced ($8 \times 10^{17}\,cm^{-3}$), which we attribute to the competition for the group-III-lattice sites in (BGaIn)As:Si.

In both systems the incorporation of Zn results in p-type conduction (Fig. 1b). The Zn-distribution coefficient is clearly reduced in $In_{0.047}Ga_{0.953}N_{0.016}As_{0.0984}$:Zn compared to $B_{0.027}Ga_{0.913}In_{0.06}As$:Zn, which might be caused by the lower effective V/III-ratio and the incorporation of Zn on interstitial sites in $In_{0.047}Ga_{0.953}N_{0.016}As_{0.0984}$:Zn [1].

Mobilities were determined with IR-SE and Hall-measurements. Generally, $B_{0.027}Ga_{0.913}In_{0.06}As$ shows higher mobilities as $In_{0.047}Ga_{0.953}N_{0.016}As_{0.0984}$ due to the lower tendency for cluster formation and/or a lower number of defects. The PL-intensities increase in both material systems with increasing Si-concentration up to $n \sim 10^{18}\,cm^{-3}$.

[1] K. Volz, J.Koch, B. Kunert, and W. Stolz, J. Cryst. Growth 248 (2002) 451.

4.3.19 Light-beam induced current imaging and SNMS depth profiling of flexible $CuInSe_2$ solar cells

M. Lorenz, T. Nobis, J. Lenzner, G. Ramm, H. Hochmuth, M. Grundmann

Light beam induced current imaging (LBIC) and secondary neutrals mass spectrometry (SNMS) depth profiling are powerful tools for optimization of serial production of $CuInSe_2$ solar cells at Solarion Photovoltaik GmbH Leipzig, as demonstrated in Figs. 1 and 2. In LBIC, the sample surface is scanned by a laser beam ($\lambda = 632\,\mathrm{nm}$, spot size $1.5\,\mu\mathrm{m}$), and the induced photocurrent (measured at the Mo bottom and ZnO:Al top contact) is imaged in dependence on laser spot position (Fig. 1). The solar cell investigated in Fig. 1 shows nearly homogeneous, and high quantum efficiency. SNMS depth profiling gives the intensity of selected isotopic species sputtered by 600 eV Ar-ions from the sample. The sputter time scale corresponds to the depth. The SNMS depth profile (Fig. 2) of the flexible solar cell demonstrates the multilayer structure ZnO:Al - ZnO:i - CdS - $CuInSe_2$ - Mo - Ti - polyimid foil. For example S, Al, and Cd show remarkable diffusion into deeper cell regions, as confirmed also by ion beam analysis.

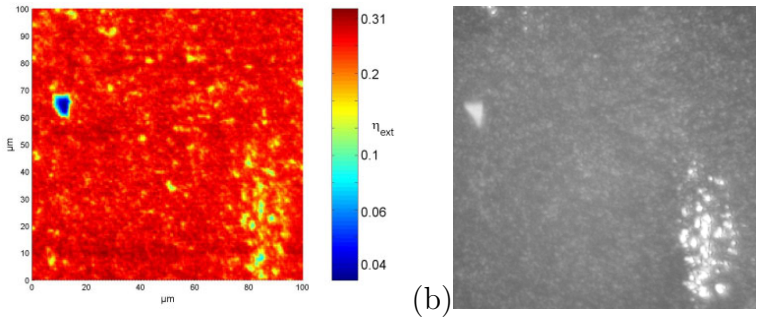

(a) (b)

Fig. 1: (a) LBIC scan ($100 \times 100\,\mu\mathrm{m}^2$) of a flexible $CuInSe_2$ solar cell (monochromatic, $\lambda = 632\,\mathrm{nm}$, quantum efficiency). The points with lower efficiency are due to surface contamination. (b) photo of the same surface area.

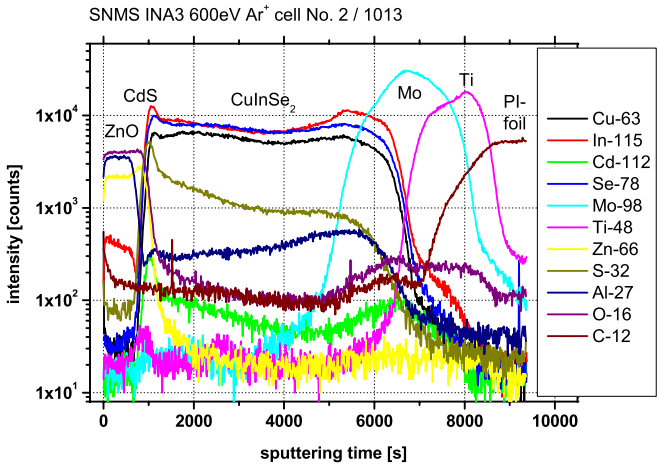

Fig. 2: SNMS isotope intensity vs. sputter time (depth) profile of a typical $CuInSe_2$ solar cell of Solarion GmbH, Leipzig.

This work was supported by BMBF Wachstumskern INNOCIS under Grant No. 03WKI09.

4.3.20 $B_xGa_yIn_{1-x-y}As$ and $In_xGa_{1-x}N_yAs_{1-y}$ as absorption materials in thin film solar cells

C. Krahmer*, G. Leibiger*, V. Gottschalch*, H. Herrnberger*, J. Bauer*,
O. Breitenstein**, M. Grundmann
*Department of Inorganic Chemistry, Semiconductor Chemistry Group, University of Leipzig
** Max-Planck-Institut für Mikrostrukturphysik, Halle/Saale

The new material systems $B_xGa_yIn_{1-x-y}As$ and $In_xGa_{1-x}N_yAs_{1-y}$ have been investigated within the BMBF "Wachstumskern INNOCIS" with the intention to use these mixed crystals as absorption materials in thin film tandem solar cells (GaAs/GaInP). Highest effiencies in tandem cells can be achieved with a combination of the band-gap energies of 1.8 eV for the upper cell and 1.1 eV for the lower cell. (BGaIn)As- and (InGa)(NAs)-mixed crystals can both reach smaller band-gap energies then GaAs due to the reduction of band-gap with increasing boron and nitrogen incorporation, respectively (Fig. 1a,b) [1,2].

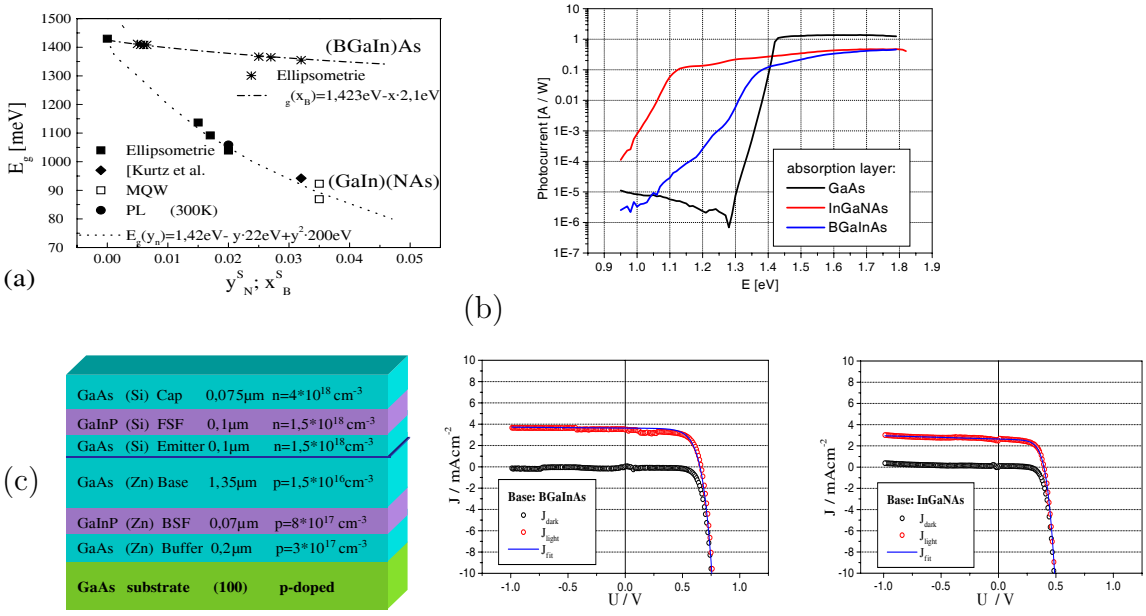

Fig. 1: (a) Reduction of band-gap energy with B or N incorporation, (b) photocurrent of a solar cells with different absorption layers. (c) Structure of a solar cell with GaAs-absorption layer and I-V-curves of cells with BGaInAs or InGaNAs absorbtion layers.

GaAs based single junction solar cells have been grown to optimize the cells for the incorporation of the alternative absorption materials (Fig. 1c). Afterwards the absorption layer in these cells has been replaced by $B_xGa_yIn_{1-x-y}As$ or $In_xGa_{1-x}N_yAs_{1-y}$. The measured I-V-curves indicate high fill factors and low series resistance (Fig. 1c). However, in comparison to the GaAs-cells the short circuit current J_{sc}, the open circuit voltage U_{oc} and the fill factor are reduced to the half of the corresponding values of GaAs-cells. This requires an improvement of the material properties. Furthermore a solar cell with a GaInP absorption layer (E_g = 1.89 eV) has been investigated as upper cell. The characteristic values from the I-V-curves are comparable with literature data. First GaAs/GaInP tandem cells have been grown with an AlGaAs/GaAs tunnel junction.

[1] D. J. Friedman et al., J. Cryst. Growth 195 (1998) 409.
[2] G. Leibiger, Dissertation, Universität Leipzig (2003).

4.3.21 MOVPE-growth of GaAs on Ge-substrates

S. Scholz*, V. Gottschalch*, G. Leibiger*, G. Benndorf, J. Lenzner, G. Wagner*
* Department of Inorganic Chemistry, Semiconductor Chemistry Group, University Leipzig

The low mismatch of the lattice constant of GaAs and Ge of (0.07%) and the low difference of their thermal expansion coefficients allow the epitaxial growth of GaAs-based solar cells on Ge-substrates [1]. With the low indirect band gap of 0.77 eV this material can be used in a separate junction. The major disadvantage is the heteroepitaxial growth of the polar $A^{III}B^{V}$-material on the nonpolar Ge-substrate resulting in anti phase domains (APD) [2]. In this study, we examine the epitaxial growth with varying growth parameters on differently oriented Ge-substrates. The grown layers were characterized by interference microscopy, wet etching technique, atomic force microscopy (AFM), photoluminescence (PL), scanning electron microscopy (SEM), transmission electron microscopy (TEM) and double crystal x-ray diffraction (XRD).

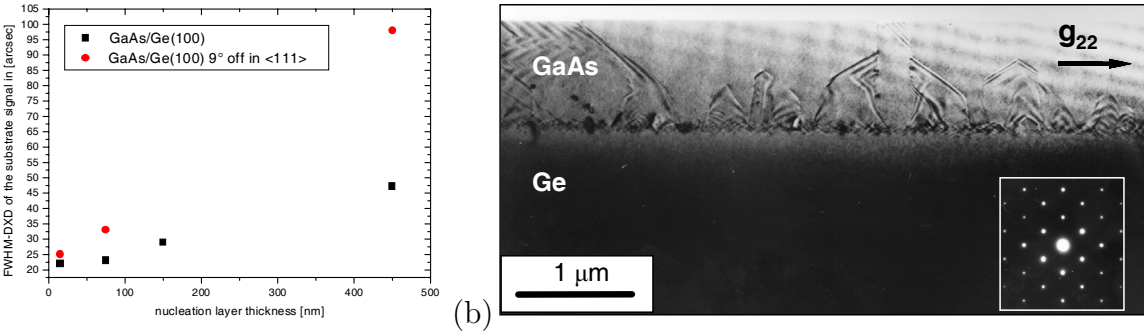

Fig. 1: (a) Correlation of XRD-FWHM of the layer signal against the thickness of the nucleation layer. (b) (110) TEM cross-sectional bright-field image of GaAs(1.2 nm)/ GaAs(990 nm)/Ge(100) grown at 550°C and 700°C, respectively; APB's are visible.

For a two step growth process it was found, that the smaller the initial grown layer, the better is the crystalline quality of the second GaAs layer (Fig. 1). For the initial layer we varied the growth temperature and the V/III-ratio to optimize the surface morphology. By observing the surface with AFM the best results are obtained at the temperature of 550°C and the V/III-ratio of 13. For the second layer we used a temperatur of 700°C and a V/III-ratio of 92 to obtain a quasi-2D-growth. Plan-view and cross-sectional TEM show the formation of antiphase boundaries (APB) in GaAs-layers on exactly oriented Ge(100)-substrates. With increasing the GaAs layer thickness the APB density decreases (Fig. 2). The interface between GaAs and Ge is quite rough and shows a transition region of 5–8 nm. The diameters of the APD are 2–5 μm and the APB's follow selected orientations. On misoriented Ge-substrates no APB's were found. Due to Ge-diffusion into the epilayer the GaAs layer is n-type. Based on our results n-p junction solar cells were grown on 9° off-oriented Ge-substrates.

[1] M. Yamaguchi, Physica E 14 (2002) 84.
[2] P.R. Pukite, P.I. Cohen, J. Cryst. Growth, 81 (1987) 214.

4.3.22 Peptide cluster ensembles on semiconductor surfaces

K. Goede, M. Grundmann

Hybrid nanostructures of organic molecules and anorganic semiconductors are a fascinating new research area in physics. The combination of single-molecule building blocks and materials which offer fast and reliable data processing may offer an unimagined range of applications from fast detection of organics and coated functionalized surfaces to true nanoscale electronics and data storage in single molecules. Self-assembly techniques seem necessary to explore this potential. In this regard, using amino-acid based molecules like peptids, proteins and DNA is one of the most promising approaches. In nature, recognition and assembly capabilities driven by amino acids govern the replication of all highly-developed living structures. Yet the application of these principles to the world of anorganic semiconductors is fundamentally new.

By recording AFM micrographs and subsequently analyzing them, we have quantitatively shown that the adhesion rate (the percentage of surface covered by peptide clusters) of a specially selected 12-mer peptide on nine different semiconductor surfaces ranges from 25% to 0% under the same standard conditions. As an example, two AFM micrographs of GaAs (100) and Si (100), respectively, are shown in Fig. 1a. By applying a washing process to remove loose, unbound peptide particles from the surface substrates, we can exclude these results stemming from (undesired) surface tension effects which might occur when the watery solution evaporates from the surface. Instead, we ascribe them to the interplay between the polar amino-acid side chains and the atoms which constitute the surface with their respective electronegativity. The different adhesion rates are qualitatively explainable by considering these values for the substrate elements under investigation.

Furthermore, we have looked at the substrate-specific differences in size and height between respective clusters ensembles. As is obvious from Fig. 1b, a low adhesion rate is accompanied by a large average cluster size and a large average cluster height. This is probably because for low adhesion rates any binding formation between peptide and semiconductor is weaker and the peptide tends to bind to other peptide molecules rather than to the substrate.

(a)

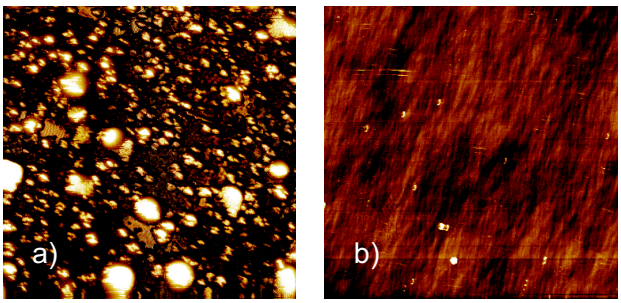

(b)

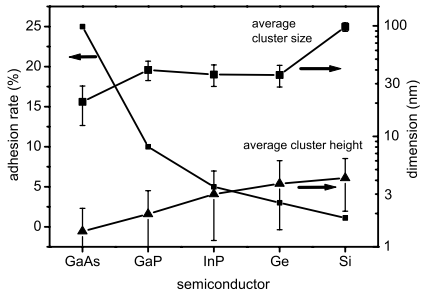

Fig. 1: (a) Two exemplary AFM micrographs of semiconductor surfaces, partly covered by a peptide. Both samples have been prepared under the same conditions. left: $(1.6\,\mu\mathrm{m})^2$ GaAs (100), showing a high adhesion rate, right: $(10\,\mu\mathrm{m})^2$ Si (100), showing a low adhesion rate. From the size of the micrograph it is obvious that this low rate on Si is typical for the whole surface and not just for a specific part. (b) Peptide adhesion rate (*left scale*) and average peptide cluster size and height (*right scale*) for different semiconductor substrates. The error bars indicate the respective standard deviation which has been obtained from measurements on eight equivalent surfaces.

4.3.23 Funding

Investigation of inter-sublevel transitions in self-organized quantum dots; development of novel infrared detectors and lasers
Prof. Dr. Marius Grundmann
DFG Gr 1011/7-3

Transferability of the codoping concept to ternary ZnO:(Cd,Mg)
Prof. Dr. Marius Grundmann, Dr. H. Schmidt
DFG Gr 1011/10-1 im DFG-Schwerpunktprogramm 1136
"Substitutionseffekte in ionischen Festkörpern"

III-V-Semiconductor Nano-Heterostructures for Advanced Opto-Electronic Devices
Prof. Dr. Bernd Rheinländer
BMBF: Bilaterale Zusammenarbeit BRD-Slowakei: SVK 01/001

New gallium phosphide grown by vertical gradient freeze method for light emitting diodes
Prof. Dr. Bernd Rheinländer
(VGF GaP - LED's) No. IST - 2001-32793
EU-FP5-Projekt und BMBF: Bilaterale Zusammenarbeit BRD-Slowakei: SVK 01/001

PLD of new dielectric and HTSC thin films for future applications in wireless and mobile communication
Dr. Michael Lorenz
BMBF-Teilprojekt FKZ 13N8158 innerhalb BMBF-Leitprojekt "Supraleiter und neuartige Keramiken für die Kommunikationstechnik der Zukunft", Förderschwerpunkt Supraleitung und Tieftemperaturtechnik.

Electronic and optical properties, in-situ Raman scattering, in-situ ellipsometry and ion beam analysis of flexible Cu-(In,Ga)-(Se,S) thin film solar cells
Prof. Dr. Marius Grundmann, Prof. Dr. Tilman Butz, Dr. Mathias Schubert
BMBF-Wachstumskern INNOCIS, Teilprojekt FKZ 03 WKI 09

Intraband and interband carrier transitions in type I and type II nanostructures with quantum dots, quantum dot molecules and impurities
Prof. Dr. Marius Grundmann
INTAS 01-0615

One-dimensional heterostructures and nano-forests
Prof. Dr. Marius Grundmann, Dr. Michael Lorenz
DFG Gr 1011/11-1
within Forschergruppe FOR 522
Architecture of nano- and microdimensional building blocks

Lateral optical confinement of microresonators
Prof. Dr. Bernd Rheinländer, Dr. V. Gottschalch
DFG Rh 28/4-1

within Forschergruppe FOR 522
Architecture of nano- and microdimensional building blocks

Interface-related properties of oxide quantum wells
Prof. Dr. Marius Grundmann, Dr. V. Gottschalch
DFG Gr 1011/14-1
within Forschergruppe FOR 404
Oxidic interfaces

Interface-induced electro-optical properties of oxide semiconductor-ferroelectric layered structures
Dr. Mathias Schubert, Dr. Michael Lorenz
within Forschergruppe FOR 404
Oxidic interfaces

Magnetoelectronics of ferromagnetic traps in TCO and of single spin traps in quantum dots
Dr. Heidemarie Schmidt
BMBF FKZ 03N8708
im BMBF-Nachwuchswettbewerb "Nanotechnologie"

4.3.24 Organizational Duties

M. Grundmann
Vertrauensdozent der Studienstiftung des deutschen Volkes
Direktor des Institut für Experimentelle Physik II
Project Reviewer: Deutsche Forschungsgemeinschaft (DFG), Alexander-von-Humboldt Stiftung (AvH), Schweizerischer Nationalfonds zur Förderung der wissenschaftlichen Forschung (FNSNF), Fonds zur Förderung der Wissenschaften (FWF)
Referee: Appl. Phys. Lett., Phys. Rev. B., Phys. Rev. Lett., Electr. Lett., Physica E, phys. stat. sol., J. Appl. Phys.

4.3.25 External Cooperations

Academic

A. F. Ioffe-Institut, St. Petersburg
Prof. Dr. Zh. I. Alferov, Dr. V. M. Ustinov, Dr. G. Cirlin

Forschungszentrum Karlsruhe, Institut für Materialforschung III
Dr. H. Heidinger, Dr. J. Halbritter

Institut für Oberflächenmodifizierung e. V., Leipzig
Prof. Dr. B. Rauschenbach, Dr. E. Schubert

Universität Leipzig, Fakultät für Biowissenschaften, Pharmazie und Psychologie
Prof. Dr. A. Beck-Sickinger

Universität Leipzig, Fakultät für Chemie und Mineralogie
Dr. V. Gottschalch

Max-Planck-Institut für Mikrostrukturphysik, Halle/Saale
Dr. O. Breitenstein, Dr. D. Hesse

St. Petersburg State Technical University
Prof. Dr. L. Vorob'jew, Dr. V. Shalygin

Slovak University of Technology, Bratislava, Slovak
Prof. Dr. J. Kovàc, Dr. F. Uherek

Oak Ridge national Laboratory, Condensed Matter Science Division, TN, U.S.A.
Dr. Hans M. Christen

Technische Universität Berlin
Prof. Dr. D. Bimberg

Universidade de Aveiro, Portugal
Prof. Dr. N. Sobolev

Kinki University, Dept. of Electronics Systems and Information Engeneering, Japan
Dr. M. Kusunoki

Paul Scherer Institut, Villingen
Prof. Dr. H. Sigg

Université Paris-Sud
Prof. Dr. F. Julien

Chinese Academy of Sciences, Institute of Physics, Beijing
Prof. Dr. Yusheng He

Universität Gießen
Prof. Dr. B. Meyer, Dr. D. Hofmann, Prof. Dr. J. Janek

Universität Magdeburg
Prof. Dr. A. Krost

Universität Bonn
Prof. Dr. W. Mader

Universität Hannover
Prof. Dr. M. Binnewies

Industry

Solarion GmbH, Leipzig
Dr. Gerd Lippold, Dr. Alexander Braun

Cryoelectra GmbH, Wuppertal
Prof. Dr. H. Diel

El-Mul Technologies, Yavne, Israel
Dr. Armin Schön

4.3.26 Publications

Journals

N. Ashkenov, G. Wagner, H. Neumann, B. N. Mbenkum, C. Bundesmann, V. Riede, M. Lorenz, E. M. Kaidashev, A. Kasic, M. Schubert, M. Grundmann
Infrared dielectric functions and phonon modes of high-quality ZnO films
J. Appl. Phys. 93, 126 (2003)

C. Bundesmann, N. Ashkenov, M. Schubert, D. Spemann, T. Butz, E. M. Kaidashev, M. Lorenz, M. Grundmann
Raman scattering in ZnO thin films doped with Fe, Sb, Al, Ga and Li
Appl. Phys. Lett. 83, 1974 (2003)

P. Busch, D. Posselt, D.-M. Smilgies, B. Rheinländer, F. Kremer, Ch. M. Papadakis
Lamellar Diblock Copolymer Thin Films Investigated by Tapping Mode Atomic Force Microscopy: Molar-Mass Dependence of Surface Ordering
Macromolecules 23 (2003) 236/03

Daniel Fritsch, Heidemarie Schmidt, and Marius Grundmann
Band-structure pseudopotential calculation of zinc-blende and wurtzite AlN, GaN, and InN
Phys. Rev. B 67, 235205 (2003)

M. Grundmann
Nanoscroll formation from strained layer heterostructures
Appl. Phys. Lett. 83, 2444 (2003)

T. Hofmann, M. Grundmann, Craig M. Herzinger, Mathias Schubert, Wolfgang Grill
Far-infrared magnetooptical generalized ellipsometry determination of free-carrier parameters in semiconductor thin film structures
Mat. Res. Soc. Symp. Proc. 744, M5.32 (2003)

Mohan V. Jacob, Janina Mazierska, M. Lorenz
Microwave characterization of YBCO films on Sapphire and $LaAlO_3$ at the interface between HTS films and substrates
Superconductor Science and Technology 16, 412-415 (2003).

E. M. Kaidashev, M. Lorenz, H. von Wenckstern, A. Rahm, H.-C. Semmelhack, K.-H. Han, G. Benndorf, C. Bundesmann, H. Hochmuth, M. Grundmann
High electron mobility of epitaxial ZnO thin films on c-plane sapphire grown by multistep pulsed-laser deposition
Appl. Phys. Lett. 82, 3901 (2003)

J. Kovac, J.Kovac,Jr., D. Pudis, J. Jakabovic, A. Vincze, V. Gottschalch, G. Benndorf, B. Rheinländer, R. Schwabe
Stimulated Red Emission from InAs Monolayers Embedded in the Active Region of $Al_xGa_{1-x}As$ Barriers
Laser Physics 13, 240 (2003)

M. Kusunoki, Y. Takano, K. Nakamura, M. Inadomaru, D. Kosaka, A. Nozaki, S. Abe, M. Yokoo, M. Lorenz, H. Hochmuth, M. Mukaida, S. Ohshima
Demonstration of surface resistance mapping of large-area HTS films using the dielectric resonator method
Physica C Superconductivity 383, 374 (2003)

M. Lorenz, E. M. Kaidashev, H. von Wenckstern, V. Riede, C. Bundesmann, D. Spemann, G. Benndorf, H. Hochmuth, A. Rahm, H.-C. Semmelhack, M. Grundmann
Optical and electrical properties of epitaxial $(Mg, Cd)_xZn_{1-x}O$, ZnO, and ZnO:(Ga, Al) thin films on c-plane sapphire grown by pulsed laser deposition
Solid State Electronics 47, 2205 (2003)

M. Lorenz, H. Hochmuth, M. Grundmann, E. Gaganidze, J. Halbritter
Microwave properties of epitaxial large-area Ca-doped $YBa_2Cu_3O_{7-\delta}$ thin films on r-plane sapphire
Solid State Electronics 47, 2183 (2003)

M. Lorenz, H. Hochmuth, M. Schallner, R. Heidinger, D. Spemann, M. Grundmann
Dielectric properties of Fe-doped $Ba_xSr_{1-x}TiO_3$ thin films on polycrystalline substrates at temperatures between -35 and $+85$°C
Solid State Electronics 47, 2199 (2003)

F. Mrowka, S. Manzoor, P. Pongpiyapaiboon, I. L. Maksimov, P. Esquinazi, K. Zimmer, M. Lorenz
Excess voltage in the vicinity of the superconducting transition in inhomogeneous $YBa_2Cu_3O_7$ thin films
Physica C Superconductivity 399, 22 (2003)

Heidemarie Schmidt, Georg Böhm
Origin of carrier localization on two-dimensional GaN substitution layers embedded in GaAs
Phys. Rev. B 67 (2003) 245306(1)

R. Schmidt, B. Rheinländer, M. Schubert, D. Spemann, T. Butz, J. Lenzner, E. M.

Kaidashev, M. Lorenz, M. Grundmann
Dielectric functions (1 to 5 eV) of wurtzite $Mg_xZn_{1-x}O$ ($0 \leq x \leq 0.29$) thin films
Appl. Phys. Lett. 82, 2260 (2003)

M. Schubert, A. Kasic, T. Hofmann, N. Ashkenov, W. Grill, M. Grundmann, E. Schubert, H. Neumann
Advances in spectroscopic ellipsometry characterization of optical thin films
Proceedings of SPIE Vol. 5250, p. XXX (2003)

in press

C. Bundesmann, N. Ashkenov, M. Schubert, A. Rahm, E. M. Kaidashev, M. Lorenz, M. Grundmann
Infrared dielectric functions and crystal orientation of a-plane ZnO thin films on r-plane sapphire determined by generalized ellipsometry
Thin Solid Films, in press

R. Schmidt-Grund, M. Schubert, B. Rheinländer, D. Fritsch, H. Schmidt, E.M. Kaidashev, M. Lorenz, H. Hochmuth, M. Grundmann
UV-VUV Spectroscopic ellipsometry of ternary $Mg_xZn_{1-x}O$ ($0 \leq x \leq 0.53$) thin films
Thin Solid Films, 455-456, pp. 500-504 (2004)

N. Ashkenov, M. Schubert, H. Hochmuth, M. Lorenz, and M. Grundmann
High-temperature band-gap energies, optical constants and in-situ growth monitoring of ZnO thin film
Thin Solid Films, in press

H. von Wenckstern, E. M. Kaidashev, M. Lorenz, H. Hochmuth, G. Biehne, J. Lenzner, V. Gottschalch, R. Pickenhain, M. Grundmann
Lateral homogeneity of Schottky contacts on n-type ZnO
Appl. Phys. Lett. 84, 79 (2004)

M. Schubert, N. Ashkenov, T. Hofmann, M. Lorenz, H. Hochmuth, H. v. Wenckstern, M. Grundmann, G. Wagner
Electro-optical properties of ZnO-$BaTiO_3$-ZnO heterostructures grown by pulsed laser deposition
Annalen der Physik 13, 61 (2004)

M. Lorenz, H. Hochmuth, R. Schmidt-Grund, E.M. Kaidashev, M. Grundmann
Advances of pulsed laser deposition of ZnO thin films
Annalen der Physik 13, 59 (2004).

M. Lorenz, J. Lenzner, E.M. Kaidashev, H. Hochmuth, M. Grundmann
Cathodoluminescence of selected single ZnO nanowires on sapphire
Annalen der Physik 13, 39 (2004)

E. Guzmán, H. Hochmuth, M. Lorenz, H. von Wenckstern, A. Rahm, E.M. Kaidashev,

M. Ziese, A. Setzer, P. Esquinazi, A. Pöppl, D. Spemann, R. Pickenhain, H. Schmidt, M. Grundmann
Pulsed laser deposition of Fe- and Fe, Cu-doped ZnO thin films
Annalen der Physik 13, 57 (2004)

D. Fritsch, H. Schmidt, M. Grundmann
Band dispersion relations of zinc-blende and wurtzite InN
Phys. Rev. B (2004), in press

T. Nobis, E. M. Kaidashev, A. Rahm, M. Lorenz, J. Lenzner, M. Grundmann
Spatially inhomogeneous impurity distribution in ZnO micropillars
Nano Letters (2004), in press.

4.3.27 Graduations

PhD

Dipl.-Phys. G. Leibiger
A^{III}-B^{V}-Mischkristallbildung mit Stickstoff und Bor

Diploma

Andreas Rahm
High Resolution X-ray Diffraction of ZnO Based Thin Films

Jens Bauer
Aufbau eines Photolumineszenzanregungsmessplatzes und Anwendung auf Halbleiterprobleme

Thomas Nobis
Ortsaufgelöste und zeitabhängige Photostromuntersuchungen an Zinkoxid-Strukturen

M.Sc.

Susanne Heitsch
Photoluminescence of p-doped ZnO thin films

Kentaro Harada
N doping of organic semiconductors by coevaporation with organic donor molecules
(Work done at TU Dresden, local supervisor Prof. K. Leo)

B.Sc.

Chegnui Bekeny
Charge Carriers in ZnO thin films and bulk material

4.3.28 Guests

Dr. Evgeni M. Kaidashev
Rostov-on-Don State University, Russia
1.1.2003 – 21.12.2003

4.4 Solid State Optics and Acoustics

4.4.1 Development of a Miniaturized Advanced Diagnostic Technology Demonstrator 'DIAMOND' - Technology Study Phase 2

W. Grill, R. Wannemacher, K. Desyllas

A miniaturized universal scanning microscope ('space microscope') is being developed for potential operation on board of the International Space Station ISS, which allows diagnostics of samples by means of optical scanning microscopy, partly combined with spectral resolution, as well as by means of acoustic microscopy with vector contrast. Foreseen microscopic techniques are confocal optical microscopy in reflection, scanning microscopy in transmission, as well as spectrally resolved fluorescence and Raman microscopy. Acoustic microscopy permits spatially resolved determination of micromechanical sample properties.

Funded by European Space Organization ESA/ESTEC

4.4.2 Ultrasound Diagnostics of Directional Solidification

W.Grill, R. Wannemacher, S. Knauth, J. Jahny, O. Lenkeit

An ultrasonic measuring device based on guided waves has been developed in order to determine the growth rate of alloys, in particular of opaque metallic alloys. Experimental tests show that a high resolution is achievable in the determination of the position of the solid-liquid interface, down to 0.01 mm. The ultrasonic technique is therefore an appropriate tool for the measurement of the solidification velocity for stable as well as unstable solidification processes. The aim consists in the investigation of the impact of process parameters on the resulting material properties. Controlled non-stationary growth presently appears to become a main research object for the next future, in particular in the context of industrial applications. The measurement of the solidification velocity by ultrasound is a diagnostic tool for directional solidification experiments. It was developed in the framework of the Technological Research Programme of the European Space Organization. An ultrasound pulse launched from the cold end of the sample and being reflected from the phase boundary of solidification allows to determine the position of the solid-liquid interface. Given the speed of sound in the sample the position of the phase boundary can be determined as a function of time and, hence, the solidification velocity via precise measurement of the propagation time by means of an autocorrelation technique.

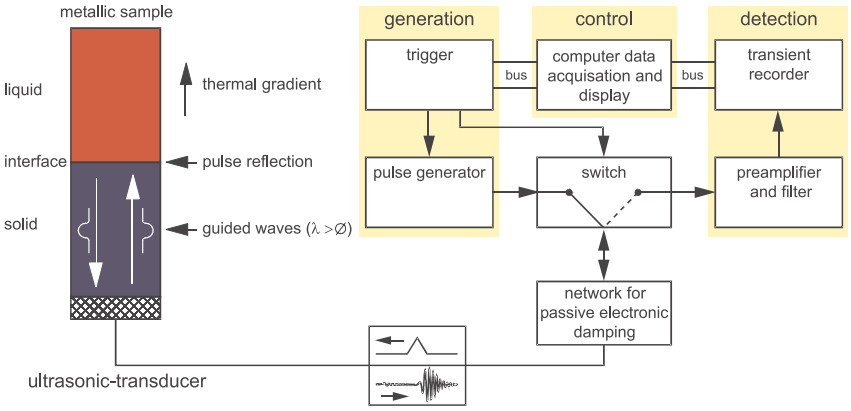
metallic sample
liquid
interface
solid
thermal gradient
pulse reflection
guided waves (λ >Ø)
ultrasonic-transducer
generation
control
detection
trigger
bus
computer data acquisation and display
bus
transient recorder
pulse generator
switch
preamplifier and filter
network for passive electronic damping

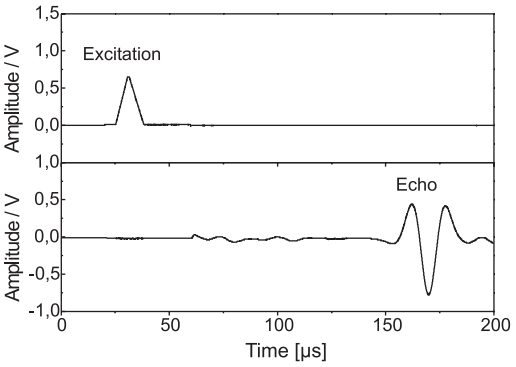
Excitation
Echo
Amplitude / V
Time [µs]

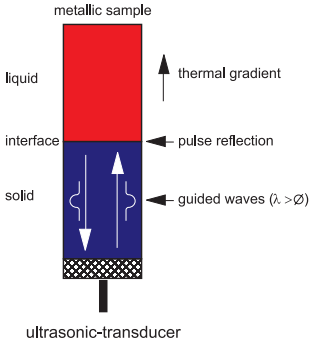
metallic sample
liquid
interface
solid
thermal gradient
pulse reflection
guided waves (λ >Ø)
ultrasonic-transducer

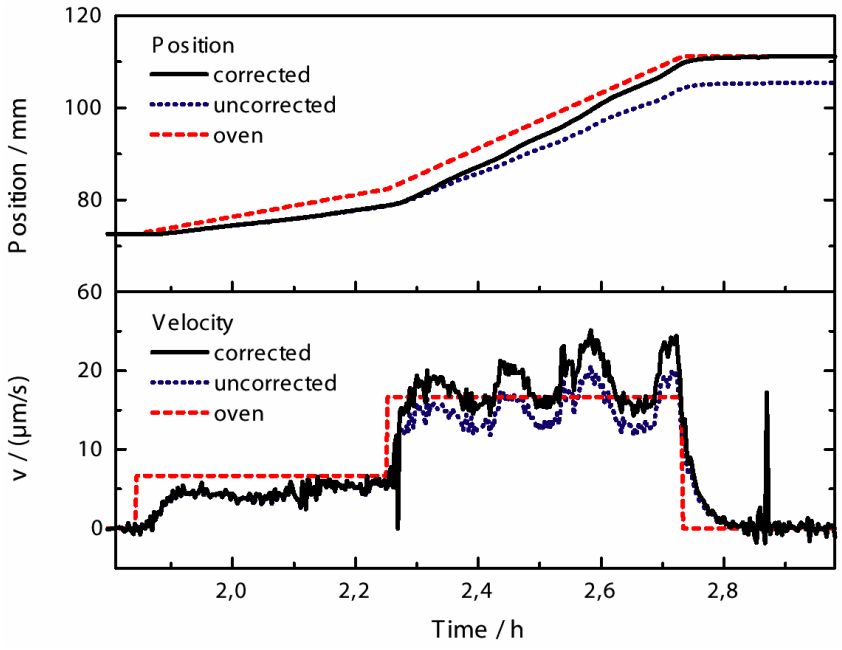
Position
corrected
uncorrected
oven
Position / mm
Velocity
corrected
uncorrected
oven
v / (µm/s)
Time / h

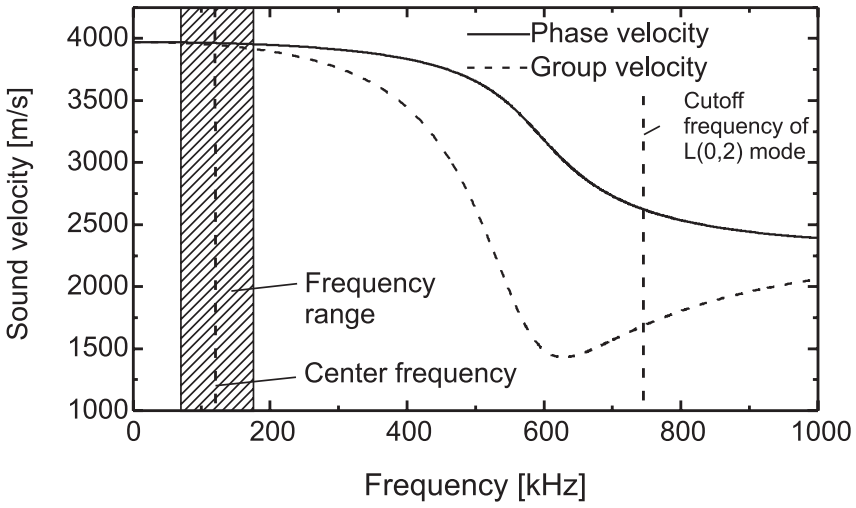

Funded by European Space Organization ESA/ESTEC

4.4.3 Development and verification of the applicability of ultrasonic methods

W. Grill, Z. Kojro

Possible applications associated with the company Schott GLAS of the ultrasound techniques developed and published by our group are investigated. Techniques, sensors, and measurement devices are being developed. The work is conducted in cooperation with Schott GLAS. New techniques were developed and tested.

Funded by Schott GLAS Mainz

4.4.4 Development of ultrasonic methods, sensors and measurement equipment

W. Grill, J. Jahny, O. Lenkeit

Based on techniques developed and published by us in the context of high-resolution ultrasound spectroscopy and time-of-flight measurements dedicated ultrasonic techniques, sensors, and devices are being developed for industrial use within the company 'Heidelberg' (printing machines). Investigations of physical and technical principles and development of appropriate models are prerequisites for the application of the techniques and devices. The work has led to new measurement techniques.

Funded by Heidelberger Druckmaschinen AG

4.4.5 Development and verification of the applicability of ultrasonic methods

W. Grill, Z. Kojro

Based on techniques developed and published by us dedicated ultrasonic techniques, sensors, and devices are being developed for use at the company PFW Technologies GmbH. The work is conducted in cooperation with PFW Technologies GmbH. The developed techniques are a spin-off of the projects of our group financed by the European Spcae Organization (ESA).

Funded by PFW Technologies GmbH

4.4.6 Fourier inversion of acoustic wave fields in anisotropic solids

M. Pluta, A. G. Every, W. Grill, T. J. Kim, E. Twerdowski

This work [1] is concerned with the analysis of acoustic wave fields encountered in phase-sensitive acoustic microscopy (PSAM) applied to elastically anisotropic solids.We show that the fast Fourier transform technique provides a computationally efficient method of calculating two-dimensional amplitude and phase images of these fields. More importantly, we demonstrate how this technique, applied to complex wave field data, can be used to treat inverse problems such as source reconstruction, image quality assessment, and the determination of elastic constants. Monochromatic and also more general time-dependent excitations, such as tone bursts and short pulses, are treated, and the resulting wave fields described. The evolution of these wave fields with increasing frequency is discussed, and emerging infinite frequency features, such as the ray surface and phonon focusing caustics, are identified. A number of numerical simulations are presented that are in good agreement with measured data from the literature. As an illustration of elastic constant determination, we use the point spread function determination based on our PSAM measurements on the longitudinal mode in silicon to determine the elastic constant C_{11} of Si.

[1] M. Pluta, A. G. Every, W. Grill, T. J. Kim, Phys. Rev. B **67**, 094117 (2003)

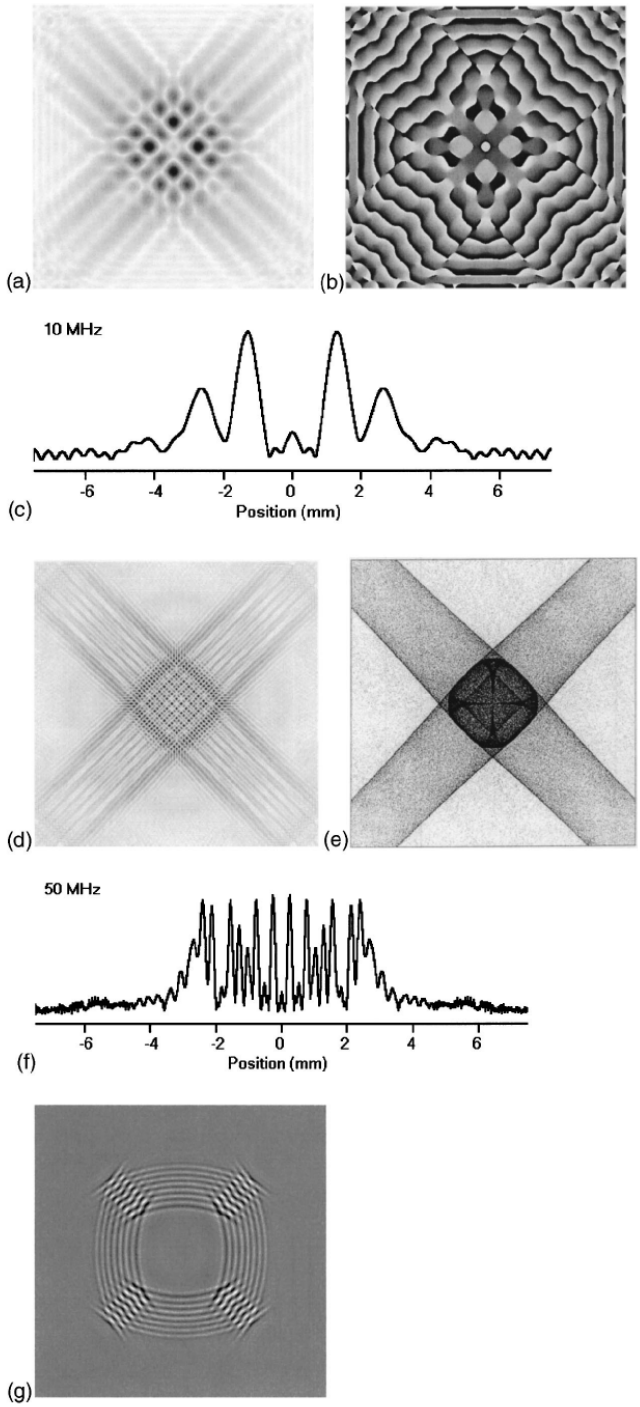

Fig. 1: (a) Amplitude and (b) phase images of silicon, representing the spatial dependence of $\tilde{G}_{33}(\vec{x}_{\|})$ in the plane $x_3 = 20\,\text{mm}$ and for frequency $f = 10\,\text{MHz}$. (d) Depicts the 2D amplitude variation at 50 MHz and (c) and (f) the amplitude variation along the central line in cases (a) and (d), respectively. (e) The infinite-frequency phonon focusing pattern for Si. (g) Response in the plane $x = 10mm$ to a 15 MHz tone burst of 8 periods as observed after a 2.15 μs delay. The reference axes are aligned along the cubic crystallographic axes, and the spatial range of the scan is $15 \times 15\,\text{mm}^2$ in each case. The darkness of the gray scale in (a) and (d) is proportional to the amplitude, in (e) to the intensity, and in (g) to the real part of the analytical signal.

4.4.7 Phase-sensitive acoustic imaging and micro-metrology of polymer blend thin films

W. Ngwa, R. Wannemacher, W. Grill, T. Kundu

Scanning acoustic microscopy with vector contrast (PSAM) at 1.2 GHz is employed for three-dimensional real-space measurements of structure in PS/PMMA (polystyrene / poly(methyl methacrylate)) blend films, spun-cast on glass and silicon substrates. Processing of the digitized phase and amplitude images yields information on the surface structure and internal structure of the blend films. The complex $V(z)$ functions render qualitative and quantitative material contrast for each image pixel and, hence, permit the characterization of individual domains. It is shown [1] that PSAM can provide valuable insights regarding the polymer blend film morphology and micro-mechanical properties, not acquirable by other ways.

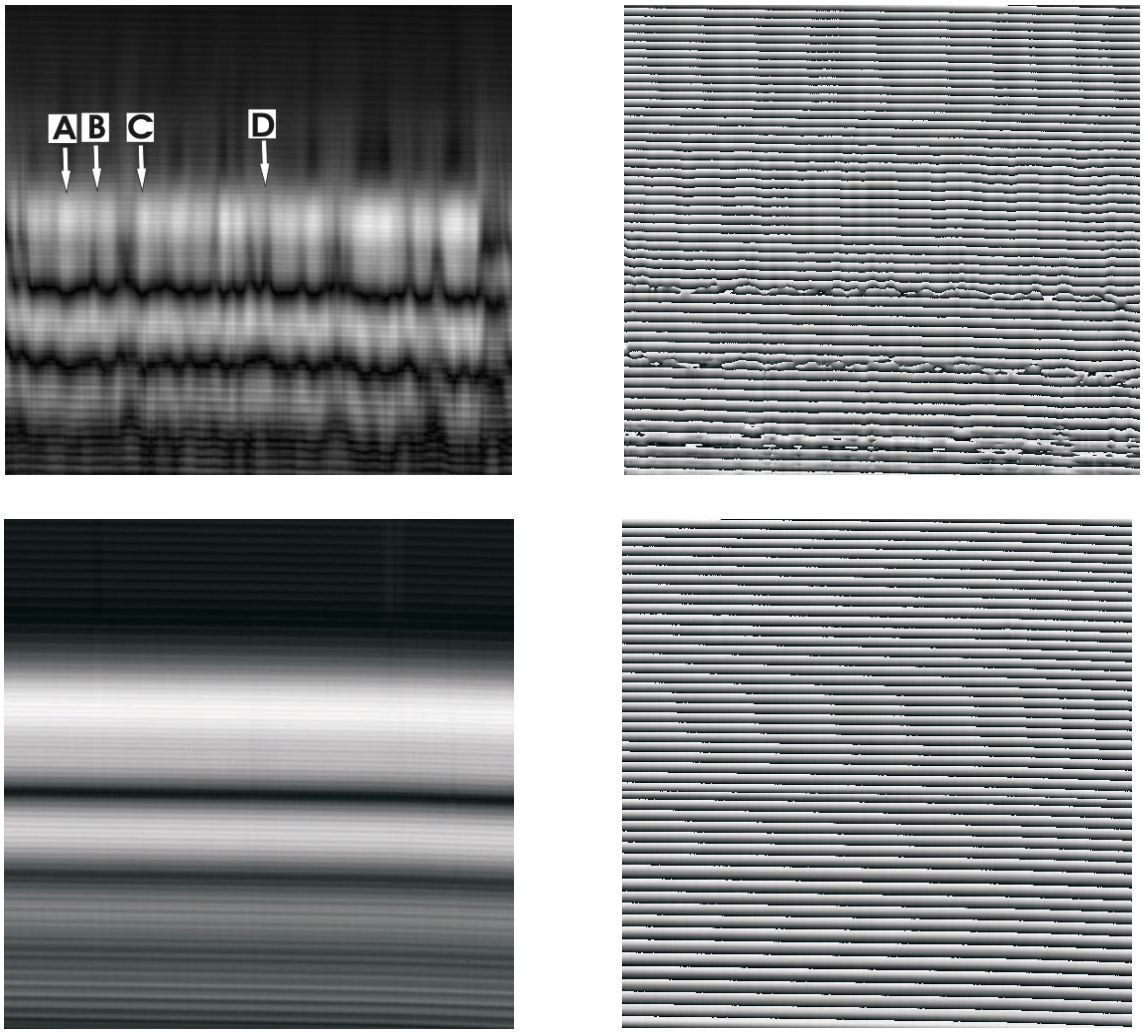

Fig. 1: ($140 \times 32\,\mu\mathrm{m}^2$) $y - -z$ amplitude and phase images, respectively, of: (a-b) a PS/PMMA blend film on glass substrate; (c-d) uncoated glass substrate for comparison. The coupling fluid for the acoustic measurements is water. The frequency used is 1.2 GHz.

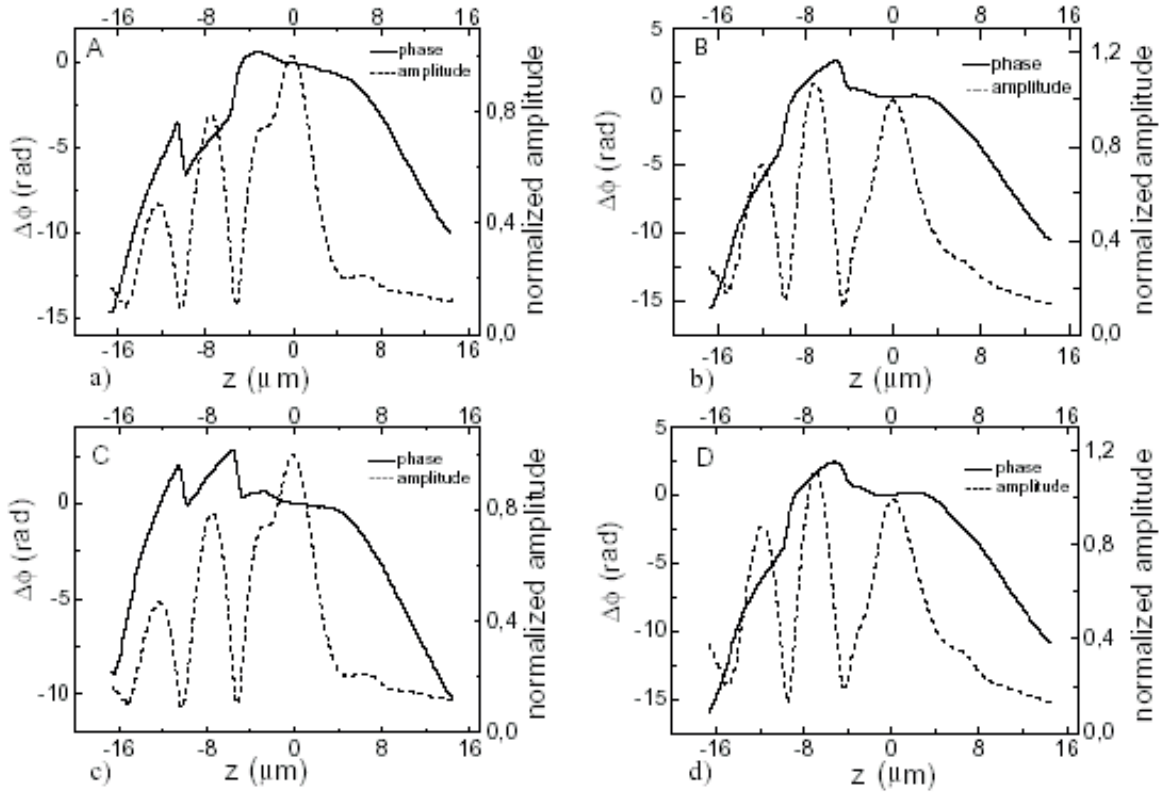

Fig. 2 - PSAM complex $V(z)$ curves from the marked spots in the $y--z$ images shown in Fig. 1a. The graphs show the dependencies of the differential phase and amplitude signals on the position of the sample along the axis of the acoustic lens for reflected ultrasonic waves. The amplitude is normalized to the first (main) maximum. The differential phase signal ($\Delta\phi$) shown is derived from the observed and tracked phase signal by subtracting a linear phase term $2kz$, where k is the wave number of water. The linear range of the phase useful for topographic imaging is in the vicinity of the focal plane (around $z = 0$). The substrate is glass, and the coupling fluid water. The frequency is 1.2 GHz. (a-d) correspond, respectively, to the points marked (A-D) with arrows in Fig. 1a.

[1] W. Ngwa, R. Wannemacher, W. Grill, T. Kundu, Europhys. Lett. **64**, 830-836 (2003)

4.4.8 Mode control by nanoengineering of light emitters in spherical microcavities

B. Möller, M. V. Artemyev, U. Woggon, R. Wannemacher

Quantum-confined semiconductor nanorods are used as highly polarized nanoemitters to actively control the polarization state of microcavity photons. A wet-chemical method to tangentially align CdSe nanorods on a polymer surface is applied to a spherical $R \approx 2\lambda$-microcavity. The cavity emission is studied by imaging spectroscopy and polarization-sensitive mode mapping. The efficient confinement of photons spontaneously emitted by nanorods into single transverse electric (TE)cavity modes is achieved while transverse magnetic modes are suppressed. A microscopic tricolor TE-emitter operating at room temperature in the visible spectral range is demonstrated [1].

[1] B. Möller, M. V. Artemyev, U. Woggon, R. Wannemacher Mode control by nanoengineering of light emitters in spherical microcavities Appl. Phys. Lett. **83**, 2686-2688 (2003)
[2] B. Möller, M. V. Artemyev, U. Woggon, R. Wannemacher, Appl. Phys. Lett. **80**,

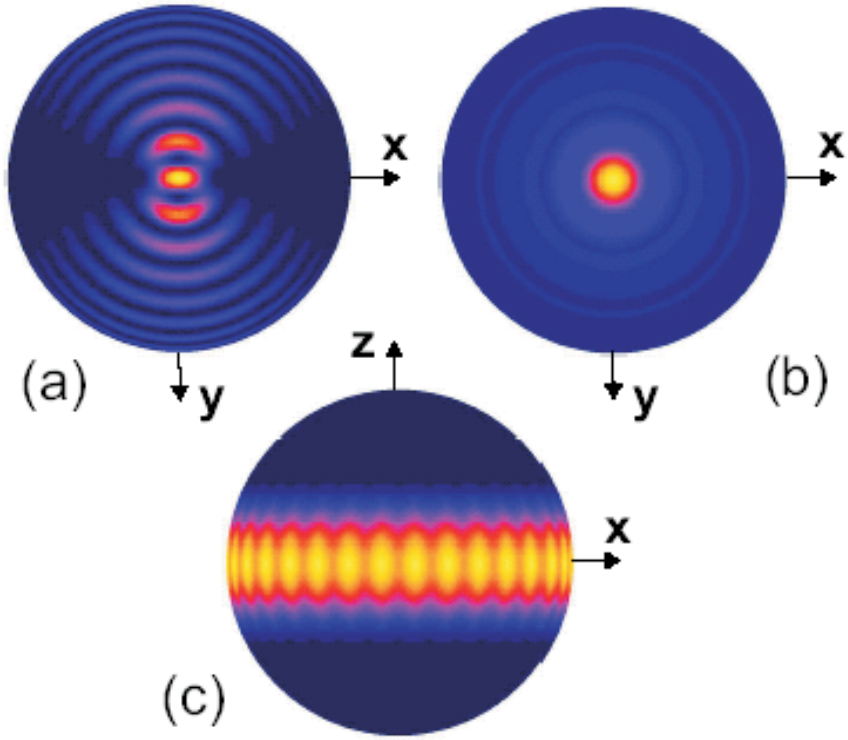

Fig. 1: Calculated electromagnetic field intensity distribution (E^2) on a sphere surface for a microsphere with $R = 1.4\,\mu$m and $n = 1.57$. (a) TE^1_{16} mode with $m = \pm 1$ ($\lambda = 688.5$ nm), dipole oscillates in x-direction, (b) TM^1_{16} mode with $m = 0$ ($\lambda = 666.9$ nm), dipole oscillates in z-direction. For comparison the corresponding picture of a whispering gallery mode TM^1_{16} with $m = 16$ is shown in (c). The intensity is color-coded in a linear scale.

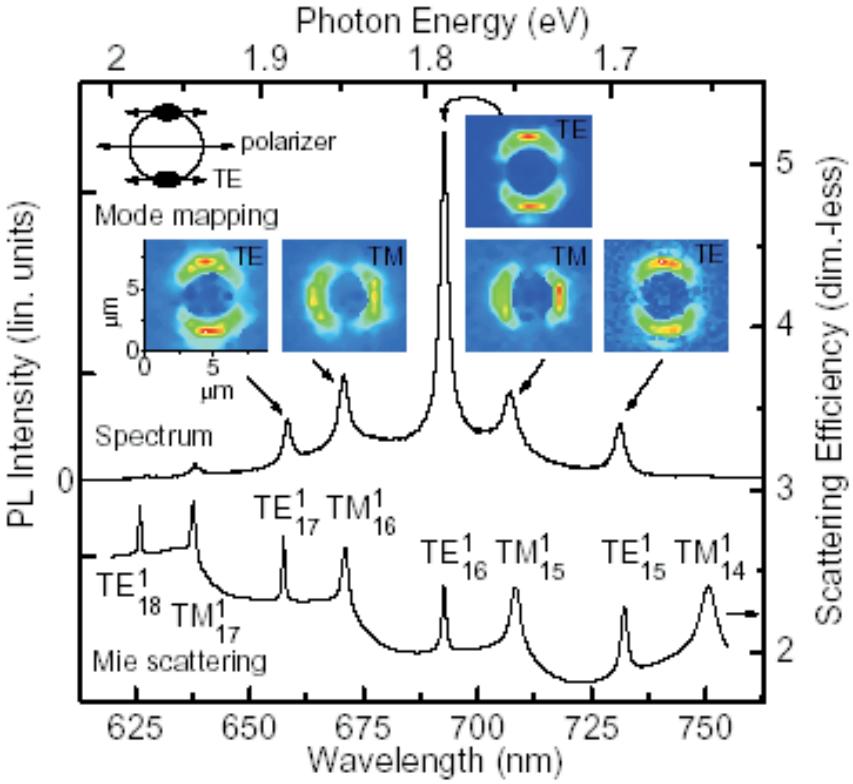

Fig. 2: Determination of cavity mode polarization by combining the results from polarization sensitive mode mapping (top), spatially resolved emission spectroscopy (middle) and Mie-calculation (bottom). The Mie-scattering efficiency is fitted by using $R = 1.397\,\mu$m for the sphere radius and $n = 1.5663 + 0.00785\,\mu\text{m}^2/\lambda^2 + 0.000334\,\mu\text{m}^4/\lambda^4$ for the refractive index. The two-dimensional $8.9\,\mu$m x $8.9\,\mu$m intensity scans (top) are performed at the spectral positions indicated by arrows with a polarizer in the detection beam ensuring polarization-sensitive detection as described in ref. [2]. $T = 300\,$K, excitation at 488 nm.

4.4.9 Dot-in-a-dot: electronic and photonic confinement in all three dimensions

U. Woggon, R. Wannemacher, M.V. Artemeyev, B. Möller, N. LeThomas, V. Anikeyev, O. Schöps

We study three-dimensionally (3D)-confined photon states in a spherical microcavity (the photonic dots) resonantly excited by photons emitted from semiconductor nanocrystals (the quantum dots). Glass and polymer microspheres with sizes of $R = 2$ to $10\,\lambda$ are characterized by spatially and temporally resolved micro-photoluminescence and the influence of nanoemitter position and orientation is analysed. The emission spectra of single, bulk and hollow, microspheres impregnated with CdSe quantum dots and rods are investigated and the modification of the quantum dot radiative lifetime by the 3D-photon confinement is discussed [1].

[1] U. Woggon, R. Wannemacher, M.V. Artemeyev, B. Möller, N. LeThomas, V. Anikeyev, O. Schöps, Appl. Phys. B **77**, 469 - 484 (2003) *invited paper*

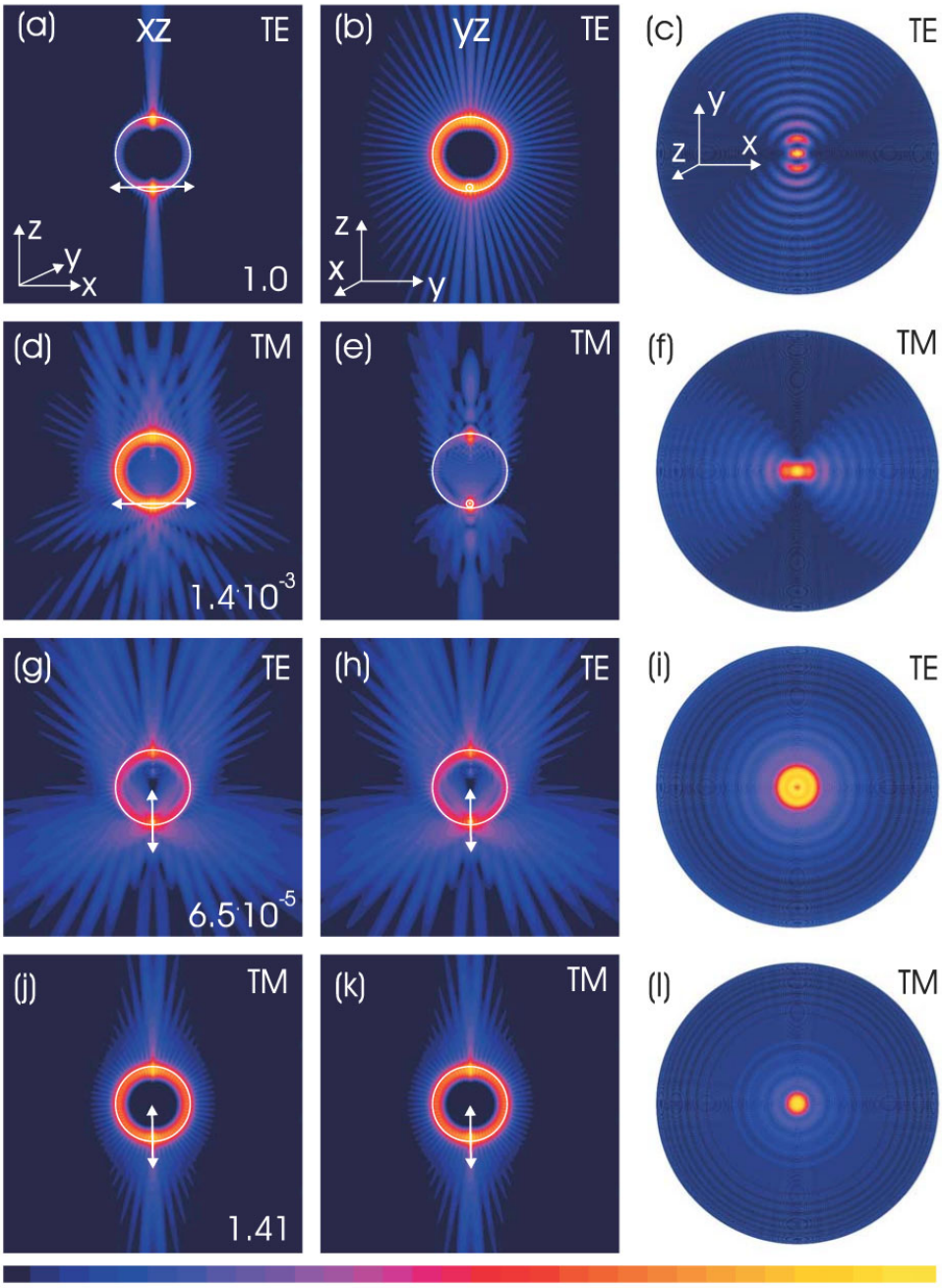

Fig. 1: Calculated electromagnetic intensity (E^2) in and outside a spherical microcavity for the case of excitation by a single dipole ($d = 1\,\text{Debye}$, position $z = 2.3\,\mu\text{m}$, sphere radius $R = 2.5\mu\text{m}$, refractive index n=1.5) with two different orientations. The dipole emission is chosen to be resonant to the $\text{TM}^1_{32,0}$-mode ($\lambda = 621.44\,\text{nm}$) or to the $\text{TE}^1_{32,1}$-mode ($\lambda = 632.83\,\text{nm}$), respectively. Plotted is the intensity in the xz-(a,c,e,g) and yz-planes (b,d,f,h) for the dipole oscillating in x-direction (a-d) and for the dipole oscillating in z-direction (e-h). Each plot represents an area of $20\,\text{mm} \times 20\,\text{mm}$. The logarithmic intensity scale covers 60 dB. The maximum intensity (a) is normalized to 1.0. For (b) to (h) the relative intensity maxima with respect to (a) are given.

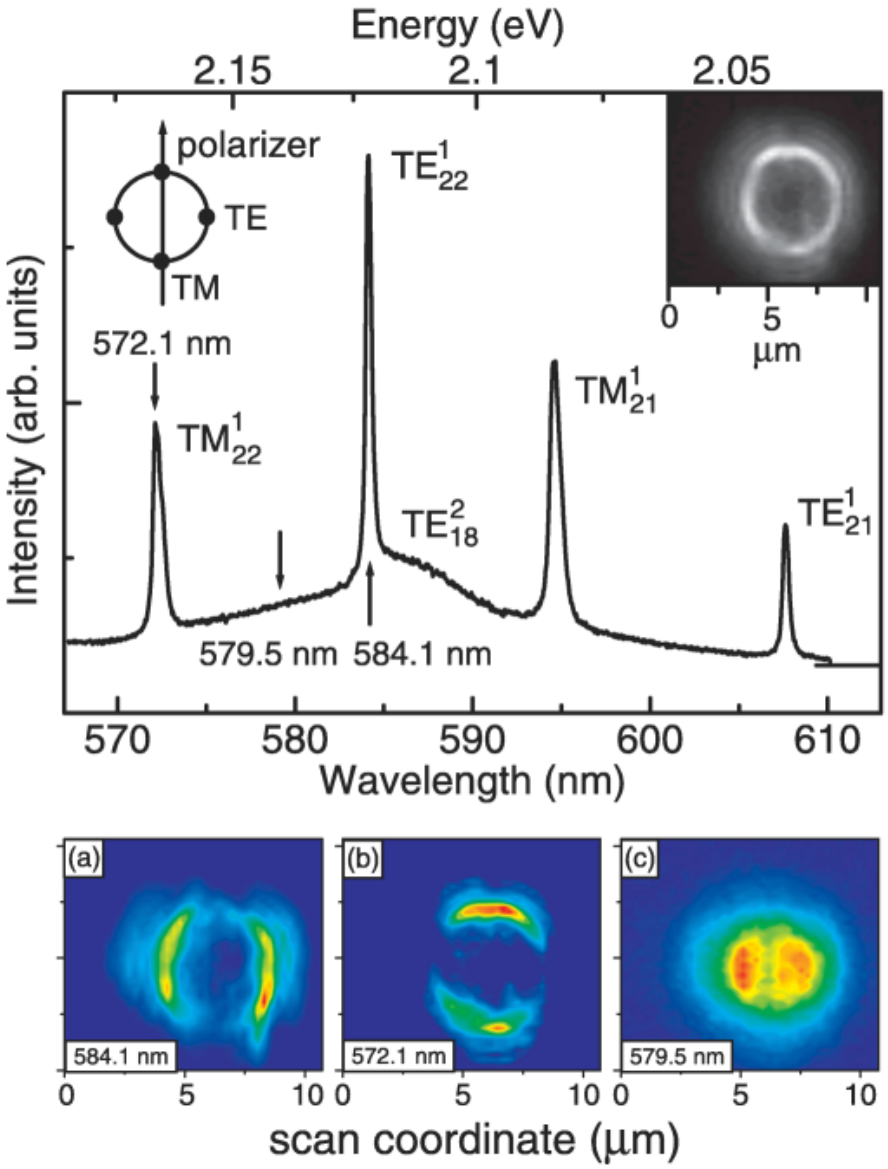

Fig. 2: Measured spectrum of CdSe QDs bound to the surface of a $R = 1.8$ μm microsphere ($\lambda_{\text{exc}} = 488$ nm, $T = 300$ K, $I_{\text{exc}} = 20$ W/cm^2). The mode quantum numbers are assigned using Mie theory. The right inset shows the microscopic image of the microsphere taken spectrally resolved at the TE^1_{22}-resonance (unpolarized detection). The left inset shows the polarizer orientation for which the mode mapping is performed at 572.1 nm (TM^1_{22}), 584.1 nm (TE^1_{22}) and 579.5 nm (background). The lower part shows the two-dimensional intensity scans (a-c)for the spectral positions indicated by arrows.

4.4.10 Apertureless near-field optical microscopy of metallic nanoparticles

A. Pack, W. Grill, R. Wannemacher

Image formation in apertureless near-field optical microscopes employing evanescent-wave excitation is studied quantitatively as a function of the polarisation and the wavelength of the excitation. Aggregate Mie theory is used to describe the probe-sample interactions self-consistently, including retardation. Only p-polarised excitation yields images, which closely reproduce the sample, and the contrast is much higher in this case than for s-polarised waves. Particular attention is paid to the case of imaging of metallic nanoparticles, for which local and nonlocal versions of aggregate Mie theory are compared. Nonlocality arises from the excitation of longitudinal bulkplasmons at the particle surface. It is shown that this effect is essential in the imaging of such particles and implies comparatively rapid convergence, in contrast to the local theory. The converged images calculated within the nonlocal theory resemble the results of the local theory, when, arbitrarily, within the latter only dipole-dipole interactions are taken into account. Significant qualitative and quantitative differences, however, are shown to exist. Signal and contrast enhancements due to resonant excitation of surface plasmon polaritons are studied quantitatively using the results of the converged nonlocal theory [1] .

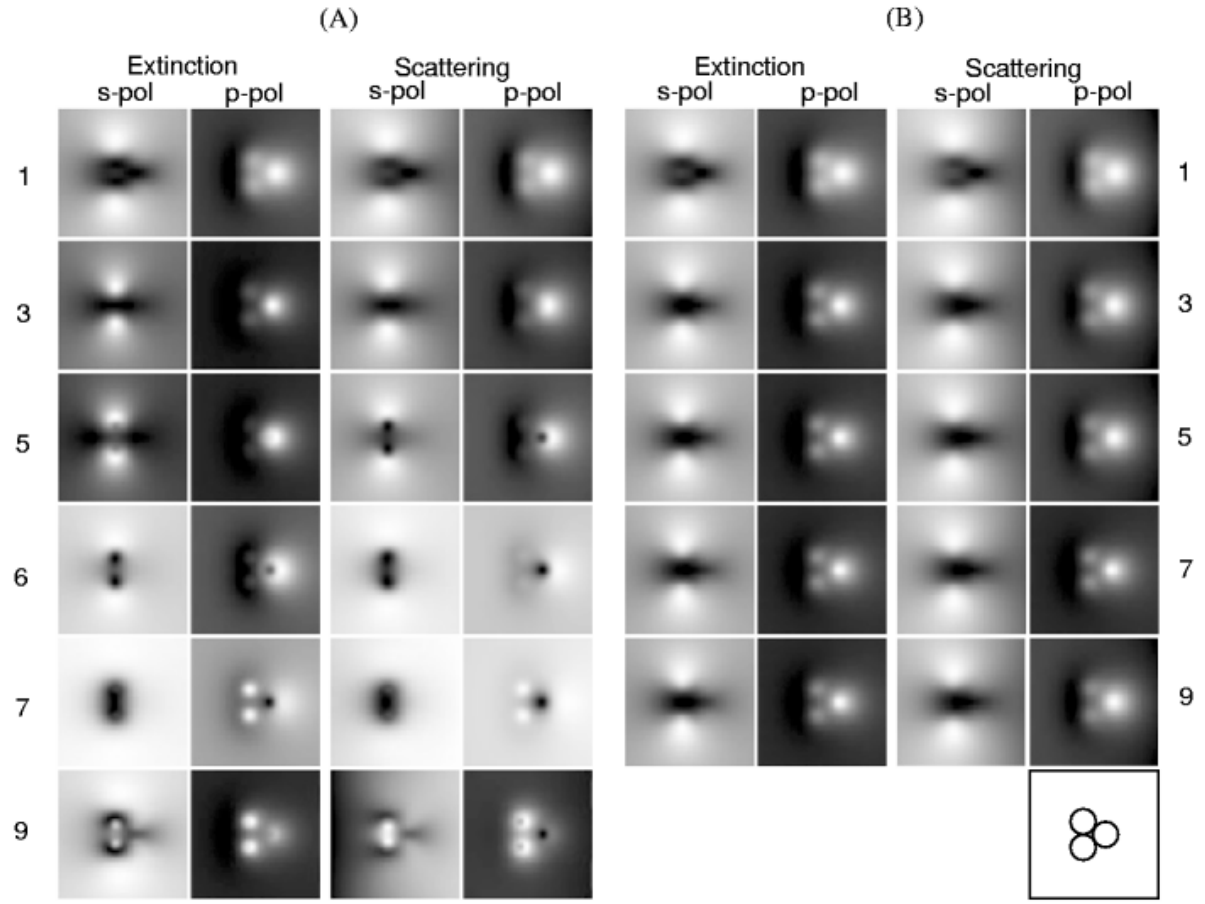

Fig. 1: Calculated apertureless near-field optical images, obtained by registering the total extinction, or scattered power, respectively, of a cluster of three silver particles, r = 5 nm,

in contact with each other, and forming an equilateral triangle, as indicated by the circles, as a function of the position of a gold probe particle, r = 5 nm scanned immediately above the silver cluster. The excitation wavelength is 460 nm. Results obtained by local (part A) and nonlocal (part B) versions of aggregate Mie theory are compared. The maximum multipole order allowed in the calculation is given in each case. Size of the images 50 × 50 nm. Rapid variations, within local aggregate Mie theory, with the maximum multipolar order used in the calculation are observed, in contrast to the nonlocal theory. This is caused by the unphysical neglection of the finite compressibility of the electron gas in the local theory.

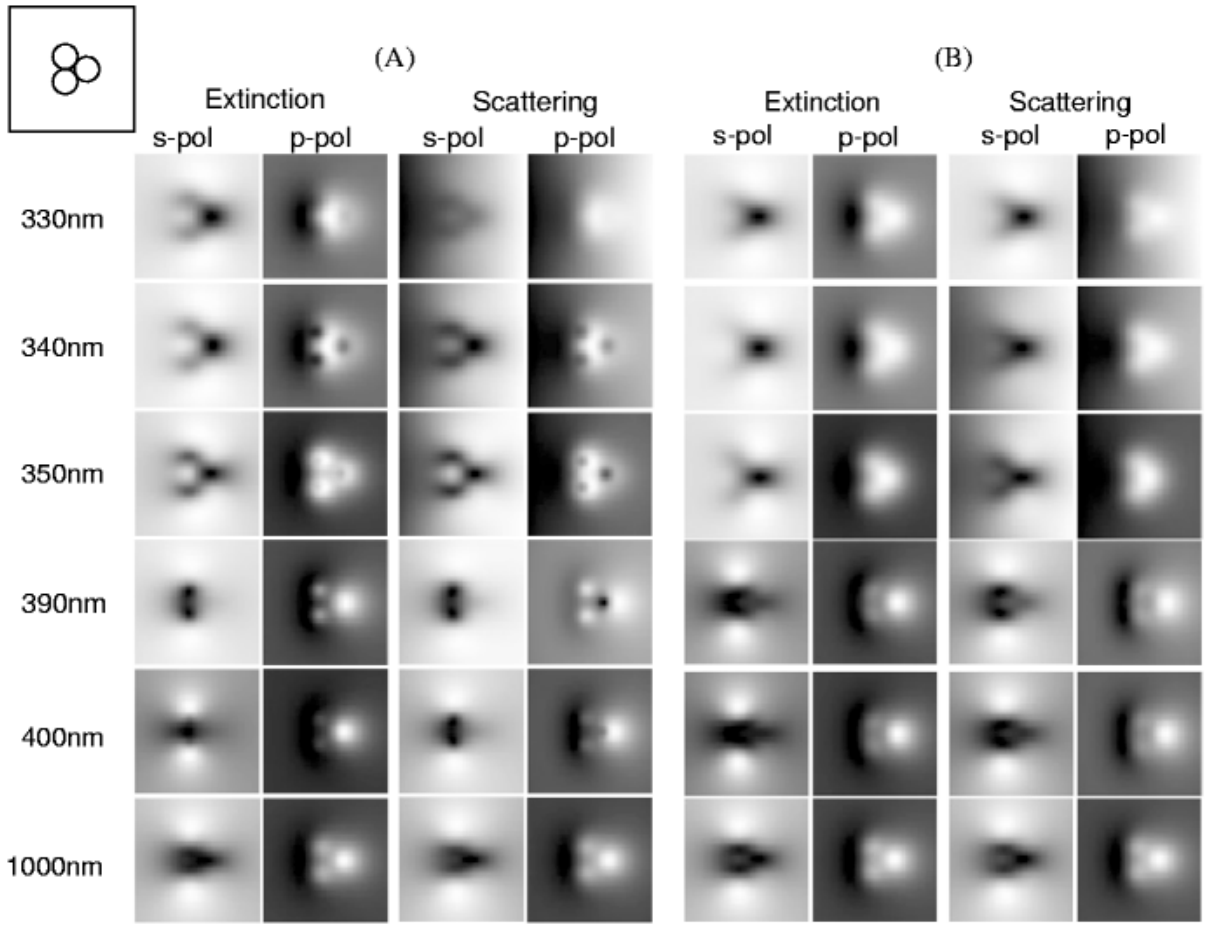

Fig. 2: Calculated apertureless near-field optical images of a cluster of three silver particles as a function of the position of a gold probe particle (as in fig. 1). Shown is here the spectral dependence of the images, with emphasis on the spectral region of the SPP resonance of the silver particles. Images on the left (part A) represent fully converged images calculated within the nonlocal version of aggregate Mie theory. Images on the right (part B) were calculated within the dipolar approximation of local aggregate Mie theory. The schematic on the top left side of the images shows again the dimensions and positions of the silver particles relative to the scan range.

[1] A. Pack, W. Grill, R. Wannemacher, Ultramicroscopy, **94**, 109-125 (2003)

4.4.11 Polarization coupling in ZnO-$BaTiO_3$ heterostructures

M. Schubert, N. Ashkenov, T. Hofmann, M. Lorenz, M. Grundmann

$BaTiO_3$ (BTO) is attractive for capacitive, piezoelectric, pyroelectric and electro-optic (EO) device applications. The electrical conductivity of the ZnO layers can be controlled over many orders of magnitude. ZnO possesses permanent spontaneous polarization. Calculations predict values similar to GaN and AlN [1],[2]. Spontaneous polarization values of BTO thin films are within the same range. Whereas the wurtzite polarization cannot be reversed, external electric fields can switch the polarization direction in the perovskite structure. Coupling effects between wurtzite and perovskite polarizations are of interest here. We report on electro-optical birefringence measurements by spectroscopic ellipsometry on ZnO-BTO-ZnO heterostructures, grown by pulsed laser deposition. Hysteresis behavior is explained by wurtzite polarization biasing the ferroelectric polarization, and ohmic-loss-induced phase transition. Thin-film-design combining remanent perovskite with permanent wurtzite polarization provide interesting grounds for new EO-device applications [3].

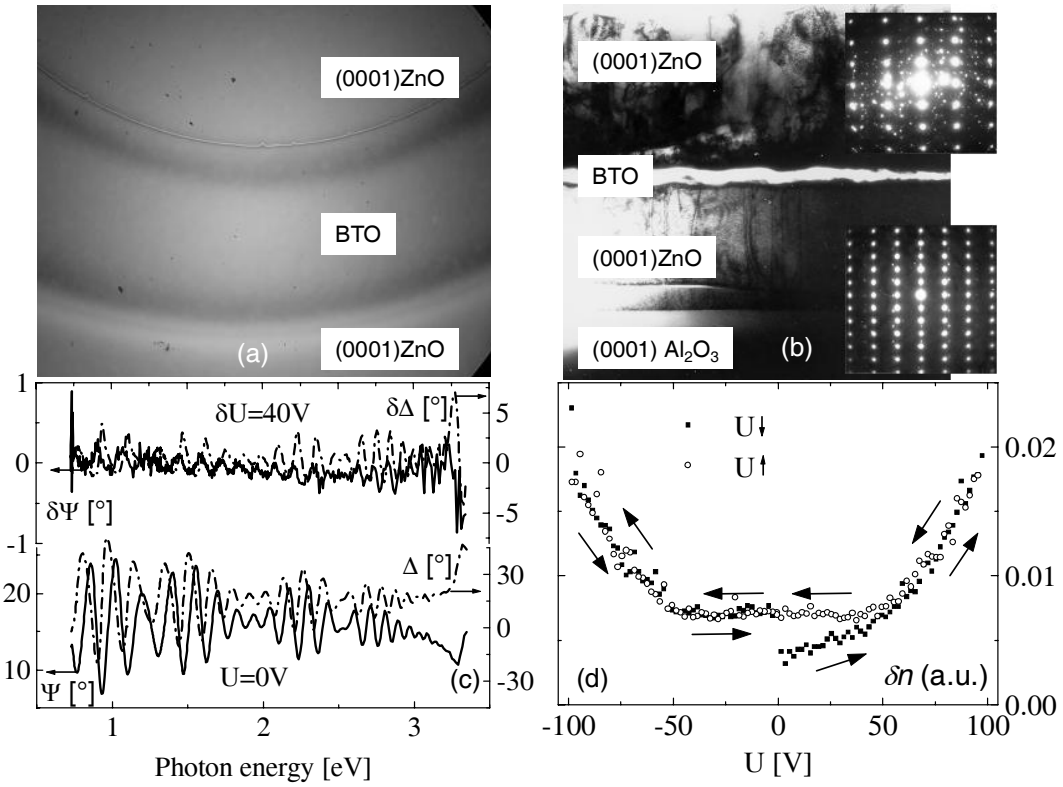

Fig. 1: ZnO(1.8 μm)/BTO/ZnO(0.4 μm) heterostructure: (a) top view, (b) TEM image and SAD pattern. (c) Ψ and Δ spectra at $U = 0$, and differences $\delta\Psi$ and $\delta\Delta$ between $U = 40$ V and $U = 0$. (d) δn versus U.

[1] F. Bernardini, V. Fiorentini, D. Vanderbilt, Phys. Rev. B **56**, R10924 (1997).
[2] O. Ambacher *et al.*, J. Appl. Phys. **87**, 334 (2000).
[3] M. Schubert *et al.*, Ann. Phys. **13**, 61 - 62 (2004)

Funded by DFG under contract SCHUH 1338/4-1,2 within FOR 404 'Oxidic Interfaces'

4.4.12 Phonon modes of stibnite determined by generalized infrared ellipsometry

M. Schubert, T. Hofmann, W. Dollase*
* Department of Earth and Space Sciences, University of California, Los Angeles, CA 90095

Generalized ellipsometry allows complete extraction of the dielectric function tensor, including orientation, from measurement of skew-cut single crystal orthorhombic absorbing materials. As an example, Stibnite (Sb_2S_3) is studied to determine fundamental phonon modes for polarization along major crystal axes **a**, **b**, and **c** from lineshape analysis of the major dielectric function spectra (Fig. 1) [1].

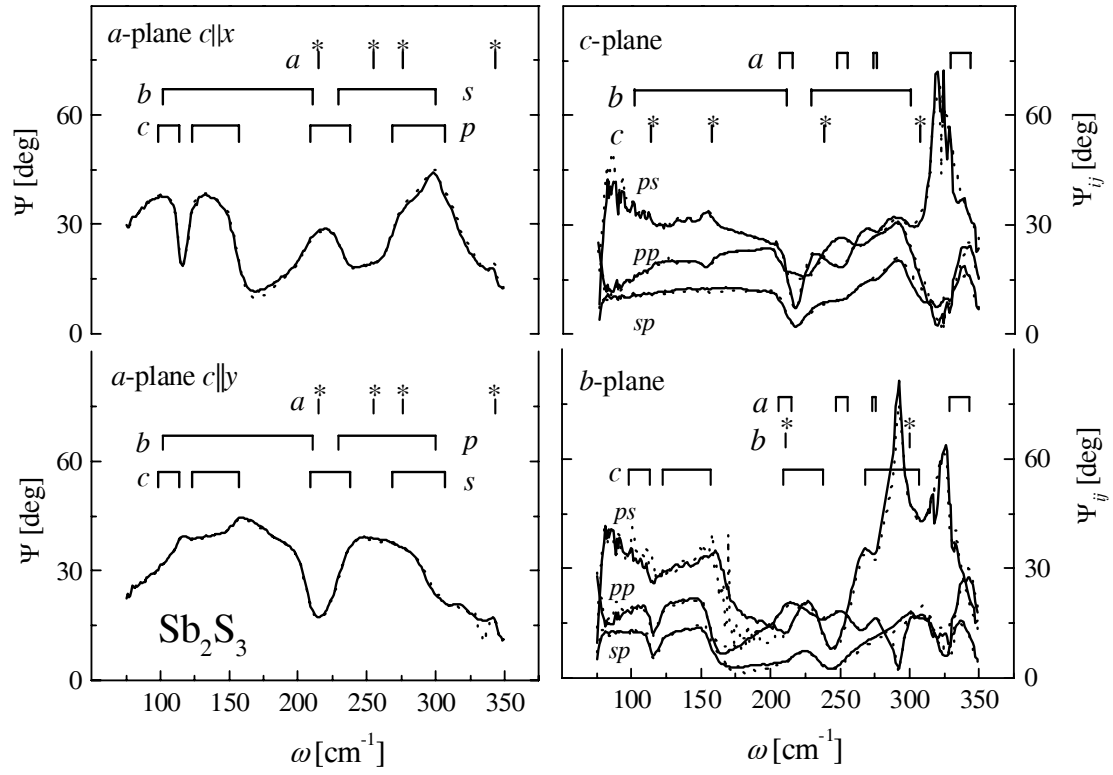

Fig. 1: Experimental (dotted lines) and best-fit (wavenmuber-by-wavenumber multiple-sample-, multiple-orientation analysis) calculated ellipsometry data (solid lines), obtained from nearly *a*-plane, *b*-plane, and *c*-plane oriented surfaces of stibnite ($\Phi_a = 70°$). Data shown for the *b*- and *c*-plane surfaces were acquired with the *a*-axis rotated $\approx 45°$ away the laboratory *x*-axis. The horizontal bars indicate the spectral regions of total reflection for *p* and *s* polarization. The labels "*a*", "*b*", "*c*" address polarizations parallel crystal axes **a**, **b**, and **c**, respectively. The vertical bars denote TO and LO frequencies. The stars indicate frequencies ω_{LO*} where dielectric loss occurs for polarization along **a**, **b**, and **c** [2].

[1] M. Schubert *et al.*, Thin Solid Films, in press.
[2] M. Schubert, *Infrared Ellipsometry on semiconductor layer structures* Springer Tracts in Modern Physics (Springer, Heidelberg, 2004/5)

4.4.13 Mo-Si soft x-ray mirror growth monitoring by in-situ ellipsometry

E. Schubert*, H. Neumann*, M. Schubert
* Wilhelm Leibnitz-Institut für Oberflächenmodifizierung Leipzig, e.V.

Fast and reliable optical in-situ process diagnostics by spectroscopic ellipsometry is demonstrated for control of dielectric multilayer mirros for soft-x-ray applications. The Mo/Si material system is a promising candidate for high - reflective normal incidence multilayer mirrors for soft-x-rays near $\lambda = 13.4$ nm. A series of Mo/Si multilayer samples with a period d =68.3 was prepared on Si (100) substrates by ion-beam deposition (Fig. 1c). The multilayer period d was monitored in-situ by visible-wavelength ellipsometry. Data of selected ellipsometry parameters are shown in Fig. 1a. Growth initiates at the silicon surface, and during deposition of the first 8 periods, the optical response of the substrate can still be seen. Measurements were done at sufficient time intervals placed within each Mo and Si sequence to ensure real-time determination of the deposition speed and the optical properties (optical constants) of both bilayer constituents. These information can be used to control the growth conditions (material stability) as well as the thickness values of each individual sublayer. A closed-loop cycle can be placed to determine the shutter opening times for each sequence to reach homogeneous thickness values over many deposition

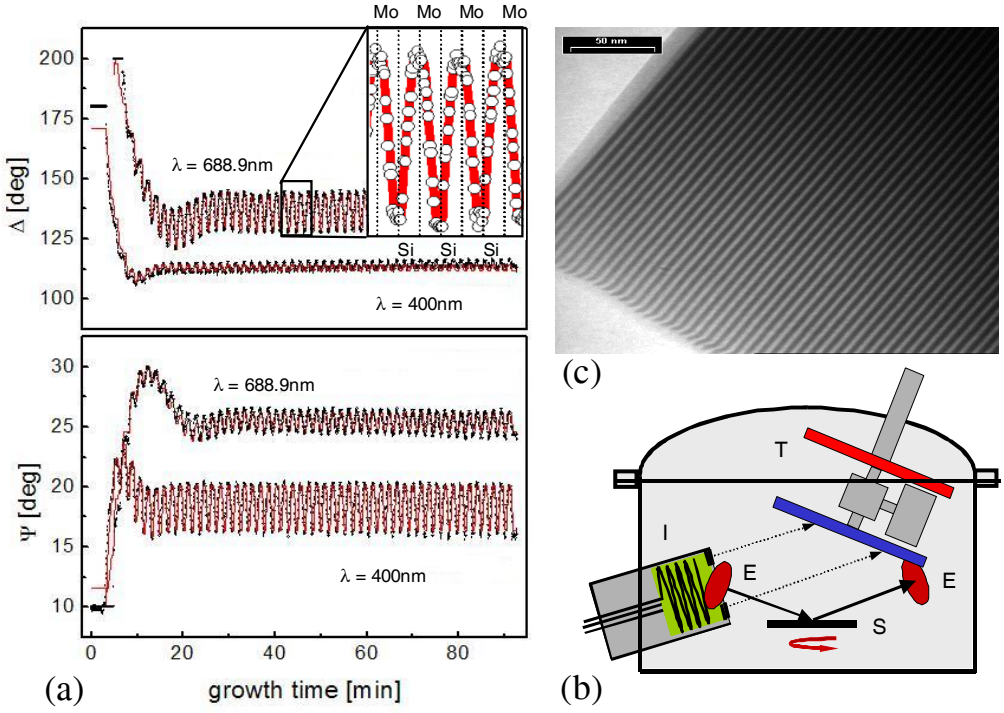

cycles.

Fig. 1: (a) Time-resolved in-situ ellipsometry data ($\lambda = 688$ nm and 400 nm) of a 50-period Mo-Si superlattice targeting a period thickness of 68.2 Å. (b) Ion-beam system for the Mo/Si multilayer deposition. The HF ion source (I) is opposed towards a switchable target (T). The substrate (S) can be rotated. The ellipsometer is attached to ports E. (c) TEM high-resolution image of the resulting SL.

4.4.14 Optical in-situ process monitoring

C. Bundesmann, N. Ashkenov, M. Schubert, G.Lippold*
* Solarion GmbH, Ostende 5, 04288 Leipzig, Germany

Optical techniques, such as spectroscopic ellipsometry and Raman scattering spectroscopy, are non-destructive, reliable and fast, and constitute almost perfect techniques for in-situ monitoring of thin film processes. While spectroscopic ellipsometry has been already applied successfully to several industrial processes, Raman scattering was still restricted to research laboratory systems. Here we report the first successful application of a Raman head fitted to an industrial thin film process. A roll-coater (Fig. 1) was designed to deposit the absorber layer of a $CuInSe_2$-based solar cell structure on flexible substrates. The performance of the absorber layer is strongly dependent on its phase compositon. Raman scattering is a perfect tool, because both wanted (α-$CuInSe_2$) and unwanted phases (e.g. γ-In_2Se_3 and Cu_2Se) produce distinct Raman or fluorescence spectra. The Raman head is an in-house built high-power large-aperture head.

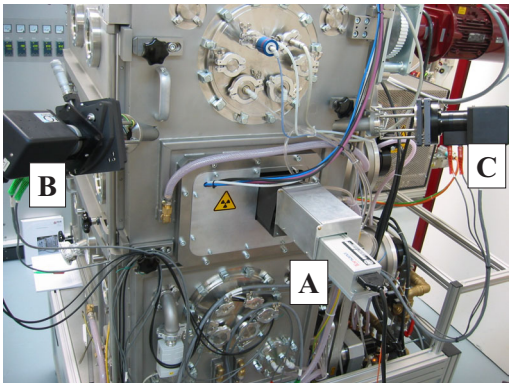

Fig. 1: Industrial roll-coater (FHR Anlagenbau GmbH, Ottendorf-Okrilla, Germany) with Raman (A) and ellipsometry (B/C) setup at the Solarion GmbH Leipzig, Germany.

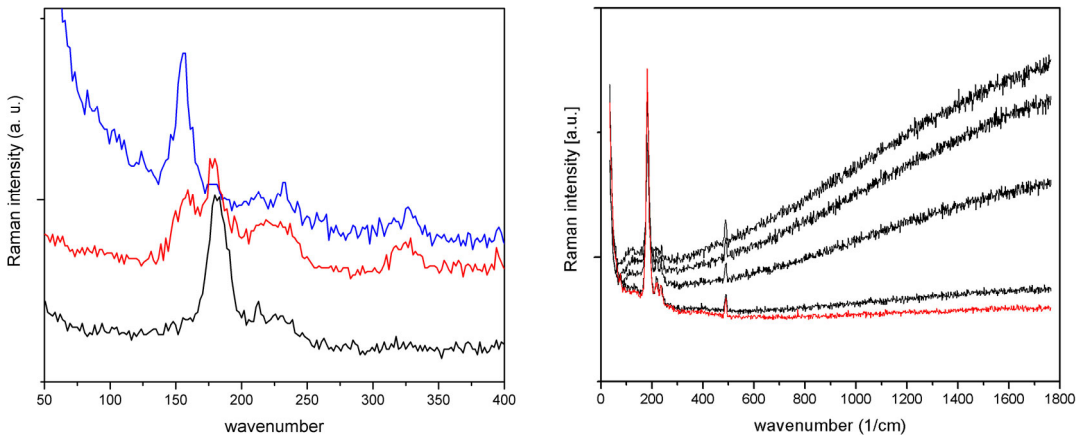

Fig. 2: Typical in-situ Raman spectra of different phases, which occur during the deposition of Cu-In-Se at different growth paramaters. *Left panel*: Raman spectra of γ-In_2Se_3 (top spectra), α-$CuInSe_2$ (bottom) and a mixture of both phases. *Right panel*: The high-temperature phase of Cu_2Se has no Raman active mode, but produces a strong fluorescence signal. The spectra were recorded with the Raman setup shown in Fig. 1 (A).

4.4.15 Phonon modes of cubic Mg-rich $Mg_xZn_{1-x}O$ thin films

C. Bundesmann, M. Schubert

Research interest is focussed on wide-band gap properties of ZnO-related compounds, such as MgZnO, which are interesting for short wavelength emitter end detector structures. In our group infrared spectroscopic ellipsometry (IRSE) and Raman scattering spectroscopy is applied to study phonon mode and free charge carrier parameters of inorganic and organic semiconductors, one example is presented here. Recent work was concerned with the infrared dielectric functions and phonon mode properties of hexagonal $Mg_xZn_{1-x}O$ thin films with $x \leq 0.52$.[1,2] Now cubic Mg-rich $Mg_xZn_{1-x}O$ thin films with $x \geq 0.67$ were studied. The samples were supplied by M. Lorenz of the Semiconductor Physics Group.

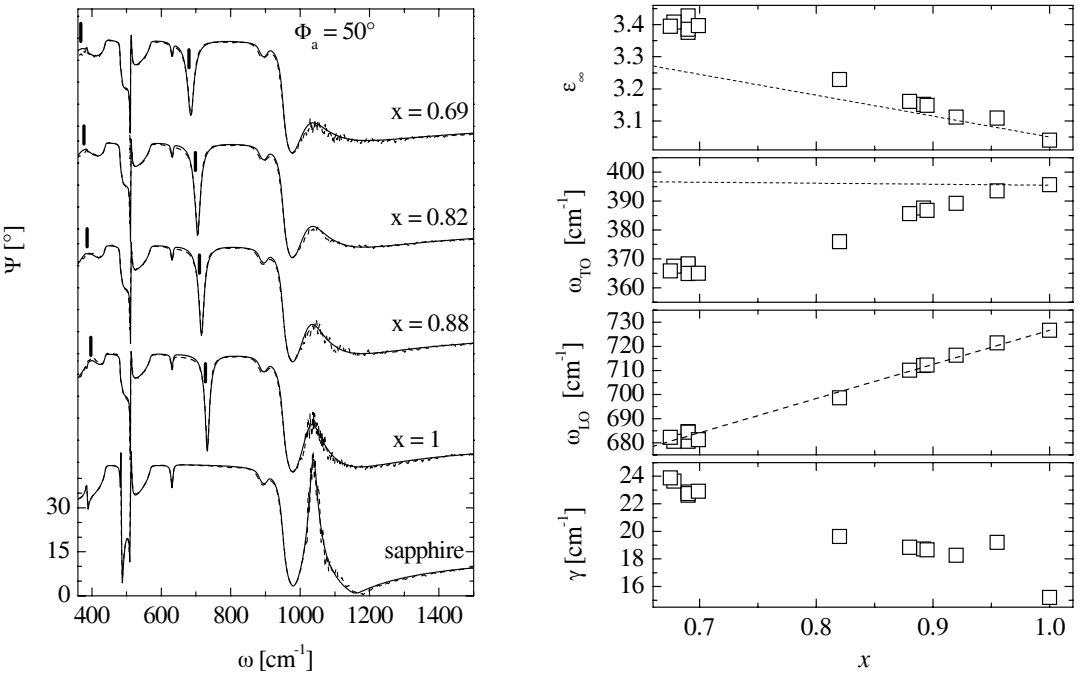

Fig. 1: Left panel: Experimental (dotted lines) and best-fit calculated (solid lines) IRSE Ψ-spectra of $Mg_xZn_{1-x}O$ thin films with $x = 0.69$, 0.82, 0.88 and 1, and a c-plane sapphire substrate. The angle of incidence is 50°. Spectra are shifted for clarity. The vertical bars indicate the frequencies of the TO and LO phonon modes obtained from best-fit model analysis. Right panel: Best-fit model dielectric function parameters of the $Mg_xZn_{1-x}O$ thin films in dependence on the Mg content x. The dashed lines are linear interpolations between the corresponding values of the binary compounds ZnO and MgO.

The infrared model dielectric function parameters of the $Mg_xZn_{1-x}O$ thin films will become useful for future free charge carrier studies of $Mg_xZn_{1-x}O$ based heterostructures.

[1] C. Bundesmann *et. al*, Appl. Phys. Lett. 81, 2376 (2002).
[2] R. Schmidt *et. al*, Proceedings of 26th ICPS, Edinburgh, UK, 2002.
[3] C. Bundesmann *et. al*, Appl. Phys. Lett. (2004) submitted.

4.4.16 Free-charge-carrier properties in AlGaAs/GaAs superlattices investigated by magnetooptic ellipsometry

T. Hofmann, C. von Middendorff, G. Leibiger*, V. Gottschalch*, and M. Schubert
*Department of Inorganic Chemistry, Semiconductor Chemistry Group, University Leipzig

Far-infrared magnetooptic ellipsometry is employed to determine the electron effective mass, the mobility and concentration in Si-doped AlGaAs/GaAs-superlattices at temperatures ranging from 10 to 290 K. The free-charge-carriers are trapped in the GaAs quantum wells, which is clearly indicated by the Fano surface polariton resonance in the vicinity of the GaAs-like longitudinal optical (LO) frequency (280 cm^{-1}). The second Fano resonance (295 cm^{-1}) is due to the undoped GaAs buffer layer on top of the Te-doped n-type GaAs substrate. We observe a directional dependence of the free-charge-carrier mobility at low temperatures. As expected for a system of reduced dimensionality the in-plane mobility ($\mu_{\parallel} = 1707\ \mathrm{cm}^2/\mathrm{Vs}$) is much larger than its out-of-plane component ($\mu_{\perp} = 1111\,\mathrm{cm}^2/\mathrm{Vs}$) at 10 K. All parameters are determined by modelling the observed magnetooptic birefringence originating from the far-infrared free-charge-carrier excitations in the AlGaAs/GaAs-heterojunctions without any need for additional electrical measurements.

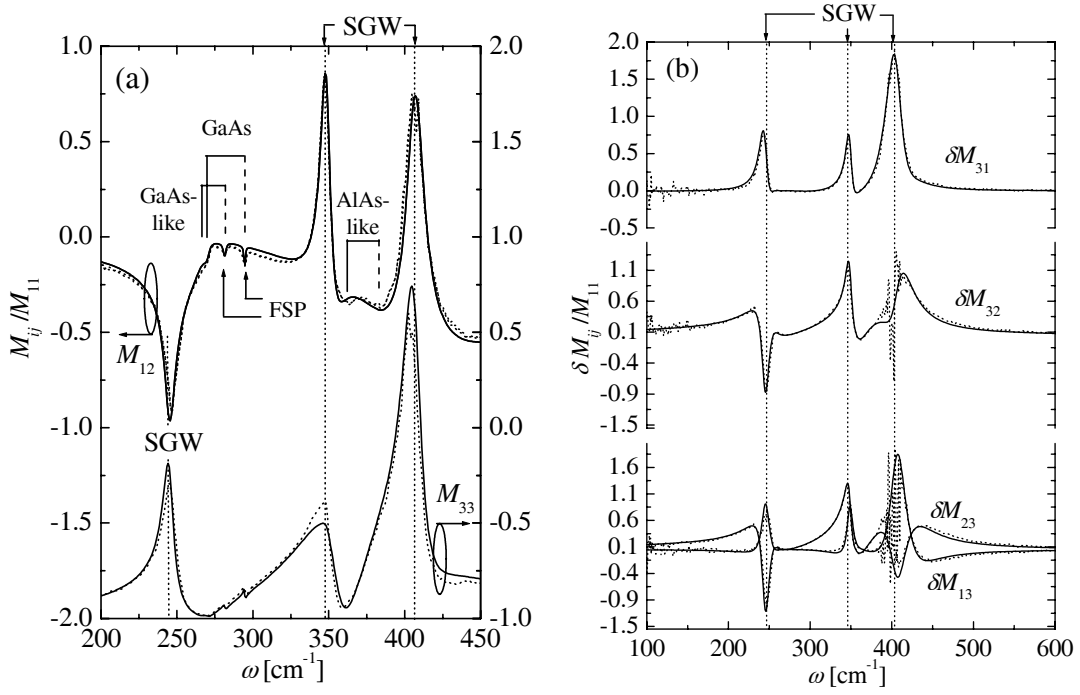

Fig. 1: (a) Experimental (dotted lines) and best-fit calculation (solid lines) Mueller matrix data. The GaAs-like and AlAs-like phonon (TO, LO) modes of the AlGaAs layers are indicated by solid and dashed vertical lines, respectively. The GaAs phonon (TO, LO) modes of the substrate, buffer, and superlattice layers are marked accordingly. The resonantly excited s- (SGW) and p-polarized transverse interface polaritons (FSP) are indicated by vertical arrows and dotted lines. (b) Experimental (dotted lines) and best-fit calculation of (solid lines) Mueller matrix element differences between those obtained at $\mu_0|\vec{H}| = -3.00(0.02)$, and $+3.00(0.02)$T. Clearly the strongest magnetooptical effects occur in the vicinity of the SGW mode resonances. The data shown in (a) and (b) were obtained at 10 K sample temperature at an angle-of-incidence of $\Phi_a = 45°$.

4.4.17 Strong increase of the electron effective mass in GaAs incorporating boron and indium

T. Hofmann, G. Leibiger*, N. Ashkenov, V. Gottschlach*, and M. Schubert
*Department of Inorganic Chemistry, Semiconductor Chemistry Group, University Leipzig

The strain-free boron- and indium-containing GaAs compounds are promising candidates for novel group-III group-V semiconductor solar cell absorber materials with lattice match to GaAs, for which experimental data of the electronic band structure are widely unknown. For non-degenerate, silicon-doped, n-type $B_{0.03}In_{0.06}Ga_{0.91}As$ with band gap energy of 1.36 eV, determined by near-infrared ellipsometry, a strong increase of the electron effective mass of 44% in $B_{0.03}In_{0.06}Ga_{0.91}As$ ($m^* = 0.093$ m$_e$) compared to $In_{0.06}Ga_{0.94}As$ ($m^* = 0.067$ m$_e$) is obtained from far-infrared magnetooptic generalized ellipsometry studies. We thereby obtain the vibrational lattice mode behavior. For BAs, an experimentally obscure compound, the curvature of the same conduction band extrapolates to the free electron mass.

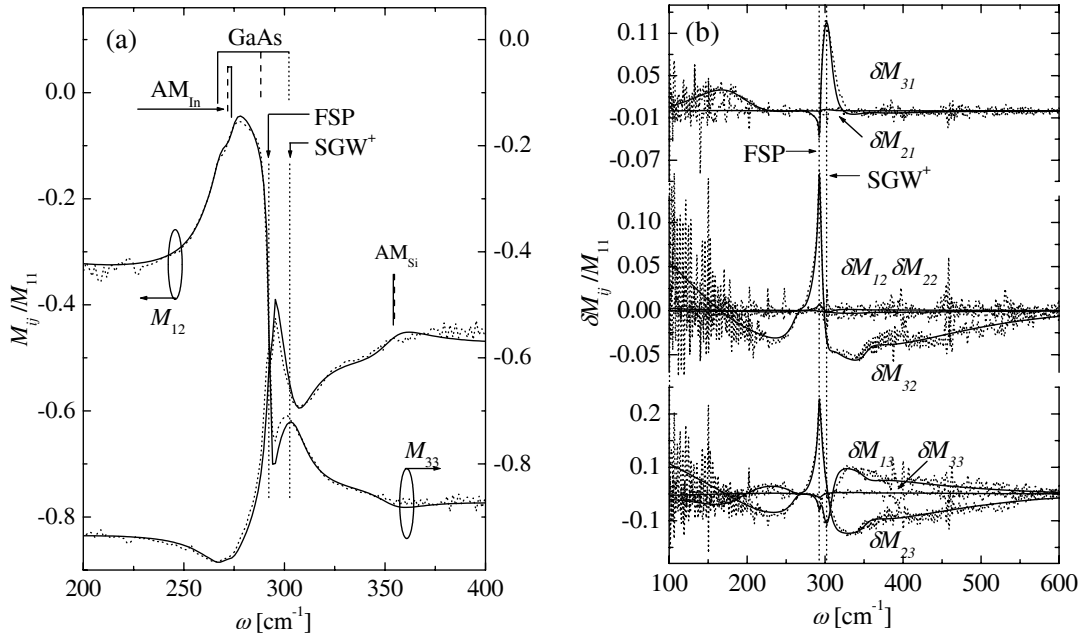

Fig. 1: (a) Experimental (dotted lines) and best-fit calculation (solid lines) ellipsometry data at $\Phi_a = 45°$. Trivial elements M_{13}, M_{22}, M_{31}, M_{23}, and M_{32} are omitted. The GaAs-like phonon (TO, LO), and phonon-plasmon (LPP$^+$) modes are indicated by solid, dashed, and dotted vertical lines, respectively. Two additional modes are attributed to InAs- and Si-like sublattice modes denoted by AM$_{In}$ and AM$_{Si}$, respectively. The sample response is further affected by excitation of s- (SGW) and p-polarized transverse interface polaritons (FSP). (b) Experimental (dotted lines) and best-fit calculation of (solid lines) Mueller matrix element differences between those obtained at $\mu_0|\vec{H}| = -3.00(0.02)$, and $+3.00(0.02)$T, obtained by magnetooptic generalized ellipsometry at $\Phi_a = 45°$.

[1] T. Hofmann, G. Leibiger, N. Ashkenov, V. Gottschlach, M. Schubert, Phys. Rev. Lett. *(submitted)*

4.4.18 Funding

Development of a Miniaturized Advanced Diagnostic Technology Demonstrator 'DIAMOND' - Technology Study Phase 2 ,
European Space Organization ESA/ESTEC

Ultrasound Diagnostics of Directional Solidification
European Space Organization ESA/ESTEC

Development and verification of the applicability of ultrasonic methods
Schott GLAS Mainz

Development of ultrasonic methods, sensors and measurement equipment
Funded by Heidelberger Druckmaschinen AG

Development and verification of the applicability of ultrasonic methods
PFW Technologies GmbH

Elektronische und optische Eigenschaften, in-situ Ramanstreuung, in-situ Ellipsometrie und Ionenstrahlanalytik von flexiblen Cu-(In,Ga)-(Se,S)-Dünnfilm-Solarzellen.
Electronic and optical properties, in-situ Ramanscattering, in-situ Ellipsometry and ion beam analysis of flexible Cu-(In,Ga)-(Se,S) thin film solar cells
M. Grundmann, M. Schubert, T. Butz
BMBF-Wachstumskern INNOCIS, Teilprojekt FKZ 03WKI09

Bestimmung der Infrarot-dielektrischen Funktion und der Eigenschaften Freier Ladungsträger in organischen Halbleiterdünnschichten
Free-carrier properties and infrared dielectric functions of organic semiconductor layers
M. Schubert
JOANNEUM Research Forschungsgesellschaft mbH, Graz, Österreich

Bestimmung der optischen Eigenschaften funktionell-optischer Dünnschichten
Determination of optical properties of functional optical thin films
M. Schubert
Flabeg GmbH, Furth im Wald

Generalized far-infrared ellipsometry of magnetooptic free-carrier-effects in III-V semiconductor layer structures
M. Schubert
DFG, SCHUH 1338/3-1

Interface-induced electro-optic properties of oxide semiconductor - ferroelectrica interfaces
M. Schubert, M. Lorenz
DFG, SCHUH 1338/4-1,2 FOR 404 'Oxidic interfaces'

4.4.19 External Cooperations

European Space Organization ESA/ESTEC
Schott GLAS Mainz
Heidelberger Druckmaschinen AG
PFW Technologies GmbH University of the Witwatersrand, Johannesburg, South Africa: Prof. Dr. A. Every
Wroclaw Institute of Technology, Wroclaw, Poland: Dr. M. Pluta
University of Arizona, Tucson, Arizona, USA: Prof. Dr. T. Kundu
Universitt Frankfurt: Prof. Dr. J. Bereiter-Hahn
Universitt Dortmund: Prof. Dr. U. Woggon
University of Nebraska-Lincoln, Lincoln, NE, USA: Prof. J. A. Woollam
Linkoping University, Linkoping, Schweden: Profs. B. Monemar, H. Arwin, O. Inganäs
University of California, Los Angelas, CA, USA: Prof. W. Dollase
Ritsumeikan University, Kusatsu, Japan: Prof. Y. Nanishi
University of Otago, Otago, New Zealand: Prof. I. Hodgkinson
Colorado State University, Fort Collins, CO, USA: Prof. H. D. Hochheimer
Joanneum Forschungsgesellschaft, Graz, Österreich: Dr. G. Jakopic
J. A. Woollam Co., Lincoln, NE, USA: Dr. C. M. Herzinger, B. Johs, Dr. T. E. Tiwald
Oak Ridge National Laboratory, TE, USA: Dr. G. E. Jellison
National Institute of Standard and Technology, Boulder, CO, USA: Dr. N. Sanford
Institut für Angewandte Optik und Feinmechanik IOF Jena: Dr. N. Kaiser, Dr. A. Duparré
Institut für Elektronenstrahl- und Plasmatechnik FEP Dresden: Dr. Hagen Bartsch, Hagen Sahm
Institut Schicht- und Oberflächentechnik IST Braunschweig: Dr. Bernd Szyska
Osram Opto Semiconductors Regensburg: Dr. K. Streubel, Dr. I. Pietzonka
Von Ardenne Anlagentechnik Dresden GmbH: Dr. M. List, Herr M. Kammer
Flabeg GmbH, Furth im Wald: Herr T. Hoeing, Herr S. Menzel
Solarion GmbH, Leipzig: Dr. G. Lippold, Dr. A. Braun
FHR Anlagenbau GmbH, Ottendorf-Okrilla: Herr W. Hentzsch, Herr F. Hammerschmidt
Roth und Rau AG: Prof. H.-U. Poll
Alanod Aluminium-Veredlung GmbH und Co. KG, Ennepetal: Dr. H. Küster, Dr. D. Peros
On Semiconductor Cooperation Terosil, Rožnov pod Radhoštem, Czech Republic: Dr. J. Šik

4.4.20 Publications

Journals

Fourier inversion of acoustic wave fields in anisotropic solids
M. Pluta, A. G. Every, W. Grill, T. J. Kim
Phys. Rev. B 67, 094117 (2003)

Phase-sensitive acoustic imaging and micro-metrology of polymer blend thin films W. Ngwa, R. Wannemacher, W. Grill,T. Kundu
Europhys. Lett. 64, 830-836 (2003)

Understanding the morphology of thin film polymer blends; Elucidations by phase-sensitive acoustic imaging
W. Ngwa, R. Wannemacher, W. Grill, and T. Kundu
Proceedings of 2nd Africa-MRS conference, 197 (2003)

Mode control by nanoengineering of light emitters in spherical microcavities
B. Möller, M. V. Artemyev, U. Woggon, R. Wannemacher
Appl. Phys. Lett. 83, 2686-2688 (2003)

Dot-in-a-dot: electronic and photonic confinement in all three dimensions
U. Woggon, R. Wannemacher, M.V. Artemeyev, B. Möller, N. LeThomas, V. Anikeyev, O. Schöps
Appl. Phys. B 77, 469 - 484 (2003) invited paper

Apertureless near-field optical microscopy of metallic nanoparticles
A. Pack, W. Grill, R. Wannemacher
Ultramicroscopy, 94, 109-125 (2003)

Phonons and free-carrier properties of binary, ternary, and quaternary group-III nitride layers measured by infrared spectroscopic ellipsometry
A. Kasic, M. Schubert, J. Off, B. Kuhn, F. Scholz, S. Einfeldt, T. Böttcher, D. Hommel, D. J. As, U. Koehler, A. Dadgar, A. Krost, Y. Saito, Y. Nanishi, M. R. Correia, S. Pereira, V. Darakchieva, B. Monemar, H. Amano, I. Akasaki, G. Wagner
In Group III-Nitrides and Their Heterostructures: Growth, Characterization and Applications edited by F. Bechstedt, B. K. Meyer and M. Stutzmann (Wiley-VCH, Berlin, 2003) ISBN 3-527-40475-9

Generalized Ellipsometry
M. Schubert
In Introduction to Complex Mediums for Optics and Electromagnetics edited by W. S. Weiglhofer and A. Lakhtakia (SPIE, Bellingham, WA, 2003) ISBN 0819449474

MOVPE growth, Phonons, Band-to-Band Transitions and Dielectric Functions of InGaNAs/GaAs Superlattices and Quantum Wells
G. Leibiger, V. Gottschalch,G. Benndorf, J. ik, M. Schubert
In Compound semiconductor heterojunctions: physics and applications edited by W. Cay and others (Research Signpost, Kerala, 2003) ISBN 8177361708

Micro-Raman scattering profiles studies on HVPE-grown free-standing GaN
A. Kasic, D. Gogova, H. Larsson, C. Hemmingsson, I. Ivanov, B. Momenar, C. Bundesmann, M. Schubert
phys. stat. sol.

Deformation potentials of the E_1(TO) and E_2 modes of InN
V. Darakchieva, P. P. Paskov, E. Valcheva, T. Paskova, B. Monemar, M. Schubert, H. Lu, W. J. Schaff

Appl. Phys. Lett.

Real-time spectroscopic ellipsometry monitoring of a ZnO thin film pulsed laser deposition growth
N. Ashkenov, M. Schubert, H. Hochmuth, M. Lorenz, M. Grundmann
Appl. Phys. Lett.

Strong increase of the electron effective mass in GaAs incorporating boron and indium
T. Hofmann, G. Leibiger, N. Ashkenov, V. Gottschalch, M. Schubert
Phys. Rev. Lett.

Temperature-dependent band-gap energies and optical constants of ZnO
N. Ashkenov, M. Schubert, W. Czakai, G. Benndorf, H. Hochmuth, M. Lorenz, M. Grundmann
Phys. Rev. B

Strain related structural and vibrational properties of thin epitaxial AlN layers
V. Darakchieva, J. Birch, M. Schubert, A. Kasic, S. Tungasmita, T. Paskova, B. Monemar
Phys. Rev. B

Phonons and polaritons in semiconductor layer structures
M. Schubert, T. Hofmann
Phys. Rev. B

Optical and structural characteristics of virtually unstrained bulk-like GaN
D. Gogova, A. Kasic, H. Larsson, B. Pcz, R. Yakimova, B. Magnusson, B. Monemar, F. Tuomisto, K. Saarinen, C. R. Miskys, M. Stutzmann, C. Bundesmann, M. Schubert
Jpn. J. Appl. Phys., accepted for publication

Optical modelling of a layered photovoltaic device with a polyfluorene-copolymer as the active layer
Nils-Krister Persson, M. Schubert, O. Inganäs
Solar Energy Materials and Solar Cells, accepted for publication

Optical properties of $Zn_{1-x}Mn_xSe$ epilayers determined by spectroscopic ellipsometry
J. Kvietkova, B. Daniel, M. Hetterich, M. Schubert, D. Spemann, P. Pfundstein, and D. Gerthsen
Thin Solid Films

Infrared to vacuum ultraviolet optical properties of 3C, 4H and 6H silicon carbide measured by spectroscopic ellipsometry
O. P. A. Lindquist, M. Schubert, H. Arwin, K. Jrrendahl
Thin Solid Films, accepted for publication

Protein adsorption in porous silicon gradients monitored by spatially-resolved spectroscopic ellipsometry

L. M. Karlsson, M. Schubert, N. Ashkenov, H. Arwin
Thin Solid Films, accepted for publication

Hydrogen implantation in InGaNAs studied by spectroscopic ellipsometry
G. Leibiger, V. Gottschalch, N. Razek, M. Schubert
Thin Solid Films, accepted for publication

UV-VUV spectroscopic ellipsometry of ternary $Mg_xZn_{1-x}O$ ($0 < x < 0.53$) thin films
R. Schmidt-Grund, M. Schubert, B. Rheinländer, D. Fritsch, H. Schmidt, E. M. Kaidashev, M. Lorenz, C. M. Herzinger, M. Grundmann
Thin Solid Films, accepted for publication

Far-infrared dielectric function and phonon modes of spontaneously ordered $(Al_xGa_{1-x)0.52}In_0.48P$
T. Hofmann, M. Schubert, V. Gottschalch
Thin Solid Films, accepted for publication

Generalized ellipsometry for orthorhombic absorbing materials: Dielectric functions, phonon modes and band-to-band transitions of Sb_2S_3
M. Schubert, T. Hofmann, C. M. Herzinger, W. Dollase
Thin Solid Films, accepted for publication

Infrared dielectric functions and crystal orientation of a-plane ZnO thin films on r-plane sapphire determined by generalized ellipsometry
C. Bundesmann, N. Ashkenov, M. Schubert, A. Rahm, H. v. Wenckstern, E. M. Kaidashev, M. Lorenz, M. Grundmann
Thin Solid Films, accepted for publication

Infrared ellipsometry characterization of conducting thin organic films
M. Schubert, C. Bundesmann, G. Jakopic, H. Maresch, H. Arwin, N.-C. Persson, F. Zhang, O. Ingans
Thin Solid Films, accepted for publication

Far-infrared magnetooptic generalized ellipsometry: Determination of free-charge-carrier parameters in semiconductor thin film structures
M. Schubert, T. Hofmann, C. M. Herzinger
Thin Solid Films, accepted for publication

Carrier redistribution in organic/inorganic (PEDOT/PSS - Si) heterojunction
M. Schubert, C. Bundesmann, H. v. Weckstern, G. Jakopic, A. Haase, N.-K. Persson, F. Zhang, H. Arwin, O. Inganäs
Appl. Phys. Lett. 84, 1311 - 1313 (2004)

Strain evolution and phonons in AlN/GaN superlattices
V. Darakchieva, P. P. Paskov, M. Schubert, E. Valcheva, T. Paskova, H. Arwin, B. Monemar, H. Amano, I. Akasaki
Mat. Res. Soc. Symp. 798, Y5.60 (2004)

Electro-optical properties of ZnO-$BaTiO_3$-ZnO heterostructures grown by pulsed laser deposition
M. Schubert, N. Ashkenov, T. Hofmann, H. Hochmuth, M. Lorenz, M. Grundmann, G. Wagner
Ann. Phys. 13, 61 - 62 (2004)

Infrared dielectric function and vibrational modes of pentacene thin films
M. Schubert, C. Bundesmann, G. Jakopic, H. Maresch, H. Arwin
Appl. Phys. Lett. 84, 200 - 202 (2004)

Generalized infrared ellipsometry study of thin epitaxial AlN layers with complex strain behavior
V. Darakchieva, M. Schubert, J. Birch, A. Kasic, S. Tungasmita, T. Paskova, B. Monemar
Physica B: Condensed Matter 340-340, 416 - 420 (2003)

Optical properties of undoped AlN/GaN superlattices grown by metal orgaic vapor phase epitaxy
V. Darakchieva, P. P. Paskov, M. Schubert, T. Paskova, B. Monemar, S. Kamiyama, M. Iwaya, H. Amano, I. Akasaki
phys. stat. sol. c 0, 1 - 4 (2003)

Raman scattering in ZnO thin films doped with Fe, Sb, Al, Ga and Li
C. Bundesmann, N. Ashkenov, M. Schubert, D. Spemann, T. Butz, M. Lorenz, E. M. Kaidashev, M. Grundmann
Appl.
Phys. Lett.83, 1974 - 1976 (2003)

Interband transitions and phonon modes in GaB_xAs_{1-x} ($0 \leq x < 0.33$) and GaN_xAs_{1-x} ($0 \leq x < 0.29$)
G. Leibiger, V. Gottschalch, V. Riede, M. Schubert, J. N. Hilfiger, T. E. Tiwald
Phys. Rev. B 67, 195205 (2003)

Optical properties of ternary MgZnO thin films
R. Schmidt, C. Bundesmann, N. Ashkenov, B. Rheinlnder, M. Schubert, M. Lorenz, E. M. Kaidashev, D. Spemann, T. Butz, J. Lenzner, M.
Grundmann
Proceedings of the International Conference on the Physics of Semiconductors (ICPS) 2002

Far-infrared magneto-optical generalized ellipsometry determination of free-carrier parameters in semiconductor thin film structures
T. Hofmann, M. Grundmann, C. M. Herzinger, M. Schubert,
W. Grill Mat. Res. Soc. Symp. 744, M5.32.1 (2003)

Far-infrared dielectric functions and phonon modes of spontaneously ordered AlGaInP

T. Hofmann, V. Gottschalch, M. Schubert
Mat. Res. Soc. Symp. 744, M5.33.1 (2003)

Far-infrared-magneto-optic Ellipsometry characterization of free-charge-carrier properties in highly-disordered n-type $Al_{0.19}Ga_{0.33}In_{0.48}P$
T. Hofmann, M. Schubert, C. M. Herzinger, I. Pietzonka
Appl. Phys. Lett. 82, 3463 - 3465 (2003)

Residual strain in HVPE GaN free-standing and re-grown homoepitaxial layers
V. Darakchieva, T. Paskova, P.P. Paskov, B. Monemar, N. Ashkenov, M. Schubert
phys. stat. sol. (a) 195 516 - 522 (2003)

Dielectric functions (1 eV to 5 eV) of wurtzite $Mg_xZn_{1-x}O$ ($0 \leq x < 0.29$) thin films
R. Schmidt, B. Rheinlnder, M. Schubert, D. Spemann, T. Butz, J. Lenzner, E. M. Kaidashev, M. Lorenz, M. Grundmann
Appl. Phys. Lett. 82, 2260 - 2262 (2003)

Infrared dielectric functions and phonon modes of high-quality ZnO films
N. Ashkenov, G. Wagner, H. Neumann, B. N. Mbenkum, C. Bundesmann, V. Riede, M. Lorenz, E. M. Kaidashev, A. Kasic, M. Schubert, M. Grundmann, V. Darakchieva, H. Arwin, B. Monemar
J. Appl. Phys. 93, 126 - 133 (2003)

Generalized far-infrared magneto-optic ellipsometry for semiconductor layer structures: Determination of free-carrier effective mass, mobility and concentration parameters in n-type GaAs
M. Schubert, T. Hofmann, C. M. Herzinger
J. Opt. Soc. Am. A 20, 347 - 356 (2003)

Invited talks

Advances in Spectroscopic Ellipsometry Characterization of Optical Thin Films
M. Schubert, A. Kasic, T. Hofmann, N. Ashkenov, W. Grill, M. Grundmann, E. Schubert, H. Neumann
Optical System Design 2003, St. Etienne, France, September 2003

Generalized magneto-optic ellipsometry
M. Schubert, T. Hofmann, C. M. Herzinger
3. International Conference on Spectroscopic Ellipsometry, Vienna, Austria, July 2003

Conference contributions

Electro-optical properties of ZnO-$BaTiO_3$-ZnO heterostructures grown by pulsed laser deposition
M. Schubert, N. Ashkenov, H. Hochmuth, M. Lorenz, M. Grundmann, G. Wagner

10th International Workshop on Oxide Electronics, Augsburg, Germany, September 11-13 2003

Generalized infrared ellipsometry study of thin epitaxial AlN layers with a complex strain behavior
V. Darakchieva, M. Schubert, J. Birch, T. Paskova, A. Kasic, S. Tungasmita, and B. Monemar
ICDS 2003

The influence of composition and strain on phonon modes and band-to-band transitions in hexagonal InGaN
A. Kasic, M. Schubert, Y. Saito, M. Kurouchi, Y. Nanishi, J. Off, F. Scholz, M. R. Correia, S. Pereira, B. Monear
5. Int. Conf. on Nitride Semiconductor Research, Nara, Japan, July 2003

High temperature optical constants and band gap energies of ZnO
N. Ashkenov, C. Bundesmann, R. Schmidt-Grund, M. Schubert, M. Lorenz, H. Hochmut, M. Grundmann
3. International Conference on Spectroscopic Ellipsometry, Vienna, Austria, July 2003

Infrared ellipsometry - a novel characterization method for group-III nitride device heterostructures
A. Kasic, M. Schubert, B. Monemar
3. International Conference on Spectroscopic Ellipsometry, Vienna, Austria, July 2003

Infrared dielectric functions and crystal orientation of a-plane ZnO thin films on r-plane sapphire determined by generalized ellipsometry
C. Bundesmann, N. Ashkenov, M. Schubert, A. Rahm, H. v. Wenckstern, E. M. Kaidashev, M. Lorenz, M. Grundmann
3. International Conference on Spectroscopic Ellipsometry, Vienna, Austria, July 2003

Optical properties of Zn1-xMnxSe epilayers determined by spectroscopic ellipsometry
J. Kvietkova, B. Daniel, M. Hetterich, M. Schubert, D. Spemann, P. Pfundstein, and D. Gerthsen
3. International Conference on Spectroscopic Ellipsometry, Vienna, Austria, July 2003

UV-VUV spectroscopic ellipsometry of ternary $Mg_xZn_{1-x}O$ ($0 < x < 0.53$) thin films
R. Schmidt-Grund, M. Schubert, B. Rheinlnder, D. Fritsch, H. Schmidt, E. M. Kaidashev, M. Lorenz, C. M. Herzinger, M. Grundmann
3. International Conference on Spectroscopic Ellipsometry, Vienna, Austria, July 2003

Infrared to vacuum ultraviolet optical properties of 3C, 4H and 6H silicon carbide measured by spectroscopic ellipsometry
O. P. A. Lindquist, M. Schubert, H. Arwin, K. Jrrendahl
3. International Conference on Spectroscopic Ellipsometry, Vienna, Austria, July 2003

Protein adsorption in porous silicon gradients monitored by spatially-resolved

spectroscopic ellipsometry
L. M. Karlsson, M. Schubert, N. Ashkenov, H. Arwin
3. International Conference on Spectroscopic Ellipsometry, Vienna, Austria, July 2003

Far-infrared dielectric function and phonon modes of spontaneously ordered $(Al_xGa_{1-x})_{0.52}In_0.48P$
T. Hofmann, M. Schubert, V. Gottschalch
3. International Conference on Spectroscopic Ellipsometry, Vienna, Austria, July 2003

Infrared ellipsometry characterization of conducting thin organic films
M. Schubert, C. Bundesmann, G. Jakopic, H. Maresch, H. Arwin, N.-C. Persson, F. Zhang, O. Ingans
3. International Conference on Spectroscopic Ellipsometry, Vienna, Austria, July 2003

Hydrogen implantation in InGaNAs studied by spectroscopic ellipsometry
G. Leibiger, V. Gottschalch, N. Razek, M. Schubert
3. International Conference on Spectroscopic Ellipsometry, Vienna, Austria, July 2003

Generalized ellipsometry for orthorhombic absorbing materials: Dielectric functions, phonon modes and band-to-band transitions of Sb_2S_3
M. Schubert, T. Hofmann, C. M. Herzinger, W.
Dollase
3. International Conference on Spectroscopic Ellipsometry, Vienna, Austria, July 2003

Far infrared magnetooptic Ellipsometry characterization of free carrier properties in highly disordered n-type AlGaInP
T. Hofmann, M. Schubert, C. M. Herzinger, I. Pietzonka
German Physical Society Spring Meeting, Dresden, March 2003

Phonons, band gap and higher interband transitions of hexagonal InGaN
A. Kasic, M. Schubert, J. Off, F. Scholz, M. R. Correia, S. Pereira, Y. Saito, M. Kurouchi, Y. Nanishi
German Physical Society Spring Meeting, Dresden, March 2003

Molekularstrahlepitaxie, Charakterisierung und Kopositionseichung von ZnMnSe Schichten
B. Daniel, J. Kvietkova, M. Hetterich, H. Priller, J. Lupaca-Schomber, C. Klingshirn, M. Schubert, N. Ashkenov, P. Pfundstein, D. Gerthsen, K. Eichhorn
German Physical Society Spring Meeting, Dresden, March 2003

Optische Übergänge und Brechungsindices von MgZnO
R. Schmidt, B. Rheinländer, M. Schubert, E. M. Kaidashev, M. Lorenz, D. Spemann, G. Wagner, A. Rahm, C. M. Herzinger, M. Grundmann
German Physical Society Spring Meeting, Dresden, March 2003

4.4.21 Graduations

Dipl.-Phys. Alexander Kasic
Phonons, free-carrier properties, and electronic interband transitions of binary, ternary, and quaternary group-III nitride layers measured by spectroscopic ellipsometry
20.01.2003

4.4.22 Guests

Dr. Mietek Pluta
Technical University of Wroclaw, Poland
4 months

Prof. Dr. Tribikram Kundu
University of Arizona
4 weeks

4.5 Superconductivity and Magnetism

4.5.1 Introduction

Research into the basic properties of ferromagnetic and superconducting materials has a long-standing tradition. The present focus of the Division of Superconductivity and Magnetism is on two branches of contemporary magnetism: (1) magnetic phenomena in carbon-based materials and (2) oxide spin-electronics.

Research highlight in the year 2003 was the discovery of ferromagnetism in proton-irradiated graphite, see P. Esquinazi *et al.*, Phys. Rev. Lett. **91**, 227201 (2003). Here the intensive cooperation between our group and the Division of Nuclear Solid State Physics lead to the observation of a clear ferromagnetic signature in irradiated highly oriented pyrolytic graphite (HOPG). This opens up a wide spectrum of further research into the magnetic and magnetotransport properties of graphite micro- and nanostructures.

In the field of oxide spin-electronics it has been a successful year with the extension of the Forschergruppe 404 'Oxidische Grenzflächen (Oxide Interfaces)' and the continuation of our project on the magnetotransport properties of magnetic oxide heterostructures. Future aims of this project are the study of magnetic oxide nanocontacts and the fabrication of spin-transistors.

4.5.2 Ferromagnetism in proton irradiated highly oriented graphite

Ferromagnetic Spots in Graphite Produced by Proton Irradiation

K.-H. Han[1], D. Spemann[2], P. Esquinazi[1], R. Höhne[1], A. Setzer[1], V. Riede[3] and T. Butz[2]
[1] *Superconductivity and Magnetism*
[2] *Nuclear Solid State Physics*
[3] *Solid-State Optics and Acoustics*

The recently discovered ferromagnetic signals in pure graphite [1,2] and in polymerized fullerenes [3] are received mainly with a mixture of surprise and scepticism by most of the scientific community. The aim of our investigation was to use samples with a very low impurity content, to measure precisely the ferromagnetic metal content and possibly to increase the intrinsic ferromagnetism. Without a sensitive and reliable method for this characterization it would not be possible to continue the research in this topic, since in several samples the measured magnetization is not much larger than the magnetization we would expect from the incorporated magnetic impurities. The basic idea was to use proton irradiation simultaneously for element analysis by "Particle Induced X-ray Emission" (PIXE) and – possibly – for the creation of magnetic domains. In the first step of our study [4] clean surfaces of a HOPG sample (Fe content < 0.3 ppm, rocking-curve width $= 0.4°$) were irradiated by 2.25 MeV protons using a microbeam applied parallel to the c-axis. Beam diameters between 1 and 2 μm, separated by 20 μm , and at different fluences and doses were chosen. The total deposited electric charge (areal) density was between 0.05 and 50 nCμm^{-2}.

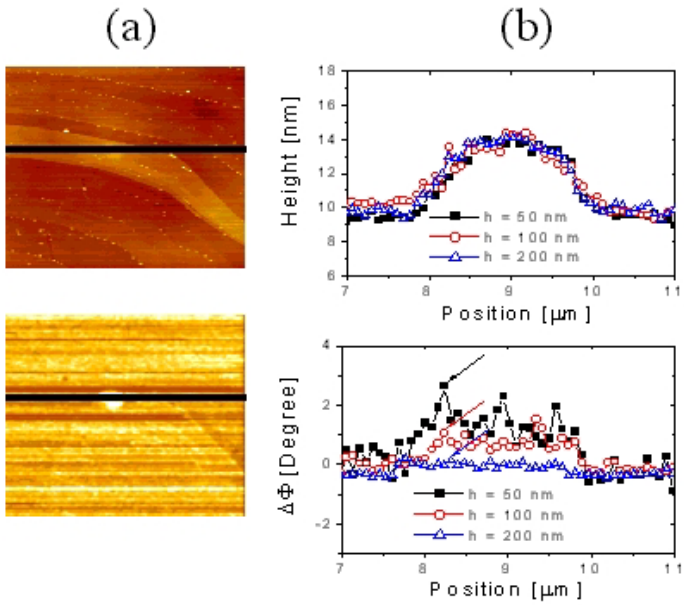

Fig. 1: (a) Topography (top) and MFM (bottom) images of a spot and its surroundings irradiated with a fluence of 0.2 nC/µm^2. The scan area was 20×20 µm^2. Horizontal black lines across the spot produce the line scans in (b) of topography (top) and MFM (bottom) images at different scan heights. The swelling height is $\sim$ 5 nm and is independent of the scan height. The magnetic image, however, shows a decrease of the phase shift from 3° to $\sim$ 0.2° after increasing the scan height from 50 nm to 200 nm.

The irradiated areas and surroundings were characterized simultaneously by atomic force (AFM) and magnetic force microscopy (MFM) at room temperature (see Fig. 1). The measured MFM phase shift is proportional to the magnetic force gradient and a measure for the ferro- or ferrimagnetic behaviour of the sample. For virgin graphite samples, even though the changes in topography are significant, one obtains in general a MFM signal with a phase shift of the order of $\pm 0.1°$, which corresponds to the noise of the microscope. The spot regions are clearly visible in the MFM signal and topography. The irradiation produces a clear swelling at the graphite surface with a height that increases with irradiation dose. It is important to note, however, that there is no clear correlation between the increase in swelling height measured by AFM and the maximum MFM phase shift change at the spot within the dose range used. Moreover, it was found that the magnetic phase shift changes sharply at the "borders" of the spot and that the magnetic force gradients measured within the area of the spots at low doses appear to be more homogeneous than that at higher doses. This behaviour rules out that topography-related spurious effects can be responsible for the MFM signals. The changes of the MFM images at the spot and in its surroundings after the application of a magnetic field also indicate that the observed magnetic contrast is not an artifact but is in favour of an intrinsic magnetic effect at the spots.

To measure the degree of disorder of the sample, Raman spectroscopy was performed. All unirradiated areas show only one pronounced peak at 1580 cm^{-1} (the E_{2g2} mode) as expected for graphite without disorder. All irradiated spots show additionally the disorder mode D at 1360 cm^{-1}.

The results demonstrate intrinsic room temperature ferromagnetism in metallic-ion-free graphite and can open the possibility of magnetically writing on carbon surfaces.

[1] Y. Kopelevich, P. Esquinazi, J. H. S. Torres and S. Moehlecke, J. Low Temp. Phys. **119**, 691 (2000).

[2] P. Esquinazi, A. Setzer, R. Höhne, C. Semmelhack, Y. Kopelevich, D. Spemann, T.

Butz, B. Kohlstrunk and M. Lösche, Phys. Rev. B **66**, 024429 (2002).
[3] T. Makarova, B. Sundqvist, R. Höhne, P. Esquinazi, Y. Kopelevich, P. Scharff, V. A. Davydov, L. S. Kashevarova and A. V Rakhmanina, Nature **413**, 716 (2001).
[4] K.-H. Han, D. Spemann, P. Esquinazi, R. Höhne, V. Riede and T. Butz, Adv. Mater. **15**, 1719 (2003).

Magnetic carbon: an explicit evidence for ferromagnetism induced by proton irradiation

P. Esquinazi[1], R. Höhne[1], K.-H. Han[1], A. Setzer[1], D. Spemann[2] and T. Butz[2]
[1] *Superconductivity and Magnetism*
[2] *Nuclear Solid State Physics*

In the next step of our studies [1] we wanted to create large irradiated areas and a large number of spots on proton irradiated HOPG to obtain enough ferromagnetic material to reach the sensitivity range of a commercial SQUID magnetometer and so to confirm the existence of magnetic domains by a completely other measuring method.
Samples of dimension $2 \times 2 \times 0.1$ mm^3 were used. Four irradiations were consecutively applied to sample 1 with total charges of 2.93 μC (No.1), 8 μC (No.2), 600 μC (No.3) and again 600 μC (No.4). Rutherford backscattering spectroscopy (RBS) and PIXE spectra were recorded simultaneously with the irradiation allowing us to check the purity of the sample at the different irradiation stages. The magnetic characterization before and after each step of irradiation was performed by SQUID measurements and MFM/AFM.
In the figure the magnetic moment measured at $T = 300$ K as a function of magnetic field is shown for sample 1 glued on a silicon substrate, after various proton irradiations. In (a) the total measured magnetic moment after irradiation No. 1 is shown, which is similar to that of the virgin sample within the scale of the figure. The main part ($\sim 90\%$) of the diamagnetic signal is due to the Si substrate. In the same figure we show the magnetic moment of the same sample after irradiation No. 3 where we can clearly recognize the *s*-shaped curve without any background subtraction. After subtraction of the magnetic moment of the substrate and graphite we obtain the results depicted in (b). A clear increase of the ferromagnetic loop in irradiation stages No. 2 and No. 3 and some decrease after irradiation No. 4 is observed.
The observed changes of the magnetic moment after the different irradiation stages are due to the irradiation and not to different misalignments of the sample position with respect to the applied field. To check this we measured sample 1 in the irradiation stages No. 3 and No. 4 for the other field direction (parallel to the c axis of graphite). After subtraction of the diamagnetic signal from graphite and Si substrate, the magnetic moment loops were similar as for the other field direction; this is an indication for a low anisotropy of the magnetism produced by the irradiation.
To check the reproducibility of our procedure as well as to rule out possible contamination during the handling of the sample, a new piece of the virgin HOPG sample was prepared in a similar way and fixed to a different Si substrate. Very good reproducibility was achieved in sample 2 for similar implanted charges. An increase of ferromagnetism was recently found in proton irradiated amorphous carbon films either [2].

Just after each irradiation the MFM and topography images were measured. The results confirm the SQUID measurements and the results found on proton irradiated microspots. The overall results indicate that room-temperature ferromagnetism in carbon-based structures containing only p- and s-electrons is a reality. The origin of the ferromagnetism in carbon is not yet well established. We speculate that the origin of the observed effect is that proton bombardment and implantation may promote the formation of sp^3 carbon creating a three-dimensional network of sp^2 and sp^3, mono- and dehydrogenated, carbon atoms. The role of hydrogen to produce magnetic moments and spontaneous magnetization in graphite has recently been treated theoretically in the literature [3].

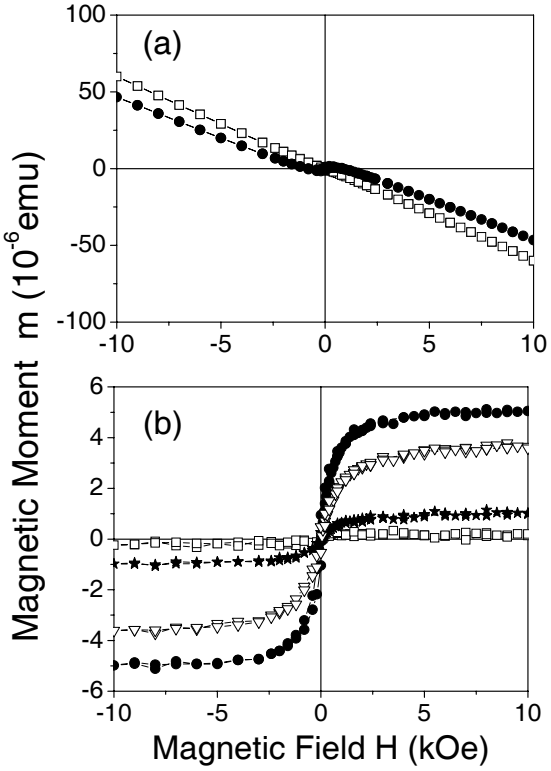

[1] P. Esquinazi, D. Spemann, R. Höhne, A. Setzer, K.-H. Han and T. Butz, Phys. Rev. Lett. **91**, 227201 (2003).
[2] R. Höhne, P. Esquinazi, K.-H. Han, D. Spemann, A. Setzer, U. Schaufuß, V. Riede, T. Butz P. Streubel and R. Hesse, Proceedings of the SMM16, 2003, to be published.
[3] K. Kusakabe and M. Maruyama, Phys. Rev. B **67**, 092406 (2003).

4.5.3 Creation and study of ferromagnetic states in fullerenes

Observation of intrinsic magnetic domains in C_{60} Polymer

K.-H. Han[1], D. Spemann[2], R. Höhne[1], A. Setzer[1], T. L. Makarova[3], P. Esquinazi[1] and T. Butz[2]
[1] *Superconductivity and Magnetism, Leipzig*
[2] *Nuclear Solid State Physics, Leipzig*
[3] *Department of Experimental Physics, Umea University, Sweden*

Our work was motivated by the recent discovery of ferromagnetic behaviour in two-dimensional polymerized highly-oriented rhombohedral C_{60} phase as well as in oriented graphite samples with Curie temperature of 500 K or above. Two questions were to be answered: do magnetic domains in a polymerized structure made solely by carbon exist and are they correlated to some structural defects or magnetically impure regions?
An undoped polymerized C_{60} sample has been characterized for the first time with respect to impurity content and ferromagnetic properties by laterally resolved PIXE, MFM and SQUID measurements [1]. The combination of these techniques unambiguously establishes the origin of the measured magnetic moment, the MFM image contrast and the

correlation with local topography, micro-magnetic structure and magnetic impurities.
For the sample studied, the average Fe concentration was (175 ± 16) μg/g, which, if all Fe behaves ferromagnetically (an unrealistic assumption), would give a saturation magnetic moment per unit mass which is three times less than the magnetization measured in our experiments by the SQUID. This excludes the possibility that the effect is due to ferromagnetic clusters formed by magnetic Fe.
From PIXE, we select two different regions for MFM measurement, a Fe-contaminated and a pure region. In the contaminated region, we found magnetic signals, which are correlated to the magnetic impurity grains. In pure regions (concentration of magnetic impurities < 1 μg/g), we found three different magnetic images. In region A, stripe domains are observed and the direction of domain magnetization appears to be oblique to the sample surface. In region B corrugated domain patterns are observed with the domain magnetization oriented approximately normal to the sample surface. In region C, however, we could not resolve any magnetic domains. The total size of the magnetic area (regions A and B) is $\sim 30\%$ of the pure sample area. In the figure the topographic (a) and magnetic force gradient (b) images taken from the pure region A are shown. Here the scan area was 10×10 μm and scan height 100 nm for the MFM image.
All of these results reveal that C_{60} polymer is a mixture of magnetic and non-magnetic parts and only part of the sample contributes to the ferromagnetism.

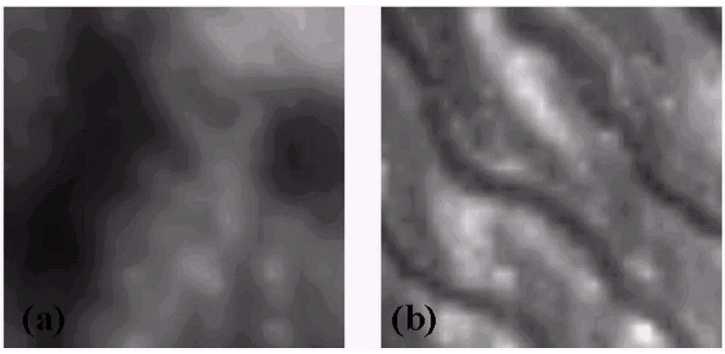

[1] K.-H. Han, D. Spemann, R. Höhne, A. Setzer, T. L. Makarova, P. Esquinazi and T. Butz, Carbon **41**, 785 (2003).

Magnetism in photo-polymerized fullerenes

T. L. Makarova[1], K.-H. Han[2], P. Esquinazi[2], R. R. da Silva[3], Y. Kopelevich[3], I. B. Zakharova[4] and B. Sundqvist[1]
[1] *Department of Experimental Physics, Umea University, Sweden*
[2] *Superconductivity and Magnetism, Leipzig*
[3] *Instituto de Física, Universidade Estadual de Campinas, Brazil*
[4] *Ioffe Physico-Technical Institute, St. Petersburg, Russia*

The aim of the study was to obtain a ferromagnetic phase in fullerenes which are polymerized by another method than by pressure.
Bulk C_{60} was polymerized by photoirradiation, whereas C_{60} films were exposed to laser- and electron-beams [1]. It was found that these treatments lead to the appearance of weak but measurable magnetic features. Nonlinear magnetization measured by SQUID

is observed only for samples irradiated in the presence of oxygen, while, in the case of pressure-polymerized C_{60}, oxygen adversely affects the magnetic properties. This could be explained by the assumption that under exposure to light, oxygen or hydrogen reacts with fullerene, producing localized spins. Magnetic force microscopy clearly shows that the laser irradiation process is followed by changes in magnetic images and topography. Laser and electron illumination enhances the roughness of the films, producing clusters. Magnetic images appear for all exposed areas. These magnetic images are highly correlated with the topographic images. The size of the topographic clusters depends on the laser and electron beam energy. The MFM images change with the direction of the magnetic field applied on the samples before MFM measurements indicating that they have a ferromagnetic origin. Using the same procedure for a non-exposed area no significant difference in the MFM signals was observed.

[1] T. Makarova, K.-H. Han, P. Esquinazi, R. R. da Silva, Y. Kopelevich, I. B. Zakharova and B. Sundqvist, Carbon **41**, 1575 (2003).

4.5.4 Transport- and magnetotransport properties of graphite: graphite as a highly correlated electron liquid

Y. Kopelevich[1], P. Esquinazi[2], J. H. S. Torres[1], R. da Silva[1] and H. Kempa[2]
[1] *Instituto de Física, Universidade Estadual de Campinas, Brazil*
[2] *Superconductivity and Magnetism, Leipzig*

Although a considerable amount of research work has been done on graphite, its physical properties are still not well understood.
The aim of our work was to study the influence of the magnetic field and its direction on the electronic conduction processes in different graphite samples and to demonstrate the two-dimensionality of the electron system in ideal graphite samples. The understanding of the transport properties in graphite is of primary interest and can provide a fundamental contribution to the physics of two-dimensional (2D) systems in general.
We have performed measurements of both basal-plane $R_b(H,T)$ and Hall $R_h(H,T)$ resistances, both as a function of temperature T and magnetic field H, on several well-characterized quasi-2D highly oriented pyrolitic graphite (HOPG) and, less anisotropic, flakes of single crystalline Kish graphite. Four HOPG samples and two Kish graphite single crystals have been studied. Low-frequency ($f = 1$ Hz) and dc standard four-probe magnetoresistance measurements were performed in the temperature interval 100 mK $\leq T \leq$ 300 K using different 9 T-magnet He-cryostats and a dilution refrigerator. The Hall resistance was measured using the van der Pauw configuration with a cyclic transposition of current and voltage leads at fixed applied field polarity, as well as magnetic field reversal; no difference in $R_h(H,T)$ obtained with these two methods was found. All resistance measurements were performed in the Ohmic regime and at various angles between applied magnetic field and the sample c-axis.
The basic results can be summarized as follows. The recently reported [1] metal-insulator transition (MIT) driven by a magnetic field applied perpendicular to the basal planes of graphite appears both in the in-plane and out-of-plane resistivity. It could be shown

that the MIT in HOPG is triggered only by magnetic fields perpendicular to the graphite layers. A clear experimental evidence was given that the MIT is absent in highly oriented graphite samples for fields applied parallel to the graphite samples [2]. Therefore, it is unlikely that spin effects play a significant role in the MIT. The transport perpendicular to the graphite layers in highly oriented and less disordered samples appears to be incoherent, demonstrating the quasi-2D character of the electron system of graphite, see Fig. 1. Sample defects lead to a better coupling between the layers, a 3D-like behaviour and coherent interlayer transport. The experimental results suggest that the low field ($\sim$ 1 kOe) metal-insulator transition is associated with the transition between Bose metal and excitonic insulator states. On the other hand, the reentrant insulator-metal transition which takes place at higher fields can consistently be understood assuming the occurrence of superconducting correlations caused by the Landau level quantization. We argue that the quantum Hall effect, observed only for strongly anisotropic quasi-2D graphite samples, and superconducting correlations may represent the same phenomenon, implying that Cooper pairs in the quasi-2D samples form a highly correlated boson liquid [3].

[1] H. Kempa, Y. Kopelevich, F. Mrowka, A. Setzer, J. H. S. Torres, R. Höhne and P. Esquinazi, Solid State Commun. **115**, 539 (2000)
[2] H. Kempa, H.-C. Semmelhack, Y. Kopelevich and P. Esquinazi, Solid State Commun. **125**, 1 (2003)
[3] Y. Kopelevich, P. Esquinazi, J. H. S. Torres, R. da Silva and H. Kempa, Adv. Solid State Phys. **43**, 207 (2003)
[4] Y. Kopelevich, J. H. S. Torres, R. R. da Silva, F. Mrowka, H. Kempa and P. Esquinazi, Phys. Rev. Lett. **90**, 156402 (2003)

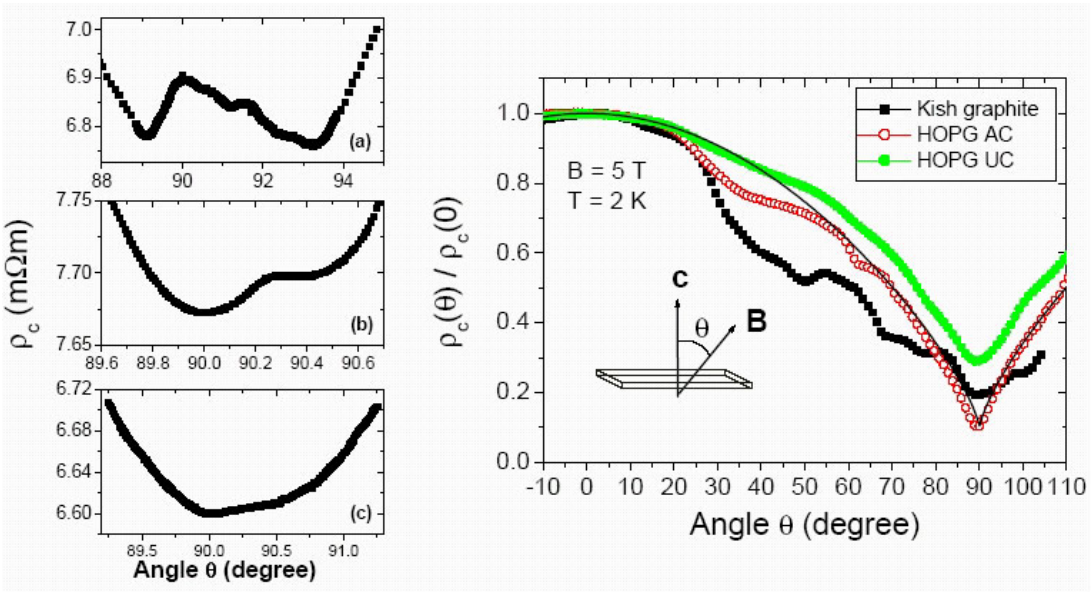

Fig. 1: (Left) Angle dependence around 90° of the c-axis resistivity of: (a) a Kish graphite sample with FWHM = 1.6°, (b) a HOPG sample with FWHM = 0.40°, and (c) a HOPG sample with FWHM = 0.24° measured at B = 9 T and at 2 K. Θ = 90° means that the field is applied parallel to the graphene planes. (Right) Angle dependence of the normalized c-axis resistance in a field of 5 T and a temperature of 2 K for the same samples as in the left figure [3].

4.5.5 Influence of thickness on microstructural and magnetic properties in magnetite thin films produced by PLD

A. Bollero, M. Ziese, R. Höhne, H.-C. Semmelhack, U. Köhler, A. Setzer and P. Esquinazi

The pulsed laser deposition technique (PLD) is an effective method to produce high-quality magnetite (Fe_3O_4) films [1]. MgO is commonly used as a substrate because of the small lattice mismatch between them of 0.3%, which allows pseudomorphic growth. The lattice constant of MgO (a=4.212 Å) is about half that of Fe_3O_4 (a=8.3987 Å) resulting in the appearance of stacking defects in the cation sublattices during growth as a consequence of the existing shift between neighbouring Fe_3O_4 islands [2]. These stacking defects are known as anti-phase domain boundaries (APBs) and have important consequences on the magnetic properties, resistivity and magneto-transport properties. $MgAl_2O_4$ has a lattice constant (a=8.080 Å) very close to that of Fe_3O_4 and the misfit between both is of about 4%; both of them exhibit spinel-type structure but APBs have been observed [3]. This could be explained on the basis that the cation interaction across the interface does not play any role for epitaxy in this case, with the continuation of the oxygen sublattice being the only restriction [4]. A systematic study of the evolution of the remanence and the coercivity, in dependence on the measuring temperature, for two films of 26 and 320 nm grown on $MgAl_2O_4$ (100) substrates [5], has shown remarkable differences which are explained in terms of: (i) decreased effect of the interfacial strain with increasing the thickness (relaxation of the film); and (ii) enlarged grains with increasing the thickness, i.e. the deposition time, and lower density of APBs which act as pinning centers for magnetic domain walls in the case of the thicker film.

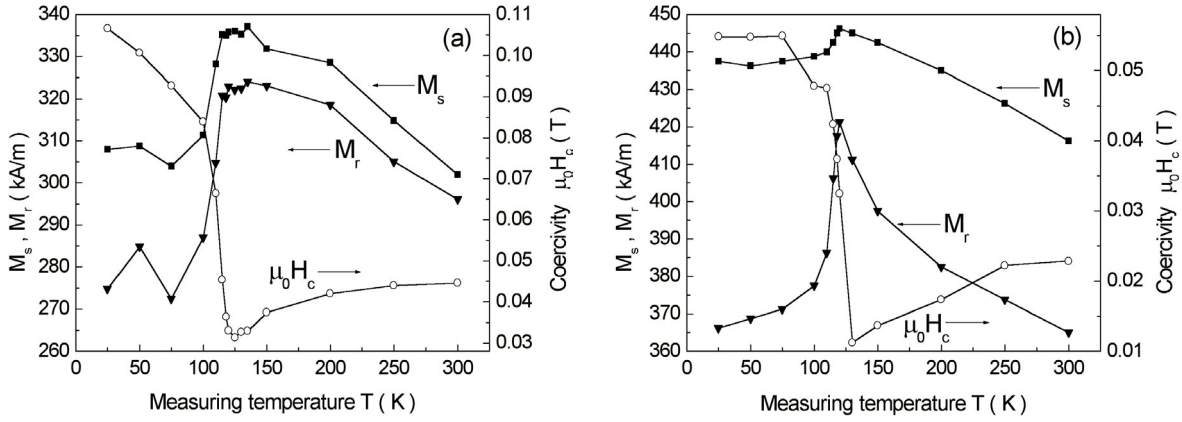

Fig. 1: Dependence of the magnetic properties on temperature for (a) 26 nm and (b) 320 nm thick Fe_3O_4 films grown on $MgAl_2O_4$ (100) substrates.

[1] C.A. Kleint, H.C. Semmelhack, M. Lorentz and M.K. Krause, J. Magn. Magn. Mater. 140, 725 (1995).
[2] D.T. Margulies, F.T. Parker, M.L. Rudee, F.E. Spada, J.N. Chapman, P.R. Aitchison and A.E. Berkowitz, Phys. Rev. Lett. 79, 5162 (1997).
[3] C.A. Kleint, M.K. Krause, R. Höhne, M. Lorentz, H.C. Semmelhack, A. Schneider, D.

Hesse, H. Sieber, J. Taubert and W. Andrä, J. Phys IV France 7, C1-593 (1997).
[4] W. Eerenstein, L. Kalev, L. Niesen, T.T.M. Palstra and T. Hibma, J. Magn. Magn. Mater. 258, 73 (2003).
[5] A. Bollero, M. Ziese, R. Höhne, C. Semmelhack, U. Köhler, A. Setzer and P. Esquinazi, to be submitted.

4.5.6 Spin injection at the Ni/GaAs interface

M. Ziese[1], H. von Wenckstern[2], R. Pickenhain[2], S. Weinhold[2], G. Biehne[2], V. Gottschalch[3], M. Grundmann[2] and P. Esquinazi[1]
[1] *Superconductivity and Magnetism*
[2] *Semiconductor Physics*
[3] *Institute for Anorganic Chemistry, University of Leipzig*

In the development of spin-electronic devices a high efficiency for spin-injection is of paramount importance. Here Schottky barriers might play a role, since these lead to an enhanced injection efficiency in comparison to ohmic metal-semiconductor contacts. It was predicted that the spin-polarization P of a metallic ferromagnet in a ferromagnet-semiconductor junction can be extracted from the analysis of the magnetic field induced variations in the Schottky barrier I-V characteristics [1]:

$$I = I_0 \exp\left(\frac{P\mu_B B}{k_B T}\right)\left[\exp\left(\frac{eV}{k_B T}\right) - 1\right].$$

Here B denotes the magnetic field, μ_B the Bohr magneton, I the current and V the applied voltage.
High quality Au/GaAs and Ni/GaAs Schottky barriers were prepared by the Semiconductor Physics Group and measurements of the Schottky characteristics in the temperature range 5 K – 300 K in magnetic field up to 9 T were performed in the Division of Superconductivity and Magnetism. The GaAs has a doping density of 4×10^{16} cm^{-3}. Small magnetic field dependent shifts of the Schottky barrier were observed for both junction types. The predicted magnetic field dependence could not be confirmed. Further work to understand the magnetic field induced features is in progress.

[1] J. Gregg in "Spin-Electronics", edited by M. Ziese and M. J. Thornton, Springer Verlag, Heidelberg, 2001, p. 24.

4.5.7 Magnetotransport properties of magnetite/Nb:$SrTiO_3$ interfaces

U. Köhler, M. Ziese, A. Bollero, R. Höhne, H.-C. Semmelhack and P. Esquinazi

For the development of the field of spin-electronics magnetic oxides might play a central role, since some ferromagnetic and ferrimagnetic oxides have spin-polarizations at the Fermi level approaching 100%. Magnetite (Fe_3O_4) is a ferrimagnet with a high Curie temperature of 860 K and, according to band-structure calculations, a spin-polarization of -100% [1]. In heterostructures the electronic properties at interfaces are of major importance and in this work we have studied the magnetotransport properties of magnetite/Nb:$SrTiO_3$ interfaces. $SrTiO_3$ was chosen, since it has a cubic crystal structure with not too large a lattice mismatch to Fe_3O_4 and since its electronic properties can be tuned from insulating to metallic by Nb-doping.
Magnetite films were deposited by pulsed laser deposition on Nb(0.1%):$SrTiO_3$ (001) substrates. Current-voltage characteristics and magnetoresistance were measured in a four-point configuration with the current perpendicular to the interface in the temperature range 60 K-300 K in magnetic fields up to 8 T. Current-voltage characteristics are shown in the figure below. On cooling through the Verwey transition the curves clearly change from being nearly linear to a strong asymmetric nonlinearity, which is reminiscent of a Schottky barrier. These characteristics have been analyzed within a model of thermionic emission and below the Verwey temperature ideality factors approaching unity and a barrier height of about 0.15 eV have been obtained. The magnetoresistance depends in a nonlinear fashion on the bias current. This proves that the magnetoresistance is dominated by the interface. The analysis using the model of the previous section leads to an estimate of the spin-polarization of about -66% at 100 K [2]. In view of the predicted half-metallic band structure this is a reasonable value.

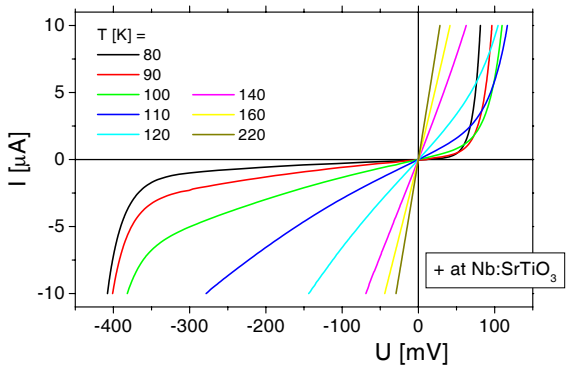

Fig. 1: Current-voltage characteristics of a Fe_3O_4/Nb:$SrTiO_3$ interface.

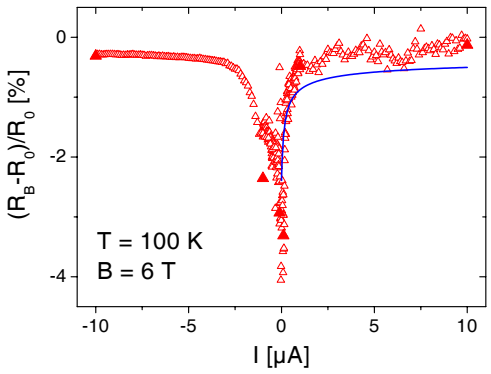

Fig. 2: Magnetoresistance of a Fe_3O_4/Nb:$SrTiO_3$ interface at 100 K.

[1] A. Yanase and N. Hamada, J. Phys. Soc. Japan **68**, 1607 (1999).
[2] U. Köhler, M. Ziese, A. Bollero, R. Höhne and P. Esquinazi, Proceedings of ICM'2003, in press.

4.5.8 Step-edge magnetoresistance in magnetite films

M. Ziese, R. Höhne, H.-C. Semmelhack, K.-H. Han, K. Zimmer and P. Esquinazi

In recent years the extrinsic magnetotransport properties of magnetic oxides have been intensely studied [1]. These effects arise from a variety of sources, especially from spin-polarized tunneling in heterostructures or at naturally grown oxide barriers. Since the extrinsic magnetoresistance is often much larger than the intrinsic one, especially in the low field regime, it was hoped to exploit these effects for potential applications.

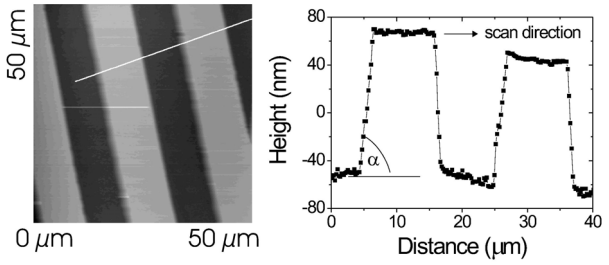

Fig. 1: AFM image and cross section of a magnetite film with step edges.

Up to now there has been promising progress in the investigation of extrinsic magnetoresistance in manganites (e.g. $La_{0.7}Sr_{0.3}MnO_3$) and CrO_2. The room temperature magnetoresistance in these compounds, however, is limited due to the comparatively low Curie temperatures.

In this work we have studied grain boundaries artificially introduced into magnetite films by growth on substrates with step-edges. Fe_3O_4 has a rather high Curie temperature of 860 K. The step-edges indeed lead to an increase of the magnetoresistance. This effect, however, occurs mainly at high magnetic fields and cannot be attributed to spin-polarized tunneling. Extensive modelling lead to the conclusion that the relevant source for the enhanced magnetoresistance is spin-dependent scattering at spin disorder near the step edges [2].

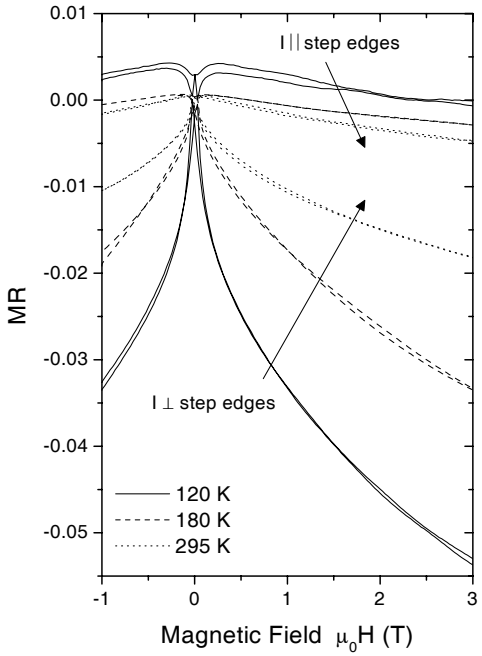

Fig. 2: Magnetoresistance of a magnetite step-edge array measured with the current flowing across and parallel to the step edges, respectively.

[1] M. Ziese, Rep. Prog. Phys. **65**, 143-249 (2002).
[2] M. Ziese, R. Höhne, H.-C. Semmelhack, K. H. Han, P. Esquinazi and K. Zimmer, to be published in J. Magn. Magn. Mater.

4.5.9 Scaling of the extraordinary Hall effect in manganite films

M. Ziese

The Hall effect in ferromagnetic systems with a strong Hund's rule coupling has attracted considerable interest in recent years. In contrast to itinerant ferromagnets, where the extraordinary Hall effect can be understood within the classical "skew-scattering" and "side-jump" models, there have been conjectures that in systems such as the manganites a new mechanism might be active [1,2]. This arises from a quantal phase which an electron acquires during movement through non-trivial spin-textures in analogy to the Hall effect in hopping systems that is due to the Aharonov-Bohm effect in a triad of sites. In [2] it was predicted that the Hall resistivity of the manganites obeys the following scaling relation as a function of the reduced magnetization $m = M_S/M_S(0)$:

$$\rho_{xy} = -\rho^0_{xy}\, m\, [(1-m^2)^2/(1+m^2)^2]\,.$$

The Hall effect, magnetization and magnetoresistance of epitaxial $La_{0.7}Ca_{0.3}MnO_3$ and $La_{0.7}Ba_{0.3}MnO_3$ films were measured in the temperature range from 10 K to 350 K in magnetic fields up to 1 T. The films were fabricated by pulsed laser deposition on $LaAlO_3$ (001) substrates. The scaling of the Hall effect was probed by plotting the Hall resistivity versus the magnetization using the magnetic induction as parameter. It is clearly evident from the figure that scaling is absent in these films. However, the scaling relation proposed is an envelope to the data. This can be understood within the classical "side-jump" model for a double exchange system and the scaling relation above can be deduced [3] from the classical model of Searle and Wang [4].

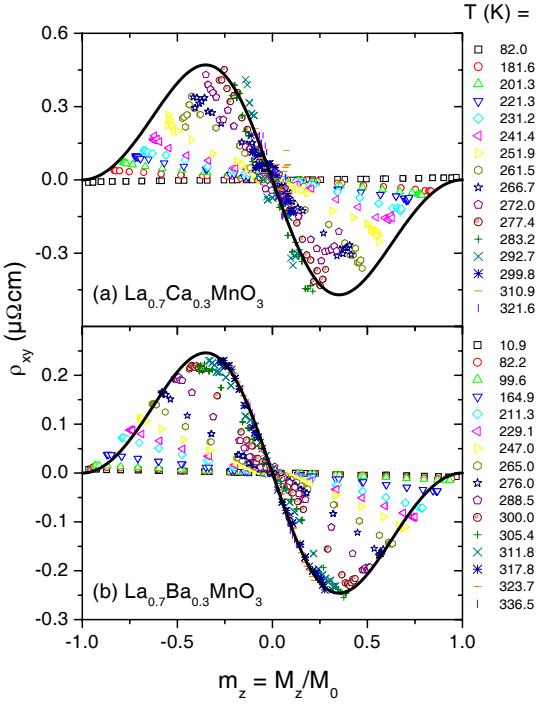

[1] J. Ye, Y. B. Kim, A. J. Millis, B. I. Shraiman, P. Majumdar and Z. Tešanović, Phys. Rev. Lett. **83**, 3737 (1999).
[2] Y. Lyanda-Geller, S. H. Chun, M. B. Salamon, P. M. Goldbart, P. D. Han, Y. Tomioka, A. Asamitsu and Y. Tokura, Phys. Rev. B **63**, 184426 (2001).
[3] M. Ziese, phys. stat. sol. (b) 241, R19 (2004).
[4] C. W. Searle and S. T. Wang, Can. J. Phys. **48**, 2023 (1970).

4.5.10 Funding

Interplay between Superconductivity and Magnetism in Graphite and Disordered Metals
Prof. P. Esquinazi
DFG Es 86/6-3

Magnetotransport in Oxide Thin Film Systems
Prof. P. Esquinazi
DFG Es 86/7-3
within Forschergruppe FOR 404
Oxidic interfaces

4.5.11 Organizational Duties

P. Esquinazi
Project Reviewer: Deutsche Forschungsgemeinschaft (DFG), National Science Foundation (USA), German-Israeli Foundation
Referee: Phys. Rev. Lett, Phys. Rev. B., Physica C, Phys. Lett. A, phys. stat. sol., J. Low Temp. Phys., Carbon

R. Höhne
Referee: phys. stat. sol., Thin Solid Films

M. Ziese
Referee: Phys. Rev. Lett., Phys. Rev. B., J. Phys. D: Appl. Phys., phys. stat. sol., J. Magn. Magn. Mater., Eur. J. Phys. B, Thin Solid Films

4.5.12 External Cooperations

Academic

State University of Campinas, Campinas, Brazil
Prof. Dr. Yakov Kopelevich

Weizmann Institute of Sciences, Israel
Prof. Dr. Eli Zeldov

Umea University, Sweden
Dr. Tatiana Makarova

Universidad Autónoma de Madrid, Spain
Prof. Dr. Miguel Angel Ramos

Universidad Autónoma de Madrid, Spain
Prof. Dr. Sebastian Vieira

Institute for Metal Physics of National Academy of Sciences of Ukraine, Kiev, Ukraine
Prof. Dr. V. M. Pan

Institut für Oberflächenmodifizierung e. V., Leipzig
Dr. Klaus Zimmer

Universität Leipzig, Fakultät für Chemie und Mineralogie
Prof. R. Szargan

University of the Negev, Beer Sheva, Israel
Dr. Evgeny Rozenberg

Trinity College Dublin
Prof. Dr. J. M. D. Coey

University of York, United Kingdom
Dr. Sarah Thompson

IFW-Dresden, Germany
Dr. Kathrin Dörr

4.5.13 Publications

Journals

P. Esquinazi, D. Spemann, R. Höhne, A. Setzer, K. H. Han and T. Butz
Induced Magnetic Ordering by Proton Irradiation in Graphite
Phys. Rev. Lett. **91**, 227201 (2003).

K. H. Han, D. Spemann, P. Esquinazi, R. Höhne, V. Riede, and T. Butz
Ferromagnetic Spots in Graphite Produced by Proton Irradiation
Adv. Mater. **15**, 1719 (2003).

R. Ocaña, P. Esquinazi, H. Kempa, J. H. S. Torres and Y. Kopelevich
Magnetothermal conductivity of highly oriented pyrolytic graphite in the quantum limit
Phys. Rev. B **68** 165408 (2003).

T. L. Makarova, K. H. Han, P. Esquinazi, R. R. da Silva, Y. Kopelevich, I. B. Zakharova and B. Sundqvist
Magnetism in photopolymerized fullerenes
Carbon **41** 1575 (2003).

K. H. Han, D. Spemann, R. Höhne, A. Setzer, T. Makarova, P. Esquinazi and T. Butz
Observation of intrinsic magnetic domains in C_{60} polymer
Carbon **41**, 785 (2003).

K. H. Han, D. Spemann, R. Höhne, A. Setzer, T. Makarova, P. Esquinazi and T. Butz
Addendum to: Observation of intrinsic magnetic domains in C_{60} polymer [Carbon **41**, 785 (2003)]
Carbon **41**, 2425 (2003).

D. Spemann, K. H. Han, R. Höhne, T. Makarova, P. Esquinazi and T. Butz
Evidence for intrinsic weak ferromagnetism in a C_{60} polymer by PIXE and MFM
Nuclear Instruments and Methods in Physics Research B **210**, 531 (2003).

Y. Kopelevich, P. Esquinazi, J. H. S. Torres, R. R. da Silva, H. Kempa, F. Mrowka and R. Ocaña
Metal-Insulator-Metal Transitions, Superconductivity and Magnetism in Graphite
Studies of High Temperature Superconductors **45**, 59 (2003).

Y. Kopelevich, J. H. S. Torres, R. R. da Silva, F. Mrowka, H. Kempa and P. Esquinazi
Reentrant Metallic Behavior of Graphite in the Quantum Limit
Phys. Rev. Lett. **90**, 156402 (2003).

H. Kempa, H.-C. Semmelhack, P. Esquinazi and Y. Kopelevich
Absence of metal-insulator transition and coherent interlayer transport in oriented graphite in parallel magnetic fields
Solid State Commun. **125**, 1 (2003).

F. Mrowka, S. Manzoor, P. Pongpiyapaiboon, I. L. Maksimov, P. Esquinazi, K. Zimmer and M. Lorenz
Excess voltage in the vicinity of the superconducting transition in inhomogeneous $YBa_2Cu_3O_7$ thin films
Physica C **399**, 22 (2003).

R. Schmidt, B. Rheinländer, M. Schubert, D. Spemann, T. Butz, J. Lenzner, E. M. Kaidashev, M. Lorenz, A. Rahm, H.-C. Semmelhack and M. Grundmann
Dielectric functions (1 to 5 eV) of wurtzite $Mg_xZn_{1-x}O$ ($x \leq 0.29$) thin films
Appl. Phys. Lett. **82**, 2260 (2003).

E. M. Kaidashev, M. Lorenz, H. von Wenckstern, A. Rahm, H.-C. Semmelhack, K.-H. Han, G. Benndorf, C. Bundesmann, H. Hochmuth and M. Grundmann
High electron mobility of epitaxial ZnO thin films on c-plane sapphire grown by multistep pulsed-laser deposition
Appl. Phys. Lett. **82**, 3901 (2003).

E. Erdem, R. Böttcher, H.-C. Semmelhack, H. J. Glasel, E. Hartmann and D. Hirsch
Preparation of lead titanate ultrafine powders from combined polymerisation and pyrolysis route
J. Mater. Science **38**, 3211 (2003).

E. Erdem, R. Böttcher, H.-C. Semmelhack, H. J. Glasel and E. Hartmann E

Multi-frequency EPR study of Cr^{3+} doped lead titanate ($PbTiO_3$) nanopowders
phys. stat. sol. (b), **239**, R7 (2003).

M. Lorenz, E. M. Kaidashev, H. von Wenckstern, V. Riede, C. Bundesmann, D. Spemann, G. Benndorf, H. Hochmuth, A. Rahm, H.-C. Semmelhack and M. Grundmann
Optical and electrical properties of epitaxial $(Mg,Cd)_xZn_{1-x}O$, ZnO, and ZnO:(Ga,Al) thin films on c-plane sapphire grown by pulsed laser deposition
Solid-State Electronics **47**, 2205 (2003).

M. Ziese
Searching for quantum interference effects in $La_{0.7}Ca_{0.3}MnO_3$ films on $SrTiO_3$
Phys. Rev. B **68**, 132411 (2003).

M. Ziese, H.-C. Semmelhack and K. H. Han
Strain-induced orbital ordering in thin $La_{0.7}Ca_{0.3}MnO_3$ films on $SrTiO_3$
Phys. Rev. B **68**, 134444 (2003).

in press

D. A. Luzhbin, A. V. Pan, V. A. Komashko, V. S. Flis, V. M. Pan, S. X. Dou and P. Esquinazi
Origin of paramagnetic magnetization in field-cooled $YBa_2Cu3O_{7-\delta}$ films
Phys. Rev. B **69**, 024506 (2004).

M. Ziese
Two-parameter scaling of the Hall effect in manganites
phys. stat. sol. (b) 241, R19 (2004).

M. Ziese, R. Höhne, H.-C. Semmelhack, P. Esquinazi and K. Zimmer
Magnetic and magnetotransport properties of magnetite films with step edges
J. Magn. Magn. Mater., in press.

A. I. Shames, E. Rozenberg, G. Gorodetsky and M. Ziese
EMR study of thin $La_{0.7}Ca_{0.3}MnO_3$ films epitaxially grown on $SrTiO_3$
Proceedings of the Workshop on Nanomagnetism, Istanbul 2003, in press.

S. A. Krasnikov, A. S. Vinogradov, K.-H. Hallmeier, R. Höhne, M. Ziese, P. Esquinazi, T Chassé and R. Szargan
Oxidation effects in epitaxial Fe_3O_4 layers on MgO and $MgAl_2O_4$ substrates studied by X-ray absorption, fluorescence and photoemission
Proceedings EMRS'2003, in press.

U. Köhler, M. Ziese, A. Bollero, R. Höhne and P. Esquinazi
On the road to an all-oxide spin-transistor: study of magnetotransport properties of magnetite/Nb:STO interfaces
Proceedings of ICM'2003, in press.

P. Esquinazi, M. Ramos and R. König
Acoustic properties of amorphous solids at very low temperatures: The quest for interacting tunneling systems
J. Low Temp. Phys. **135**, 27 (2004).

Conference Contributions

(T: talk, inv. T: invited talk, P: poster)

Magnetic Carbon (inv. T)
P. Esquinazi
Frontiers in Nanomagnetism, 294. WE-Heraeus-Seminar, 6.-8. 01. 2003, Bad Honnef (Germany)

Some random results of our research on magnetite and the manganites (inv. T)
M. Ziese
Physics Department, Trinity College Dublin, 11.02.2003.

Untersuchung der Wechselfeldsuszeptibilität von $La_{0.7}Ca_{0.3}MnO_3$ und $La_{0.7}Sr_{0.3}MnO_3$ Schichten (P)
M. Ziese
Frühjahrstagung des Arbeitskreises Festkörperphysik, Dresden 2003

Untersuchung der Magnetotransporteigenschaften von Magnetit-Nb:$SrTiO_3$-Grenzflächen (P)
U. Köhler, M. Ziese, R. Höhne and P. Esquinazi
Frühjahrstagung des Arbeitskreises Festkörperphysik, Dresden 2003

Detailed studies of the magnetoresistance at the metal-insulator transition of graphite (P)
H. Kempa and P. Esquinazi
Frühjahrstagung des Arbeitskreises Festkörperphysik, Dresden 2003

A field-effect transistor from graphite - no effect of low gate fields (P)
P. Esquinazi and H. Kempa
Frühjahrstagung des Arbeitskreises Festkörperphysik, Dresden 2003

Magnetic carbon: magnetic images in photopolymerized fullerenes (P)
K.-H. Han, P. Esquinazi, T. Makarova, B. Sundqvist, Y. Kopelevich and I. Zakharova
Frühjahrstagung des Arbeitskreises Festkörperphysik, Dresden 2003

Magnetic carbon: ferromagnetism in graphite-sulfur composites (P)
U. Schaufuß, R. R. da Silva, A. Setzer, R. Höhne, P. Esquinazi and Y. Kopelevich
Frühjahrstagung des Arbeitskreises Festkörperphysik, Dresden 2003

Magnetic carbon: observation of intrinsic magnetic domains in C_{60} polymer (P)
K.-H. Han, D. Spemann, R. Höhne, A. Setzer, T. Makarova, P. Esquinazi and T. Butz

Frühjahrstagung des Arbeitskreises Festkörperphysik, Dresden 2003

Reentrant metallic behaviour of graphite in the quantum limit (P)
Y. Kopelevich, J. H. S. Torres, R. R. da Silva, F. Mrowka, H. Kempa and P. Esquinazi
Frühjahrstagung des Arbeitskreises Festkörperphysik, Dresden 2003

Vanishing of the nodal properties with temperature in the longitudinal thermal conductivity of $YBa_2Cu_3O_7$ (P)
R. Ocaña and P. Esquinazi
Frühjahrstagung des Arbeitskreises Festkörperphysik, Dresden 2003

Quasiparticles in the mixed state of Y123 crystals: What do we learn from thermal magnetoconductivity tensor results ? (inv. T)
P. Esquinazi
7^{th} International Conference on Materials and mechanisms of Superconductivity and High Temperature Superconductors, Rio de Janeiro, 25.-30. May 2003.

Magnetotransport-Eigenschaften halbmetallischer Oxide (inv. T)
M. Ziese
Kolloquium der Fakultät für Physik und Geowissenschaften, 3. June 2003.

Magnetic Carbon: Experimental evidence vs. scientific scepticism (inv. T)
P. Esquinazi
selected as "Hot Topic" at the International Conference of Carbon, "Carbon2003", Oviedo (Spain), 6.-10. 07. 2003

Magnetotransport-Eigenschaften halbmetallischer Oxide (inv. T)
M. Ziese
Workshop on Condensed Matter Systems, University of Braunschweig, July 2003.

On the road to an all-oxide spin-transistor: study of magnetotransport properties of magnetite/Nb:STO interfaces (P)
U. Köhler, M. Ziese, R. Höhne and P. Esquinazi
International Conference on Magnetism, Rome, 2003

Study of the ac-susceptibility of manganite films (P)
M. Ziese
International Conference on Magnetism, Rome, 2003

Magnetism of pure, disordered carbon films prepared by pulsed laser deposition (P)
R. Höhne, K.-H. Han, P. Esquinazi, A. Setzer, H.-C. Semmelhack, D. Spemann and T. Butz
International Conference on Magnetism, Rome, 2003

Photoinduced magnetic changes in C_{60} films (P)
I. B. Zakharova, T. L. Makarova, K.-H. Han and P. Esquinazi
International Conference on Magnetism, Rome, 2003

Magnetic signals of proton irradiated spots created on highly oriented pyrolytic graphite surface (P)
K.-H. Han, D. Spemann, P. Esquinazi, R. Höhne, V. Riede and T. Butz
International Conference on Magnetism, Rome, 2003

Ferromagnetic spots in graphite produced by proton irradiation (P)
R. Höhne, P. Esquinazi, K.-H. Han, D. Spemann, A. Setzer, V. Riede and T. Butz
Conference Soft Magnetic Materials 16, Düsseldorf, Sept.2003

Magnetic Carbon: Experimental evidence vs. scientific scepticism (inv. T)
P. Esquinazi
National Conference of the Argentine Association of Physics (AFA), Bariloche, 22.-25. 09. 2003

Acoustic Properties of Amorphous Solids at Very Low Temperatures: The quest for Interacting Tunneling Systems (inv. T)
P. Esquinazi
International Workshop in honour of Francisco de la Cruz, Bariloche, 25. 09. 2003

Magnetic Carbon (inv. T)
P. Equinazi
International Symposium on Structure and Dynamics of Heterogeneous Systems, SDHS'03, Duisburg, 20.-21. 11. 2003

Magnetic Carbon: Experimental evidence vs. scientific scepticism (inv. T)
P. Esquinazi
Rossendorf (Dresden), December 2003

4.5.14 Graduations

PhD

Dipl.-Phys. Falk Mrowka
Globale und nichtlokale Untersuchungen an Hochtemperatursupraleitern mit Hilfe der Wechselfeldsuszeptibilitäts-, Transport- und Vibrating-Reed-Technik

Diploma

Ulrike Köhler
Untersuchung der Magnetotransporteigenschaften von Magnetit-Nb:$SrTiO_3$-Grenzflächen

4.5.15 Guests

Prof. Dr. Jorge Ossandón
Depto. de Ciencias de la Ingeniería, Universidad de Talca, Chile
18.08.2002 – 15.02.2003

Prof. Dr. Miguel Angel Ramos
Universidad Autónoma de Madrid, Spain
21.04.2003 – 20.07.2003

5

Institute for Theoretical Physics

5.1 Introduction

The aim of the research at the Institute for Theoretical Physics (ITP) is to explore the theoretical and mathematical fundamentals of physics. The key areas of research are the theory of elementary particles and the theory of condensed matter, which fruitfully complement each other. Fundamental problems of the structure of space, time and matter (from the smallest conceivable unit of length up to cosmic dimensions) are examined and practical problems of complex physical systems with mesoscopic dimensions are tackled.

The institute consists of the following research groups:

- **Quantum Field Theory (QFT)** – fundamental problems of mathematical physics, general structure of gauge theories, primary and effective interactions of elementary particles.
- **Particle Physics Group (TET)** – quantum field theory of elementary particles, supersymmetrical theories, quantum chromodynamics, lattice gauge theory.
- **Theory of Condensed Matter (TKM)** – noise-induced phenomena, structure formation in liquid crystals, non-linear dynamics in biological models, immune system, strongly coupled electron systems.
- **Computer-Oriented Quantum Field Theory (CQT)** – computer simulations of phase transitions and critical phenomena, physics of soft matter and disordered systems, quantum magnets.
- **Molecule Dynamics/Computer Simulation (MDC)** – computer simulations of molecules at interfaces, computations of structural data, studies of thermodynamic parameters and transport coefficients.
- **Statistical Physics (STP)** – interacting many-particle systems, statistical and quantum-field theoretical methods.

In the respective subsections, for each group a short overview of the research profile is followed by extended abstracts describing their most relevant current projects. Added is a subsection devoted to the Graduate Studies Programme 'Quantum Field Theory', which plays an important integrating role not only within the ITP, but also for the scientific

interaction with the Department of Mathematics and Computer Sciences and the Max-Planck Institute for Mathematics in the Sciences (MIS). In addition the research groups of the ITP take part in many of the interdisciplinary research projects of the Centre for Theoretical Sciences (NTZ) which is part of the Centre of Advanced Studies (ZHS) of the University of Leipzig. The publications of members of the ITP of the year 2003 and organizational activities of ITP members are also listed at the level of each group .

K. Sibold

March 2003

5.2 Quantum Field Theory

5.2.1 Quantum Field Theory under the Influence of External Conditions

M. Bordag, D.V. Vassilevich, I. Drosdow

The vacuum of quantum fields shows a response to changes in external conditions with measurable consequences. The investigation of vacuum corrections to string like configurations had been investigated in two examples. In [1] the fluctuations of the gluon field have been calculated for a color magnetic flux tube as a contribution to the investigation of a candidate for a stable vacuum state. It had been shown, however, that in the considered configuration tachyonic modes are present so that the color string will be unstable. In [2] the vacuum energy of a spinor field in the background of a Abrikosov-string in the Abelian-Higgs model was calculated. The developed earlier technique had been generalized to handle numerically given backgrounds too. In [3] qunatum corrections to the mass of the supersymmetric Abrikosov-Nielsen-Olesen vortec was studied. Contrary to earlier calculations a non-zero value of the mass shift was obtained. This value was later confirmed in [4]. The paper [5] studies chiral anomaly for local (bag) boundary conditions.

Recent and earlier advances of the heat kernel technique with applications to quantum field theory are summarised in the review paper [6].

[1] M. Bordag, Phys. Rev. D 67, 065001 (2003).
[2] M. Bordag and I. Drozdov, Phys. Rev. D 68, 065026 (2003).
[3] D.V. Vassilevich, Phys. Rev. D 68, 045005 (2003). [arXiv:hep-th/0304267].
[4] A. Rebhan, P. van Nieuwenhuizen and R. Wimmer, Nucl. Phys. B 679, 382 (2004); hep-th/0307282.
[5] V. N. Marachevsky and D. V. Vassilevich, Nucl. Phys. B 677, 535 (2004); hep-th/0309019.
[6] D. V. Vassilevich, Phys. Rept. **388**, 279 (2003); hep-th/0306138.

5.2.2 Gravity in two dimensions

D.V. Vassilevich

Two-dimensional gravity is a good testing ground for various ideas of classical and quantum general relativity and of the black hole physics. In [1] we have tested whether one can formulate a meaningful local gravity theory starting from the so-called double-scale special relativity and from the kappa-deformed Poincare symmtery. In two dimensions the answer is negative: the resulting theory is either indistinguishable from standard theories or is not diffeomorphism invariant. The papers [2] and [3] studied applications of two-dimensional gravity to strings. In [2] the Green functions corresponding to the virtual black hole exchange [4] were constructed. Due to the conformal symmetry of string gravity they exhibit a very simple structure. In [3] radiative correction to the specific heat of the string black hole are calculated. It appeares that quantum corrected specific heat is positive, which may provide an explanation to the information paradox of quantum black holes.

[1] D. Grumiller, W. Kummer and D. V. Vassilevich, Ukr. J. Phys. 48, 329 (2003); hep-th/0301061.
[2] D. Grumiller, W. Kummer and D. V. Vassilevich, Eur. Phys. J. C 30, 135 (2003).
[3] D. Grumiller, W. Kummer and D. V. Vassilevich, JHEP 0307, 009 (2003); hep-th/0305036.
[4] D. Grumiller, W. Kummer and D. V. Vassilevich, Nucl. Phys. B 580, 438 (2000); gr-qc/0001038.

5.2.3 Quantum field theory of light-cone dominated hadronic processes

B. Geyer, J. Eilers

Light-cone dominated, polarized hadronic processes at large momentum transfer factorize into process-dependent hard scattering amplitudes and process-independent non-perturbative generalized distribution amplitudes. Growing experimental accuracy requires the entanglement of various twist as well as (target) mass contributions and radiative corrections. Their quantum field theoretic prescription is based on the nonlocal light-cone expansion [1].

The group theoretical procedure allowing for the decomposition of nonlocal tensor-valued light-ray operators into tensorial harmonic operators with well-defined geometric twist (τ = dimension − spin), thereby taking trace terms correctly into account [2], has been studied and applied further:

• A rigorous treatment of the (infinite) twist decomposition off the light-cone for non-local vector operators has been given and applied to relevant QCD operators thereby determining the power resp. target mass corrections being essential for the related distribution amplitudes [3].

• These results are applied to virtual (non-forward) Compton scattering in order to rigorously obtain the target mass dependence of their double-distribution amplitudes in leading twist approximation [4]. Thereby, the generalization of the Wandzura-Wilczek representation for the distribution amplitudes from forward to non-forward case - together with

new distribution amplitudes - and analogous representations for distribution amplitudes of the symmetric part of the Compton amplitude has been found.
• A general, constructive procedure of determining the (infinite) spin resp. twist decomposition of non-local off-cone tensor operators of any rank and arbitrary symmetry type, in any space-time dimension d, has been given and implemented in a `Java` programme [5]. It has been applied to the twist decomposition for non-local (in x-space) QCD operators of rank 2 and 3.

[1] S.A. Anikin, O.I. Zavialov, Ann. Phys. (N.Y.) **116**, 135 (1978); D. Müller, D. Robaschik, B. Geyer, F.-M. Dittes and J. Hořejši, Fortschr. Phys. **42**, 101 (1994).
[2] B. Geyer, M. Lazar and D. Robaschik, Nucl. Phys. **B 559**, 339 (1999); **B 618**, 99 (2001); B. Geyer and M. Lazar, Nucl. Phys. **B 581**, 341 (2000), Phys. Rev. **D 63**, 094003 (2001); J. Eilers and B. Geyer, Phys. Lett. **B 546**, 78 (2002).
[3] J. Eilers, B. Geyer, and M. Lazar, Phys. Rev. **D 69**, 034015 (2004).
[4] B. Geyer, D. Robaschik, J. Eilers, and J. Blümlein, *Virtual Compton scattering and non-forward Wandzura-Wilczek representation*, in preparation.
[5] J. Eilers, Thesis, Leipzig 2004.

5.2.4 Quantum symmetries of general gauge theories

B. Geyer

General gauge theories are characterized by local symmetries whose generators, in contrast to the well-known Yang-Mills theories, not necessarily obey a Lie algebra structure. Their gauge algebra may be open, i.e., closed modulo equations of motion, and, in addition, may be reducible (up to any finite order of reducibility) requiring for the introduction of various extra ghost and auxiliary fields. Nevertheless, the quantum symmetries of such theories [including higher dimensional and $N-$extended super Yang-Mills theories (SYM), (super) string theories and topological field theories (TQFT)] are governed by (extended) BRST operations resp. master equations. – Two different routes of research have been considered:

Lagrangian Quantization of General Gauge Theories: The well-known Batalin-Vilkovisky (BV) quantization using a master equation in terms of fields and antifields (sources) found various extensions in the past.
• Continuing previous work [1], we applied the $Sp(2)-$symmetric quantization of Batalin, Lavrov & Tyutin [2] to W_3-gravity [3], the simplest model with open gauge algebra, studied the arbitrariness in the realization of the gauge algebra as well as problems related to the Hamiltonian approach; we showed by explicit construction that solutions of the related classical master equation necessarily exceed third order in (anti)ghost and auxiliary fields.
• A former partial study of (modified) triplectic quantization [4] in general coordinates [5] has been extended to the case when the basic manifold consists of fields with both even and odd Grassmann parity [6]; a superfield formulation of that approach has been found [7]. In addition, we introduced Fedosov supermanifolds and showed that their Ricci curvature in the even resp. odd case vanishes resp. (in general) does not vanish [8].

[1] B. Geyer, P.M. Lavrov, P.Yu. Moshin, Int. J. Mod. Phys. **A 16**, 4297 (2001).
[2] I.A. Batalin, P.M. Lavrov, I.V. Tyutin, J. Math. Phys. **31**, 1487 (1990); *ibid.* **32**, 532

(1990); *ibid.* **32**, 2513 (1990).
[3] B. Geyer, D.M. Gitman, P.M. Lavrov, P.Yu. Moshin, Int. J. Mod. Phys. **A18**, 5099 (2003).
[4] I.A. Batalin, R. Marnelius, Phys. Lett. **B 350**, 44 (1995); Nucl. Phys. **B 465**, 521 (1996); I.A. Batalin, R. Marnelius, A.M. Semikhatov, Nucl. Phys. **B 446**, 249 (1995); B. Geyer, D.M. Gitman, P.M. Lavrov, Mod. Phys. Lett. **A 14**, 661 (1999); Theor. Math. Phys. **123**, 813 (2000).
[5] B. Geyer, P.M. Lavrov, A.P. Nersessian, Phys. Lett. **B 512**, 211 (2001); Int. J. Mod. Phys. **A 17**, 349 (2002).
[6] B. Geyer and P.M. Lavrov, hep-th/0304011.
[7] B. Geyer, D.M. Gitman, P.M. Lavrov, P.Yu. Moshin, Int. J. Mod. Phys. **A 19**, 737 (2004).
[8] B. Geyer, P.M. Lavrov, hep-th/0306218.

Cohomological Gauge Theories: Topological quantum field theories are the simplest QFT's with the defining property that their Green functions are independent of the local Riemannian structure of the underlying manifold.
• Continuing our constructions of cohomological gauge theories of Hodge type [9] (i.e., gauge theories where the generators of the topological shift, co-shift and gauge symmetry together with a discrete Hodge-type $\star-$operation obey a complex being completely analogous to the de Rham complex) we studied the basic cohomology of the twisted $N = 16, D = 2$ super Maxwell theory, showed that the corresponding BRST-Laplacian *on-shell* does not vanish and constructed the basic topological invariants [10].
• We studied cohomological gauge theories with special holonomy group $\mathcal{H} \in SO(D)$ in $D > 4$ dimensions being invariant under metric variations respecting $\mathcal{H}$. First, we explicitly constructed the Euclidean SYM on a hyper Kähler eightfold with $N_T = 3$ and $Sp(4)$–holonomy [11], second, we found a cohomological extension of the $Spin(7)-$invariant, $D = 8$ SYM [12] and, finally, we determined the G_2-invariant $D = 7$ SYM by dimensional reduction of $Spin(7)-$invariant, $N_T = 1, D = 8$ SYM thereby showing that it constitutes a higher-dimensional analogue of the $D = 3$ super BF theory [13].

[9] B. Geyer, D. Mülsch, Phys. Lett. **B 518**, 181 (2001); Int. J. Mod. Phys. **A 17**, 4425 (2002); Nucl. Phys. **B 662**, 531 (2003).
[10] B. Geyer, D. Mülsch, Phys. Lett. **B 575**, 349 (2003)
[11] D. Mülsch, B. Geyer, hep-th/0310275.
[12] D. Mülsch, B. Geyer, hep-th/0304096.
[13] D. Mülsch, B. Geyer, hep-th/0310237.

5.2.5 Casimir effect and real media

M. Bordag, B. Geyer

The vacuum of quantum fields shows a response to changes in external conditions with measurable consequences. The investigation of the electromagnetic vacuum in the presence of real media is of actual interest in view of current experiments as well as nanoscopic electro-mechanical devices [1]. In recent experiments using atomic force microscopy the Casimir effect had been measured with high accuracy. This required a detailed investigation of the influence of real experimental structures on the corresponding force.

Using the surface impedance approach we derived the Lifschitz formula for the free energy and the Casimir force between real metals in perfect agreement with thermodynamics; thereby a longstanding controversy could be resolved [2]. The result has been applied to a configuration of two parallel plates of gold; the dependence on the temperature has been determined.

[1] M. Bordag, U. Mohideen, V. M. Mostepanenko, Phys. Rept. **353**, 1 (2001).
[2] B. Geyer, G. L. Klimchitskaya, V. M. Mostepanenko, Phys. Rev. A **67**, 062102 (2003).

5.2.6 Structure of the gauge orbit space and study of gauge theoretical models

G. Rudolph, Ch. Fleischhack, M. Schmidt, Sz. Charzynski

Based upon our results on the structure of the gauge orbit space [1] and on lattice gauge theories [3–5], we continued to investigate non-perturbative aspects of quantum gauge theory with special emphasis on the following items:
i) The study of singular Marsden-Weinstein reduction [6] and geometric quantization of singular Marsden-Weinstein quotients [7] for model spaces like $SU(3) \times \cdots \times SU(3)$ was pushed forward. Such spaces arise as configuration spaces in lattice QCD. This work aims at clarifying the role of nongeneric strata in quantum gauge theory. From the mathematical point of view, nontrivial problems of classical invariant theory and complex geometry arise. Neglecting some delicate mathematical aspects, the analogous problem for full Yang-Mills theory on compact manifolds is under investigation, too.
ii) The study of non-perturbative aspects of gauge theories on the lattice in terms of observables was continued. Applying similar techniques as for lattice QED, see [3,4], the observable algebra and the charge superselection structure of QED was investigated, see [5]. Further publications are in preparation.
iii) Studying the structure of the observable algebra for lattice QCD in purely algebraic (representation independent) terms, we were led to investigate generalizations of ordinary superalgebras, see [8]. This is a promising field of pure mathematics, with applications in different areas of physics.
(iv) Christian Fleischhack continued the study of gauge theories within the Ashtekar approach, with special emphasis on noncompact structure groups and applications in quantum gravity.

[1] G. Rudolph, M. Schmidt, I.P. Volobuev, J. Math. Phys. Anal. Geom. **5**, 201–241 (2002); J. Geom. Phys. **42**, 106-138 (2002); J. Phys. A: Math. Gen. **35**, R1–R50 (2002).
[3] J. Kijowski, G. Rudolph, A. Thielmann, Commun. Math. Phys. **188**, 535–564 (1997).
[4] J. Kijowski, G. Rudolph and C. Śliwa, Annales H. Poincaré **4**, 1137 (2003).
[5] J. Kijowski, G. Rudolph, J. Math. Phys. **43**, 1796 (2002).
[6] R. Sjamaar, E. Lerman, Ann. Math. (2), **134**, 375 (1991).
[7] J. Huebschmann, math-dg/0104213.
[8] P. Jarvis and G. Rudolph, J. Phys. A, **36**, No. 20, 5531 (2003).

5.2.7 Noncommutative geometry

G. Rudolph, O. Richter

The study of the theory of foliations in the sense of Connes [1] was continued. Two papers on the subject have been published [2]. These contain results about spectral triples related to the Kronecker foliation of the 2-torus. In particular, the associated differential calculi were analyzed explicitly and for one spectral triple a topological invariant (Chern character) was calculated.

The study of quantum principal bundles was continued. Papers on quantum discs and quantum real projective space as quotients of Podles quantum spheres and their interpretation in terms of graph C^*-algebras have been published [3]. Concerning the study of quantum Hopf bundles, Chern-Connes pairings between traces on the basis algebra and the K^0-classes for projectors of line bundles associated with a quantum Hopf bundle were calculated for the locally trivial bundle [4,5] and the Hopf bundle over the generic Podleś spheres [6]. This way, one obtains the winding numbers of these line bundles and one can conclude the topological non-triviality of the quantum Hopf bundle. These results are published in [7].

The example of a locally trivial Hopf bundle has been generalized, leading to two nonisomorphic quantum principal bundles living over two different quantum two-spheres. One of these two-spheres is topologically the generic Podleś sphere, the other one results from a gluing of two quantum discs with an extra twist. The total spaces of the bundles coincide and are hybrids of the 3-sphere of the locally trivial bundle and the 3-sphere of Matsumoto [8]. Many of the results mentioned above (in particular Chern numbers) are true also for these new examples. The total space can be viewed as quantum analog of a Heegaard splitting of the 3-sphere, and its topological properties (in particular K-theory) are still investigated.

[1] A. Connes, H. Moscovici, GAFA **5** (2), 174–243 (1995).
[2] R. Matthes, O. Richter and G. Rudolph, J. Geom. Phys. **46**, 48 (2003); Banach Center Publications **61**, 125–147 (2003).
[3] P.M. Hajac, R. Matthes, W. Szymański, Algebras and Representation Theory **6**, 169–192 (2003); Rep. Math. Phys. **51**, 215–224 (2003).
[4] D. Calow, R. Matthes, J. Geom. Phys. **41**, 114–165 (2002).
[5] P.M. Hajac, R. Matthes, W. Szymański, to appear in Algebras and Representation Theory.
[6] T. Brzeziński, S. Majid, Commun. Math. Phys. **213**, 491–521 (2000).
[7] P.M. Hajac, R. Matthes, W. Szymański, C. R. Acad. Sci. Paris, Ser. I **336**, 925–930 (2003).
[8] K. Matsumoto, Japan J. Math. **17**, 333–356 (1991).

5.2.8 One-particle properties of quasiparticles in the half-filled Landau level

W. Weller

Using field theoretical methods, two-dimensional electron systems in strong magnetic fields were studied. The investigations were concentrated on the half-filled lowest Landau level.

The theory for the half-filled lowest Landau level of Halperin *et al.* [1] transforms from the electrons to Chern–Simons fermions by eliminating the external magnetic field. The theory leads to an infrared divergent energy. It was shown [2] that this is due to missing diagrams and to the fact that in [1] the ordering of the operators in the path integral was changed. The correct formulation yields a three-particle interaction. For this interaction, a path integral representation was developed [2] with correct ordering of the operators by using time steps with intermediate times.

The energy was computed by evaluating the path integral in various approximations. The calculated energies are convergent and agree well with numerical simulations. The idea of the Singwi-Sj"olander approach to the 3d Coulomb problem was extended to the Chern-Simons theory [3] with even better results for the energies.

An approximation scheme was developed conserving the particle number and the constraints. Now, the conserving Hartree–Fock approximation is being numerically evaluated. The self energy of the Chern–Simons fermions is until now infrared divergent. For the solution of that problem we started investigations based on a transformation introduced by Bohm and Pines and by Shankar and Murthy [4]; that transformation transforms from the Chern–Simons fermions to the composite fermions (CF), which include the correlation hole. The conserving approximations are extended to the CF.

[1] B.I. Halperin, P.A. Lee, N. Read, Phys. Rev. B **47**, 7312 (1993).
[2] W. Weller, J. Dietel, Th. Koschny, W. Apel in R. Casalbuoni et al. (eds.), 6th Int. Conf. on Path Integrals, World Scientific, Singapore 1999, p. 466.
[3] J. Dietel, W. Weller, Phys. Rev. B **64**, 195307 (2001).
[4] R. Shankar, G. Murthy, Phys. Rev. Lett. **79**, 4437 (1997).

5.2.9 Funding

Graduiertenkolleg Quantenfeldtheorie: Mathematische Struktur und Anwendungen in der Elementarteilchen- und Festkörperphysik
Spokesman: Prof. Dr. B. Geyer
DFG GRK 52/3-03

Lokale Methoden zur Berechnung der Vakuumpolarisation
Dr. M. Bordag
DFG Bo 1112/12-1

Reimar-Lüst-Stipendium der Max-Planck-Gesellschaft
Dr. Ch. Fleischhack

Lagrangian quantization of general gauge theories with extended BRST symmetry: Triplectic quantization and Fedosov manifolds
Prof. Dr. B. Geyer
DFG Ge 696/7-1

Casimir force between real boundaries
Prof. Dr. B. Geyer
SMWK Az.: 4-7531.50-04-0361-03/1

Untersuchungen zur physikalischen Bedeutung der Stratifizierung des Eichorbitraumes
Prof. G. Rudolph
DFG RU 692/3-1

One-particle properties of quasiparticles in the half-filled Landau level
W. Weller
DFG-Schwerpunktprogramm "Quanten-Hall-Systeme", WE 480/3-2

5.2.10 Organizational Duties

Priv.-Doz. Dr. Michael Bordag
Referee: J. Phys. A, Phys. Rev. D, J. Math. Phys.
Head of International Organizing Committee for the 'Workshop on Quantum Field Theory under the influence of external conditions', held Sept. 2003 in Oklahoma

Dr. Christian Fleischhack
Spokesman Arbeitsgruppe Wissenschaftspolitik der Jungen Akademie, since October, 2003
Corrector for the Mathematics Olympiad

Prof. Dr. Bodo Geyer
Spokesman of the Graduiertenkolleg Quantenfeldtheorie: Mathematische Struktur und Anwendungen in Elementarteilchen- und Festkörperphysik
Member of scientific advisory board of Andrejewski Foundation (up to 2/2003)
Member of electing board Latin America-South of DAAD
Vertrauensdozent of the Gesellschaft Dt. Naturforscher und Ärzte
Referee: DFG, DAAD, Humboldt Foundation

Prof. Dr. Gerd Rudolph
Referee: Rep. Math. Phys., J. Phys. A, J. Geom. Phys., Class. Quant. Grav., J. Math. Phys.

Dr. Dmitri V. Vassilevich
Referee: Class. Quant. Grav., J. Phys. A, Nucl. Phys. B, Mod. Phys. Lett. A, J. High Energy Phys., Nuovo Cimento B, London Math. Soc.
Coordinator, Program on Gravity in Two Dimensions, ESI (Wien)

Program Committee, Fock School on Advances in Physics (St.Petersburg)

Prof. em. Wolfgang Weller
Board member: Physikalische Blätter

5.2.11 External Cooperations

Academic

National University, Dnepropetrovsk
Prof. V. Skalozub

Technische Universität Wien
Prof. Dr. W. Kummer, Dr. D. Grumiller

State University of New York at Stony Brook
Prof. P. van Nieuwenhuizen

University of Oregon
Prof. P.B. Gilkey

St. Petersburg University
Dr. V. Marachevsky

DESY-Institute of High Energy Physics, Zeuthen
Dr. Johannes Blümlein

Max-Planck Institute for Mathematics in the Sciences, Leipzig
Dr. Markus Lazar

Institute of Theoretical Physics, Brandenburg Technical University Cottbus
Prof. Dr. Dieter Robaschik

Institute of Nuclear Physics, University of São Paulo
Prof. Dr. Dmitry M. Gitman
Dr. P.Yu. Moshin (on absence of Pedagogical University Tomsk)

Department of Mathematical Physics, Pedagogical University Tomsk
Prof. Dr. Petr M. Lavrov

Wissenschaftszentrum Leipzig e.V.
Dr. Dietmar Mülsch

Russian Academy of Science, Lebedev Institute, Moscow
Prof. Dr. Igor V. Tyutin

Dept. of Physics, North-West Polytechnical University St. Petersburg
Prof. Dr. Galina L. Klimchitskaya

A. Friedmann Laboratory of Theoretical Physics, St. Petersburg
Prof. Dr. Vladimir M. Mostepanenko

Technische Universität Clausthal-Zellerfeld
Dr. R. Matthes

Polish Academy of Sciences, Center for Theoretical Physics, Warsaw
Prof. J. Kijowski

Polish Academy of Sciences, Mathematics Institute and University of Warsaw
Prof. P. Hajac

Skobeltsyn Institute of Nuclear Physics, Lomonosov Moscow State University
Dr. I.P. Volobuev

University of Tasmania, Hobart
Prof. P. Jarvis

Université des Sciences et Technologies de Lille
Prof. J. Huebschmann

University of Newcastle
Prof. W. Szymanski

Center for Gravitation Physics and Geometry, Penn State University
Prof. A. Ashtekar, Dr. H. Sahlmann

Institute for Theoretical Physics, University of Warsaw
Prof. J. Lewandowski

Physikalisch-technische Bundesanstalt
Dr. W. Apel

5.2.12 Publications

Journals

M. Bordag
Vacuum energy of a color magnetic vortex
Phys. Rev. D **67**, 065001 (2003).

M. Bordag and I. Drozdov

Fermionic vacuum energy from a Nielsen-Olesen vortex
Phys. Rev. D **68**, 065026 (2003).

Ch. Fleischhack
Hyphs and the Ashtekar-Lewandowski Measure
J. Geom. Phys. **45**, 231–251 (2003).

Ch. Fleischhack
On the Gribov Problem for Generalized Connections
Commun. Math. Phys. **234**, 423–454 (2003).

Ch. Fleischhack
Regular Connections among Generalized Connections
J. Geom. Phys. **47**, 469–483 (2003).

B. Geyer, D.M. Gitman, P. Lavrov and P. Moshin
On Problems of the Lagrangian Quantization of W_3 gravity
Int. J. Mod. Phys. **A 18**, 5099–5125 (2003).

B. Geyer, D.M. Gitman, and I.V. Tyutin
Canonical form of Euler-Lagrange equations and gauge symmetries
J. Phys. A: Math. Gen. **36**, 6587–6609 (2003).

B. Geyer, D.M. Gitman, and I.V. Tyutin
Reduction of Euler-Lagrange equations in gauge symmetries
Int. J. Mod. Phys. **A 18**, 2077–2084 (2003).

B. Geyer, G.L. Klimchitskaya, and V.M. Mostepanenko
Surface-impedance approach solves problems with the thermal Casimir force between real metals
Phys. Rev. **A 67**, 062102 (2003).

B. Geyer, P. Lavrov and A. Nersessian
Extended BRST quantization in general coordinates,
Proc. 3rd Int. Sacharov Conference on Physics, Singapore 2003, Vol. II, pp. 94–103.

B. Geyer and D. Mülsch
Higher dimensional analogue of the Blau-Thompson model and $N_T = 8$, $D = 2$ Hodge type cohomological gauge theories
Nucl. Phys. **B 662**, 531–553 (2003).

B. Geyer and D. Mülsch
$N_T = 8, D = 2$ Hodge type cohomological gauge theory with global $SU(4)$ symmetry
Proc. 3rd Int. Sacharov Conference on Physics, Singapore 2003, Vol. II, pp. 45–53.

B. Geyer and D. Mülsch
The basic cohomology of the twisted $N = 16, D = 2$ super Maxwell theory

Phys. Lett. **B 575**, 349–357 (2003).

P. Gilkey, K. Kirsten and D. Vassilevich
Heat trace asymptotics defined by transfer boundary conditions
Lett. Math. Phys. **63**, 29 (2003).

P. Gilkey, K. Kirsten, D. Vassilevich and A. Zelnikov
Duality symmetry of the p-form effective action and super trace of the twisted de Rham complex
Nucl. Phys. B **648**, 542 (2003).

D. Grumiller, W. Kummer and D.V. Vassilevich
Virtual black holes in generalized dilaton theories and their special role in string gravity
Eur. Phys. J. C **30**, 135 (2003).

D. Grumiller, W. Kummer and D.V. Vassilevich
A note on the triviality of kappa-deformations of gravity
Ukr. J. Phys. **48**, 329 (2003).

D. Grumiller, W. Kummer and D.V. Vassilevich
Positive specific heat of the quantum corrected dilaton black hole
JHEP **0307**, 009 (2003).

P.M. Hajac, R. Matthes, W. Szymański
Quantum real projective space, disc and spheres
Algebras and Representation Theory **6**, 169–192 (2003).

P.M. Hajac, R. Matthes, W. Szymański
Chern numbers for two families of noncommutative Hopf fibrations
C. R. Acad. Sci. Paris, Ser. I **336** (11), 925–930 (2003).

P.M. Hajac, R. Matthes, W. Szymański
Graph C^*-algebras and $\mathbb{Z}_2$-quotients of quantum spheres
Rep. Math. Phys. **51**, 215–224 (2003).

P. Jarvis and G. Rudolph
Polynomial super-Gl(n) algebras
J. Phys. A, Vol. 36, No. 20, 5531–5555 (2003).

J. Kijowski, G. Rudolph
How to define Coulor Charge in Quantum Chromodynamics
in: J.-P. Gazeau et.al. (eds.), Group 24: Physical and Mathematical Aspects of Symmetries, Institute of Physics, Conference Series Number 173, Bristol and Philadelphia, 2003, pp. 359-362.

J. Kijowski, G. Rudolph and C. Śliwa
Charge Superselection Sectors for Scalar QED on the Lattice

Annales H. Poincaré **4**, 1137–1167 (2003).

R. Matthes
A locally trivial quantum Hopf bundle
in: J.-P. Gazeau et.al. (eds.), Group 24: Physical and Mathematical Aspects of Symmetries, Institute of Physics, Conference Series Number 173, Bristol and Philadelphia, 2003, pp. 455–459.

R. Matthes, O. Richter and G. Rudolph
Spectral triples and differential calculi related to the Kronecker foliation
J. Geom. Phys. **46**, 48-73 (2003).

R. Matthes, O. Richter and G. Rudolph
Generalized signature operators and spectral triples for the Kronecker foliation
in: P.M. Hajac and W. Pusz (eds.), Noncommutative Geometry and Quantum Groups, Banach Center Publications **61**, 2003, pp. 125–147.

M. Schmidt
How to study the physical relevance of gauge orbit space singularities?
Rep. Math. Phys. **51**, 325–333 (2003).

D.V. Vassilevich
Quantum corrections to the mass of the supersymmetric vortex
Phys. Rev. D **68**, 045005 (2003).

D.V. Vassilevich
Heat kernel expansion: User's manual
Phys. Rept. **388**, 279 (2003).

P. M. Alberti
Playing with Fidelities
Rep. Math. Phys. **53**, No. 1, 87–125 (2003).

In press

J. Eilers, B. Geyer, and M. Lazar
Complete twist decomposition for nonlocal QCD vector operators in x-space
Phys. Rev. **D 69** 034015 (2004), hep-ph/0306269.

Ch. Fleischhack
Parallel Transports in Webs
Math. Nachr. **263–264**, 83–102 (2004); math-ph/0304001.

Ch. Fleischhack
Proof of a Conjecture by Lewandowski and Thiemann
math-ph/0304002; Commun. Math. Phys.

B. Geyer, D.M. Gitman, P. Lavrov and P.Yu. Moshin
Superfield extended BRST quantization in general coordinates
Int. J. Mod. Phys. **A 19**, 737–750 (2004), hep-th/0310143.

B. Geyer, D.M. Gitman, and I.V. Tyutin
Reduction of Euler-Lagrange equations in general gauge theories with external fields
Contribution to: Proc. 6. Int. Friedman Seminar, Oklahoma, Sept. 2003

B. Geyer and P. Lavrov
Modified triplectic quantization in general coordinates
Int. J. Mod. Phys. A, hep-th/0304011.

B. Geyer and P.M. Lavrov
Fedosov supermanifolds: Basic properties and the difference in even and odd cases
Int. J. Mod. Phys. A, hep-th/0306218.

D. Mülsch and B. Geyer
Euclidean super Yang-Mills theory on a quaternionic Kähler manifold
Int. J. Mod. Phys. **A** , hep-th/0304096.

D. Mülsch and B. Geyer
Cohomological extension of $Spin(7)$ invariant super Yang-Mills theory in eight dimensions
Int. J. Mod. Phys. **A** , hep-th/0310275.

D. Mülsch and B. Geyer
An abelian cohomological gauge theory
Contribution to : Proc. X. Int. Marcel Grossmann Conf., Rio de Janeiro, July 2003

D.V. Vassilevich
Non-commutative heat kernel
hep-th/0310144; Lett. Math. Phys.

D.V. Vassilevich and A. Yurov
Space-time non-commutativity tends to create bound states
hep-th/0311214, Phys. Rev. D.

Conference contributions

Fermionic vacuum energy in the Abelian-Higgs model (inv. T)
M. Bordag
Fifth Workshop on Quantum Field Theory under the Influence of external Conditions, Oklahoma, September 20, 2003

Stratification of the Space of Distributional Connections (inv.T)
Ch. Fleischhack
Center for Geometry and Mathematical Physics Seminar Series (Penn State University) February 19, 2003.

Diffeomorphism Invariance in the Smooth Category I and II (inv.T)
Ch. Fleischhack
Gravity Theory Series at the Center of Gravitational Physics and Geometry (Penn State University), University Park, April 28 and May 2, 2003

Geometry of the Generalized Gauge Orbit Space in the Ashtekar Program
Ch. Fleischhack
Evaluation of the Max Planck Institute for Mathematics in the Sciences, Leipzig, Mai 8, 2003

Ashtekar Gravity – Overview and Problems
Ch. Fleischhack
12. Workshop Grundlagen und konstruktive Aspekte der QFT, Leipzig, May 23–24, 2003

Proof of the Lewandowski-Thiemann Conjecture
Ch. Fleischhack
Conference on Gravitation: A Decennial Perspective, University Park, June 8–12, 2003

Combinatorics of Parallel Transports: Implementation of Diffeomorphism Invariance into Loop Quantum Gravity (inv.T)
Ch. Fleischhack
Seminarium KMMF, Warszawa, October 16, 2003

Geometry of the Configuration Space in Quantum Gauge Field Theory and Quantum Gravity (inv.T)
Ch. Fleischhack
Relativity Seminar, Warszawa, October 17, 2003

Hopf type cohomological gauge theories (inv.T)
B. Geyer
Fourth Workshop on Gauge Fields and Strings, Jena, Febr. 25 - March 01, 2003

An abelian cohomological gauge theory (T)
D. Mülsch and *B. Geyer*
X. Int. Marcel Grossmann Conf., Rio de Janeiro, July 19 - 26, 2003

Reduction of Euler-Lagrange equations in general gauge theories with external fields (inv.T)
B. Geyer, D.M. Gitman, and I.V. Tyutin
6. Int. Friedman Seminar, Oklahoma, September 14 - 19, 2003

Observable algebras and charge superselection structures of gauge theories on the lattice (P)
J. Kijowski, G. Rudolph
Int. Congress on Mathematical Physics, Lissabon, July 28 – August 02, 2003

Spectral actions for leaf spaces of foliations (P)
O. Richter
Int. Congress on Mathematical Physics, Lissabon, July 28 – August 02, 2003

Stratification of the gauge orbit space for gauge group SU(n) (inv.T)
M. Schmidt
Miniworkshop on quantization of Poisson spaces with singularities, Oberwolfach, January 19–25, 2003

Spectral problems from quantum field theory (inv. T)
D.V. Vassilevich
Workshop on Spectral Geometry, Holbaek, August 7, 2003

Non-commutative heat kernel (inv. T)
D.V. Vassilevich
Workshop on Gravity in Two Dimensions, Wien, September 29, 2003

Heat kernel methods in quantum field theory (inv. T)
D.V. Vassilevich
Fock School on Advances in Physics, St.Petersburg, October 29, 2003

5.2.13 Graduations

Habilitation

Dr. Olaf Richter
Physically reasonable solutions to the Ernst equation and their twistor theory

Diploma

Tobias Fischer
Untersuchung axialsymmetrischer und stationärer Raum-Zeit mit Methoden der algebraischen Geometrie

5.2.14 Guests

Dr. J. Blümlein
DESY-IfH Zeuthen
January 15/16, 2003

Prof. Dr. M. Forger
Department of Mathematics, University of São Paulo
June 11/12, 2003

Dr. D. Fursaev
JINR Dubna
November 23–December 14, 2003

Prof. Dr. D.M. Gitman
Institute of Nuclear Research, University of São Paulo
September 03– November 04, 2003

Prof. Dr. P. Hajac
Unversity of Warsaw
September 1–30, 2003
funded by GK QFT

Prof. Dr. M. Henneaux
Université Libre Bruxelles
May 12–23, 2003

Prof. Dr. J. Huebschmann
Université des Sciences et Technologies de Lille
May 19–24, 2003
December 1–5, 2003
funded by GK QFT

Prof. Dr. J. Kijowski
Center for Theoretical Physics, Polish Academy of Sciences, Warsaw
September 1–30, 2003
funded by MPI MIS

Prof. Dr. G.V. Klimchitskaya
Department of Physics, North-West Polytechnical University, St. Petersburg
February 10–April 09, 2003

Prof. Dr. P.M. Lavrov,
Department of Mathematical Physics, Pedagogical University Tomsk
January 15–July 15, 2003

Dr. V. Marachevsky
St.Pteresburg University (Russia)
April 6–May 5, 2003

Prof. Dr. V.M. Mostepanenko
A. Friedmann Laboratory of Theoretical Physics, St. Petersburg
February 10–April 09, 2003

Prof. Dr. S. Odintsov
Department of Mathematical Physics, Pedagogical University Tomsk
February 12–20, 2003

Dr. Pirozhenko
JINR Dubna

November 30–December 14, 2003

Dr. O. Richter
Inst. of Mathematics, Ohio State University
October 20–28, 2003

Prof. Dr. D. Robaschik
BTU Cottbus
February 9–March 10, 2003

Prof. A. Saharyan
University of Yerevan (Armenia)
October 25–December 25, 2003

Prof. Dr. I.P. Volobuev
Skobeltsyn Institute of Nuclear Physics, Moscow State University
October 1–December 15, 2003
funded by GK QFT

Prof. Dr. A. Yurov
University of Kaliningrad
October 16–November 30, 2003

5.3 Theory of Elementary Particles

5.3.1 Introduction

The Particle Physics Group performs basic research in the quantum field theoretic description of elementary particles and in phenomenology. Topics of current interest are conformal symmetry and its breaking in the context of supersymmetric theories, renormalization problems, electroweak matter at finite temperature and the derivation of Regge behaviour of scattering amplitudes from Quantum Chromodynamics. Perturbative and non-perturbative methods are applied to answer the questions. In perturbation theory the work is essentially analytical using computers only as a helpful tool. Lattice Monte Carlo calculations as one important non-perturbative approach however are based on computers as an indispensable instrument. Correspondingly the respective working groups are organized: in analytical work usually very few people collaborate, in the lattice community rather big collaborations are the rule. Our group is involved in many cooperations on the national and international level (DESY, Munich; France, Russia, Armenia, USA, Japan). Since elementary particles are very tiny (of the order of 10^{-15} m) and for the study of their interactions large accelerators producing enormously high energy are needed, it is clear that results in this direction of research do not have applications in daily life immediately. To clarify the structure of matter is first of all an aim in its own and is not pursued for other reasons. But particle theory has nevertheless a very noticeable impact on many other branches by its power of providing new methodological insight. Similarly for the student specializing in this field the main benefit is her/his training in analysing complex situations and in applying tools which are appropriate for the respective problem. As a rule there will be no standard procedures which have to be learned and then followed, but the student has to develop her/his own skill according to the need that arises. This may be a mathematical topic or a tool in computer application. Jobs which plainly continue these studies are to be found at universities and research institutes only. But the basic knowledge which one acquires in pursuing such a subject opens the way to many fields where analytical thinking is to be combined with application of advanced mathematics. Nowadays this seems to be the case in banks, insurance companies and consulting business.

5.3.2 High-energy asymptotics and integrable quantum systems

R. Kirschner

The aim of this project is to develop methods for treating the Regge and Bjorken limits in gauge theories like QCD. We rely on the idea of the high-energy effective action [1] which we have shown in recent years to be a useful tool for analyzing the asymptotics of scattering amplitudes. In the Regge case the action describes the scattering by the exchange of reggeized quarks and gluons. The reggeon and parton interactions exhibit remarkable symmetry properties and can be related to integrable quantum systems.

In 2003 we have studied the construction of intergrable quantum systems based on the Jordanian deformation of $sl(2)$ symmetry [2]. In our application to conformal transformation of the light ray this deformation results in a breaking of scaling symmetry but preserves the translation symmetry. This is similar to the conformal symmetry breaking

in field theories.

We have formulated representations of the deformed symmetry in terms of polynomials and solved the Yang-Baxter relation for generic infinite-dimensional representations both in spectral and integral form.

This work continues previous investigations, where Yang-Baxter solutions with supersymmetric extension and standard quantum deformation of conformal symmetry [3,4]

[1] L.N. Lipatov, Nucl. Phys. B365(1991)614;
R. Kirschner, L.N. Lipatov and L. Szymanowski, Nucl. Phys. B452(1994)579; Phys. Rev. D51(1995)838;
L.N. Lipatov, Nucl. Phys. B452(1995)369;
R. Kirschner and L. Szymanowski, Phys. Rev. D52(1995)2333; Phys. Lett. B419 (1998) 348; Phys. Rev. D58(1998) 014004.

[2] S. Derkachov, D. Karakhanyan and R. Kirschner,
Universal R operator with Jordanian deformation of conformal symmetry,
Nucl. Phys. B 681 (2004) 295, [arXiv:nlin.si/0310019].

[3] S. E. Derkachov, D. Karakhanyan and R. Kirschner,
Universal R-matrix as integral operator ,
nlin.si/0102024, Nucl. Phys B 618[FS] (2001) 589-616.

[4] D. Karakhanyan, R. Kirschner and M. Mirumyan,
Universal R operator with deformed conformal symmetry,
Nucl. Phys. B 636 (2002) 529 [arXiv:nlin.si/0111032].

Funding

Integrable systems nd high-energy asymptotics
Dr. R. Kirschner
SMWK Forschungsförderung 2003, Support of the visit by Dr. S.E. Derkachov at ITP.

Two.dimensional intergrable theories in application to high energy scattering
Dr. R. Kirschner
BMBF/IB, WTZ ARM 00/001, Bilateral Cooperation with Phys. Institut Yereva, Armenia.

Organizational Duties

R. Kirschner
Referee: Eur. Physics Journal C, Phys. Rev. D, Progr. Part. Nucl. Phys.

External Cooperations

Academic

St. Petersburg, Nuclear Physics Institute
Prof. L.N. Lipatov

St. Petersburg, University and Technology Institute
Dr. S.E. Derkachov

Yerevan Physics Institute, Theory Dept.
Prof. Ara Sedrakyan

Soltan Institut of Nucl. Studies, Warsaw
Dr. Lech Szymanowski

Univ. Hamburg, Inst. f. Theor. Physik/ DESY
Prof. J. Bartels

Universität Regensburg, Inst.f. Theor. Physik
Prof. A. Schäfer, Prof. V. Braun

5.3.3 The Nucleon in a Finite Volume and in Chiral Perturbation Theory

M. Göckeler

Monte Carlo simulations of lattice QCD with $N_f = 2$ dynamical quarks are now delivering physical results. In particular, several groups have computed the nucleon mass for a variety of lattice actions, quark masses and volumes [1-3]. Due to limited computer resources, the quark masses are larger than in reality and the volumes are relatively small. Still one would like to extract as much physically relevant information from the simulations as possible. One way of doing so consists in comparing with formulae from chiral perturbation theory. Considering the underlying chiral effective field theory in a finite volume one can describe the dependence of the nucleon mass on the quark mass and on the volume in a unified framework, where the finite size effects are due to pions "propagating around the spatial box".

In Ref. [4] it has been demonstrated that relativistic baryon chiral perturbation theory leads to a good chiral extrapolation function for the nucleon mass in a large ("infinite") volume connecting available lattice results with the physical value.

In this project we have worked out the finite size effects for the nucleon mass on the basis of the same chiral effective field theory in the first two nontrivial orders ($O(p^3)$ and $O(p^4)$) [5]. We find for a spatial box of length L

$$m_N(L) - m_N(\infty) = \Delta_3(L) + \Delta_4(L) + O(p^5)\,,$$

where the $O(p^3)$ contribution is given by

$$\Delta_3(L) = \frac{3g_A^2 m_0 m_\pi^2}{16\pi^2 f_\pi^2} \int_0^\infty \mathrm{d}x \sum_{\vec{n}\neq\vec{0}} K_0\left(L|\vec{n}|\sqrt{m_0^2 x^2 + m_\pi^2(1-x)}\right)$$

and the correction of $O(p^4)$ reads

$$\Delta_4(L) = \frac{3m_\pi^4}{4\pi^2 f_\pi^2} \sum_{\vec{n}\neq\vec{0}} \left[(2c_1 - c_3)\frac{K_1(L|\vec{n}|m_\pi)}{L|\vec{n}|m_\pi} + c_2 \frac{K_2(L|\vec{n}|m_\pi)}{(L|\vec{n}|m_\pi)^2}\right] .$$

Here $K_\nu(z)$ are modified Bessel functions and m_0 denotes the nucleon mass in the chiral limit. The coupling constants g_A, f_π, c_i appear already in the infinite volume theory. They do not depend on L and are also taken in the chiral limit. The finite volume does not introduce any new parameter! Therefore we can take the values of the coupling constants from the analysis of the nucleon masses in large volumes, supplemented by some phenomenological input, to obtain a parameter-free prediction of the finite size effects. In Fig. 1 this is compared with Monte Carlo data [3] for $m_\pi = 545\,\mathrm{MeV}$ demonstrating a surprisingly good agreement. So we think that we have made some progress towards a better understanding of the nucleon.

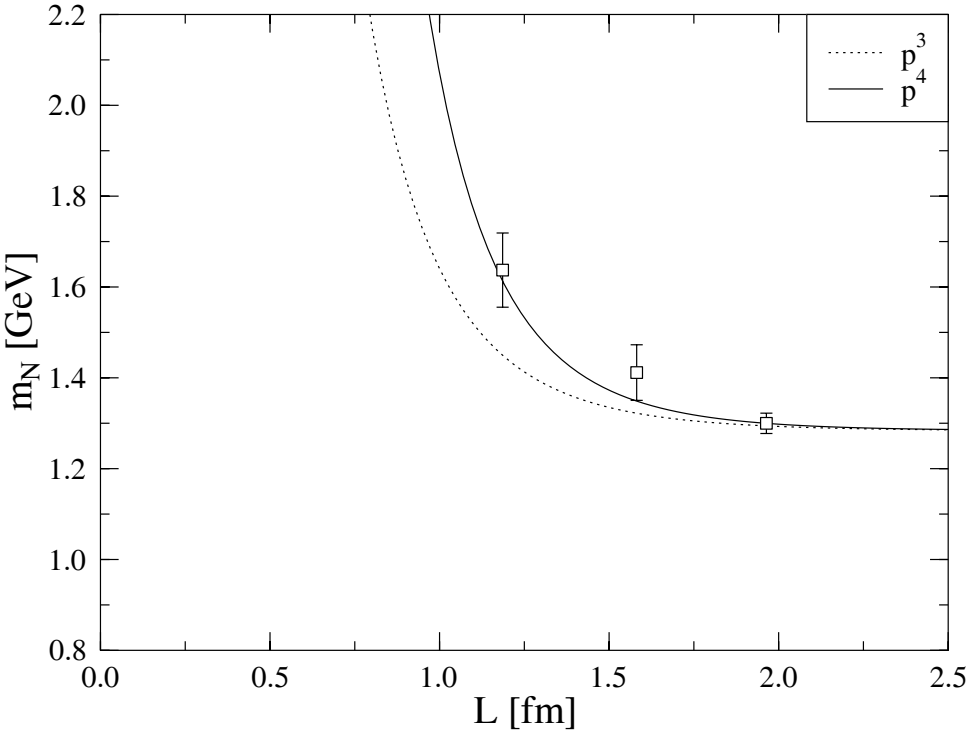

Fig. 1: Volume dependence of the nucleon mass for $m_\pi = 545\,\mathrm{MeV}$. The dotted curve shows the contribution of the p^3 term, while the solid curve includes also the p^4 correction.

[1] C. R. Allton, S. P. Booth, K. C. Bowler, J. Garden, A. Hart, D. Hepburn, A. C. Irving, B. Joó, R. D. Kenway, C. M. Maynard, C. McNeile, C. Michael, S. M. Pickles, J. C. Sexton, K. J. Sharkey, Z. Sroczynski, M. Talevi, M. Teper and H. Wittig, Phys. Rev. D **65** (2002) 054502.

[2] A. Ali Khan, S. Aoki, G. Boyd, R. Burkhalter, S. Ejiri, M. Fukugita, S. Hashimoto, N. Ishizuka, Y. Iwasaki, K. Kanaya, T. Kaneko, Y. Kuramashi, T. Manke, K. Nagai, M. Okawa, H. P. Shanahan, A. Ukawa and T. Yoshié (CP-PACS Collaboration), Phys. Rev. D **65** (2002) 054505; Erratum ibid. D **67** (2003) 059901.

[3] S. Aoki, R. Burkhalter, M. Fukugita, S. Hashimoto, K.-I. Ishikawa, N. Ishizuka, Y. Iwasaki, K. Kanaya, T. Kaneko, Y. Kuramashi, M. Okawa, T. Onogi, N. Tsutsui, A. Ukawa, N. Yamada and T. Yoshié (JLQCD Collaboration), Phys. Rev. D **68** (2003) 054502.

[4] M. Procura, T. R. Hemmert and W. Weise, Phys. Rev. D **69** (2004) 034505.

[5] A. Ali Khan, T. Bakeyev, M. Göckeler, T. R. Hemmert, R. Horsley, A. C. Irving, B. Joó, D. Pleiter, P. E. L. Rakow, G. Schierholz and H. Stüben, arXiv:hep-lat/0312030.

External Cooperations

Academic

A. Ali Khan (Humboldt Universität zu Berlin)
T. Bakeyev (Joint Institute for Nuclear Research, Dubna)

T.R. Hemmert (Technische Universität München)
R. Horsley and B. Joó (University of Edinburgh)
A.C. Irving and P. E. L. Rakow (University of Liverpool)
D. Pleiter (John von Neumann–Institut für Computing NIC, Zeuthen)
G. Schierholz (John von Neumann–Institut für Computing NIC, Zeuthen, and DESY, Hamburg)
H. Stüben (Konrad-Zuse-Zentrum für Informationstechnik Berlin)

Funding

This project has been supported in part by the European Community's Human Potential Program under contract HPRN-CT-2000-00145, Hadrons/Lattice QCD and by the DFG (Forschergruppe Gitter-Hadronen-Phänomenologie).
The numerical calculations have been performed on the Hitachi SR8000 at LRZ (Munich), on the Cray T3E at EPCC (Edinburgh) under PPARC grant PPA/G/S/1998/00777, on the Cray T3E at NIC (Jülich) and ZIB (Berlin), as well as on the APE1000 and Quadrics at DESY (Zeuthen). We thank all institutions for their support.

5.3.4 The photon propagator in compact QED(2+1): The effect of wrapping Dirac strings

A. Schiller

In this project we continue to study the photon propagator in three dimensions.

We discuss the influence of closed Dirac strings on the photon propagator in the Landau gauge emerging from a study of the compact U(1) gauge model in 2+1 dimensions. This gauge also minimizes the total length of the Dirac strings. Closed Dirac strings are stable against local gauge-fixing algorithms only due to the torus boundary conditions of the lattice. We demonstrate that these left-over Dirac strings are responsible for the previously observed unphysical behavior of the propagator of space-like photons (D_T) in the deconfinement (high temperature) phase. We show how one can monitor the number N_3 of thermal Dirac strings which allows to separate the propagator measurements into N_3 sectors. The propagator in $N_3 \neq 0$ sectors is characterized by a non–zero mass and an anomalous dimension similarly to the confinement phase. Both mass squared and anomalous dimension are found to be proportional to N_3. Consequently, in the $N_3 = 0$ sector the unphysical behavior of the D_T photon propagator is cured and the deviation from the free massless propagator disappears.

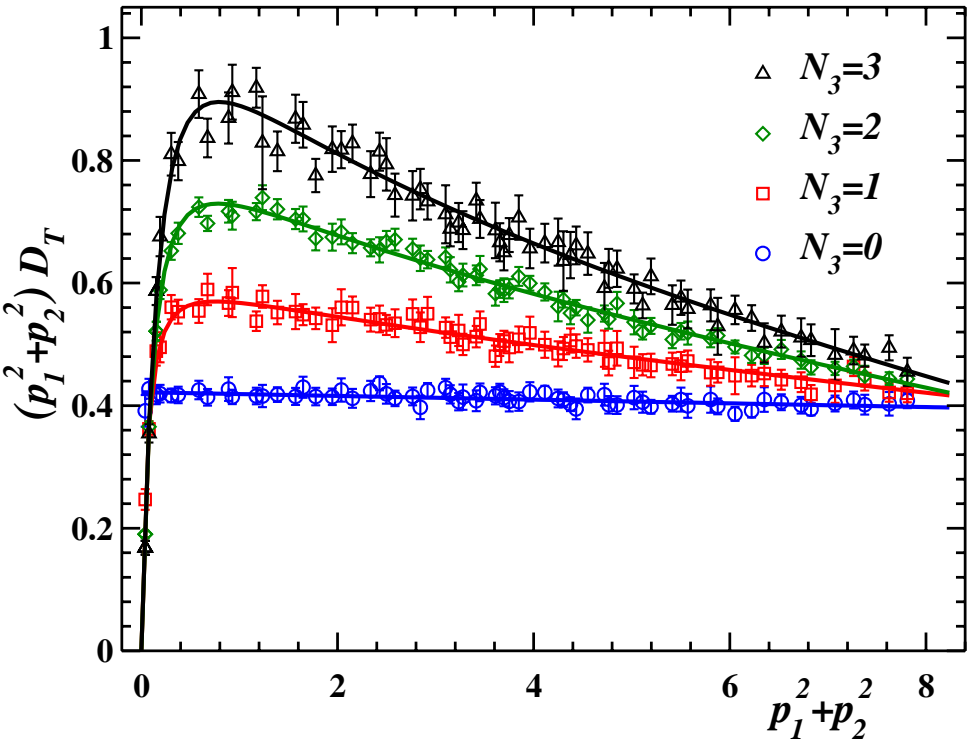

Fig. 1: The total form factor D_T for spatial photons in the different thermal Dirac string sectors

[1] M. N. Chernodub, E. M. Ilgenfritz and A. Schiller, Phys. Rev. D **67** (2003) 034502

[2] M. N. Chernodub, E. M. Ilgenfritz and A. Schiller, arXiv:hep-lat/0311033, Phys. Rev. D to appear (2004)

External Cooperations

Academic

M.N. Chernodub (Kanazawa U., Inst. Theor. Phys. & Moscow, ITEP)
E.-M. Ilgenfritz (Humboldt U., Berlin)

Organizational Duties

A. Schiller
Referee: Phys. Rev. D

Funding

The project is supported from the grants RFBR 01-02-17456, DFG 436 RUS 113/73910 and RFBR-DFG 03-02-04016. and by DFG through the DFG-Forschergruppe "Lattice Hadron Phenomenology" (FOR 465).

5.3.5 Quark spectra and light hadron phenomenology from overlap fermions with improved gauge field action

A. Schiller (UKQCD-QCDSF-collaboration)

Lattice calculations at small quark masses, i.e. in the chiral regime, require actions with good chiral properties. Overlap fermions have an exact chiral symmetry on the lattice and thus are predestined for this task. A further advantage of overlap fermions is that they are automatically $O(a)$ improved.

The massive overlap operator is defined by

$$D = \big(1 - \frac{am_q}{2\rho}\big)\, D_N + m_q\,, \quad D_N = \frac{\rho}{a}\big(1 + \frac{X}{\sqrt{X^\dagger X}}\big)\,, \quad X = D_W - \frac{\rho}{a},$$

where D_W is the Wilson-Dirac operator.

We present first results from a simulation of quenched overlap fermions with improved gauge field action. Among the quantities we study are the spectral properties of the overlap operator, the chiral condensate and topological charge, quark and hadron masses, and selected nucleon matrix elements. To make contact with continuum physics, we compute the renormalization constants of quark bilinear operators in perturbation theory and beyond.

[1] D. Galletly, M. Gürtler, R. Horsley, B. Joo, A.D. Kennedy, H. Perlt, B.J. Pendleton, P.E.L. Rakow, G. Schierholz, A. Schiller, T. Streuer, arXiv:hep-lat/0310028.

[2] T. Bakeyev *et al.* [QCDSF-UKQCD Collaboration], arXiv:hep-lat/0311017.

External Cooperations

Academic

T. Bakeyev (Dubna, JINR)
D. Galletly, R. Horsley, B. Joo, A.D. Kennedy, B. Pendleton (Edinburgh U.)
M. Gürtler, D. Pleiter, T. Streuer (NIC, Zeuthen & DESY Zeuthen)
H. Perlt (Regensburg U.)
P.E.L. Rakow (Liverpool U., Dept. Math.)
G. Schierholz (NIC, Zeuthen & DESY Hamburg)
H. Stuben (NIC, Zeuthen & Konrad Zuse Zent. Informationstech.)

Funding

This work is supported by the European Community's Human Potential Program under contract HPRN-CT-2000-00145 Hadrons/Lattice QCD and by DFG under contract FOR 465 (Forschergruppe Gitter-Hadronen-Phänomenologie).
The numerical calculations have been performed at NIC Jülich, ZIB Berlin and NeSC Edinburgh (IBM Regatta), NIC Zeuthen and Southampton (PC Cluster), and HPCF Cranfield (SunFire). We thank these institutions for support.

5.3.6 Double gauging of $U(1)$ symmetry on noncommutative space

Yi Liao, Klaus Sibold

Charge is a global property of fields. Its conservation implies a global $U(1)$ symmetry. When the symmetry is gauged on ordinary spacetime, the charge of a field specifies how the field transforms locally together with the gauge field. This gauging procedure may be generalized to field theory on noncommutative (NC) spacetime in the approach of the Moyal-Weyl correspondence. In $U(1)$ gauge theory, the following types of matter field transformation rules have been studied [1]

$$\begin{aligned} \psi_+(x) &\to U(x) \star \psi_+(x), \\ \psi_-(x) &\to \psi_-(x) \star U^{-1}(x), \\ \psi_0(x) &\to U(x) \star \psi_0(x) \star U^{-1}(x), \end{aligned}$$

besides the trivial identity representation. In our work [2] we pointed out a new transformation rule for matter fields that is more general than the ones listed above, i.e.,

$$\varphi(x) \to U_L(x) \star \varphi(x) \star U_R^{-1}(x),$$

where $U_{L,R}(x)$ are two independent starred exponentials. This generalization is based on the following observation. The fact that the φ field carries a conserved, additive charge is strong enough to fix uniquely its local transformation rule on ordinary spacetime but not so on NC spacetime where the commutative point-wise multiplication is replaced by the noncommutative star product. The order of factors becomes relevant as we already saw in the transformation rules for the above ψ fields. On the other hand, as far as charge is concerned, the requirement that must be met is the global transformation rule of the charged field for which there is no difference between the point-wise and star product. This is indeed the case for the new rule: for constant $U_{L,R}$, only the combination $U = U_L U_R^{-1}$ is relevant. Furthermore, multiplying more factors like $U_{L,R}(x)$ from the left or right is ambiguous because the order of these factors, while relevant due to the star, is not a well-defined concept. This makes the new rule the most general transformation that can be assumed for a charged field.

The implementation of the new transformation rule necessarily demands two $U(1)$ gauge bosons and thus a double gauging of one global $U(1)$ symmetry on NC space. We suggested how the resulting theory should be interpreted in terms of physical degrees of freedom that are identified using the global property of charge: one gauge boson interacts with the charge while the other interacts only noncommutatively and thus decouples on ordinary space. We have also shown that the interactions in this theory have a richer structure than those obtained by a direct gauging of the charge $U(1)$ symmetry.

[1] M. Hayakawa, Phys. Lett. B478, 394 (2000) and hep-th/9912167.
[2] Y. Liao, K. Sibold, Phys. Lett. B586, 420 (2004).

5.3.7 CKM matrix renormalization

Yi Liao

Since the Cabibbo-Kobayashi-Maskawa (CKM) matrix appearing in the charged current sector of the standard model (SM) contains free physical parameters, it will generally be subject to renormalization. However, compared to other physical parameters in SM, there is no renormalization scheme that is more physically motivated than others. The necessity to renormalize the CKM matrix in order to obtain an ultraviolet (UV) finite result for a physical amplitude was first emphasized in Ref. [1] for two generations. The case of three generations was then studied in Ref. [2] in the on-shell renormalization scheme of SM. Unfortunately, the prescription proposed by the latter was shown to contain a UV finite part that is gauge parameter dependent [3], which must be avoided for physical parameters. Other alternative prescriptions were also suggested [4]. All of these differ only in a UV finite and gauge parameter independent part in the counterterm for the CKM matrix and can thus be understood as renormalization scheme dependence.

In our work [5] we showed how a simple inspection of the one loop contribution to quark self-energies suggests a way of splitting them: one part that is UV divergent but gauge parameter independent, to be absorbed into the CKM matrix counterterm, and the other that is UV finite but gauge parameter dependent, to be put back to form renormalized physical amplitudes. The CKM matrix counterterm so obtained shares with all proposals made so far the requisite properties: gauge parameter independence, unitarity constraints and absorption of the remaining UV divergence in physical amplitudes. It also enjoys a nice feature that is incorporated in some of those prescriptions; namely, the renormalized physical amplitudes are smooth when the up-type (or down-type) quark masses approach each other. We also made a point that seems to have not been emphasized in the literature. When one works in a specific representation of the CKM matrix which is often convenient in practical calculations, caution must be exercised in interpreting the CKM matrix counterterm in terms of its rotation angles and CP phase. There is a relative rephasing, i.e., a change of representations between the bare and renormalized CKM matrices due to renormalization effects. This rephasing must be removed before one can write down the counterterms for those angles and phase. We showed how this can be done using the degrees of freedom available in the on-shell renormalization scheme.

[1] W.J. Marciano, A. Sirlin, Nucl. Phys. B93, 303 (1975).
[2] A. Denner, T. Sack, Nucl. Phys. B347, 203 (1990).
[3] P. Gambino, P.A. Grassi, F. Madricardo, Phys. Lett. B454, 98 (1999).
[4] B.A. Kniehl, *et. al.*, Phys. Rev. D62, 073010 (2000); A. Barroso, *et. al.*, Phys. Rev. D62, 096003 (2000); K.-P.O. Diener and B.A. Kniehl, Nucl. Phys. B617, 291 (2001); Y. Yamada, Phys. Rev. D64, 036008 (2001); A. Pilaftsis, Phys. Rev. D65, 115013 (2002); D. Espriu, *et. al.*, Phys. Rev. D66, 076002 (2002); Y. Zhou, J. Phys. G29, 1031 (2003).
[5] Y. Liao, Phys. Rev. D69, 016001 (2004).

External Cooperations

DESY in Hamburg
Prof. Dr. P.M. Zerwas

5.3.8 $N = 4$ supersymmetric Yang-Mills theory

P. Heslop

There has been greatly renewed interest in the study of superconformal field theories in four dimensions, following from the conjectured correspondence connecting these with supergravity or string theory on anti de-Sitter spacetime backgrounds: the AdS/CFT correspondence [1]. Superconformal field theories and in particular $N = 4$ super Yang-Mills (SYM) theory are also of great interest in their own right. $N = 4$ SYM is the most symmetric known flat space quantum field theory in four dimensions (more than 4 supersymmetries leads to curved spacetime.) It is a gauge theory whose classical Lagrangian is uniquely determined given the gauge group and a value of the coupling constant. These properties give the theory great theoretical and pedagogical interest: one studies this theory as a stepping stone for learning more about more complicated but phenomenologically more interesting gauge theories such as QCD or GUTs. In particular one would like to study the extent to which the theory is determined by its symmetries.

A program was initiated in [2] to study Greens functions of certain operators- known as chiral primary operators (CPOs)- in $N = 4$ SYM. In particular one wishes to solve the superconformal Ward identities which are assumed to hold for these correlation functions, with the aid of a particular superspace known as analytic superspace [3]. This superspace has many nice properties: the entire superconformal symmetry is manifest; superconformal fields satisfy simple analyticity constraints only; it has a structure which is very similar to Minkowski space.

In [4] we have extended this analysis to completely solve (at least in principle) the Ward identities for all Greens functions of all gauge invariant operators in the theory. We have also performed a complete analysis of an additional $U(1)$ group which is a symmetry of a sector of the theory and which leads to the non-renormalisation of some Greens functions via the reduction formula.

In [5] we wrote explicitly the four-point functions of CPOs of arbitrary charge for the first time, allowing a comparison with supergravity on AdS via the AdS/CFT correspondence. A summary of analytic superspace and its application to $N = 4$ SYM is given in [7].

In [6] we considered the next simplest operators in $N = 4$ SYM (after the CPOs) known as quarter BPS operators. By finding the perturbative two point functions of these operators and considering them on a different analytic superspace ideally suited for these operators we were able to resolve a puzzle concerning the compatibility of these with superconformal symmetry.

[1] J. M. Maldacena, Adv. Theor. Math. Phys. **2** (1998) 231 [Int. J. Theor. Phys. **38** (1999) 1113]; E. Witten, Adv. Theor. Math. Phys. **2** (1998) 253; S. S. Gubser, I. R. Klebanov and A. M. Polyakov, Phys. Lett. B **428** (1998) 105.

[2] P. S. Howe and P. C. West, Int. J. Mod. Phys. A **14** (1999) 2659.

[3] P. S. Howe and G. G. Hartwell, Class. Quant. Grav. **12** (1995) 1823.

[4] P. J. Heslop and P. S. Howe, JHEP **0401** (2004) 058.

[5] P. J. Heslop and P. S. Howe, JHEP **0301** (2003) 043.

[6] P. J. Heslop, arXiv:hep-th/0403144.

[7] E. D'Hoker, P. Heslop, P. Howe and A. V. Ryzhov, JHEP **0304** (2003) 038.

Funding

The project is supported by a grant from DESY in Zeuthen.

5.3.9 Organizational duties

Klaus Sibold
Vice dean of the faculty "Physics and earth sciences"
Director of the ITP
Member of the "Forschungskommission" of the university
Member of the "Ger"atekommission" of the university
Member of the "Graduiertenkolleg: Quantenfeldtheorie"
Associated member of the Graduiertenkolleg: Analysis, Geometrie und die Naturwissenschaften"
Coorganizer of the "Mitteldeutsche Phyik-Combo" (joint graduate lecture courses with universities Jena and Halle)

5.3.10 Publications

Journals

1. A. Ivanov and R. Kirschner,
   Electroproduction of vector mesons: Factorization of end-point contributions,
   Eur. Phys. J. C **29** (2003) 353 [arXiv:hep-ph/0301182].

2. Ali Khan, A., Bakeyev, T., Göckeler, M., Horsley, R., Pleiter, D., Rakow, P., Schäfer, A., Schierholz, G., Stüben, H.
   Accelerating the hybrid Monte Carlo algorithm.
   Phys. Lett. **B564** (2003) 235-240.

3. Braun, V.M., Burch, T., Gattringer, C., Göckeler, M., Lacagnina, G., Schaefer, S., Schäfer, A.
   Lattice calculation of vector meson couplings to the vector and tensor currents using chirally improved fermions
   Phys. Rev. **D68** (2003) 054501-(1-6).

4. M. N. Chernodub, E. M. Ilgenfritz and A. Schiller,
   Confinement and the photon propagator in 3D compact QED: A lattice study in Landau gauge at zero and finite temperature
   Phys. Rev. D **67** (2003) 034502-(1-16).

5. M. N. Chernodub, E. M. Ilgenfritz and A. Schiller,
   More on string breaking in the 3D Abelian Higgs model: The photon propagator,
   Phys. Lett. B **555** (2003) 206-214.

6. C. Carimalo, A. Schiller and V. G. Serbo,
New method for calculating helicity amplitudes of jet-like QED processes i for high-energy colliders. II: Processes with lepton pair production,
Eur. Phys. J. C **29** (2003) 341-351.

7. P. J. Heslop and P. S. Howe,
Four-point functions in N = 4 SYM.
JHEP **0301** (2003) 043 [arXiv:hep-th/0211252].

8. E. D'Hoker, P. Heslop, P. Howe and A. V. Ryzhov,
Systematics of quarter BPS operators in N = 4 SYM.
JHEP **0304** (2003) 038.

9. J. M. Drummond, P. J. Heslop, P. S. Howe and S. F. Kerstan,
Integral invariants in N = 4 SYM and the effective action for coincident D-branes.
JHEP **0308** (2003) 016.

10. P. J. Heslop and P. S. Howe,
Aspects of N = 4 SYM.
JHEP **0401** (2004) 058.

11. Y. Liao, C. Dehne
Some phenomenological consequences of the time-ordered perturbation theory of QED on noncommutative spacetime
Eur. Phys. J. C29, 125 (2003)

in press

1. S. Derkachov, D. Karakhanyan and R. Kirschner
Universal R operator with Jordanian deformation of conformal symmetry,
Nucl. Phys. B in press, [arXiv:nlin.si/0310019].

Conference contributions

1. A. Ivanov and R. Kirschner,
Electroproduction of vector mesons
XI Intenational Workshop on Deep Inelastic Scattering, St. Petersburg April 2003,
Talk published in Proceedings,
V.T. Kim and L.N. Lipatov (eds.), publisher Petersburg Nuclear Physics, Institute Gatchina 2003, pp. 272 - 276.

2. R. Kirschner,
Prospects of Quantum Informatics ,
Second International Symposium on Stochastic Algorithms, SAGA 2003, Hatfield, UK, Sept. 2003, inv talk, published in the Proceedings:
Springer Lecture Notes in Computer Science No. 2827, A. Albrecht, K. Steinhöfel (eds.)
Springer Verl. 2003, pp. 1 - 9.

3. Göckeler, M., Horsley, R., Pleiter, D., Rakow, P.E.L., Schäfer, A., Schierholz, G.
Calculation of moments of structure functions
Nucl. Phys. B (Proc. Suppl.) 119 (2003) 32-40.

4. Göckeler, M., Horsley, R., Pleiter, D., Rakow, P.E.L., Schierholz, G.
Structure functions near the chiral limit
Nucl. Phys. B (Proc. Suppl.) 119 (2003) 398-400.

5. Ali Khan, A., Bakeyev, T., Göckeler, M., Horsley, R., Irving, A.C., Pleiter, D., Rakow, P., Schierholz, G., Stüben. H.
Finite size effects in nucleon masses in dynamical QCD
Nucl. Phys. B (Proc. Suppl.) 119 (2003) 419-421.

6. Bakeyev, T., Göckeler, M., Horsley, R., Pleiter, D., Rakow, P.E.L., Schäfer, A., Schierholz, G., Stüben. H.
A non-perturbative determination of Z_V and b_V for $O(a)$ improved quenched and unquenched Wilson fermions
Nucl. Phys. B (Proc. Suppl.) 119 (2003) 467-469.

7. Gattringer, C., Göckeler, M., Hasenfratz, P., Hauswirth, S., Holland, K., Jörg, T., Juge, K.J., Lang, C.B., Niedermayer, F., Rakow, P.E.L., Schaefer, S., Schäfer, A.
Quenched QCD with fixed-point and chirally improved fermions
Nucl. Phys. B (Proc. Suppl.) 119 (2003) 796-812.

8. M. N. Chernodub, E. M. Ilgenfritz and A. Schiller,
Monopoles, confinement and the photon propagator in QED_3
Nucl. Phys. Proc. Suppl. **119** (2003) 766-768.

9. M. N. Chernodub, E. M. Ilgenfritz and A. Schiller,
Confinement, deconfinement and the photon propagator in 3D cQED on the lattice
Gargnano 2002, Quark confinement and the hadron spectrum, World Scientific 2003, 249-251.

10. C. Carimalo, A. Schiller and V. G. Serbo,
A new method for calculating jet-like QED processes
Proc. Photon 2003: Int. Conference on the Structure and Interactions of the Photon and 15th Int. Workshop on Photon-Photon Collisions, Frascati
arXiv:hep-ph/0305293, pp 1-6

11. P. J. Heslop,
Superconformal field theories in analytic superspace.
Proceedings of the International Workshop "Supersymmetries and Quantum Symmetries" (SQS'03, 24-29 July, 2003), JINR Publishing, Dubna, Russia.

5.3.11 Graduations

PhD

Yong Zhang
Conformal symmetry and the S-matrix

5.4 Theory of Condensed Matter

5.4.1 General Scientific Goals

The topics of research in the Theory of Condensed Matter group are stochasticity and disorder as well as structure formation in soft condensed matter and solids, models of complex biological systems, strongly correlated electron systems, and superconducting materials. Investigations using modern analytic methods and computer applications complement and stimulate each other. Research is performed in cooperation with mathematicians as well as with theoretical and experimental physicists, biologists and researchers in medicine. There are well established collaborations with research groups in France, Germany, Italy, Russia, Switzerland, UK, and USA.

Noise induced phenomena are studied in a number of different systems. Structure formation, stochastic stability, and on-off intermittency is investigated in liquid crystals driven by stochastic electric fields (Cooperation with the Institute for Experimental Physics I). Noise induced non-equilibrium phase transitions are studied in coupled arrays of stochastically driven nonlinear systems. The statistics of first passage times and self-organized criticality is investigated in stochastic nonlinear systems with time delay.

Mathematical modeling of the immune system. Using methods of nonlinear dynamics and statistical physics, we study the architecture and the random evolution of the idiotypic network of the B-cell subsystem and describe the regulation of balance of Th1/Th2-cell subsystems, its relation to allergy and the hyposensitization therapy (Cooperation with the Institute for Clinical Immunology and Transfusion Medicine).

Strongly correlated electron systems. The unconventional magnetic properties of transition metal oxides, such as the mixed-valency manganites, are investigated on the basis of correlation models including anisotropic Heisenberg-type exchange interactions. Using Green's function techniques the effects of magnetic short-range order at arbitrary temperatures are studied in comparison with experiments.

Superconductors. Conventional and high-temperature superconductivity are studied within a gauge field theory by drawing parallels between an Abelian Higgs-like model in the isotropic case and a time-dependent Lawrence-Doniach model for layered high-T_c cuprates. The aim is the macroscopic derivation of an effective action to describe the dynamics of the superconducting condensate at zero temperature in the presence of electromagnetism.

5.4.2 Nonlinear Dynamics and Statistical Physics of the Immune System

Ulrich Behn, Markus Brede and Jan Richter

The immune system is a hierarchically organized natural adaptive system built by a macroscopic number of constituents which shows a very complex behavior on several scales of temporal, spatial, and functional organization. It is thus naturally a subject of modelling with methods of statistical physics and nonlinear dynamics, for recent reviews see, e.g., [1-3]. We investigate models describing the architecture of the idiotypic network formed by the subsystem of B-lymphocytes and the regulation of the Th1-Th2 balance of the T-lymphocyte subsystem.

B-cells express on their surface receptors (antibodies) of a given specificity (idiotype). Crosslinking these receptors by complementary structures (antigen or antibodies) stimulates the lymphocyte to proliferate. Thus even without antigen there is a large functional network of interacting lymphocytes, the idiotypic network. Both the potential repertoire and the number of idiotypes expressed by an individual at a given time (the expressed repertoire) are of macroscopic order. In the frame of a simple bit-string model we investigate the architecture of a randomly generated idiotypic network [4,5]. We identify a working regime above the percolation transition where a giant cluster coexists with many small clusters, such that immunological demands as the completeness of the repertoire and a persistent immunological memory preserved by the internal image of antigen can be fulfilled. The dynamics of the idiotypic network is driven by the influx of new idiotypes randomly produced in the bone marrow and by the population dynamics of the lymphocytes themself. Modelling this dynamics by simple cellular automata rules we describe the architecture of the idiotypic network as the highly organized product of a random temporal evolution.

T-helper lymphocytes have subtypes which differ in their spectrum of secreted cytokines. These cytokines have autocrine effects on the own subtype and cross-suppressive effects on the other subtype and regulate further the type of immunoglobulines secreted by B-lymphocytes. The balance of Th1- and Th2-cells is perturbed in several diseases. For example, in allergy the response to allergen is Th2-dominated. A widespread and successful therapy consists in the injection of increasing doses of allergen following empirically justified protocols of administration. We seek an explanation of this therapy studying the nonlinear dynamics of a nonautonomous system of few variables which describes the Th1/Th2 populations in the sense of a mean field theory [6-9]. Indeed, the system is driven by proper injections of allergen towards new attractors, where the response is Th1-dominated as for healthy individuals. The target of the initial phase of the therapy whith increasing doses of allergen is in our view not primarily the T-cell system but it is to desensitize mast cells and basophils, so that the larger doses during the maintenance phase of the therapy do not cause allergic symptoms. This is corroborated by a model describing the dynamics of the mast cell stimulation and the intracellular Calcium response that triggers the release of inflammatory mediators. A clinical study [9] shows a significant decrease of specific IgE accompanied by an increase of specific IgG4 due to the therapy in accordance with predictions of the model. These investigations are performed in collaboration with Prof. G. Metzner (Institute of Clinical Immunology).

The project is supported by the Graduiertenförderung des Freistaates Sachsen.

[1] A. S. Perelson and G. Weisbuch, Rev. Mod. Phys. **69** 1219 (1997).
[2] U. Behn, F. Celada, and P. E. Seiden, in: *Frontiers of Life*, Vol. II, Part Two: *The Immunological System*, eds. A. Lanzavecchia, B. Malissen and R. Sitia, (Academic Press, London, 2001), p. 611.
[3] U. Behn, M. Brede, and J. Richter, in: Function and regulation of cellular systems: Experiments and Models, A. Deutsch, J. Howard, M. Falcke, W. Zimmermann (Eds.), Birkhäuser, Basel (2004), 399-410.
[4] M. Brede and U. Behn, Phys. Rev. E **64**, 011908 (2001), ibid. **67**, 031920 (2003).
[5] M. Brede, *Randomly evolving idiotypic networks: Dynamics and architecture*, PhD thesis, University of Leipzig 2003.
[6] J. Richter, G. Metzner and U. Behn, J. Theor. Med. **4**, 119 (2002).
[7] J. Richter, *Nonlinear Dynamics of Models Describing Th1/Th2 Regulation, Allergy and Venom Immunotherapy*, PhD thesis, University of Leipzig 2003.
[8] J. Richter, U. Behn, and G. Metzner, in: Clinical Immunology and Allergy in Medicine, Proc. 21st EAACI Congress 2002, Naples, G. Marone (Ed.), JGC Editions, Naples (2003), 257-262.

5.4.3 On-off Intermittency in Nematic Liquid Crystals Driven by Multiplicative Noise

Ulrich Behn, Thomas John, Ralf Stannarius

Electrohydrodynamic convection (EHC) in liquid crystals is a well investigated phenomenon of pattern formation, its physical mechanism is understood and it is easily accessible to experimental control and observation. This allows a quantitative comparison of theoretical models with experimental results; for a recent review see [1]. We investigate on-off intermittency [2] in electrohydrodynamic convection of nematic liquid crystals driven by a stochastic dichotomous electric voltage.

If the characteristic times of the system are well separated from the correlation time of the noise, the onset of the roll pattern is sharp, similar to the case of deterministic driving. If these times are of the same order as it is typical for pure stochastic driving one observes outbursts of spatially regular roll pattern which interrupt quiescent (laminar) periods. The phenomenon is related to the persistence problem of a suitable random walk. At the sample stability threshold [3] the probability distribution of laminar periods is a power law with exponent -3/2 over several decades. We found a quantitative agreement of experiment, analytical results, and simulations of the nemato-electrohydrodynamic equations of the basic model. The phenomenon represents thus a first example of on-off intermittency in a spatially extended dissipative system [4].

In addition to the previous experiment based on orthoscopic microscopy the distribution of laminar periods and other statistical characteristics of the stochastic signal as the distribution of amplitudes and the power spectrum are determined by laser scattering techniques [5] and compared with theoretical results and simulations [6,7]. Again, at the stochastic stability threshold universal scaling laws are found over several orders of magnitude. Using laser scattering technique first explorations of noise induced wave number selection have been performed.

Our theoretical and experimental findings are corroborated by investigations of a phenomenological Swift-Hohenberg model by Fujisaka and coworkers [8].

The project is supported by the Deutsche Forschungsgemeinschaft (BE 1417/4-2).

[1] W. Pesch and U. Behn, in *Evolution of Spontaneous Structures in Dissipative Continuous Systems*, eds. F. H. Busse and S. C. Mueller (Springer, Berlin, 1998), p. 335.
[2] H. Fujisaka and T. Yamada, Progr. Theor. Phys. **74**, 918 (1985); N. Platt, E. A. Spiegel and C. Tresser, Phys. Rev. Lett. **70** 279 (1993); J. F. Heagy, N. Platt and S. M. Hammel, Phys. Rev. E **49** 1140 (1994).
[3] U. Behn, A. Lange and T. John, Phys. Rev. E **58** 2047 (1998).
[4] T. John, R. Stannarius and U. Behn, Phys. Rev. Lett. **83**, 749 (1999).
[5] T. John, U. Behn and R. Stannarius, Europhys. J. B. **35**, 267 (2003).
[6] U. Behn, T. John and R. Stannarius, in: *Proc. 6th Experimental Chaos Conference, 22-26 July 2001, Potsdam, Germany*, eds. S Boccaletti, B. J. Gluckman, J. Kurths, L. M. Pecora, M. L. Spano, AIP Conference Proceedings **622** (American Institute of Physics, Melville, New York, 2002), p. 381.
[7] T. John, U. Behn and R. Stannarius, Phys. Rev. E **65**, 046229 (2002).
[8] H. Fujisaka, K. Ouchi, H. Ohara, Phys. Rev. E **64** 036201 (2001); H. Ohara, H. Fujisaka, K. Ouchi, Phys. Rev. E 67 **67** 046223 (2003).

5.4.4 Noise Induced Phenomena in Nonlinear Systems

Ulrich Behn, Micaela Krieger-Hauwede, Arne Traulsen, Edgar Martin

We describe non-equilibrium phase transitions [1] in arrays of spatially coupled dynamical systems with cubic nonlinearity driven by multiplicative Gaussian white noise (Stratonovich models). Depending on the sign of the harmonic spatial coupling we observe transitions from a state with zero order parameter to a ferromagnetic [2] or an antiferromagnetic stationary state varying the control parameter. Antiferromagnetic ordering is considered for the first time in this class of models. We determine the phase diagram, the order of the transitions [3], and the critical behaviour for both global coupling and nearest neighbour coupling on simple cubic lattices comparing analytical results in mean field approximation and numerical simulations. In mean field approximation we give an analytical result for the critical exponent of the magnetization which exhibits a transition from the classical universal value 1/2 to a non-universal behaviour with increasing ratio of noise strength and magnitude of the spatial coupling [4]. The critical exponent of the magnetization as a function of the strength of the spatial coupling has been determined. Similar results can be obtained for models with other nonlinearities, universality classes have been determined [5].

Spatially coupled stochastically driven systems are considered in the continuum limit which leads to stochastic partial differential equations. We show that it is preferable to use spatiotemporal colored noise in order to avoid unphysical divergencies in this limit [6]. A generalization of the Ornstein-Uhlenbeck process in $1 + 1$ dimensions is proposed [7].

For a class of stochastically driven nonlinear systems with delayed time argument we investigated the persistence problem and determined the probability density of first passage times. For systems spontaneously evolving to a marginally stable state the density is a power law over several decades in close analogy to self-organized criticality in spatially extended systems. The marginally stable linear system was considered in the parameter range where the instability is towards oscillating solutions and the corresponding characteristic exponent was determined.

For a class of generalized diffusion processes the asymptotic behavior of the distribution of first return times is analytically determined [8].

[1] C. Van den Broeck, J. M. R. Parrondo and R. Toral, Phys. Rev. Lett. **73**, 3395 (1994); J. Garcia-Ojalvo, J. M. Sancho, *Noise in Spatially Extended Systems*, (Springer, New York, 1999).
[2] W. Genovese and M. A. Muñoz, Phys. Rev. E **60**, 69 (1999).
[3] R. Müller, K. Lippert, A. Kühnel and U. Behn, Phys. Rev. E **56**, 2658 (1997).
[4] T. Birner, K. Lippert, R. Müller, A. Kühnel and U. Behn, Phys. Rev. E **65**, 046110 (2002).
[5] J. Przybilla, *Kritisches Verhalten in global gekoppelten rauschgetriebenen nichtlinearen Systemen*, Diploma thesis, University of Leipzig (2002).
[6] A. Traulsen, *Coupled stochastically driven systems in the continuum limit*, Diploma thesis, University of Leipzig (2002).
[7] A. Traulsen, K. Lippert, U. Behn, Phys. Rev. E **69**, 026116 (2004).
[8] O. E. Martin, *Wiederkehrzeitverteilungen in rauschgetriebenen nichtlinearen Systemen*, Diploma thesis, University of Leipzig (2003).

5.4.5 Spin Correlations in Manganites

D. Ihle, I. Junger and H. Fehske (Universität Greifswald)

The manganites $R_{1-x}A_xMnO_3$ ($R = La, Pr, Nd$ and $A = Sr, Ca, Ba, Pb$) have attracted renewed attention when the phenomenon of colossal magnetoresistance near the phase transition from the ferromagnetic metallic to the paramagnetic insulating phase was discovered [1,2]. It is important to understand first of all the observed magnetic and orbital order and the low-energy excitations in the undoped insulating compound $LaMnO_3$. Neutron-scattering experiments [2] yield strong evidence for a pronounced ferromagnetic short-range order (SRO) in the paramagnetic phase. The magnetic properties of the $S = 2$ spin system $LaMnO_3$ may be described by an effective extended Heisenberg model including a ferromagnetic intraplane and an antiferromagnetic interplane exchange interaction as well as a single-ion easy-axis spin anisotropy [2]. To provide a good description of SRO at arbitrary temperatures, the standard spin-wave approaches cannot be adopted.

In this project low-dimensional quantum spin models with a single-site easy-axis spin anisotropy were considered, and a second-order Green's-function theory along the lines indicated in Refs. [3] and [4] was developed. For comparison, exact finite-lattice diagonalizations (ED) were performed. For the one- and two-dimensional $S = 1/2$ Heisenberg ferromagnet in a magnetic field, the thermodynamic properties (magnetization, isothermal magnetic susceptibility, specific heat) at arbitrary temperatures and fields were calculated in good agreement with ED, Bethe-Ansatz [5], and Monte-Carlo data [6]. In one dimension and at very low fields, for the first time two maxima in the temperature dependence of the specific heat were found. Considering the $S = 1$ ferromagnet with a single-ion spin anisotropy, additional vertex parameters have to be introduced as compared with the case $S = 1/2$, and a good agreement with ED results was obtained.

The project is supported by the DFG through the graduate college "Quantum Field Theory".

[1] A. P. Ramirez, J. Phys.: Condens. Matter **9**, 817 (1997).
E. L. Nagaev, Phys. Rep. **346**, 387 (2001).
[2] F. Moussa *et al.*, Phys. Rev. B **54**, 15149 (1996).
K. Hirota, N. Kaneko, A. Nishizawa and Y. Endoh, J. Phys. Soc. Jpn. **65**, 3736 (1996).
[3] S. Winterfeldt and D. Ihle, Phys. Rev. B **56**, 5535 (1997); ibid. **59**, 6010 (1999).
[4] D. Ihle, C. Schindelin and H. Fehske, Phys. Rev. B **64**, 054419 (2001).
[5] M. Takahashi, Phys. Rev. B **44**, 12382 (1991); H. Nakamura and M. Takahashi, J. Phys. Soc. Jpn. **63**, 2563, (1994).
[6] P. Henelius, A. W. Sandvik, C. Timm and S. M. Girvin, Phys. Rev. B **61**, 364 (2000).

5.4.6 Magnetic Systems with Frustration

J. Richter (Universität Magdeburg), D. Schmalfuss (Universität Magdeburg) and D. Ihle

The exciting magnetic properties of several low-dimensional quantum spin systems with frustration, such as the layered copper oxychlorides $M_2Cu_3O_4Cl_2$ ($M = Ba, Sr$) [1] and the Kagomé antiferromagnet [2], have attracted much attention. To describe the magnetic short-range order at arbitrary temperatures, especially in the spin-liquid phase, one has to go beyond the usual spin-wave approaches [3]. Previously, it was shown that frustration effects in the two-dimensional Heisenberg model with antiferromagnetic nearest- and next-nearest-neighbor couplings ($J_1 - J_2$ model) may be described successfully by a spin-rotation-invariant Green's-function theory [4,5]. The role of the interplane coupling in the stabilization of long-range order in non-frustrated systems was also well described by this theory [6].

In this project, the second-order Green's-function approach of Refs. [4] to [6] was extended to a theory for frustrated spin lattices with basis, where the formal structure of the theory turned out to be of much higher complexity as compared with previous situations. In the Kagomé antiferromagnet the influence of the interplane coupling on the spin correlation functions and the thermodynamic properties was investigated. As the main result, the spin-liquid phase was found to be stable with respect to the interplane coupling. To shed more light into the suppression of long-range order by frustration, the three-dimensional Kagomé ferromagnet was considered, where quantum fluctuations and frustration effects occur at non-zero temperatures only. The Curie temperature was calculated to be lower than that of the simple cubic ferromagnet having an equal coordination number.

The work is supported by the DFG through the projects RI 615/12-1 and IH 13/7-1.

[1] H. Rosner, R. Hayn and J. Schulenburg, Phys. Rev. B **57**, 13660 (1998).
J. Richter, A. Voigt, J. Schulenburg, N. B. Ivanov and R. Hayn, J. Magn. Magn. Mat. **177-181**, 737 (1998).
[2] J. Schulenburg, A. Honecker, J. Schnack, J. Richter and H. J. Schmidt, Phys. Rev. Lett. **88**, 167207 (2002).
[3] A. B. Harris *et al.*, Phys. Rev. B **64**, 024436 (2001).
[4] L. Siurakshina, D. Ihle and R. Hayn, Phys. Rev. B **64**, 104406 (2001).
[5] S. Winterfeldt and D. Ihle, Phys. Rev. B **56**, 5535 (1997); **59**, 6010 (1999).
[6] D. Ihle, C. Schindelin and H. Fehske, Phys. Rev. B **64**, 054419 (2001).

5.4.7 Quantum Fluctuations at Superconductivity

W. Kolley

Density and current fluctuations in a superconductor create electric and magnetic fields which in turn couple to the condensate field. The minimum coupling of the gauge field to the matter field can be described within a modified Abelian Higgs model, which is gauge invariant but not Lorentz invariant. This is a phenomenological model for, e.g., weak-coupling s-wave superconductivity at zero temperature (cf., e.g., [1]). The modification means that the sound velocity enters the kinematical matter part, i. e., the phonon metric and the photon metric differ in the Lagrange density. This allows one to study low-energy quantum fluctuations in four-dimensional space-time around a constant background (in the preferred rest frame of the lattice), provided that the ground-state is a currentless condensate. Low-energy relativistic spectra with quantum behaviour are extracted along three scales (in increasing order of magnitude): Debye screening length, London penetration depth, and coherence length.

The kinematics inherent in the condensate wave function can be expressed in terms of the
(i) supercurrent velocity, involving the gradient of the phase and corresponding to the centre-of-mass motion;
(ii) "osmotic" velocity, due to the amplitude gradient, yielding an internal motion, some kind of Zitterbewegung [2,3,4].

Thus the motion is decomposed in the classical (i) and quantum (ii) contributions, respectively. The equations of motion for the matter part result in a continuity equation and a relativistic Hamilton-Jacobi-type equation. This Hamilton-Jacobi equation endowed with the acoustic metric includes, in addition to the Higgs potential, a quantum potential [5,6] connected with the quantum velocity (ii). This interpretation gives an insight into the compatibility of the macroscopic quantum phenomenon and relativity.

[1] A. van Otterlo, D. S. Golubev, A. D. Zaikin, and G. Blatter, Eur. Phys. J. B **10**, 131 (1999).
[2] G. Salesi, Mod. Phys. Lett. A **11**, 1815 (1996).
[3] S. Rupp, T. Sigg, and M. Sorg, Int. J.Theor. Phys. **39**, 1543 (2000).
[4] J. H. Lee and O. K. Pashaev, Teor. Mat. Fiz. **127**, 432 (2001).
[5] D. Bohm, Phys. Rev. **85**, 166 (1952).
[6] R. P. Holland, *The Quantum Theory of Motion*, Cambridge University Press, Cambridge, 1993.

5.4.8 Funding

Statistische Charakterisierung stochastisch getriebener elektrohydrodynamischer Konvektion in Nematen: Experiment und Theorie
Prof. Dr. U. Behn, PD Dr. R. Stannarius
DFG BE1417/4-2

Rotationsinvariante Greenfunktionsmethode für Quantenspingitter
Prof. Dr. J. Richter (Magdeburg), Prof. Dr. D. Ihle
DFG RI615/12-1, IH13/7-1

5.4.9 Organizational Duties

U. Behn
Referee: Physical Review Letters, Physical Review E, Journal Theoretical Biology, Advances in Complex Systems, Journal of Physics CM

D. Ihle
Referee: phys. stat. sol. (b)
Member of the Commission for Graduate Studies of the University

W. Kolley
Member of the Promotionsauschuß of the Faculty

A. Kühnel
Member of the Executive Commitee of the *International Center for Scientific Cooperation* with residence in Tübingen

5.4.10 External Cooperations

Academic

Prof. Dr. Gerhard Metzner, Institut für Klinische Immunologie, Universität Leipzig

Prof. Dr. Franco Celada, Department of Oncology, Biology and Genetics, University of Genoa

Prof. Dr. Valentin Zagrebnov, Centre de Physique Theorique, CNRS, Marseille

Prof. Dr. Slava Priezzhev, Bogolyubov Laboratory of Theoretical Physics, JINR, Dubna

Prof. Dr. Hirokazu Fujisaka, Department of Applied Analysis and Complex Dynamical Systems, Kyoto University

Prof. Dr. Ralf Stannarius, Institut für Experimentelle Physik, Otto-von-Guericke-Universität Magdeburg

Dr. Angela Stevens, Max Planck Institute for Mathematics in Science, Leipzig

Dr. Jan Richter, Cyprus Institute of Neurology and Genetics, Nicosia

Dr. Markus Brede, Center for Complex Systems Science, CSIRO, Canberra

Prof. Dr. Holger Fehske, Institut für Physik, Ernst-Moritz-Arndt-Universität Greifswald

Prof. Dr. Johannes Richter, Institut für Theoretische Physik, Otto-von-Guericke-Universität Magdeburg

Prof. Dr. Nikolai M. Plakida, Bogolyubov Laboratory of Theoretical Physics, JINR, Dubna

Prof. Dr. Peter Wachter, Laboratorium für Festkörperphysik, ETH Zürich

5.4.11 Publications

M. Brede, U. Behn, *Patterns in randomly evolving networks: Idiotypic networks*, Phys. Rev. E **67**, 031920-1/18 (2003).

T. John, U. Behn, R. Stannarius, *Laser diffraction by periodic dynamic patterns in anisotropic fluids*, Eur. Phys. J. B **35**, 267-278 (2003).

J. Richter, U. Behn, G. Metzner, *Modelling of Th1-Th2 Regulation, Allergy and Venom Immunotherapy*, in: Clinical Immunology and Allergy in Medicine, Proc. 21st EAACI Congress 2002, Naples, G. Marone (Ed.), JGC Editions, Naples (2003), 257-262.

in press

U. Behn, M. Brede, J. Richter, *Nonlinear dynamics and statistical physics of models for the immune system*, in: Function and regulation of cellular systems: Experiments and Models, A. Deutsch, J. Howard, M. Falcke, W. Zimmermann (Eds.), Birkhäuser, Basel (2004), 399-410.

A. Traulsen, K. Lippert, U. Behn, *Generation of spatiotemporal correlated noise in 1+1 dimensions*, Phys. Rev. E **69**, 026116-1/9 (2004).

Conference contributions

U. Behn, M. Brede
Random evolution towards highly organized structures in idiotypic networks (inv. T)
2nd Workshop "Computational Biology in Saxony: Problems and Perspectives", TU Dresden, 14.3.03

U. Behn
Random evolution of idiotypic networks (inv. T)
8. Herbstseminar 'Strukturbildung in Chemie und Biophysik', Salzwedel, 29.9.03

U. Behn, T. Birner, K. Lippert, R. Müller, A. Kühnel
Critical behaviour of non-equilibrium phase transitions (T)
CompPhys03, 4th NTZ Workshop on Computational Physics, Leipzig, 5.12.03

T. John, R. Stannarius, U. Behn
Mode selection in a spatial extended pattern forming system at noise excitation (T)
DPG-Frühjahrstagung, Dresden, 24.–28.3.2003

T. John, U. Behn, R. Stannarius
Laser diffraction by periodic dynamic patterns in anisotropic fluids (T)
31. Arbeitstagung Flüssigkristalle, Mainz, 19.–21.03.2003

T. John, U. Behn, R. Stannarius
Laser diffraction study of stochastically excited nematic electroconvection (P)
DPG-Frühjahrstagung, Dresden, 24.–28.3.2003

5.4.12 Graduations

PhD

Jan Richter
Nonlinear Dynamics of Models Describing Th1/Th2 Regulation, Allergy and Venom Immunotherapy
12.2.2003

Markus Brede
Randomly evolving idiotypic networks: Dynamics and architecture
4.6.2003

Diploma

Otto Edgar Martin
Wiederkehrzeitverteilungen in rauschgetriebenen nichtlinearen Systemen
4.4.2003

5.5 Computational Quantum Field Theory

5.5.1 Introduction

The Computational Physics Group performs basic research in classical and quantum statistical physics with special emphasis on phase transitions and critical phenomena. In the centre of interest are currently spin glasses, diluted magnets and other physical systems with quenched, random disorder, a geometrical approach to the statistical physics of topological defects with applications to superconductors and superfluids, biologically motivated problems (e.g., protein folding and semiflexible polymers), fluctuating geometries with applications to quantum gravity (e.g., dynamical triangulations) and soft condensed matter physics (e.g., membranes and interfaces). Supported by a Development Host grant of the European Commission, currently also research into the physics of anisotropic quantum magnets is established.

The methodology is a combination of analytical and numerical techniques. The numerical tools are currently mainly Monte Carlo computer simulations and high-temperature series expansions. The computational approach to theoretical physics is expected to gain more and more importance with the future advances of computer technology, and will probably become the third basis of physics besides experiment and analytical theory. Already now it can help to bridge the gap between experiments and the often necessarily approximate calculations of analytical work. To achieve the desired high efficiency of the numerical studies we develop new algorithms, and to guarantee the flexibility required by basic research all computer codes are implemented by ourselves. The technical tools are Fortran, C, and C++ programs running under Unix or Linux operating systems and computer algebra using Maple or Mathematica. The software is developed and tested at the Institute on a cluster of PC's and workstations, where also most of the numerical analyses are performed. Large-scale simulations requiring vast amounts of computer time are carried out at the Institute on a recently installed Beowulf cluster with 40 Athlon MP1800+ CPU's and a brandnew Opteron cluster with 18 processors of 64-bit architecture, at the parallel computers of the University computing center, and upon grant application at the national supercomputing centres in Jülich and München on T3E, IBM and Hitachi parallel supercomputers. This combination of various platforms gives good training opportunities for the students and offers promising job perspectives in many different fields for their future career.

The research is embedded in a wide net of national and international collaborations funded by network grants of the European Commission and the European Science Foundation, and by binational research grants with scientists in Great Britain, France, and Israel. Close contacts are also established with research groups in Armenia, Austria, China, Italy, Russia, Spain, Taiwan, and the United States.

5.5.2 Monte Carlo Studies of Spin Glasses

B. A. Berg*, A. Billoire**, E. Bittner, W. Janke, A. Nußbaumer, D. B. Saakian***
* Florida State University, Tallahassee, USA, ** CEA/Saclay, Gif-sur- Yvette, France,
*** Yerevan Physics Institute, Yerevan, Armenia

Spin glasses are examples for an important class of materials with random, competing interactions [1]. This leads to "frustration", since no unique spin configuration is favored by all interactions, and a rugged free energy landscape with many minima separated by barriers. Standard Monte Carlo simulations are very inefficient in such a case since they overcome the barriers only very rarely and hence run into ergodicity problems. To elucidate the scaling behaviour of the barriers with system size we therefore developed a multi-overlap Monte Carlo algorithm [2] which can be optimally tailored [3] for the sampling of rare-events. Recently we have further improved this method by combining it with parallel tempering and N-fold way ideas [4]. First tests indicate [5] that the new algorithm will enable us to push the studies of the spin-glass phase further towards the physically more interesting low-temperature regime. As in our previous work at higher temperatures [6] we focus on the free-energy barriers F_B^q in the probability density $P_{\mathcal{J}}(q)$ of the Parisi overlap parameter q [7] which can be defined in terms of the autocorrelation times τ_B^q of auxiliary Markov chains.

Along a second line of research we have also investigated the diluted generalized random-energy model (DGREM) which provides an approximation to the ground-state energy of spin glasses. Applications to two-dimensional q-state Potts models and a comparison with numerically determined ground-state energies are reported in Ref. [8].

[1] K. H. Fischer and J. A. Hertz, *Spin Glasses* (Cambridge University Press, 1991).

[2] B. A. Berg and W. Janke, Phys. Rev. Lett. **80**, 4771 (1998).

[3] W. Janke, B. A. Berg and A. Billoire, Ann. Phys. (Leipzig) **7**, 544 (1998); Comp. Phys. Comm. **121-122**, 176 (1999).

[4] A. Nußbaumer, E. Bittner and W. Janke, to be published.

[5] A. Nußbaumer, Diploma Thesis, University of Leipzig (2003).

[6] B. A. Berg, A. Billoire and W. Janke, Phys. Rev. B **61**, 12143 (2000); Physica A **321**, 49 (2003).

[7] G. Parisi, Phys. Rev. Lett. **43**, 1754 (1979).

[8] E. Bittner, W. Janke and D. B. Saakian, Phys. Rev. E **67**, 016105 (2003).

5.5.3 Monte Carlo Studies of Diluted Magnets

B. Berche*, P.-E. Berche**, C. Chatelain* and W. Janke
* Université Nancy, France, ** Université Rouen, France

The influence of quenched, random disorder on phase transitions has been the subject of exciting experimental, analytical and numerical studies in the past few years. To date most theoretical studies have concentrated on two-dimensional (2D) models with site- or bond-dilution or bond-disorder [1]. Generically one expects that quenched disorder, under certain conditions, will modify the critical behaviour at a second-order transition (Harris criterion) and can soften a first-order transition of the pure system to a second-order one [2]. In three dimensions (3D), numerical studies have mainly focused on the site-diluted Ising model [3] where good agreement with field theory was obtained. For the case of a first-order transition in the pure model, large-scale simulations have only been performed for the 3-state Potts model with site-dilution [4].

In this project we have performed intensive Monte Carlo studies of the 3D Ising and 4-state Potts models with *bond*-dilution [5]. We have determined the phase diagrams of the diluted models, starting from the pure model limit down to the neighbourhood of the percolation threshold, in very good agreement with a single-bond effective-medium approximation. For the estimation of critical exponents in the Ising case [6], we have first performed a finite-size scaling study, where we concentrated on three different dilutions to check the stability of the disorder fixed point. We emphasize in this work the great influence of the cross-over phenomena between the pure, disorder and percolation fixed points which lead to effective critical exponents dependent on the concentration. In a second set of simulations, the temperature behaviour of physical quantities has been studied in order to characterize the disorder fixed point more accurately. In particular this allowed us to estimate universal ratios of some critical amplitudes which are usually more sensitive to the universality class than the critical exponents. Moreover, the question of non-self-averaging at the disorder fixed point is investigated and compared with recent results for the bond-diluted 4-state Potts model. We obtain very good agreement with approximate analytical calculations by Aharony and Harris. Overall our numerical results provide evidence that, as expected on theoretical grounds, the critical behaviour of the bond-diluted model is indeed governed by the same universality class as the site-diluted model.

[1] B. Berche and C. Chatelain, in *Order, Disorder, and Criticality*, edited by Yu. Holovatch (World Scientific, Singapore, 2004), p. 147 [cond-mat/0207421].

[2] A. B. Harris, J. Phys. C **7**, 1671 (1974).
Y. Imry and M. Wortis, Phys. Rev. B **19**, 3580 (1979).

[3] S. Wiseman and E. Domany, Phys. Rev. Lett. **81**, 22 (1998); Phys. Rev. E **58**, 2938 (1998).
H. G. Ballesteros, L. A. Fernández, V. Martín-Mayor, A. Muñoz Sudupe, G. Parisi and J. J. Ruiz-Lorenzo, Phys. Rev. B **58**, 2740 (1998).

[4] H. G. Ballesteros, L. A. Fernández, V. Martín-Mayor, A. Muñoz Sudupe, G. Parisi and J. J. Ruiz-Lorenzo, Phys. Rev. B **61**, 3215 (2000).

[5] W. Janke, P.-E. Berche, C. Chatelain and B. Berche, in: *NIC-Symposium 2004*, edited by D. Wolf, G. Münster and M. Kremer, NIC Series, Vol. **20**, pp. 241–250 (2003).

[6] P.-E. Berche, C. Chatelain, B. Berche and W. Janke, cond-mat/0402596, to appear in Eur. Phys. J. **B** (in print).

5.5.4 High-Temperature Series Expansions for Spin Glasses and Disordered Magnets

M. Hellmund* and W. Janke
* Fakultät für Mathematik und Informatik

Despite considerable efforts there are still many open problems in the physics of disordered systems. One alternative to large-scale numerical simulations are systematic series expansions. Such expansions for statistical models defined on a lattice are a well-known method to study phase transitions and critical phenomena [1]. The extension of this method to disordered systems [2] demands the development of new graph theoretical and algebraic algorithms.

Using the method of "star-graph expansion", we calculate, e.g., free energies and susceptibilities for disordered q-state Potts models on d-dimensional hypercubic lattices. The probability distribution of couplings is parametrized by $P(J_{ij}) = p\delta(J_{ij} - J_0) + (1 - p)\delta(J_{ij} - RJ_0)$, which includes spin glasses, diluted ferromagnets, random-bond models and transitions between them. First results for the random-bond Ising [3] and Potts [4] model demonstrate the feasibility of the method to complement Monte Carlo [5] and field theoretic studies of phase transitions in disordered systems.

For the bond-diluted 4-state Potts model in three dimensions, which exhibits a rather strong first-order phase transition in the undiluted case, we obtained results [6] for the transition temperature and the effective critical exponent γ as a function of p from analyses of susceptibility series up to order 18. A comparison with recent Monte Carlo data [5] shows signals for the softening to a second-order transition at finite disorder strength. Further new results were also obtained for the three-dimensional bond-diluted resp. random bond Ising model and the $q \to 1$ percolation limit for different dimensionalities d [7].

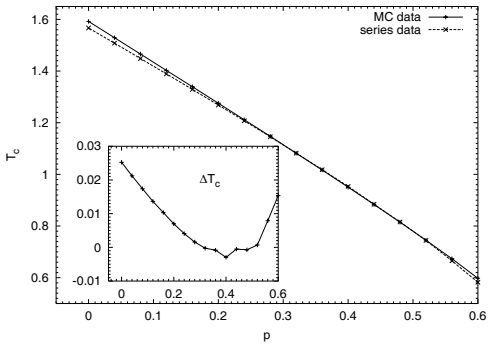

Critical temperature for different dilutions p as obtained from Monte Carlo (MC) simulations [5] and DLog-Padé series analyses [6]. The inset shows the difference between the two estimates.

[1] C. Domb and M. S. Green, eds, *Phase Transitions and Critical Phenomena*, Vol. 3 (Academic Press, New York, 1974).

[2] R. R. P. Singh and S. Chakravarty, Phys. Rev. B **36**, 546 (1987).

[3] M. Hellmund and W. Janke, Comp. Phys. Comm. **147**, 435 (2002).

[4] M. Hellmund and W. Janke, Nucl Phys. B (Proc. Suppl.) **106/107**, 923 (2002).

[5] C. Chatelain, B. Berche, W. Janke and P.-E. Berche, Phys. Rev. E **64**, 036120 (2001).

[6] M. Hellmund and W. Janke, Phys. Rev. E **67**, 026118 (2003).

[7] M. Hellmund and W. Janke, to be published.

5.5.5 Harris-Luck Criterion and Potts Models on Random Graphs

W. Janke, G. Kähler and M. Weigel

The Harris criterion judges the relevance of uncorrelated, quenched disorder for altering the universal properties of systems of statistical mechanics close to a continuous phase transition [1]. For this situation, as e.g., in the paradigmatic case of a quenched random-bond or bond diluted model, a change of universal properties is expected for models with a positive specific heat exponent α, i.e., the relevance threshold is given by $\alpha_c = 0$. For the physically more realistic case of spatially correlated disorder degrees of freedom, Harris' scaling argument can be generalised, yielding a shifted relevance threshold $-\infty < \alpha_c \leq 1$ known as Luck criterion [2]. The value of α_c depends on the quality and strength of the spatial disorder correlations as expressed in a so-called geometrical fluctuation or *wandering exponent*.

We consider the effect of a different, topologically defined type of disorder on the universal behaviour of coupled spin models, namely the result of *connectivity disorder* produced by placing spin models on *random graphs*. As it turns out, the Harris-Luck argument can be generalised to this situation, leading to a criterion again involving a suitably defined wandering exponent of the underlying random graph ensemble. Using a carefully tailored series of finite-size scaling analyses, we precisely determine the wandering exponents of the two-dimensional ensembles of Poissonian Voronoï-Delaunay random lattices as well as the quantum gravity graphs of the dynamical triangulations model, thus arriving at explicit predictions for the relevance threshold α_c for these lattices [3].

As a result, for Poissonian Voronoï-Delaunay random graphs the Harris criterion $\alpha_c = 0$ should stay in effect, whereas for the dynamical triangulations the threshold is shifted to a negative value, $\alpha_c \approx -2$. The latter result is in perfect agreement with Monte Carlo simulations of the q-states Potts model [4] as well as an available exact solution of the percolation limit $q \to 1$ [5]. For the Poissonian Voronoï-Delaunay triangulations, the Ising case $q = 2$ with $\alpha = 0$ is marginal and a change of universal properties cannot normally be expected. The $q = 3$ Potts model with $\alpha = 1/3$, on the other hand, should be shifted to a new universality class. Following up on a first exploratory study for small graphs [6], we performed high-precision cluster-update Monte Carlo simulations for rather large lattices of up to 80 000 triangles to investigate this model. Astonishingly, however, the (exactly known) critical exponents of the square-lattice $q = 3$ Potts model are reproduced to high precision [7]. To clarify this situation, a generalised model introducing a distance dependence of the interactions is currently under investigation.

[1] A. B. Harris, J. Phys. C **7**, 1671 (1974).

[2] A. Weinrib and B. I. Halperin, Phys. Rev. B **27**, 413 (1983).
J. M. Luck, Europhys. Lett. **24**, 359 (1993).

[3] W. Janke and M. Weigel, Phys. Rev. B **69** (2004), in print [cond-mat/0310269].

[4] W. Janke and D. A. Johnston, Nucl. Phys. B **578**, 681 (2000).

[5] V. A. Kazakov, Mod. Phys. Lett. A **4**, 1691 (1989).

[6] F. W. S. Lima, U. M. S. Costa, M. P. Almeida and J. S. Andrade, Eur. Phys. J. B **17**, 111 (2000).

[7] W. Janke and M. Weigel, Acta Phys. Polon. B **34**, 4891 (2003).

5.5.6 The F Model on Quantum Gravity Graphs

W. Janke, D. A. Johnston* and M. Weigel
* Heriot-Watt University, Edinburgh, Scotland

As an alternative to various other approaches towards a theory of quantum gravity, the *dynamical triangulations* method has proved to be a successful discrete formulation of Euclidean quantum gravity in two dimensions. There, the necessary integration over all metric tensors as the dynamic variables of the theory, is performed as a discrete summation over all possible gluings of equilateral triangles to form a closed surface of a given (usually planar) topology. The powerful methods of matrix integrals and generating functions allow for an exact solution of the pure gravity model in two dimensions. Furthermore, matrix models can be formulated for the coupling of spin models of statistical mechanics to the random graphs and some of them could be solved analytically. More generally, the "dressing" of the weights of $c < 1$ conformal matter on coupling it to quantum gravity in two dimensions is predicted by the KPZ/DDK formula [1], in agreement with all known exact solutions.

One of the most general classes of models in statistical mechanics is given by Baxter's 8-vertex model [2]. Thus its behaviour on coupling it to dynamical *quadrangulations*, i.e., surfaces built from simplicial squares, is of general interest. Although a solution of special slices of this model could recently be achieved [3], the general model could not yet be solved. Heading for computer simulations, one first has to ensure the correct handling of the (quite unorthodox) geometry of four-valent graphs or quadrangulations in the dual language. While simulations of three-valent graphs have already been extensively done, the code for ϕ^4-graphs had to be newly developed and tested [4]. Due to the fractal structure of the graphs being described as a self-similar tree of "baby universes", this local dynamics suffers from critical slowing down. To alleviate the situation, we adapted a non-local update algorithm known as "minBU surgery" [5].

Combining the developed techniques, we simulated the F model, a symmetric case of the 8-vertex model, coupled to planar random ϕ^4 graphs. On regular as well as random lattices, this model is expected to exhibit a Kosterlitz-Thouless transition to an anti-ferroelectrically ordered state [2, 3]. The numerical analysis of this model turned out to be exceptionally difficult due to the combined effect of the highly fractal structure of

the lattices and the presence of strong logarithmic corrections, leading to rather extreme finite-size effects. Nevertheless, a scaling analysis of the staggered polarizability yields results [6] in agreement with the predictions of Ref. [3] as far as the order of the transition and the location of the transition point are concerned.

[1] V. Knizhnik, A. Polyakov and A. Zamolodchikov, Mod. Phys. Lett. A **3**, 819 (1988).
F. David, Mod. Phys. Lett. A **3**, 1651 (1988).
J. Distler and H. Kawai, Nucl. Phys. B **321**, 509 (1989).

[2] R. Baxter, *Exactly Solved Models in Statistical Mechanics* (Academic Press, London, 1982).

[3] V. A. Kazakov and P. Zinn-Justin, Nucl. Phys. B **546**, 647 (1999).
I. Kostov, Nucl. Phys. B **575**, 513 (2000).
P. Zinn-Justin, Europhys. Lett. **50**, 15 (2000).

[4] M. Weigel and W. Janke, Nucl. Phys. B (Proc. Suppl.) **106–107**, 986 (2002).
M. Weigel, Ph.D. Thesis, University of Leipzig (2002).

[5] J. Ambjørn, P.Bialas, J. Jurkiewicz, Z. Burda and B. Petersson, Phys. Lett. B **325**, 337 (1994).

[6] M. Weigel and W. Janke, to be published.

5.5.7 Conformational Transitions of Lattice Heteropolymers

M. Bachmann, W. Janke, R. Schiemann and T. Vogel

The native conformation of a protein is strongly correlated with the sequence of amino acid residues building up the heteropolymer. The sequence makes the protein unique and assigns it a specific function within a biological organism. The reason is that the different types of amino acids vary in their response to the environment and in their mutual interaction. Since many diseases (e.g., Alzheimer's, Creutzfeld-Jacob, type II diabetes) are due to protein misfolds, it is an important task to reveal on what general principles the folding process of a protein is based. Models differ extremely in their level of abstraction, ranging from simple and purely qualitative lattice models to highly sophisticated all-atom off-lattice formulations with explicit solvent that partially yield results comparable with experimental data. Due to the enormous computational effort required for simulations of realistic proteins, usually characteristic properties of a protein with a given sequence are studied in detail. Much simpler, but by no means trivial, lattice models enjoy a growing interest, since they allow a more global view on, for example, the analysis of the relation between sequence and structure.

We focused ourselves on the study of thermodynamic properties of lattice proteins at all temperatures. In particular, this includes the investigation of the transitions between the different classes of states: lowest-energy (hydrophobic-core) states, compact globules, and random coils. Since the ground-state–globule transition occurs at rather low temperatures, a powerful algorithm is required that in particular allows a reasonable sampling of the low-lying energy states. To this end we combined multicanonical strategies [1] with chain growth algorithms [2] to a new method [3]. We applied this method to different

lattice proteins, modeled by the simplest lattice formulation for heteropolymers, the HP model [4]. In this model, only two types of monomers enter, hydrophobic (H) and polar (P) residues. The model is based on the assumption that the hydrophobic interaction is one of the fundamental principles in protein folding. An attractive hydrophobic interaction provides for the formation of a compact hydrophobic core that is screened from the aqueous environment by a shell of polar residues.

For different sequences with lengths between 42 and 103 monomers, we analyzed in detail the temperature-dependent behavior of radius of gyration, end-to-end distance, as well as their fluctuations, and compared it with the specific heat in order to elaborate relations between characteristic properties of these curves (peaks, "shoulders") and conformational transitions not being transitions in a strict thermodynamic sense due to the impossibility to formulate a thermodynamic limit for proteins. Therefore, we identified temperature regions, where global changes of protein conformations occur. These transition regions separate "phases", where random coils, maximally compact globules, or states with compact hydrophobic core dominate. As an interesting by-product, we not only confirmed the known global-minimum energies for these examples, but we even found a new minimum for the 103mer being the longest sequence under consideration [3].

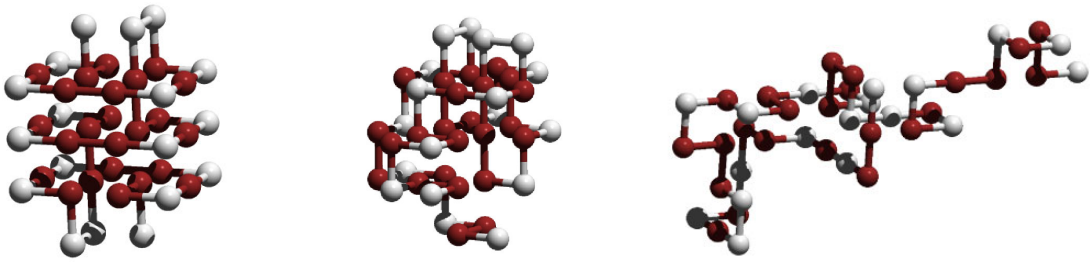

bad solvent poor solvent good solvent

In another project [5] we exactly analyzed the combined space of sequences and conformations for proteins on the simple cubic lattice for HP-type models that differ in the contact energy between hydrophobic and polar monomers. Since there were only a few known exact results for heteropolymers in 3D, in particular on compact cuboid lattices, we generated by exact enumeration the sets of designing sequences (i.e. sequences with nondegenerate ground state) and native conformations on simple cubic lattices. We studied, how their properties, measured, e.g., in terms of quantities like end-to-end distance, radius of gyration, designability, etc., differ from the bulk of all possible sequences and all self-avoiding conformations, respectively. We confirmed that the ground-state conformations are very compact, but not necessarily maximal compact. We studied also energetic thermodynamic properties, in order to investigate how characteristic the low-temperature behavior of designing compared to non-designing sequences is and found that designing sequences show up a pronounced low-temperature peak in the specific heat being related to a conformational transition between low-energy states with hydrophobic core and highly compact globules. While designing sequences behave similarly for very low temperature, nondesigning sequences react quite differently on changes of the temperature, over the

entire range of temperatures.

We also investigated the HP model on more general lattices, e.g. the triangular lattice in 2D and the face-centered cubic (fcc) lattice in 3D [6]. Comparing for given sequences the results obtained on the fcc lattice with results from considerations on the simple cubic lattice, it turned out that there was in most cases no qualitative coincidence. In particular, for exemplified sequences exhibiting a distinct "three-phase" behavior on the simple cubic lattice, we did not find a clear indication for the low-temperature transition between globules and hydrophobic-core conformations on the fcc lattice. Consequently, ground-state properties and thermodynamic properties for given sequences strongly depend on the type of the lattice used. This does not render lattice models completely irrelevant for qualitative studies of heteropolymers, but it shows that, just for this reason, HP proteins on the simplest lattices will not adequately describe properties of a realistic amino acid sequence that was translated into the corresponding HP sequence.

[1] B. A. Berg and T. Neuhaus, Phys. Lett. B **267**, 249 (1991); Phys. Rev. Lett. **68**, 9 (1992).

[2] P. Grassberger, Phys. Rev. E **56**, 3682 (1997).
H.-P. Hsu, V. Mehra, W. Nadler and P. Grassberger, J. Chem. Phys. **118**, 444 (2003).

[3] M. Bachmann and W. Janke, Phys. Rev. Lett. **91**, 208105 (2003); J. Chem. Phys. **120**, 6779 (2004).

[4] K. A. Dill, Biochemistry **24**, 1501 (1985).
K. F. Lau and K. A. Dill, Macromolecules **22**, 3986 (1989).

[5] R. Schiemann, M. Bachmann and W. Janke, to be published.

[6] T. Vogel, M. Bachmann and W. Janke, to be published.

5.5.8 Thermodynamic Properties of Simple Off-Lattice Models for Proteins

H. Arkın*, M. Bachmann and W. Janke
* Hacettepe University, Ankara, Turkey

The understanding of protein folding is one of the most challenging objectives in biochemically motivated research. Although the physical principles are known, the complexity of proteins as being macromolecules consisting of numerous atoms, the influence of quantum chemical details on long-range interactions as well as the role of the solvent, etc. makes an accurate analysis of the folding process of realistic proteins extremely difficult. Therefore, one of the most important questions in this field is how much detailed information can be neglected to establish effective models yielding reasonable, at least qualitative, results that allow for, e.g., a more global view on the relationship between the sequence of amino acid residues and the existence of a global, funnel-like energy minimum in a rugged free-energy landscape.

Within the past two decades much work has been done to introduce minimalistic models based on general principles that are believed to primarily control the structure formation of proteins. One of the most prominent examples is the HP model of lattice

proteins [1] which has been exhaustively investigated without revealing all secrets, despite its simplicity. The only explicit interaction is between non-adjacent but next-neighbored hydrophobic monomers. This interaction of hydrophobic contacts is attractive to force the formation of a compact hydrophobic core which is screened from the (hypothetic) aqueous environment by the polar residues.

A manifest off-lattice generalization of the HP model is the AB model [2], where the hydrophobic monomers are labeled by A and the hydrophilic ones by B. The contact interaction is replaced by a distance-dependent Lennard-Jones type of potential accounting for short-range excluded volume repulsion and long-range interaction, the latter being attractive for AA and BB pairs and repulsive for AB pairs of monomers. An additional interaction accounts for the bending energy of any pair of successive bonds. This model was first applied in two dimensions [2] and generalized to three-dimensional AB proteins, partially with modifications taking into account the additional torsional degree of freedom of each bond [3].

We have studied thermodynamic and ground-state properties of known AB sequences for two representations [2, 3] of the AB model. In order to more accurately resolve the low-temperature behavior we applied a multicanonical Monte Carlo algorithm with an appropriate update mechanism, which enabled us to sample the density of states over more than 70 *orders of magnitude* [4]. This allowed us to calculate fluctuating quantities such as the specific heat with very high accuracy for almost all temperatures. We also obtained with this method a very good estimate for the ground-state energies. These values are in very good agreement with results achieved by means of the energy landscape paving (ELP) minimizer [5], which was designed just for this purpose.

[1] K. F. Lau and K. A. Dill, Macromolecules **22**, 3986 (1989).

[2] F. H. Stillinger, T. Head-Gordon and C. L. Hirshfeld, Phys. Rev. E **48**, 1469 (1993). F. H. Stillinger and T. Head-Gordon, Phys. Rev. E **52**, 2872 (1995).

[3] A. Irbäck, C. Peterson, F. Potthast and O. Sommelius, J. Chem. Phys. **107**, 273 (1997).

[4] H. Arkın, M. Bachmann and W. Janke, to be published.

[5] U. H. E. Hansmann and L. T. Wille, Phys. Rev. Lett. **88**, 068105 (2002).

5.5.9 Phase Transitions in Ginzburg-Landau Theory

E. Bittner, W. Janke, A. Krinner and S. Wenzel

Scalar fields with n components and a fourth-order O(n)-symmetric quartic self-interaction are so far the best understood examples of systems, whose second-order phase transitions can be treated with field-theoretic techniques [1, 2]. Universality ensures that spin models which describe only directional fluctuations show the same critical properties as scalar fields with $n \geq 2$ components, and the precise reason for this can easily be understood [3]. In particular, this equivalence holds for the superfluid phase transition which can be described either by a directional XY model or by an O(2)-symmetric scalar field theory, whose Hamiltonian is of the Ginzburg-Landau form with a complex field $\psi(\vec{r}) = |\psi(\vec{r})|e^{i\phi(\vec{r})}$. Therefore the model can equivalently be represented as a partition

function of a dual theory where the elementary excitations are closed vortex lines, i.e. loops. The loops of the dual theory may therefore play an important role in determining the properties of the phase transition. A seemingly natural approach to study the vortex degrees of freedom is to decompose every spin configuration generated in a lattice Monte Carlo simulation [4] into a number of vortex loops. The hope is then that the transition will be signalized by a non-zero probability for finding vortex loops that extend through the whole system [5], a phenomenon which is often called percolation.

Percolation has been used to study phase transitions in various different theories. From studies of the Ising model, where a different kind of percolation may occur, related to spin clusters instead of vortex lines, it is known that one has to be quite careful with the interpretation [6]. In discussing the phase transition of the Ginzburg-Landau theory, we study a geometrically defined vortex loop network as well as the magnetic properties of the system in the vicinity of the critical point. Using high-precision Monte Carlo techniques we consider an alternative formulation of the geometrical excitations in relation to the global O(2)-symmetry breaking, and check if both of them exhibit the same critical behaviour leading to the same critical exponents and therefore to a consistent description of the phase transition. Different percolation observables are taken into account and compared with each other.

[1] J. Zinn-Justin, *Quantum Field Theory and Critical Phenomena*, 3rd ed. (Clarendon Press, Oxford, 1996).

[2] H. Kleinert and V. Schulte-Frohlinde, *Critical Properties of* Φ^4*-Theories* (World Scientific, Singapore, 2001).

[3] H. Kleinert, Phys. Rev. Lett. **84**, 286 (2000).

[4] N. Metropolis, A.W. Rosenbluth, M.N. Rosenbluth, A.H. Teller and E. Teller, J. Chem. Phys. **21**, 1087 (1953).

[5] K. Kajantie, M. Laine, T. Neuhaus, A. Rajantie and K. Rummukainen, Phys. Lett. B **482**, 114 (2000).

[6] S. Fortunato, J. Phys. A **36**, 4269 (2003).

5.5.10 Equilibrium Crystal Shapes in Three Dimensions

E. Bittner, W. Janke and A. Nußbaumer

The free energy of the three-dimensional Edwards-Anderson Ising model in the low temperature phase shows a multi-valley structure. Multicanonical simulations, e.g. for the overlap parameter, were expected to remove these valleys and to lead to a random walk behaviour in the corresponding observable. In fact there are still jumps in the time series which were attributed to so-called "hidden barriers". Recently, Neuhaus and Hager [1] explained such barriers in the magnetisation M for the much simpler case of the two-dimensional Ising model. Based on the analytic work of Leung and Zia [2], they identified a geometrically induced first-order transition from a droplet to a strip domain and showed that even a perfect multimagnetic simulation operating with the optimal weights needs exponential time to overcome the associated free energy barrier. To obtain more qualitative

insights, we determined directly the anisotropy of a configuration by measuring a structure function. Simulating different system sizes with Kawasaki dynamics (M = const.), the scaling of the anisotropy leads to a value for the barrier height in good agreement with the theoretical prediction (see Fig. 1). By generalising these considerations to the case of the three-dimensional Ising model, new transitions could be identified analytically and verified numerically, and the crystal shapes emerging during the transition were visualised.

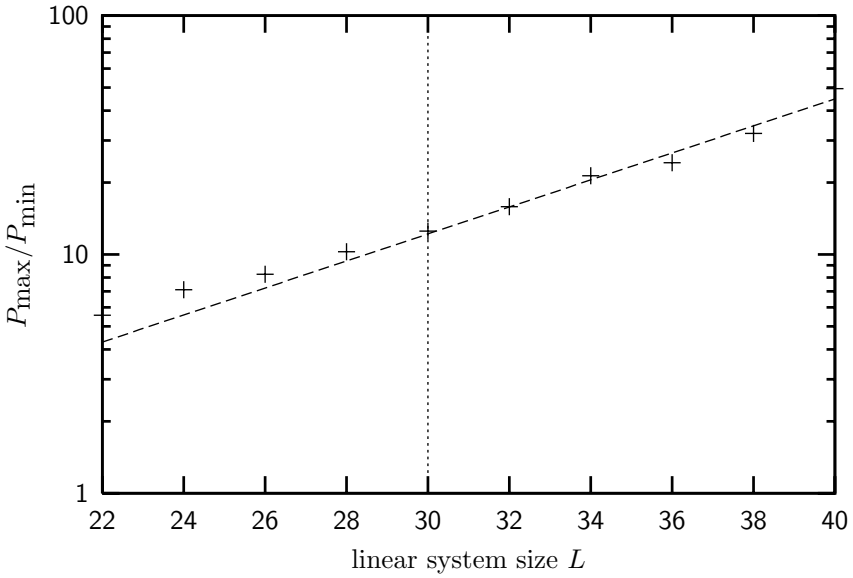

Fig. 1: Linear fit to $\ln(P_{\max}/P_{\min})$ in the range $L = 30$ to $L = 40$. The measured value $\alpha = 1.30 \pm 0.01$ is to be compared with the analytic value [2] of $\alpha = 1.35$.

[1] T. Neuhaus and J. Hager, Stat. Phys. **113**, 47 (2003).

[2] K. Leung and R. Zia, J. Phys. A **23**, 4593 (1990).

5.5.11 Geometrical Approach to Phase Transitions

W. Janke and A. M. J. Schakel

The geometrical approach to phase transitions is an exciting research topic in contemporary physics. The prototype of this approach is percolation theory, describing clusters of (randomly) occupied sites on a lattice. The fractal structure of these geometrical objects and whether or not a cluster percolates the lattice are central topics addressed by the theory. Percolation theory is easily adapted to describe other geometrical objects such as lines and (hyper)surfaces as well. Typical line objects featuring in phase transitions that can be described in this way are, for example, (i) vortex lines in systems with spontaneously broken global U(1) or local gauge symmetries, (ii) worldlines in Bose-Einstein condensates, and (iii) graphs in high-temperature representations of spin models.

(i) Because of topological constraints, vortices generally form closed loops. Whereas in the broken-symmetry phase only finite vortex loops are present, at the critical point, loops of all sizes appear. This vortex proliferation is in complete analogy to what happens with clusters at the percolation threshold. The disordering effect of the proliferating vortices

destroys superfluidity in superfluids, and leads to charge confinement in certain gauge theories.

(ii) Boson worldlines at finite temperature also form closed loops in imaginary time. Feynman's theory of Bose-Einstein condensation asserts that upon lowering the temperature, small loops describing single particles hook up to form larger exchange rings, so that the particles become indistinguishable. At the critical temperature, again as in percolation phenomena, worldlines proliferate and loops of arbitrary size appear, signalling the onset of Bose-Einstein condensation.

(iii) The high-temperature representation of spin models can be visualized by closed graphs on the lattice (see Fig. 1), making these models eligible to a geometrical description. In this project, the fractal structure of two-dimensional spin models was investigated and a close connection between different models established. To support our theoretical findings, the high-temperature representation of the Ising model was simulated by means of a Metropolis plaquette update. It was shown that (a) large graphs are exponentially suppressed in the high-temperature phase, and that (b) graphs percolate the lattice and proliferate precisely at the thermal critical point. From the percolation strength (defined as the number of bonds in the largest graph) and the average graph size, the fractal dimension of the graphs is extracted through finite-size scaling [1]. The resulting value was found to agree with theoretical predictions [2].

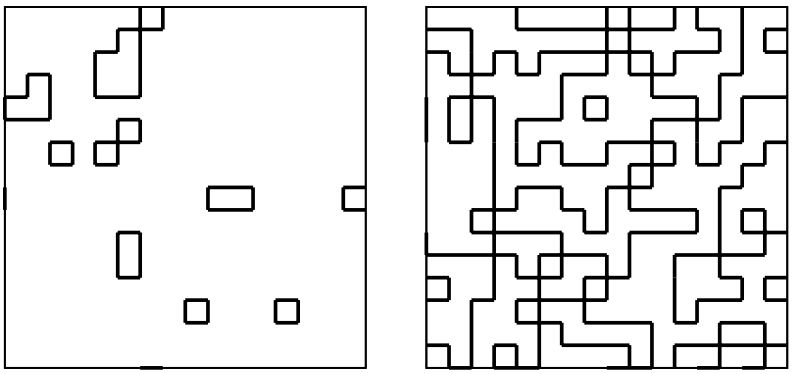

Fig. 1. Typical graph configurations generated on a 16×16 square lattice with periodic boundary conditions in the high- (*left panel*) and low-temperature (*right panel*) phase of the two-dimensional Ising model.

[1] W. Janke and A. M. J. Schakel, cond-mat/0311624.

[2] B. Duplantier and H. Saleur, Phys. Rev. Lett. **61**, 1521 (1988).

5.5.12 Information Geometry and Phase Transitions

W. Janke, D. A. Johnston*, R. Kenna** and R. P. K. C. Malmini***
* Heriot-Watt University, Edinburgh, Scotland, ** Coventry University, England,
*** University of Sri Jayewardenepura, Sri Lanka

Various authors, motivated by ideas in parametric statistics [1], have discussed the advantages of taking a geometrical perspective on statistical mechanics [2]. The "distance" between two probability distributions in parametric statistics can be measured using a

geodesic distance which is calculated from the Fisher information matrix for the system. To this end the manifold $\mathcal{M}$ of parameters is endowed with a natural Riemannian metric, the Fisher-Rao metric [1]. For a spin model in field, $\mathcal{M}$ is a two-dimensional manifold parametrised by $(\theta^1, \theta^2) = (\beta, h)$. The components of the Fisher-Rao metric take the simple form $G_{ij} = \partial_i \partial_j f$ in this case, where f is the reduced free energy per site and $\partial_i = \partial/\partial\theta^i$. A natural object to consider in any geometrical approach is the scalar or Gaussian curvature $\mathcal{R}$ which in various two-parameter calculable models has been found to diverge at the phase transition point β_c according to the scaling relation $\mathcal{R} \sim |\beta - \beta_c|^{\alpha-2}$, where α is the usual specific heat critical exponent. For spin models the necessity of calculating in non-zero field has limited analytic consideration to 1D, mean-field and Bethe lattice Ising models [3].

In this project we used the exact solution in field of the Ising model on an ensemble of fluctuating planar random graphs (where $\alpha = -1,\ \beta = 1/2,\ \gamma = 2$) [4] to evaluate the scaling behaviour of the scalar curvature explicitly, and find $\mathcal{R} \sim |\beta - \beta_c|^{-2}$ [5]. The apparent discrepancy with the general scaling postulate is traced back to the effect of a *negative* α [5]. As anticipated, the same effect is found [6] in exact calculations for the *three*-dimensional spherical model, which was solved (in field) in the classic Berlin and Kac paper [7] and shares the same critical exponents as the Ising model on *two*-dimensional planar random graphs. We mainly concentrated on the 3D case, but also discussed other dimensions [6], in particular the mean-field like behaviour which sets in at $D = 4$.

[1] R. A. Fisher, Phil. Trans. R. Soc. Lond., Ser. A **222**, 309 (1922).
C. R. Rao, Bull. Calcutta Math. Soc. **37**, 81 (1945).

[2] G. Ruppeiner, Rev. Mod. Phys. **67**, 605 (1995).
D. Brody and N. Rivier, Phys. Rev. E **51**, 1006 (1995).
D. Brody and L. Hughston, Proc. Roy. Soc. London A **455**, 1683 (1999).

[3] B. P. Dolan, D. A. Johnston and R. Kenna, J. Phys. A **35**, 9025 (2002).

[4] D. V. Boulatov and V. A. Kazakov, Phys. Lett. B **186**, 379 (1987).

[5] W. Janke, D. A. Johnston and R. P. K. C. Malmini, Phys. Rev. E **66**, 056119 (2002) [cond-mat/0207573].

[6] W. Janke, D. A. Johnston and R. Kenna, Phys. Rev. E **67**, 046106 (2003).
D. A. Johnston, W. Janke and R. Kenna, Acta Physica Polonica B **34**, 4923 (2003).

[7] T. Berlin and M. Kac, Phys. Rev. **86**, 821 (1952).

5.5.13 Funding

1. *Discrete Random Geometries: From Solid State Physics to Quantum Gravity.*
W. Janke.
EU-Network "EUROGRID".
Grant No. HPRN-CT-1999-000161.

2. *Statistical Physics of Random Structures with Applications to Life and Material Sciences.*
W. Janke.
German-Israel-Foundation (GIF).
Grant No. I-653-181.14/1999.

3. *Hochtemperaturreihen für Random-Bond-Modelle und Spingläser.*
W. Janke.
Deutsche Forschungsgemeinschaft (DFG).
Grant Nos. JA 483/17-1 and 17-3.

4. *Two-Dimensional Magnetic Systems with Anisotropy.*
W. Janke.
EU-Marie Curie Development Host Fellowship.
Grant No. IHP-HPMD-CT-2001-00108.

5. *Quantenfeldtheorie: Mathematische Struktur und Anwendungen in der Elementarteilchen- und Festkörperphysik.*
Dozenten der Theoretischen Physik und Mathematik (Sprecher B. Geyer).
Deutsche Forschungsgemeinschaft (DFG).
Graduiertenkolleg, Grant No. 52.

6. *Geometry and Disorder: From Membranes to Quantum Gravity.*
W. Janke.
ESF-Network.

7. *Challenges in Molecular Simulations: Bridging the Length and Time-Scale Gap.*
W. Janke.
ESF-Programme "SIMU".

8. *Statistical Physics of Glassy and Non-Equilibrium Systems.*
W. Janke.
ESF-Programme "SPHINX".

9. *Multi-Overlap Simulationen von Spingläsern.*
W. Janke.
NIC Jülich (computer time grant).
Grant No. hmz09.

10. *Ungeordnete Ferromagnete.*
W. Janke.
NIC Jülich (computer time grant).
Grant No. hlz06.

11. *Disordered Ferromagnets*.
    W. Janke.
    LRZ München (computer time grant).
    Grant No. h0611.

12. *Studentenstipendium*.
    R. Schiemann.
    Studienstiftung des deutschen Volkes.

13. *Studentenstipendium*.
    S. Wenzel.
    Studienstiftung des deutschen Volkes.

5.5.14 Organizational Activities

Wolfhard Janke:

1. Member of Advisory Committee, *YALELAT03 – 13. Workshop on Lattice Field Theory*, Yale University, New Haven, USA, May 1–3, 2003.

2. Organizer of the Workshop *CompPhys03 – 4. NTZ-Workshop on Computational Physics*, ITP, University of Leipzig, December 4–5, 2003.

3. Permanent Member of International Advisory Board, *Conference of the Middle European Cooperation in Statistical Physics (MECO)*.

4. Member of Scientific Organizing Committee, *Fourth Eurogrid Meeting – Random Geometry: Theory and Applications*, Les Houches, March 22–26, 2004.

5. Director of the Naturwissenschaftlich-Theoretisches Zentrum (NTZ) at the Zentrum für Höhere Studien (ZHS), University of Leipzig.

5.5.15 External Cooperations

1. EU-Network "EUROGRID" – *Discrete Random Geometries: From Solid State Physics to Quantum Gravity* with 11 teams throughout Europe.

2. GIF-Network *Statistical Physics of Random Structures with Applications to Life and Material Sciences* with Joan Adler (Technion, Haifa), Amnon Aharony (Tel Aviv Univ.), Eytan Domany (Weizmann Inst., Rehovot), Kurt Binder (Mainz), Peter Grassberger (Jülich and Wuppertal), Thomas Nattermann (Köln), and Dietrich Stauffer (Köln).

3. Prof. Dr. Bernd A. Berg, Dept. of Physics, Florida State University, Tallahassee, USA.

4. Dr. Alain Billoire, CEA/Saclay, Service de Physique Théorique, France.

5. Prof. Dr. Desmond A. Johnston, School of Mathematical and Computer Sciences, Heriot-Watt University, Edinburgh, Scotland.

6. Dr. Ralph Kenna, School of Mathematical and Information Sciences, Coventry University, England.

7. Prof. Dr. Bertrand Berche and Dr. Christophe Chatelain, Laboratoire de Physique des Matériaux (UMR CNRS No 7556), Université Henri Poincaré, Nancy, France.

8. Dr. Pierre-Emmanuel Berche, Groupe de Physique des Matériaux (UMR CNRS No 6634), Université de Rouen, France.

9. Dr. Handan Arkın, Dept. of Physics, Hacettepe University, Ankara, Turkey.

10. Prof. Dr. Peter Grassberger and Dr. Hsiao-Ping Hsu, NIC, Forschungszentrum Jülich.

11. Prof. Dr. Hagen Kleinert and Prof. Dr. Bodo Hamprecht, Inst. für Theoretische Physik, FU Berlin.

12. Prof. Dr. Harald Markum and Dr. Rainer Pullirsch, Atominstitut, TU Wien, Austria.

13. Priv.-Doz. Dr. Rudolf Hilfer, IAC-1, Universität Stuttgart.

14. Dr. Simon Hands, Dept. of Physics, University of Wales Swansea, Swansea, Wales.

15. Priv.-Doz. Dr. Thomas Neuhaus, Inst. für Theoretische Physik, Universität Bielefeld.

16. Prof. Dr. Lev N. Shchur, Landau Institute for Theoretical Physics, Chernogolovka, Russia.

17. Prof. Dr. David B. Saakian, Yerevan Physics Institute, Yerevan, Armenia.

18. Prof. Dr. Bo Zheng and Prof. Dr. He-Ping Ying, Zhejiang University, Hangzhou, P.R. China.

5.5.16 Publications

Published in 2003

[1] Bachmann, M.; Janke, W.
Density of States for HP Lattice Proteins.
Acta Physica Polonica **B34** (2003) 4689–4697.

[2] Bachmann, M.; Janke, W.
Multicanonical Chain Growth Algorithm.
Phys. Rev. Lett. **91** (2003) 208105-1–4.

[3] Berche, P.-E.; Chatelain, C.; Berche, B.; Janke, W.
Monte Carlo Studies of Three-Dimensional Bond-Diluted Ferromagnets.
In: Wagner, S.; Hanke, W.; Bode, A.; Durst, F. (Eds.): *High Performance Computing in Science and Engineering, Munich 2002*.
Berlin: Springer, 2003; pp. 227–238.

[4] Berg, B.A.; Billoire, A.; Janke, W.
Numerical Study of the Two-Replica Overlap of the 3D Edwards-Anderson Ising Spin Glass.
Physica **A321** (2003) 49–58.

[5] Bittner, E.; Janke, W.; Saakian, D.B.
Approximate Calculation of the Ground-State Energy for Potts Spin-Glass Models using DGREM.
Phys. Rev. **E67** (2003) 016105-1–8.

[6] Bittner, E.; Janke, W.; Markum, H.
On the Continuum Limit of the Discrete Regge Model in 4d.
Nucl. Phys. **B** (Proc. Suppl.) **119** (2003) 924–926.

[7] Bittner, E.; Janke, W.
Generalized Complex $|\Psi^4|$ Model.
Acta Physica Polonica **B34** (2003) 4727–4737.

[8] Hellmund, M.; Janke, W.
Star-Graph Expansions for Bond-Diluted Potts Models.
Phys. Rev. **E67** (2003) 026118-1–9.

[9] Hilfer, R.; Biswal, B.; Mattutis, H.G.; Janke, W.
Multicanonical Monte Carlo Study and Analysis of Tails for the Order-Parameter Distribution of the Two-Dimensional Ising Model.
Phys. Rev. **E68** (2003) 046123-1–9.

[10] Janke, W.; Johnston, D.A.; Kenna, R.
The Information Geometry of the Spherical Model.
Phys. Rev. **E67** (2003) 046106-1–4.

[11] Janke, W.; Johnston, D.A.; Kenna, R.
New Methods to Measure Phase Transition Strength.
Nucl. Phys. **B** (Proc. Suppl.) **119** (2003) 882–884.

[12] Janke, W.; Billoire, A.; Berg, B.A.
Extreme Order Statistics.
Nucl. Phys. **B** (Proc. Suppl.) **119** (2003) 867–899.

[13] Janke, W.; Weigel, M.
Effects of Connectivity Disorder on the Potts Model.
Acta Physica Polonica **B34** (2003) 4891–4907.

[14] Janke, W.; Berg, B.A.; Billoire, A.
Simulating Rare Events in Spin Glasses.
Acta Physica Polonica **B34** (2003) 4909–4921.

[15] Janke, W.
First-Order Phase Transitions.
In: Dünweg, B.; Landau, D.P.; Milchev, A.I. (Eds.): *Computer Simulations of Surfaces and Interfaces*.

NATO Science Series, II. Mathematics, Physics and Chemistry – Vol. **114**, Proceedings of the NATO Advanced Study Institute, Albena, Bulgaria, 9 – 20 September 2002.
Dordrecht: Kluwer, 2003; pp. 111–135.

[16] Janke, W.
Histograms and All That.
In: Dünweg, B.; Landau, D.P.; Milchev, A.I. (Eds.): *Computer Simulations of Surfaces and Interfaces*.
NATO Science Series, II. Mathematics, Physics and Chemistry – Vol. **114**, Proceedings of the NATO Advanced Study Institute, Albena, Bulgaria, 9 – 20 September 2002.
Dordrecht: Kluwer, 2003; pp. 137–157.

[17] Janke, W.; Berche, P.-E., Chatelain, C; Berche, B.
Phase Transitions in Disordered Ferromagnets.
In: Wolf, D.; Münster, G.; Kremer, M. (Eds.): *NIC-Symposium 2004*, Proceedings.
Jülich: John von Neumann Institute for Computing NIC Series, Vol. **20**, 2003; pp. 241–250.

[18] Johnston, D.A.; Janke, W.; Kenna, R.
Information Geometry, One, Two, Three (and Four).
Acta Physica Polonica **B34** (2003) 4923–4937.

Published in 2004

[19] Bachmann, M.; Janke, W.
Thermodynamics of Lattice Heteropolymers.
J. Chem. Phys. **120** (2004) 6779–6791.

[20] Janke, W.; Johnston, D.A.; Kenna, R.
Information Geometry and Phase Transitions.
Physica **A336** (2004) 181–186.

[21] Janke, W.; Johnston, D.A.; Kenna, R.
Phase Transition Strength through Densities of General Distributions of Zeroes.
Nucl. Phys. **B682** (2004) 618–634.

To appear in 2004 (in print)

[22] Berche, P.-E.; Chatelain, C.; Berche, B.; Janke, W.
Bond Dilution in the 3D Ising Model: A Monte Carlo Study.
e-print cond-mat/0402596, to appear in Eur. Phys. J. **B** (in print).

[23] Bittner, E.; Janke, W.; Markum, H.
Discretization and Continuum Limit of Quantum Gravity on a Four-Dimensional Space-Time Lattice.
e-print hep-lat/0311031, to appear in: *Difference Equations and Special Functions*, International Conference "Bexbach Colloquium on Science", Bexbach, Germany, October 26–30, 2002 (in print).

[24] Bittner, E; Hands, S.; Markum, H.; Pullirsch, R.
Quantum Chaos in Supersymmetric QCD at Finite Density.
e-print hep-lat/0402015, to appear in Progress of Theoretical Physics Supplement (in print).

[25] Janke, W.; Berche, P.-E.; Chatelain, C.; Berche, B.
Quenched Disorder Distributions in Three-Dimensional Diluted Ferromagnets.
To appear in: Landau, D.P.; Lewis, S.P.; Schüttler H.-B. (Eds.): *Computer Simulation Studies in Condensed-Matter Physics XVI*.
Berlin: Springer, 2004 (in print).

[26] Janke, W.; Weigel, M.
The Harris-Luck Criterion for Random Lattices.
e-print cond-mat/0310269, to appear in Phys. Rev. **B** (in print).

[27] Janke, W.; Schakel, A.M.J.
Geometrical vs. Fortuin-Kasteleyn Clusters in the Two-Dimensional q-State Potts Model.
e-print cond-mat/0311624, to appear in Nucl. Phys. **B** (in print).

[28] Janke, W.; Weigel, M.
Monte Carlo Studies of Connectivity Disorder.
To appear in: *High Performance Computing in Science and Engineering, Munich 2004*, proceedings of the *Second Joint HLRB and KONWIHR Result and Reviewing Workshop* (in print).

Talks and Posters 2003

Michael Bachmann:

1. *Energy Density of HP Lattice Proteins*,
(with Janke, W.) 28th Conference of the Middle European Cooperation in Statistical Physics (MECO28), Saarbrücken, March 20–22 (P).

2. *Energy Density of Heteropolymers*,
DPG-Frühjahrstagung Dresden, March 24–28 (T).

3. *Multicanonical Chain Growth Algorithm*,
Seminar *Theory of Complex Systems*, John von Neumann Institute for Computing (NIC), Forschungszentrum Jülich, April 24 (T).

4. *Density of States for HP Lattice Proteins*,
(with Janke, W.) Workshop on *Random Geometry* and EU-Network Meeting, Krakow, Poland, May 15–17 (P).

5. *Energetic Properties of Heteropolymers*,
(with Janke, W.) 2nd Day of Biotechnology, Leipzig, May 21 (P).

6. *Exact Analysis of Designing Sequences*,
(with Schiemann, R.; Janke, W.) 2nd Day of Biotechnology, Leipzig, May 21 (P).

7. *Generalized-Ensemble Simulations of Off-Lattice Heteropolymers*,
Computational Physics Workshop (CompPhys03), Leipzig, December 4–5 (T).

Elmar Bittner:

1. *Nature of Phase Transitions in a Generalized Complex $|\psi|^4$ Model*,
(with Janke, W.) 28th Conference of the Middle European Cooperation in Statistical Physics (MECO28), Saarbrücken, March 20–22 (P).

2. *Zum Phasenübergang in der komplexen $|\psi^4|$ Theorie*,
DPG-Frühjahrstagung, Arbeitskreis Festkörperphysik, TU Dresden, March 24–28 (T).

3. *Generalized Comlex ψ^4 Model*,
(with Janke, W.) Workshop on *Random Geometry* and EU-Network Meeting, Krakow, Poland, May 15–17 (P).

4. *Phase Structure of a Generalized ψ^4 Model*,
Computational Physics Workshop (CompPhys03), Leipzig, December 4–5 (T).

Meik Hellmund:

1. *Star-Graph Expansions for Bond-Diluted Potts Models*,
(with Janke, W.) DPG-Frühjahrstagung, Arbeitskreis Festkörperphysik, TU Dresden, March 24–28 (P).

Wolfhard Janke:

1. *Phasenübergänge in ungeordneten Ferromagneten*,
Theorie-Kolloquium, Universität Mainz, January 16 (T).

2. *Partition Function Zeroes for Fluctuating Graphs*,
Seminaire LPM, Université Henri Poincaré, Nancy, France, January 23 (T).

3. *Quenched Disorder in Three-Dimensional Ferromagnets*,
16th Workshop on *Recent Developments in Computer Simulation Studies in Condensed Matter Physics*, The University of Georgia, Athens, Georgia, USA, February 24–28 (T).

4 *Information Geometry and Phase Transitions*,
(with Johnston, D.A.; Kenna, R.; Malmini, R.P.K.C.) 28th Conference of the Middle European Cooperation in Statistical Physics (MECO28), Saarbrücken, March 20–22 (P).

5. *Phase Transitions of the Diluted 3D 4-State Potts Model*,
DPG-Frühjahrstagung, Arbeitskreis Festkörperphysik, TU Dresden, March 24–28 (T).

6. *Quenched Disorder in Ferromagnets*,
invited talk, *Yalelat03* – 13. Workshop on Lattice Field Theory, Yale University, New Haven, USA, May 1–3 (T).

7. *Simulating Rare Events in Spin Glasses*,
   invited talk, Workshop on *Random Geometry* and EU-Network Meeting, Krakow, Poland, May 15–17 (inv. T).

8. *Quenched Connectivity Disorder*,
   invited talk, Atelier Nancy, Université Henri Poincaré, Nancy, Frankreich, May 21–22 (inv. T).

9. *Ground States of Lattice Proteins*,
   invited talk, Dagstuhl-Seminar on *New Optimization Algorithms in Physics*, Wadern, September 14–19 (inv. T).

10. *Overcoming Slow Dynamics in Generalized Ensemble Simulations*,
    invited talk, Workshop NesPhy03, MPI-PKS Dresden, September 22 – October 10 (inv. T).

Andreas Nußbaumer:

1. *Parallel Tempering at Second-Order Phase Transitions*,
   (with Bittner, E.; Janke, W.) DPG-Frühjahrstagung, Arbeitskreis Festkörperphysik, TU Dresden, March 24–28 (P).

2. *Ising Droplets in Action*,
   Computational Physics Workshop (CompPhys03), Leipzig, December 4–5 (T).

Adriaan Schakel:

1. *Physics in Geometrical Potts Clusters*,
   Computational Physics Workshop (CompPhys03), Leipzig, December 4–5 (T).

Reinhard Schiemann:

1. *Exact Statistical Analysis of Native Ground States of Lattice Proteins*,
   (with Bachmann, M.; Janke, W.) DPG-Frühjahrstagung, Arbeitskreis Festkörperphysik, TU Dresden, March 24–28 (P).

Thomas Vogel:

1. *Monte Carlo Simulations of the 2D Ising Model with Brascamp-Kunz Boundary Conditions*,
   (with Krinner, A.; Janke, W.) DPG-Frühjahrstagung, Arbeitskreis Festkörperphysik, TU Dresden, March 24–28 (P).

Martin Weigel:

1. *Effects of Connectivity Disorder on the Potts Model*,
   (with Janke, W.) 28th Conference of the Middle European Cooperation in Statistical Physics (MECO28), Saarbrücken, March 20–22 (P).

2. *Effects of Connectivity Disorder on the Potts Model*,
(with Janke, W.) DPG-Frühjahrstagung, Arbeitskreis Festkörperphysik, TU Dresden, March 24–28 (P).

3. *Effects of Connectivity Disorder on the Potts Model*,
(with Janke, W.) Workshop on *Random Geometry* and EU-Network Meeting, Krakow, Poland, May 15–17 (P).

4. *The Harris-Luck Criterion for Random Lattices*,
Institute for Theoretical Physics, University of Leipzig, October 8 (T).

5. *The Harris-Luck Criterion for Random Lattices*,
Condensed Matter Theory Seminar, University of Waterloo, Canada, November 4 (T).

6. *Harris Criterion and Correlated Disorder from Random Graphs*,
Emerging Materials Knowledge Meeting, University of Waterloo, Canada, December 18 (T).

Andreas Wernecke:

1. *Q-state Potts Models on Quenched Random Planar ϕ^3 Graphs*,
(with Janke, W.) DPG-Frühjahrstagung, Arbeitskreis Festkörperphysik, TU Dresden, March 24–28 (P).

5.5.17 Graduations

Diploma and Master Theses

1. Andreas Nußbaumer, *Rare-Event Sampling of Spin Glasses*, Diploma Thesis, April 2003.

2. Reinhard Schiemann, *Exact Enumeration of 3D Lattice Proteins*, Diploma Thesis, September 2003.

3. Sandro Wenzel, *Monte Carlo Simulations of the 3D Ginzburg-Landau Model with Compact U(1) Gauge Field*, Master Thesis, December 2003.

4. Thomas Vogel, *HP-Proteine auf verallgemeinerten Gittern und Homopolymerkollaps*, Diploma Thesis, January 2004.

5. Axel Krinner, *Nature of Phase Transitions in a Generalized Complex Ginzburg-Landau*, Diploma Thesis, March 2004.

5.5.18 Guests

Short-term guests

1. Dr. Pai-Yi Hsiao, Laboratoire de Physique Théorique de la Matière Condensée, University Paris 7, France,
NTZ-Kolloquium, January 9, 2003: *Critical Behavior of the Ferromagnetic Ising*

Model on the Fractals,
Period: January 8–11, 2003.

2. Prof. Dr. Yuko Okamoto, Dept. of Theoretical Studies, Institute for Molecular Science, Okazaki, Aichi 444-8585, Japan,
TKM-Seminar, May 20, 2003: *Protein Folding Simulations by Generalized-Ensemble Algorithms*,
Period: May 19–21, 2003.

3. Prof. Dr. Royce Zia, Virgina Tech. Univ., USA,
NTZ-Kolloquium, November 27, 2003: *Non-Equilibrium Statistical Mechanics*,
Period: November 26–28, 2003.

4. Prof. Dr. Bernd A. Berg, Florida State University, Tallahassee, USA,
NTZ-Kolloquium, December 18, 2003: *A Biased Metropolis Sampling Method for Peptides*,
Period: December 16–19, 2003.

Long-term guests

1. Adriaan Schakel (FU Berlin): June–July 2003.

2. Handan Arkın (Hacettepe University, Ankara, Turkey): July–October 2003.

3. Thomas Neuhaus (Univ. Bielefeld): November–December 2003.

4. Adriaan Schakel (FU Berlin): November–December 2003.

5. Thomas Neuhaus (Univ. Bielefeld): January–February 2004.

5.6 Molecular Dynamics/Computer Simulations

5.6.1 Introduction

Using methods of statistical physics and computer simulations we investigate classical many-particle systems interacting with interfaces. One aim of the research in our department is to built up a bridge between theoretical and experimental physics.

By means of analytical theories of statistical physics and computer simulations (Molecular dynamics, Monte Carlo procedures, percolation theories) using modern workstations and supercomputers we examine subjects for which high interest exists in basic research and industry as well. The examinations involve transport properties (diffusion of guest molecules) in zeolites and the structural and phase behaviour of complex fluids on bulk conditions and in molecular confinements. Especially we are interested to understand

- the diffusion behaviour of guest molecules in zeolites in dependence on thermodynamic parameters, steric conditions, intermolecular potentials and the concentration of the guest molecules,
- structure and phase behaviour of dense fluids in pores, slits and model membranes in dependence on geometric and thermodynamic conditions
- and the migration of waste in deposits by use of percolation theories

in microscopic detail and to compare the results with experimental data. The use of a network of PC's and workstations (Unix, Linux, Windows), the preparation and application of programs (Fortran, C, C^{++}) and the interesting objects (zeolites, membranes) give excellent possibilities for future careers of undergraduates, graduate students and postdocs.

Our research in 2003 was part of several national and international programs (DFG - Schwerpunktprogramm 1155, an International Research Graduate Training program a joint research project DFG/TRF-Thailand, a joint research project DAAD/TRF-Thailand, and a NATO grant). We have a close collaboration with the Institute of Experimental Physics I (Physics of Interfaces and Biomembranes) of Leipzig University and many institutions in several countries (University of California, Irvine; University of Massachusetts, Amherst; University of Guelph, Canada; Athens/Patras; Charles University Prague; Sassari, Italy; Bangkok; Bordeaux; Warschau; Wien; Regensburg; MPI Mainz; Bundesanstalt für Geologie und Rohstoffe (BGR) Hannover).

5.6.2 Investigation of diffusion mechanisms of non-spherical molecules in cation free zeolites

A. Schüring, S. M. Auerbach*, S. Fritzsche, R. Haberlandt
* University Amherst, Massachusetts, USA

Explaining a surprising temperature dependence of the self diffusion coefficient D of ethane in the cation free LTA zeolite it could be shown that this dependence is caused by an entropic barrier [1]. Random walk treatment reduced the description of the underlying diffusion process on the essentials and could explain the effect in terms of jump rates that can be calculated analytically by use of the transition state theory or evaluated from Molecular Dynamics (MD) computer simulations. Investigations of the local free energy, defined as in [2], which is also the potential of mean force, show that the temperature

dependence of the jump rates is in some cases dominated by entropic barriers [3,4]. These investigations are now extended to other systems.

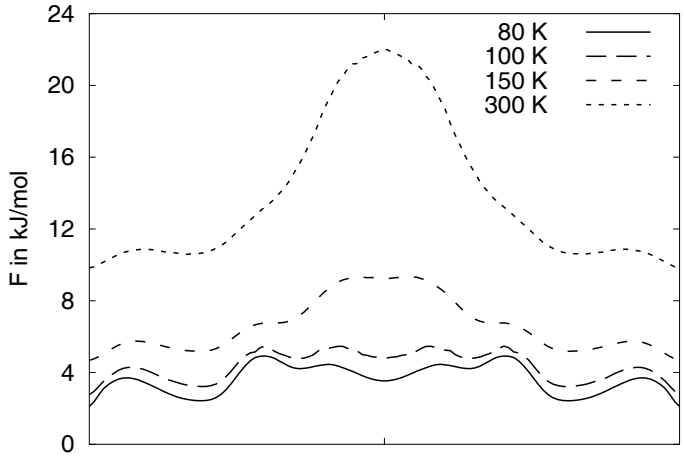

Fig. 1: The local free energy for a methane molecule in the LTA zeolite at positions along a line through the center of a window connecting two cavity centers for different temperatures.

From the Fig. 1 it can clearly be seen that for higher temperatures a barrier for the methane molecule appears in the window.

5.6.3 Analytical Theory and MD Simulations of special effects connected with diffusion of guest molecules in channels

S. Fritzsche, A. Schüring with J. Kärger* and S. Vasenkov*
* Institute for Experimental Physics I, University Leipzig

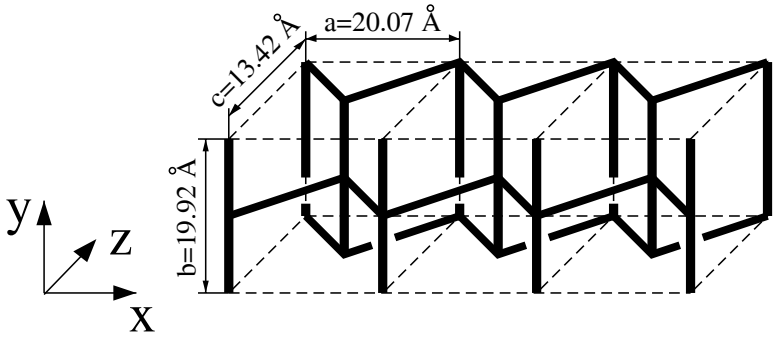

Fig. 2: Channel structure of Silicalite–1.

In this project effects of correlated anisotropic diffusion and effects in the transition region channel / gas phase are investigated.

Summing up infinite series of transition probabilities between intersections in silacalite–1 it has been shown, that in the case of uncorrelated movements, which is a good approx-

imation in many cases for small molecules, the elements of the diffusion tensor obey the relationship [5]

$$\frac{c^2}{D_z} = \frac{a^2}{D_x} + \frac{b^2}{D_y} \tag{5.1}$$

with a, b and c denoting the unit cell extensions in x–, y– and z–direction. Deviations from eq. (5.1) have been quantified by introducing a memory parameter β in ref. [6]

$$\beta = \frac{c^2/D_z}{a^2/D_x + b^2/D_y}. \tag{5.2}$$

Such processes are examined with inclusion of correlations e.g. in [7, 8, 9].

If channels of zeolites end at the zeolite surface, where the exchange of guest molecules with the gas phase takes place, pecularities with respect to diffusion have been observed. There is a region within the channel close to the end, where a special diffusion regime rules the migration of guest molecules [10]. These effects are investigated by analytical calculations in connection with dynamical Monte Carlo simulations and Molecular Dynamics simulations.

5.6.4 Investigation of the influence of zeolite lattice vibrations and molecule vibrations on the diffusion of guest molecules

S. Fritzsche, R. Haberlandt, M. Wolfsberg*
* UCI, Institute for Surface and Interface Science, Irvine, CA 92697-2025, USA

In the literature a strong influence of the lattice vibrations on the diffusion of methane the cation free A zeolite was found in [11, 12]. But our investigations showed by Molecular Dynamics Computer Simulations that the diffusion coefficient of the guest molecules was nearly the same for the rigid and the vibrating lattice for this system [13] and we gave an explanation of the discrepancy. This earlier result could be confirmed and understood in more detail by investigating the equilibration of kinetic energy differences in small zeolite cavities [14] using e.g. the one particle kinetic energy autocorrelation function.

The investigations have been extended to methane in silicalite–1 and the influence of the molecule vibrations has now been included as well. It could be shown that for the diffusion of methane in silicalite–1, contrary to the cation free LTA zeolite, the lattice vibration have some influence on the value of D while the influence of the molecule vibrations is negligible [15].

5.6.5 Water in chabazite

S. Jost, S. Fritzsche, R. Haberlandt, Ph. A. Bopp*
* University of Bordeaux, France

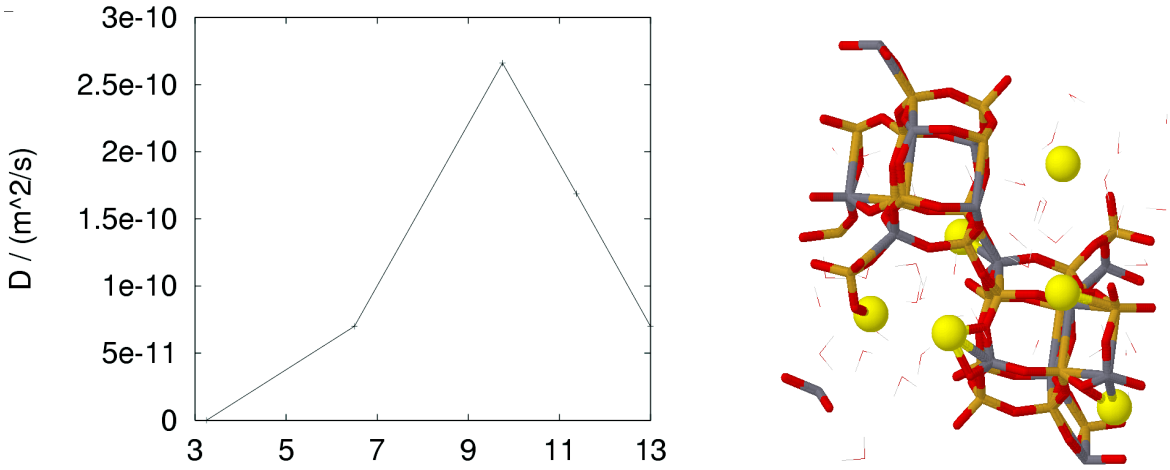

Fig. 3: Left: Mean diffusion coefficient versus Loading (molecules per unit cell) at $T = 600\,\mathrm{K}$. Right: Snapshot from the MD-Simulation. Cations are bright, water molecules are represented by small ticks.

In this project methodical developments and Molecular Dynamics Computer Simulations are combined. The simulation of this diffusional process [16, 17] turned out to be at the limit of the computational capabilities, so we had to increase the temperature up to $T = 600\,\mathrm{K}$, to get mean square displacements, which are large enough, to evaluate diffusion coefficients. At this temperature the system shows a quite uncommon dependence on the loading (Fig. 3): For the almost dehydrated zeolite with only one quarter of the full loading, there is a very slow diffusion. Then the diffusion coefficient increases with increasing loading, up to a maximum value for 75% of the full loading. Then it decreases with further increasing loading.

This abnormal behaviour can be explained by the knowledge about the adsorption places. At approximately half of the maximum loading, almost all preferred places in the hydration shells of the cations are filled up. Therefore, at higher loadings there are some water molecules which are only loosely bound and relatively free to move. With further increase in the loading, the fraction of mobile molecules increases, leading to more diffusional motion, but with more molecules, the number of potential collision partners increases as well, which limits the increase of D and dominates for the highest loadings.

5.6.6 How do guest molecules enter zeolite pores? Quantum Chemical calculations and classical MD simulations

R. Haberlandt, S. Fritzsche, C. Bussai*, S. Hannongbua*
* Chulalongkorn University, Bangkok

This research is based on a joint project of the DFG (Germany) and the TRF (Thailand). After water in silicalite-1 was examined in cooperation with experimentally working physicists [18] these investigations are now extended to the surface. Fitted potentials developped from ab inition calculations for several thousand configurations of an water molecule in silicalite have been calculated [19, 20, 21]. This potential has then been used in Molecular Dynamics simulations [18, 20, 22, 23]. For the water/water interaction a well established potential from the literature has been used [24]. The investigations have also been started for methane in silicalite–1 [25] and on its external surface.

5.6.7 Force Field Calculation and MD–Simulation of Pentane in Silicalite–1

S. Fritzsche, A. Loisruangsin*, S. Hannongbua*
* Chulalongkorn University, Bangkok

This research is based on a joint project of the DAAD (Germany) and the TRF (Thailand). Force fields for the pentane/pentane interaction and the interaction of pentane with the silicalite–1 lattice are developped. This is done by fitting potential parameters to the results of MP2 *ab initio* calculations. Different from most *ab initio* calculations the present ones are not only done on the Hartree–Fock level. In Hartree–Fock calculations the electron correlations are neglected hence, the dispersive forces (Van der Waals interactions) are not reproduced. Instead, in the more accurate MP2 calculations these effects are taken into account. In comparison to several well known force fields in the literature the newly developped potentials show better agreement with the *ab initio* results [26].

5.6.8 Statistical mechanics of associating fluids: Chemical potentials, phase equilibria, and critical properties

H. L. Vörtler, I. Nezbeda*, M. Kettler**
* Charles University, Prague, ** Frankfurt

The project is part of a long-term research program dealing with the equilibrium statistical mechanics of molecular and associating fluids on both bulk conditions and geometrical restrictions using Monte Carlo simulations and analytical (perturbation) theories.

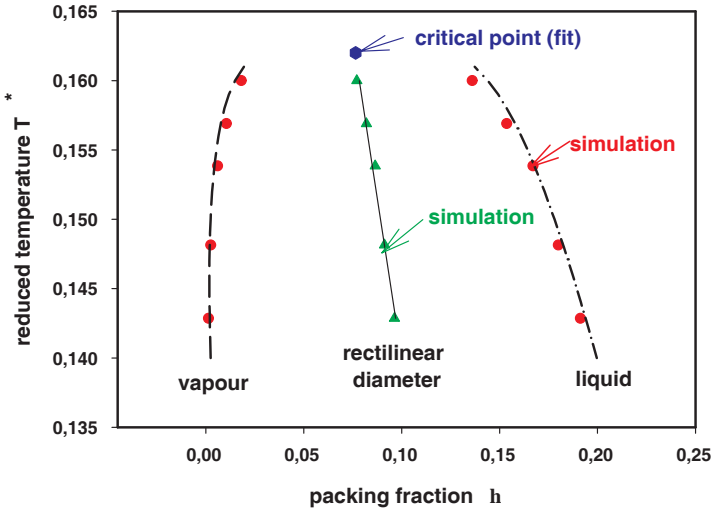

Vapour-liquid equilibrium and critical point EPM 5 water

We discuss recent Monte Carlo computer simulation techniques to calculate efficiently chemical potentials of short-ranged primitive models of associating (water-like) fluids [27], where the conventional Widom test-particle method fails because of the very low insertion probability of a test particle at moderate to high densities. Therefore, gradual particle insertion [28] and monomer insertion techniques [29] are used to overcome these problems.

Novel simulation results for chemical potential versus density isotherms of primitive water models which show typical van der Waals loops at sub-critical temperatures are use to estimate the densities of the coexisting fluid phases by means of a Maxwell equal-area construction [30].

From the vapour-liquid equilibrium data we calculate the critical temperatures and the critical densities of primitive water using classical scaling theory arguments.

The obtained chemical potentials and coexistence properties are pseudo-experimental reference data for analytical theories of associating fluids. Fields of applications are aqueous solutions, water confined to microporous media or thin water films in biological systems. The project is part of an international collaboration.

5.6.9 Cavity Distribution Functions and Solubility of Fused Hard Sphere Fluids

H. L. Vörtler and W. R. Smith*
* University of Guelph, Ontario, Canada

We continue our studies of the molecular structure of bulk and inhomogeneous fluids in terms of cavity distribution functions [31] which are of special interest for both developing analytical closures of the BGY integral equation hierarchy [32] connecting cavity distribution functions of different order and calculating efficiently excess chemical potentials and background correlation functions.

On the basis of novel virtual particle/cavity insertion simulation techniques we have calculated efficiently cavity pair distribution functions of confined hard-sphere systems using virtual particle/cavity insertion moves in a canonical ensemble. Extensive simulation studies have been performed for conditional distribution functions of pairs of hard-sphere cavities in fluids confined to slit-like micropores and thin films. The results – which represent the first quantitative data of such functions available – are summarized in papers [33, 34].

The next step of the project – which is at present under consideration – deals with the extension to m-body cavity functions, where the corresponding cavity is a fused-hard-sphere (FHS) cavity (molecule) of m HS cavities, the individual spheres of which may be overlapping. The corresponding m-particle cavity distribution function $n(\mathbf{1}, \mathbf{2}, \ldots, \mathbf{m})$ is the probability that the FHS cavity can be inserted into the system, and is related to its dimensionless excess chemical potential at infinite dilution, $\beta\mu^e(\mathbf{1}, \mathbf{2}, \ldots, \mathbf{m})$, via

$$n(\mathbf{1}, \mathbf{2}, \ldots, \mathbf{m}) = \exp[-\beta\mu^e(\mathbf{1}, \mathbf{2}, \ldots, \mathbf{m})] \tag{5.3}$$

$\beta\mu^e(\mathbf{1}, \mathbf{2}, \ldots, \mathbf{m})$ is equivalent to the dimensionless excess chemical potential at infinite dilution of a molecule corresponding to the m-particle cavity in the fluid. $\beta\mu^e(\mathbf{1}, \mathbf{2}, \ldots, \mathbf{m})$ is directly related to the solubility of the corresponding FHS-molecule in a hard sphere fluid at infinite dilution.

Therefore estimations of m-body cavity functions in geometric restricted fluids provide a direct route to study solubility and sorption phenomena of polyatomic molecules in confined fluids on a molecular level.

The project is part of an international collaboration.

References

[1] A. Schüring, S. M. Auerbach, S. Fritzsche, and R. Haberlandt, J. Chem. Phys. **116**, 10890 (2002).

[2] D. Chandler, *Introduction to Modern Statistical Mechanics*, Oxford University Press, New York, 1987.

[3] A. Schüring, *Molekulardynamik-Simulationen und Sprungmodelle zur Diffusion in Zeolithen*, PhD thesis, University of Leipzig, 2003.

[4] A. Schüring, S. M. Auerbach, S. Fritzsche, and R. Haberlandt, Capturing geometric correlations for ethane diffusion in cation-free LTA zeolite through the vacancy correlation factor , in preparation.

[5] J. Kärger, J. Phys. Chem **95**, 5558 (1991).

[6] E. J. Maginn, A. T. Bell, and D. N. Theodorou, J. Phys. Chem **100**, 7155 (1996).

[7] S. Fritzsche and J. Kärger, Europhys. Lett. **63**, 465 (2003).

[8] S. Fritzsche and J. Kärger, J. Phys. Chem. B **107**, 3515 (2003).

[9] S. Fritzsche, A. Schring, S. Vasenkov, and J. Kärger, Poster, 85th Bunsen Colloquium on Atomic Transport in Solids: Theory and Experiments, 31th October 2003 Rauischholzhausen / Gieen, Germany (2003).

[10] S. Vasenkov and J. Kärger, Phys. Rev. E **66**, 0526011 (2002).

[11] P. Demontis and G. B. Suffritti, Chem. Phys. Lett. **223**, 355 (1994).

[12] P. Demontis and G. B. Suffritti, Molecular Dynamics Simulations of Diffusion in a Cubic Symmetry Zeolite, in *Zeolites and Related Microporous Materials: State of the Art*, edited by J. Weitkamp, H. G. Karge, H. Pfeifer, and W. Hoelderich, pages 2107–2113, Elsevier, Amsterdam, 1994, Proceedings of the the 10th International Zeolite Conference, Garmisch– Partenkirchen, 1994.

[13] S. Fritzsche et al., Chem. Phys. Lett. **296**, 253 (1998).

[14] S. Fritzsche, M. Wolfsberg, and R. Haberlandt, Chem. Phys. **253**, 283 (2000).

[15] S. Fritzsche, M. Wolfsberg, and R. Haberlandt, Chem. Phys. **289**, 321 (2003).

[16] S. Jost, S. Fritzsche, and R. Haberlandt, Studies in Surface Science and Catalysis **142**, 1947 (2002).

[17] S. Jost, *Untersuchung struktureller und dynamischer Eigenschaften von Wasser in Zeolithen am Beispiel von Chabasit mit Hilfe von MD – Simulationen*, PhD thesis, University of Leipzig, 2004.

[18] C. Bussai et al., Applied Catalysis A **232**, 59 (2002).

[19] C. Bussai, S. Hannongbua, and R. Haberlandt, J. Phys. Chem. B **105**, 3409 (2001).

[20] C. Bussai, R. Haberlandt, S. Hannongbua, S. Jost, and S. Fritzsche, Computer Simulations of Water in Zeolites, in *Studies in Surface Science and Catalysis*, edited by A. Galarneau, F. D. Renzo, F. Fajula, and J. Vedrine, volume 106, Elsevier, Amsterdam, 2001.

[21] C. Bussai, S. Hannongbua, S. Fritzsche, and R. Haberlandt, Chem. Phys. Lett. **354**, 310 (2002).

[22] C. Bussai, S. Hannongbua, S. Fritzsche, and R. Haberlandt, Studies in Surface Science and Catalysis **142**, 1979 (2002).

[23] C. Bussai, S. Fritzsche, S. Hannongbua, and R. Haberlandt, J. Phys. Cem. B **107**, 12444 (2003).

[24] P. Bopp, G. Jancso, and K. Heinzinger, Chem. Phys. Lett. **98**, 129 (1983).

[25] C. Bussai, S. Hannongbua, S. Fritzsche, and R. Haberlandt, to be published (2004).

[26] A. Loisruangsin, S. Fritzsche, and S. Hannongbua, Chemical Physics Letters, submitted (2004).

[27] I. Nezbeda, J. Mol. Liquids, **73-74**, 317 (1997).

[28] I.Nezbeda; J. Kolafa; Molec.Simulation. **5**, 391 (1991); M. Kettler, H.L. Vörtler, I. Nezbeda and M. Strnad, Fluid Phase Equilib. **181**, 83 (2001).

[29] S. Tripathi, S., W.G. Chapman, Mol. Phys. **101** 1199 (2003)

[30] H. L. Vörtler, M. Kettler, Chem. Phys. Letters **377** 557 (2003)

[31] R. Speedy, J. Chem. Soc. Faraday II, **76**, 693 (1980)

[32] S. Labìk, W. R. Smith, and R. Speedy, J. Chem.Phys. **88**, 1944 (1987)

[33] W.R. Smith and H.L. Vörtler, Mol. Phys. **101**, 805 (2003)

[34] S. Fritzsche and R. Haberlandt and H. L. Vörtler; *Modelling and Simulation of Structure, Thermodynamics and Transport of Fluids in Molecular Confinements*, in *Lecture Notes in Physics*, Vol 634,
Eds. R. Haberlandt et al., Springer, Berlin, 2004

5.6.10 Funding

- Project *How do guest molecules enter zeolite pores? Quantum Chemical calculations and classical MD simulations*, German project leader: PD Dr. Fritzsche. Common project of the TRF (Thailand) and the DFG (DFG - grant numbers: FR1486/1-1, FR1486/1-3).

- Project *Analytical Treatment and Computer Simulations of Anomalous Diffusion in the Transition Region Gas/Adsorbent*, Project leader PD Dr. Fritzsche and Dr. Sergey Vasenkov. Schwerpunktprogramm 1155 Molekulare Modellierung und Sim-

ulation in der Verfahrenstechnik (DFG - Fördernummer: FR1486/2-1),

- Project *Statistical mechanics of associating fluids: Chemical potentials, phase equilibria, and critical properties.* Project leader: Dr. Vörtler. The project is part of an international collaboration supported by NATO (Grant PST.CLG.978178/6343CRG).

- *Cavity Distribution Functions and Solubility of Fused Hard Sphere Fluids.* Project leader: Dr. H. L. Vörtler. The project is part of an international collaboration supported by NATO (Grant PST.CLG.978178/6343CRG) and the Parallel Computer Network SHARCNET (Ontario, Canada).

- *Force Field Calculation and MD–Simultion of Pentane in Silicalite–1* common project DAAD/TRF-Thailand, German project leader PD Dr. S. Fritzsche, (DAAD Grant A/01/19909), Thailand Research Fund, *Royal Golden Jubilee*, Grant No. A/03/28658)

5.6.11 External Academic Cooperations

1. Chulalongkorn University, Bangkok, Inst. of Chemistry, Prof. Dr. S. Hannongbua, projects 5.6.6, 5.6.7

2. Charles University, Prague, Inst. of Theoretical Physics, Prof. Dr. I. Nezbeda, project 5.6.8

3. University of Guelph, Ontario, Canada, Institute of Technology, Prof. Dr. W. R. Smith, project 5.6.9

4. University of California, Irvine, Inst. of Chemistry, Prof. Dr. M. Wolfsberg, project 5.6.4

5. University of Massachusetts, Amherst, Inst. of Chemistry, Prof. Dr. S. M. Auerbach, project 5.6.2

6. University of Bordeaux I, Inst. of Chemistry, Prof. Dr. P. A. Bopp, project 5.6.5

7. Dr. K. Heinzinger, Max-Planck-Inst. f. Chemie, Dept. Physical Chemistry

5.6.12 Publications in 2003

In Journals

1) S. Fritzsche and J. Kärger, *Memory Effects in Correlated Anisotropic Diffusion*, Europhys. Lett. **63**, 465 (2003)

2) S. Fritzsche and J. Kärger, *Tracing Memory Effects in Correlated Diffusion Anisotropy in MFI–Type Zeolites by MD Simulation* J. Phys. Chem. B **107**, 3515 (2003).

3) W.R. Smith and H.L. Vörtler, *Computer Simulation of Cavity Pair Distribution Functions of Hard Spheres in a Hard Slit Pore*, Mol. Phys. **101**,805 (2003).

4) H. L. Vörtler, M. Kettler, *Computer Simulations of chemical potentials of primitive models of water*, Chem. Phys. Letters **377**, 557 (2003).

5) S. Fritzsche, M. Wolfsberg, and R. Haberlandt, *The Importance of Various Degrees of Freedom in the Theoretical Study of the Diffusion of Methane in silicalite–1*, Chem. Phys. **289**, 321 (2003).

6) C. Bussai, S. Fritzsche, S. Hannongbua, and R. Haberlandt, *Formation of Low-Density Water Clusters in the Silicalite-1 Cage: A Molecular Dynamics Study*, J. Phys. Cem. B **107**, 12444 (2003).

7) A. S. Cukrowski and S. Fritzsche and M. J. Cukrowski, *A large nonequilibrium effect of decrease of the bimolecular chemical reaction rate in a dilute gas*, Chem. Phys. Letters **379**, 193 (2003).

8) A. S. Cukrowski and S. Fritzsche, *Analysis of nonequilibrium effects in a bimolecular chemical reaction in a dilute gas*, Acta Phys. Polon. B. **34**, 3607 (2003)

Poster

1) S. Fritzsche, A. Schüring, S. Vasenkov, and J. Kärger, *Correlated Anisotropic Diffusion*, Poster, 85th Bunsen Colloquium on Atomic Transport in Solids: Theory and Experiments, 31th October 2003 Rauischholzhausen / Gießen, Germany (2003).

Talks

1. H. L. Vörtler, *Estimation of Cavity distribution functions*, University of Guelph, (Ontario), Canada, March 3, 2003

2. H. L. Vörtler *MC simulation of associating fluids: Chemical potentials, phase equilibria, and critical properties*, 4rd Workshop on Computational Physics CompPhys03, Leipzig, December 03, 2003

3. S. Fritzsche, *About Some Notions of Statistical Physics*, invited lecture at the Third Mahidol Summer School on Advanced Research (MSAR2003), Bangkok, February 27th 2003

4. S. Fritzsche, *Classical Molecular Dynamics Computer Simulations*, invited lecture at the Third Mahidol Summer School on Advanced Research (MSAR2003), Bangkok, February 28th 2003

5. S. Fritzsche and A. Schüring, *A Random Walk Model for Ethane Self–Diffusion in the Cation–Free LTA Zeolite*, Chemistry Departement of the Chulalongkorn University, Bangkok, March 7th 2003

5.6.13 Graduations

A. Schüring
Molekulardynamik-Simulationen und Sprungmodelle zur Diffusion in Zeolithen
PhD thesis, University of Leipzig, 2003. date of defense July 2nd 2003, academic title acknowledged August 11th 2003.

5.7 Statistical Physics

5.7.1 Introduction

We work on the connections of statistical mechanics to quantum field theory, on the mathematical and physical aspects of renormalization group (RG) theory and on its applications to condensed matter physics, and on quantum kinetic theory. Our methods range from mathematical proofs to computational solution of large differential equations.

One of the central topics in our current research is an RG approach to many–fermion systems, which is used to investigate the properties of the Hubbard model in the parameter range relevant for high–temperature superconductivity. The RG method applied here is an exact functional transformation of the action of the system, which leads to an infinite hierarchy of equations for the Green functions. Truncations of this hierarchy are used in applications. In a number of nontrivial cases, this truncation can be justified rigorously, so that the method lends itself to mathematical studies. These mathematical aspects are also under investigation.

At present, we have collaborations with ETH Zurich, the Max–Planck Institute for Solid State Research in Stuttgart, the University of British Columbia, Vancouver, the University of Munich, and Stanford University.

5.7.2 Fermi surfaces with singularities

J. Feldman, M. Salmhofer, E. Trubowitz

Fermi surfaces with van Hove singularities are interesting both from the point of view of applications (high–temperature superconductors) and from the theoretical point of view. The logarithmic singularity in the density of states caused by the zero of the bare Fermi velocity gives rise to new marginally relevant terms in the RG equation [FRS]. In this situation, the renormalization of the Fermi velocity and the quasiparticle weight differ strongly. We have an all–order proof of C^1 regularity of the Fermi velocity (to appear). Work on the question of an inversion theorem generalizing that proven in [FST] for regular Fermi surfaces is in progress.

[FRS] N. Furukawa, T.M. Rice, M. Salmhofer, *Phys. Rev. Lett.* **81** (1998) 3195–3198

[FST] J. Feldman, M. Salmhofer, E. Trubowitz, *Comm. Pure Appl. Math.* **53** (2000) 1350–1384

5.7.3 Fermi Surface Flows

W. Pedra, M. Salmhofer

The method of posing counterterms in constructive field theoretic studies of two–dimensional fermion systems leads to the inversion problem which has been solved to all orders in perturbation theory [FST2] but not yet nonperturbatively. We introduce a new RG flow where the Fermi surface is adjusted dynamically in the flow. This allows us to give a nonperturbative construction of two–dimensional Fermi systems with a regular Fermi surface at the temperature above the critical temperature for superconductivity without using

counterterms. In the proof we combine the tree expansion of [SW] with the arch expansion of Iagolnitzer and Magnen (see [DR]) to extract overlapping loops [FST1] which are crucial for the regularity properties of the selfenergy [PS].

[FST1] J. Feldman, M. Salmhofer, E. Trubowitz, *J. Stat. Phys.* **84** (1996) 1209–1336

[FST2] J. Feldman, M. Salmhofer, E. Trubowitz, *Comm. Pure Appl. Math.* **53** (2000) 1350–1384

[DR] M. Disertori, V. Rivasseau, *Comm. Math. Phys.* **215**, 251,291 (2000)

[PS] W. Pedra, M. Salmhofer, Fermi Systems in Two Dimensions and Fermi Surface Flows, to appear in the Proceedings of the ICMP 2003 and papers to appear

[SW] M. Salmhofer, C. Wieczerkowski, *J. Stat. Phys.* **99** (2000) 557–586

5.7.4 RG flows with symmetry breaking

C. Honerkamp, O. Lauscher, W. Metzner, M. Salmhofer

The flow to strong coupling observed in many RG studies of interacting fermion systems [HSFR,HM] indicates the occurrence of symmetry breaking. It is also a major technical problem for the attempt to give a more detailed description of the symmetry–broken phases of such models. Tendencies for a suppression of the quasiparticle weight are weaker than the drive towards symmetry breaking instabilities [HS]. We have developed techniques for flows in which symmetry breaking can occur and studied the flow of a BCS gap in detail (to appear). We are also working on the question of how Ward identities that are broken by the RG flow are restored at the end of the flow.

[HM] C. Halboth, W. Metzner, *Phys. Rev.* **B 61** (2000) 7364; *Phys. Rev. Lett.* **85** (2000) 5162;

[HSFR] C. Honerkamp, M. Salmhofer, N. Furukawa, T.M. Rice, *Phys. Rev.* **B 63**, 035109 (2001)

[HS] C. Honerkamp, M. Salmhofer, *Phys. Rev.* **B 67**, 174504 (2003)

5.7.5 Ferromagnetism and Superconductivity

C. Husemann, M. Salmhofer

We study the interplay of ferromagnetism and superconductivity in the two–dimensional Hubbard model with hopping amplitudes t between nearest neighbours and t' between next–to–nearest neighbours, in the regime $0.3 < -t'/t < 0.5$. In this regime, the temperature–flow RG predicts a zero–temperature transition between d–wave superconductivity and ferromagnetism if the Fermi surface has van Hove singularities [HS]. We have performed a mean–field analysis of possible coexistence (diploma thesis of C. Husemann). Work on an RG treatment that allows for an analysis of this transition and on possible other symmetry breaking effects is in progress.

[HS] C. Honerkamp, M. Salmhofer, *Phys. Rev. Lett.* **87** (2001) 187004, *Phys. Rev.* **B 64** (2001) 184516

5.7.6 Quantum Boltzmann Equation

L. Erdős, M. Salmhofer, H.–T. Yau

We study the emergence of the quantum Boltzmann equation from the reversible dynamics given by the N–particle Schrödinger equation for fermions, on the kinetic timescale $t \sim \lambda^{-2}$. We have shown that the problem can be reduced to showing restricted quasifreeness of the time–evolved state on this timescale [ESY]. The mathematical investigation of this property is work in progress.

[ESY] L. Erdős, M. Salmhofer, H.-T. Yau, On the Quantum Boltzmann Equation, J. Stat. Phys., in press

5.7.7 Quantum Diffusion

L. Erdős, M. Salmhofer, H.–T. Yau

We study the long–time limit of the quantum Lorentz gas. We prove that, for a weakly coupled system with coupling strength λ, the time evolution on timescale $t \sim \lambda^{-2-\eta}$, $\eta > 0$, is given by a diffusion equation (to appear). This is the first time that a proof of the behaviour of these systems on time scales bigger than $O(\lambda^{-2})$ is given. The essential complication is that the number of collisions that happen on such timescales diverges as an inverse power of λ.

5.7.8 Funding

W. Pedra is a PhD student funded by the Max–Planck Institute for Mathematics in the Sciences. The visit of Joel Feldman was funded by Max–Planck Institute for Mathematics in the Sciences and the Graduiertenkolleg *Quantenfeldtheorie* at the ITP.

5.7.9 Organizational Duties

M. Salmhofer

Leiter, DPG–Fachverband *Theoretische und mathematische Grundlagen der Physik*

Reports for the Fonds zur Förderung der Wissenschaften (FWF)

Refereeing for Phys. Rev. Lett., Phys. Rev. B, Rev. Math. Phys.

5.7.10 External Cooperations

L. Erdős, LMU München
J. Feldman, UBC, Vancouver
C. Honerkamp, MPI–FKF Stuttgart
C. Landim, IMPA, Rio de Janeiro
W. Metzner, MPI–FKF Stuttgart
J. Quastel, University of Toronto
T.M. Rice, ETH Zürich
E. Trubowitz, ETH Zürich
H.–T. Yau, Stanford University

5.7.11 Publications

published

C. Honerkamp, M. Salmhofer
Flow of the quasiparticle weight in the N–patch renormalization group scheme
Phys. Rev. B 67, 174504 (2003)

in press

C. Landim, J. Quastel, M. Salmhofer, H.T. Yau
Superdiffusivity of asymmetric exclusion processes in dimensions one and two
Communications in Mathematical Physics, in press

L. Erdős, M. Salmhofer, H.-T. Yau
On the Quantum Boltzmann Equation
J. Stat. Phys., in press

Conference proceedings

W. Pedra, M. Salmhofer
Fermi Systems in Two Dimensions and Fermi Surface Flows
invited talk at the 14th International Congress of Mathematical Physics, Lisbon, 2003, to appear in the Proceedings of the ICMP 2003

Carsten Honerkamp, Manfred Salmhofer
Ferromagnetism and triplet superconductivity in the two-dimensional Hubbard model
Proceedings of M2S-Rio, Rio de Janeiro 2003, Physica C, to appear

5.7.12 Guests

Prof. Joel S. Feldman, (UBC, Vancouver), September 15 – December 14, 2003.

5.8 Graduate Studies Programme 'Quantum Field Theory' (GSP)

Host institution: Center for Theoretical Sciences (NTZ) at Center of Advanced Studies (ZHS)
Cooperating institutions: Institute for Theoretical Physics, Mathematical Institute and Max-Planck-Institute "Mathematics in the Sciences".

Quantum field theory (QFT) is the basis of the overwhelming part of modern Theoretical Physics. Up to now it is by no means exhausted concerning its rich mathematical structures, its far-reaching physical consequences and also its conceptual meaning. Together with classical field theory, on which it rests, as well as with statistical and computational physics it is the most effective methodology of Theoretical Physics. QFT has essential applications reaching from the subnuclear through nuclear, atomic, molecular and mesoscopic systems up to the realm of cosmology. Much effort is required in order to fully understand all the topics in QFT which grow up in these areas. The history of QFT is closely connected with the development in many fields of modern mathematics. Obviously, no real success in QFT will be possible without evolving and intensively studying also its mathematical structures.

The closely related **Research Areas** of the Graduate Studies Programme, having a longstanding tradition at the University of Leipzig and being in accordance with the international state-of-the-art, are:

(1) The investigations of the *Mathematical Structures of Quantum Field Theory* and of its conceptual content are of principal as well as of methodological interest. They are motivated partly by actual physical problems, partly they grow up because of their pure mathematical relevance. The main methods to be applied are (non-commutative) differential geometry, theory of Lie (super)groups and their representations, theory of operator algebras and (nonlinear) functional analysis as well as functional integration.

(2) *Relativistic Quantum Field Theory* is the generally accepted frame for describing the primary interactions of elementary particles with each other, with external fields and under various boundary conditions. The actual investigations are directed especially to the perturbative as well as nonperturbative treatment of the Standard Model and its supersymmetric extensions, to the theory of strings, on lattice approximations and computer simulations, as well as to QFT under external conditions.

(3) The *Nonrelativistic Quantum Field Theory* is one of the outstanding methods to study basic properties of condensed matter and various many body systems; it is closely related to the methods of statistical and computational physics. The actual investigations are on (strong) correlations in spin and low-dimensional electron systems and on scaling behaviour, phase transitions and finite- size effects in ordered and disordered systems.

The Graduate Studies Programme contains also a well established **Academic Training Program** consisting of a thematically coordinated Course of Main Lectures and various Specialized Lectures covering the whole research area. This is supported by the weekly Colloquium and three Main Seminars on "Mathematical Physics", "Quantum Field Theory" and "Theory of Condensed Matter". The PhD students also profit from the running scientific activities (including periodic workshops, schools and conferences), from the guest programs and the scientific spirit of the cooperating institutions. Any of these research fields are investigated in cooperation with various national and interna-

tional partners. The majority of the related projects – which are considered in detail in the description of the various research groups – belong to the *interdisciplinary area of Mathematical Physics*. Research and Education profits very much from the scientific (and spatial) neighbourhood of mathematicians and theoreticians and from the longstanding, fruitful cooperation between the three cooperating institutions – being unique in Germany.

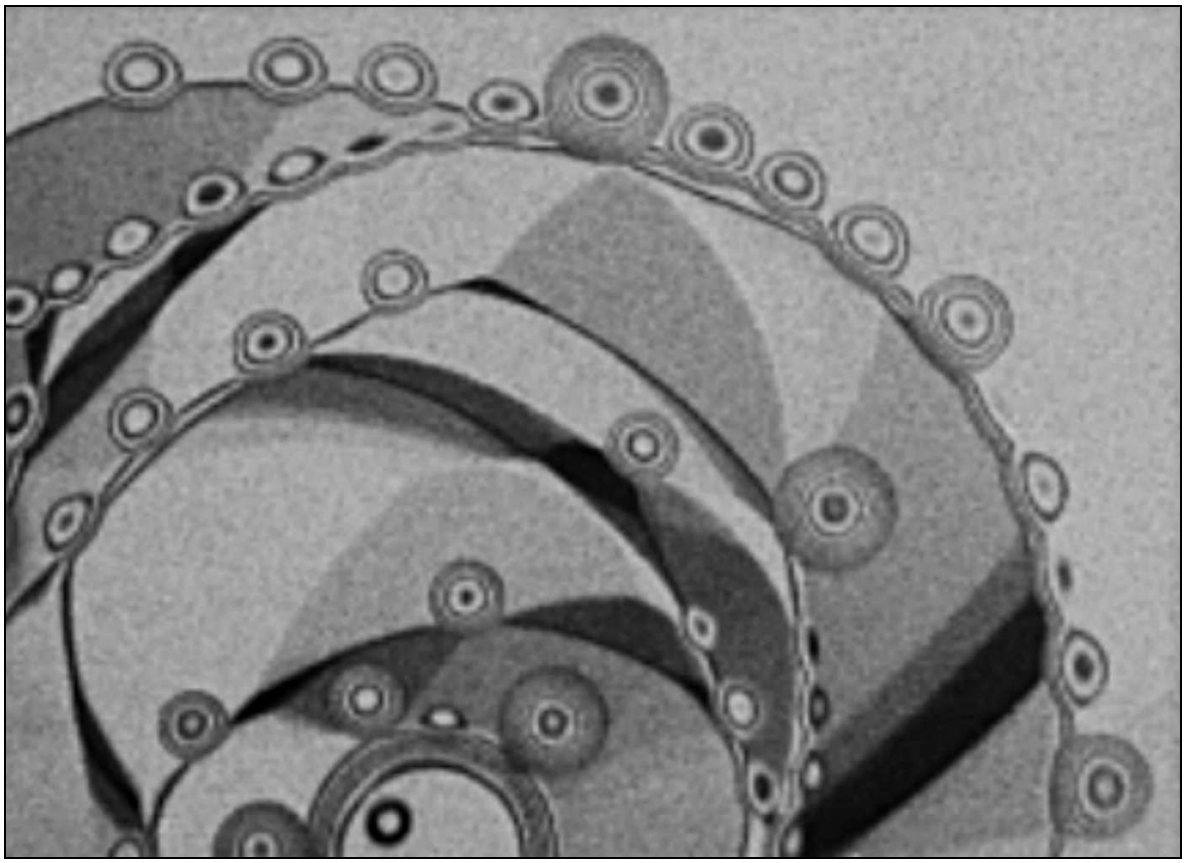

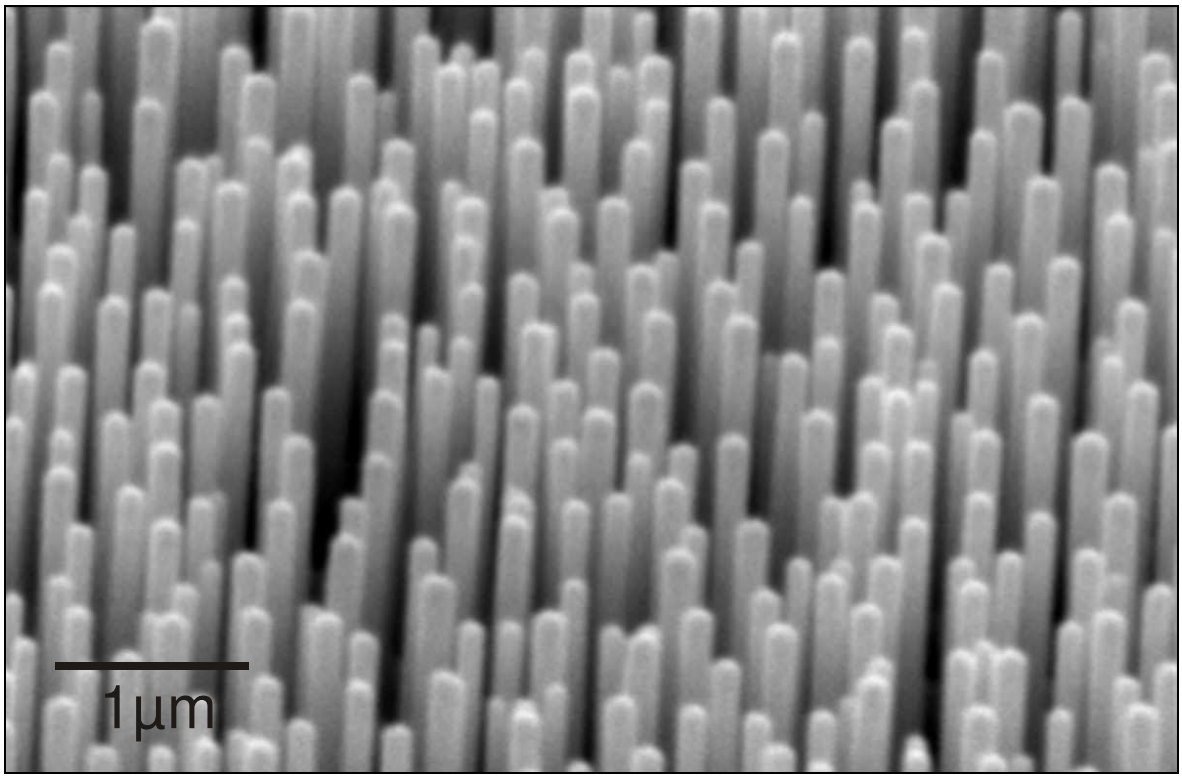

ISBN 3-934178-33-2